THE VISCERAL RESPONSE TO UNDERBODY BLAST

Andrew Phillip Pearce

Dissertation submitted in fulfilment of the requirements for the degree of:

Doctor of Philosophy

Department of Bioengineering, Imperial College London

October 2018

DECLARATION OF ORIGINALITY

The work presented in this thesis is my own and all else is appropriately referenced.

COPYRIGHT DECLARATION

ACKNOWLEDGEMENTS

A recurring theme in this thesis is the importance of an interdisciplinary approach to research. The Royal British Legion Centre for Blast Injury Studies epitomises this approach and I am forever indebted to the Centre and its personnel for providing me with the opportunity to undertake my work with them.

I first must thank my two supervisors, Professor Anthony Bull and Colonel Jon Clasper without whom this work would certainly not have been possible. They have shaped my project, nurtured my research skills, patiently critiqued my work, and taught me a great deal. I must also thank those other Centre academics: Dr Spyros Masouros, Dr Bill Proud, Dr Hari Arora, and Dr Warren Macdonald, all of whom have provided with me expertise in specialist subjects crucial to the foundations of my work.

I am incredibly grateful to my centre colleagues, both fellow PhD students and post docs, who have been working at the coal face of this research with me and who have aided me in the engineering and physics components of my work. Thanks then, to Dr Nic Newell. Dr Dilen Carpanen, Dr Grigorios Grigoriadis, and Dr Thuy Tien Nguyen. This group has, without hesitation, answered every annoyingly basic mechanics question that I could think of. My experiments would not have been completed without them. In the same regard, I must thank Mr Satpal Sangha for his technical and manufacturing expertise.

I am one in a line of military clinicians to have come though the Centre and I am grateful to those who preceded me for paving the path. In particular, I would like to thank Lt Col Arul Ramasamy and Lt Col James Singleton, whose works form the foundation for this thesis. A big thank you to Lt Col Dan Stinner, who in the two years that we sat next to each other taught me just how important it is to find good mentors.

This work would not have happened without the support of the Defence Medical Services. I am exceptionally grateful to Surg Capt Rory Rickard for his support both before and during this work. I did not make it easy for him and would not recommend the “Pearce Method” for seeking research approval!

Finally, and most importantly, I must thank my family. My wife Kate, to whom this thesis is dedicated, has been nothing but supportive in its development. She has listened with (perhaps feigned) interest when I have been discussing results and ideas and has always encouraged me to think about things in different ways.

To my two boys, Gabriel and Benjamin, I expect that you will in the future remember little of this period of our lives but it has been wonderful to spend so much time with you both. I suspect that this book is still a little too old for you though so please put it back on the shelf…

ABSTRACT

Blast is the most common cause of injury and death in contemporary warfare. Blast injuries may be categorised based upon their mechanism with underbody blast describing the effect of an explosive device detonating underneath a vehicle. Torso injuries are highly lethal within this environment and yet their mechanism in response to underbody blast is poorly understood. This work seeks to understand the pattern and mechanism of these injuries and to link them to physical underbody blast loading parameters in order to enable mitigation and prevention of serious injury and death.

An analysis of the United Kingdom Joint Theatre Trauma Registry for underbody blast events demonstrates that torso injury is a major cause of morbidity and mortality from such incidents. Mediastinal injury, including those trauma to the heart and thoracic great vessels is shown confer the greatest lethality within this complex environment.

This work explores the need for a novel *in vivo* model of underbody loading in order to explore the mechanisms of severe torso injury and to define the relationship between the "dose" of underbody loading and resultant injury. The work includes the development of a new rig which causes underbody blast analogous vertical accelerations upon a seated rat model.

Injuries causes by this loading to both the chest and abdomen can be best predicted by the examining the kinematic response of the torso to the loading. Axial compression of the torso, a previously undescribed injury metric is shown to be the best predictor of injury. The ability of these results to translate to a human model is explored in detail, with focus upon the biomechanical rationale; that torso organ injuries occur through both direct compression and shearing of tethering attachments.

Survivability of underbody blast could be improved by applying these principles to the design and modification of seats, vehicles and posture.

CONTENTS

LIST OF FIGURES

LIST OF TABLES

ABBREVIATIONS

Abbreviation	Explanation
ADMEM	Academic Department of Military Emergency Medicine
AC	Anterior Caudate lobe
AIC	Abdominal Injury Criterion
AIS	Abbreviated Injury Scale
ANOVA	Analysis of Variance
AP	Anatomic Profile
APF	Abdominal Peak Force
ASPA	Animals (Scientific Procedures) Act 1986
ATD	Anthropomorphic Test Device
AUROC	Area under the Receiver Operating Curve
AWERB	Animal Welfare and Ethical Review Board
BTAR	Blunt Traumatic Aortic Rupture
CAD	Computer Aided Design
CL	Caudate Lobe
CBIS	Centre for Blast injury Studies
CFR	Case Fatality Rate
CMax	Maximum Compression
CT	Computed Tomography
DMS	Defence Medical Services
DRI	Dynamic Response Index
DOW	Died of Wounds
GCS	Glasgow Comma Score
GI	Gastrointestinal
GSW	Gunshot Wound
HE	High Explosives
IED	Improvised Explosive Device
ICD	International Classification of Diseases
IRL	Inferior Right Lobe

IQR	Inter-Quartile Range
ISO	International Standards Organisation
ISS	Injury Severity Score
IVC	Inferior Vena Cava
JTTR	Joint Theatre Trauma Registry
KIA	Killed in Action
ML	Median Lobe
LLL	Left Lateral Lobe
LML	Left Medial Lobe
NATO	North Atlantic Treaty Organisation
NCIS	Normalised Confidence Interval Size
NCTH	Non-Compressible Torso Haemorrhage
NISS	New Injury Severity Score
NS	Non-Survivable
OR	Odds Ratio
PBLI	Primary Blast Lung Injury
PC	Pulmonary Contusion
PCL	Posterior caudate lobe
PMHS	Post-Mortem Human Surrogates
PPE	Personnel Protective Equipment
PS	Potentially Survivable
PV	Portal Vein
RCDM	Royal Centre for Defence Medicine
REBOA	Resuscitative Endovascular Balloon Occlusion of the Aorta
RivUL	Rig for *in vivo* Underbody Loading
RL	Right Lobe
RTS	Revised Trauma Score
SD	Standard Deviation
SE	Standard Error
SRL	Superior Right Lobe
SVC	Superior Vena Cava
TBI	Traumatic Brain Injury
TM	Tympanic Membrane

TNT	Trinitrotoluene
TRISS	Trauma and Injury Severity Score
TTI	Thoracic Trauma Index
UBB	Under-Body Blast
UK	United Kingdom
US	United States
VC	Viscous Response
WWI	World War 1
WWII	World War 2

CHAPTER 1

INTRODUCTION

1.1 Scope of the thesis

This thesis concerns the analysis of torso injuries sustained in response to explosions detonated underneath military vehicles, along with a novel *in vivo* model of these injuries which may be used to predict likelihood of severe injury.

1.2 General introduction

Explosions are now the most common weapon of warfare. These weapons may cause injury and death by a variety of means. The signature weapon of conflicts in Iraq and Afghanistan has been the Improvised Explosive device, or "roadside bomb" (Ramasamy *et al.*, 2008, 2009). These devices cause injury to those on foot (dismounted) and those in vehicles (mounted). The pattern of injury between the two is different with extremity and junctional injury predominant in the dismounted group (Singleton *et al.*, 2013). Under vehicle or underbody (mounted) blast is characterised by a wider spectrum of injuries with those to the head and torso most severe (Singleton *et al.*, 2013).

Advances and innovation in deployed military healthcare have led to hitherto unseen levels of survival from battlefield injuries. Those casualties who survive evacuation to a medical treatment facility are very likely to survive overall, such that the vast majority of fatalities in recent conflicts were deemed to have an unsurvivable injury burden. (Russell *et al.*, 2014). Improvements in future survival are therefore more likely gained from mitigation of these unsurvivable injuries.

1.3 Aims

Despite a relatively large body of international research into underbody blast as a cause of injury and death, some aspects of the injury pattern remain poorly understood. Musculoskeletal injuries have been the dominant research focus, partly due to the common nature of these injuries and the relative ease of studying them. There remains, however, little knowledge of the effect of this environment upon the internal organs of the torso nor of the role in which torso injuries play in overall survival.

The overall aims of this thesis are therefore to characterise the pattern of torso injuries caused by underbody blast and demonstrate the relationship of these injuries in regards to blast loading. It is anticipated that a quantative understanding of this relationship will ultimately enable improved survival by enabling the mitigation of injury.

1.4 Structure of the thesis

The thesis is separated into 3 main sections.

1.4.1 Section A: Blast Injury

This section on blast injury comprises Chapter 2 and is an overview of the relevant blast physics. The chapter separates out the injurious effects of blast with a latter emphasis upon the mounted blast environment. This initial understanding of the blast physics is essential for describing the relationship between injury and loading.

1.4.2 Section B: Clinical analysis of blast survivability and torso injury

Chapter 3 presents contemporary definitions of survivability. The use and limitations of current scoring systems and scores to describe battlefield injury is described. The chapter focuses upon improvements made in survivability and concludes that further improvements in survival can be gained by protective and mitigative strategies.

Chapter 4 is a detailed analysis of torso injuries sustained by UK deployed forces in Iraq and Afghanistan. The chapter shows the diverse range of injuries and demonstrates the importance of particular injuries in affecting survival using a binomial logistic regression model.

Chapter 5 analyses the association between torso injuries and musculoskeletal injuries. This analysis aims to describe the loading pathway of the injuries and demonstrates two disparate injury complexes related to the seat and floor respectively.

1.4.3 Section C: The biomechanics of torso injury in response to underbody blast

Following the finding of two distinct injury complexes, this section focus on torso injury biomechanics, starting with a literature review (Chapter 6). The chapter discusses the relevant organ anatomy before assessing existing models of impact and accelerative models of torso injury. The chapter includes a discussion and critique of current injury criteria and concludes that a novel model of *in vivo* injury with novel injury criteria is required for underbody torso injury.

Chapter 7 describes the specification, design, and construction of a new rig for analogous vertical loading of a rodent model.

Chapter 8 is a novel *in vivo* study of torso injury in a rat model in response to high rate vertical loading. The chapter describes similarities and differences in anatomy between the species. Necropsy, imaging, and histological injury data is presented alongside physical and biomechanical injury parameters.

Chapter 9 discusses the translation of this rodent model to human injury with a discussion of scaling laws, and mechanical analogues. The chapter uses the injury data from Chapter 8 to construct injury risk curves from the novel parameters and suggests that high rate measures of axial torso compression are the best predictors of injury.

Finally, Chapter 10 is a summary of the work presented above and discussion of the future work required both to further characterise these injuries and to improve blast survivability.

CHAPTER 2

BLAST INJURY

2.1 Scope of the chapter

This thesis concerns severe injury following blast. This chapter places these injuries into context by describing the increasing incidence of blast as a mechanism of battlefield wounding. The chapter describes the fundamental physics, which underlie blast processes, and details the methods used to classify blast injury. Particular emphasis is placed upon the mechanism of underbody blast and the transfer of load following detonation of a buried explosive device.

2.2 Blast Injury

Explosives are "materials which reacts to produce a violent expansion of hot gas which rapidly delivers energy to its surroundings" (Proud, 2013a). The injurious effects of any explosion are varied and depend upon both the type of explosive, design (if applicable) of the explosive device, and environmental factors (Horrocks, 2001). Blast injury, sustained as a consequence of explosions is not exclusive to deliberate acts of warfare or terrorism but weapon technology has led to the ubiquity of blast in modern conflict. Although injuries occurred as a consequence of explosions during the First World War, there were no systematic accounts of blast specific injuries from this. Interest in blast injury as a phenomenon became particularly important during the Second World War with the widespread use of both aircraft and air weapons (Benzinger, 1950). Eloquently described as "a shot without a bullet, a slash without a sword" (Benzinger, 1950), research interest in blast injury initially focussed upon the effect of the primary blast wave.

2.3 The changing nature of warfare.

Explosive technology has evolved and changed. Although not ubiquitous in warfare, explosive devices vary widely concerning their application and sophistication of design. The increasing availability of explosives in a variety of forms is reflected in the increasing incidence of blast related injuries as a proportion of all combat casualties. Table 2.1 (adapted from Owens *et al.*, 2008) illustrates the change in the mechanism of injuries amongst US service personnel in conflicts ranging from the US Civil War through to operations in Iraq and Afghanistan.

Conflict	Mechanism of Wounding	
	Gunshot Wound (%)	Blast (%)
US Civil War	91	9
WWI	65	35
WWII	27	73
Korea (1950-1953)	31	69
Vietnam (1966-1967)	35	65
Iraq and Afghanistan (2001-2005)	19	81

Table 2.1: Mechanisms of wounding in historical and recent conflicts. Adapted with permission from Owens *et al*. (2008).

The predominance of explosive injuries during large scale conflicts since the Second World War has been due to changes in the availability of explosive weapons, increasing sophistication of delivery methods (including air power) and growing expertise within military and insurgent groups. Explosive weapons have also been used by terrorist groups with increasing frequency (Edwards *et al.*, 2016).

2.4 Blast Physics

Explosive weapons can be classified in several ways. The most common distinction is between low-order and high-order explosives which differ in the speed at which an exothermic reaction propagates through the material. The basic chemical components of an explosive are a combustible fuel, an oxidiser, and a material that allows rapid ignition. Explosive materials do not necessarily release more energy than other chemical reactions. Both petrol and butter release more energy per molecule oxidised that trinitrotoluene (TNT) (Proud, 2016), but explosives have both fuel and oxidiser intimately mixed which speeds up the reaction process.

High-order explosives or simply high explosives (HE), which include TNT, have these necessary constituents within one chemically pure mixture. These materials explode in a process called detonation whereby the explosive shock front passes through the material faster than the speed of sound. The velocity of the detonation wave in such materials is around 8000m/s with a resultant energy release rate in the order of several Gigawatts.

Low-order explosives are separate fuel and oxidiser that are mixed. Gun powder is the most widely known example. These mixtures explode by a process of rapid burning, called deflagration. Although the total energy of the resultant reaction may be the same, the reaction rate is around a thousand time slower than the shock front of HE.

Given that an explosion by definition results in the formation of a gas, the rate of formation of this gas is dependent upon the explosive type. Detonation of high-order explosives produces gas products which expand rapidly. Gas products expand with velocity of approximately ¼ of the detonation velocity (around 2000m/s) (Proud, 2016). The interaction of these hot product gases with the surrounding environment results in a high velocity stress wave. A stress wave is the propagation of localised compression though the material. Stress waves travelling faster than the speed of sound (>330m/s) are referred to as shock waves. The resultant velocity of materials affected by the stress wave is dependent upon energy transmission through these materials and is governed by material properties.

Equation 2.1 is one of the "Rankin-Hugoniot" equations, where σ is stress, ρ is density of the material, U_S is the wave velocity, and δu_p is the change in material velocity. The equation, derived from fundamental equations of motion and momentum conservation, shows that the change in velocity of a material is dependent upon density of material and the velocity of stress transmission. The initial effect of a detonation wave outside of the energetic material itself is to transmit stress into the surrounding casing, causing fragmentation of this material and acceleration of the resultant fragments (Proud, 2016).

$$\sigma = \rho \, U_S \, \delta u_p \qquad [2.1]$$

Given that a shock wave is localised compression of the relevant medium, the pressure of that localised region is accordingly increased during the brief period of stress propagation. The characteristic description of the resultant pressure changes due to detonation of HE within an open field is given by the Friedlander curve (Figure 2.1).

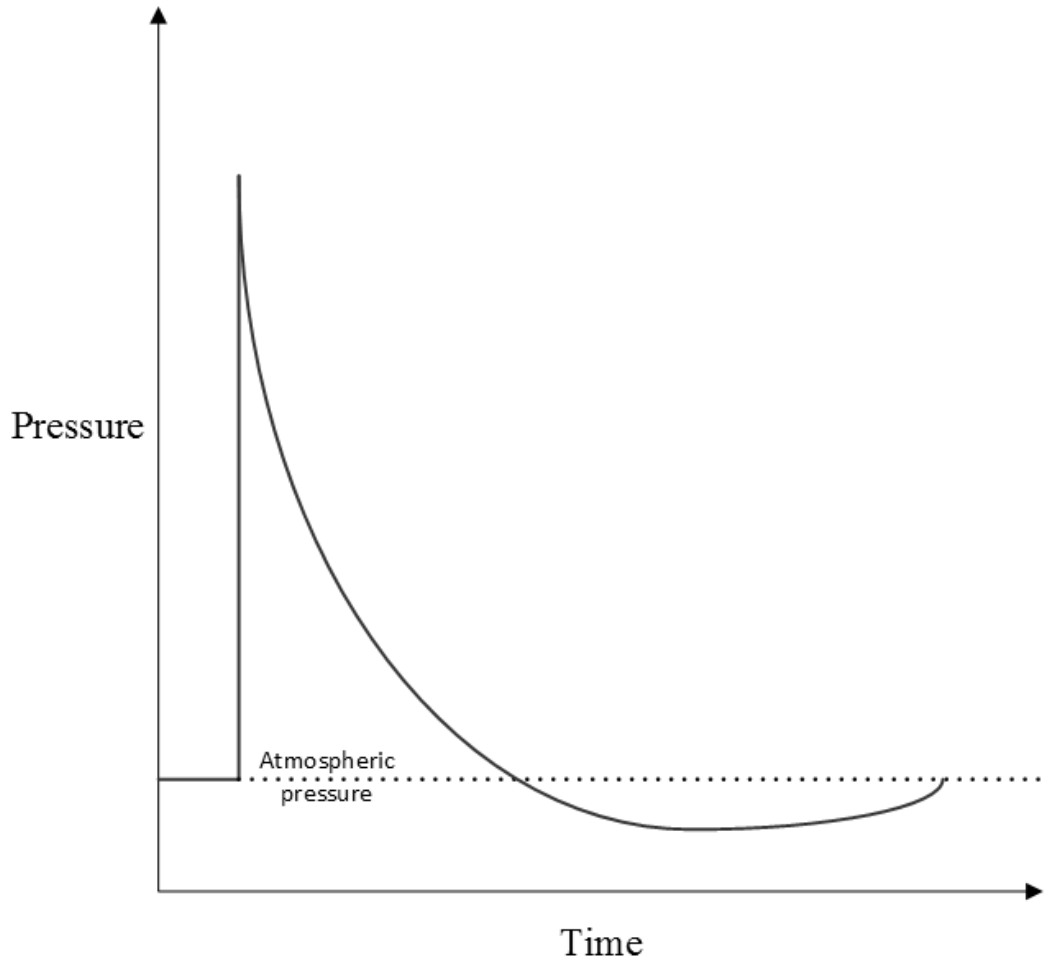

Figure 2.1: Friedlander curve showing quasi-instantaneous rise in pressure following detonation in a theoretical open field.

The high rate nature of the detonation is illustrated by the quasi-instantaneous rise in surrounding pressure before resultant decay. Although a useful illustration, this waveform is to some degree only theoretical as reflection of the shock wave off surrounding surfaces inevitably leads to some degree of wave complexity. In the free-field scenario, the shock wave expands as a sphere away from the point of detonation with equal pressure changes at each point on the sphere. As a consequence of this three-

dimensional energy transmission, the energy carried by the blast wave at any particular point away from the source is inversely proportional to the cube of the distance from the source. Stand-off from any explosive device is therefore an important mitigative principle.

Behind the supersonic shock front is a region of accelerated gas products and air, the so called "blast wind". The velocity of this wind may be as high as 560 m/s (2000 km/h). Given that the blast wind has both mass and velocity, it is able to transfer momentum to objects and cause gross physical displacement of people and objects (including small fragments). When the shock wave has passed, a "release" wave occurs as both air and gases expand out beyond the source and leave a relative vacuum with sub-atmospheric pressure. This negative pressure is shown in Figure 2.1 as the pressure line going below atmospheric pressure. Air and gas now move backwards (with a slower velocity than the blast wind) to occupy this space and equalise the pressure. The push-pull effect of these changes can be damaging to both structures and biological tissues (Proud, 2016).

As already mentioned, the precise description of the blast wave and resultant overpressure by the Friedlander curve is probably only true in a theoretical open space. A compressive wave hitting a solid surface leads to reflection of (some of) that wave with resultant increase in stress. Stress following reflection of a wave may double but is dependent upon how much of the stress is transmitted through the material of the solid surface. An explosive within an enclosed or partially enclosed space may lead to multiple reflected waves with subsequent complex changes in both magnitude and duration of pressure. An example of the pressure profile with a theoretical enclosed space is shown in Figure 2.2.

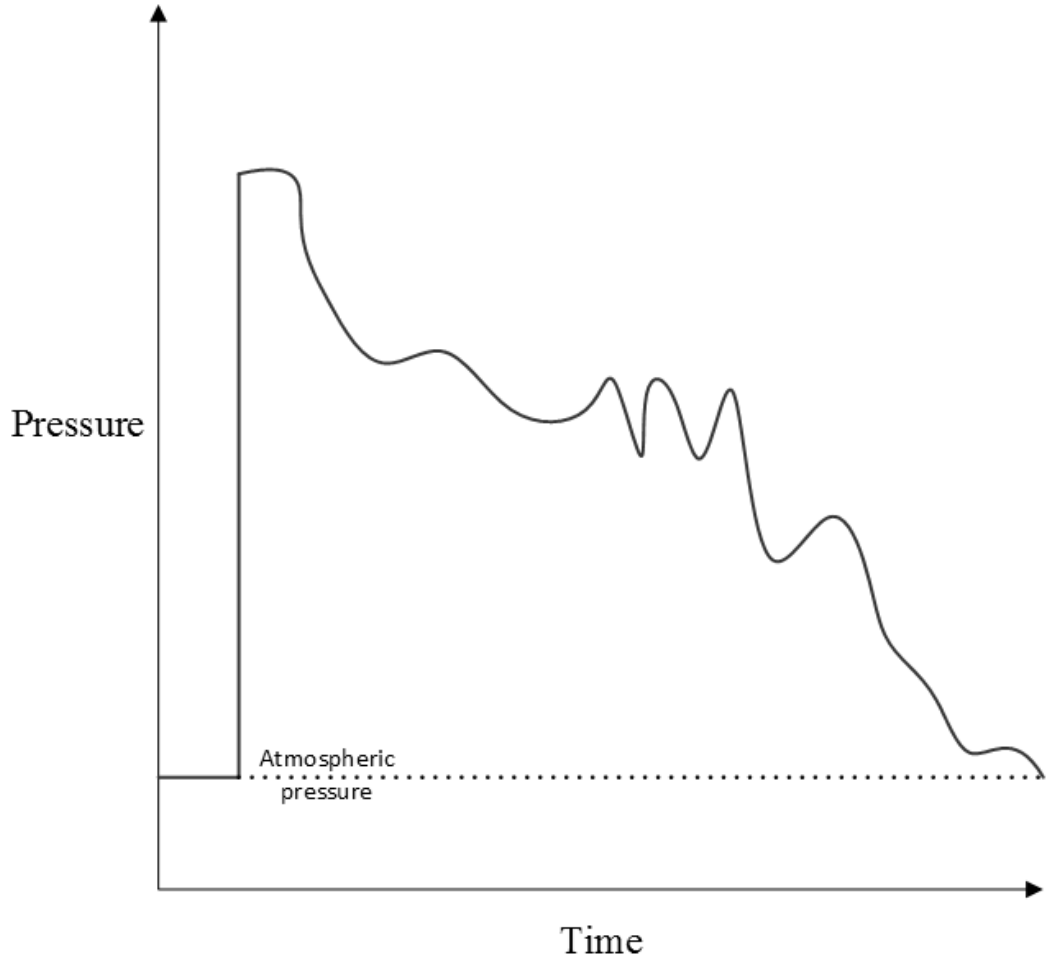

Figure 2.2: Pressure changes following explosion within theoretical enclosed space showing longer duration and increased magnitude of pressure.

The change in pressure profile is best measured by the blast impulse, which is the integral of the pressure-time curve (Proud, 2016). The impulse is increased by both increased magnitude and duration of pressure and allows easy numerical comparison of the two scenarios. An explosive detonated at ground level in an otherwise "free field" is also subject to the effect of wave reflection from the ground itself. Resultant combination of reflected and incident wave forms the "Mach stem", a region of even higher peak overpressure travelling parallel to the ground beneath the point of interaction (the triple point).

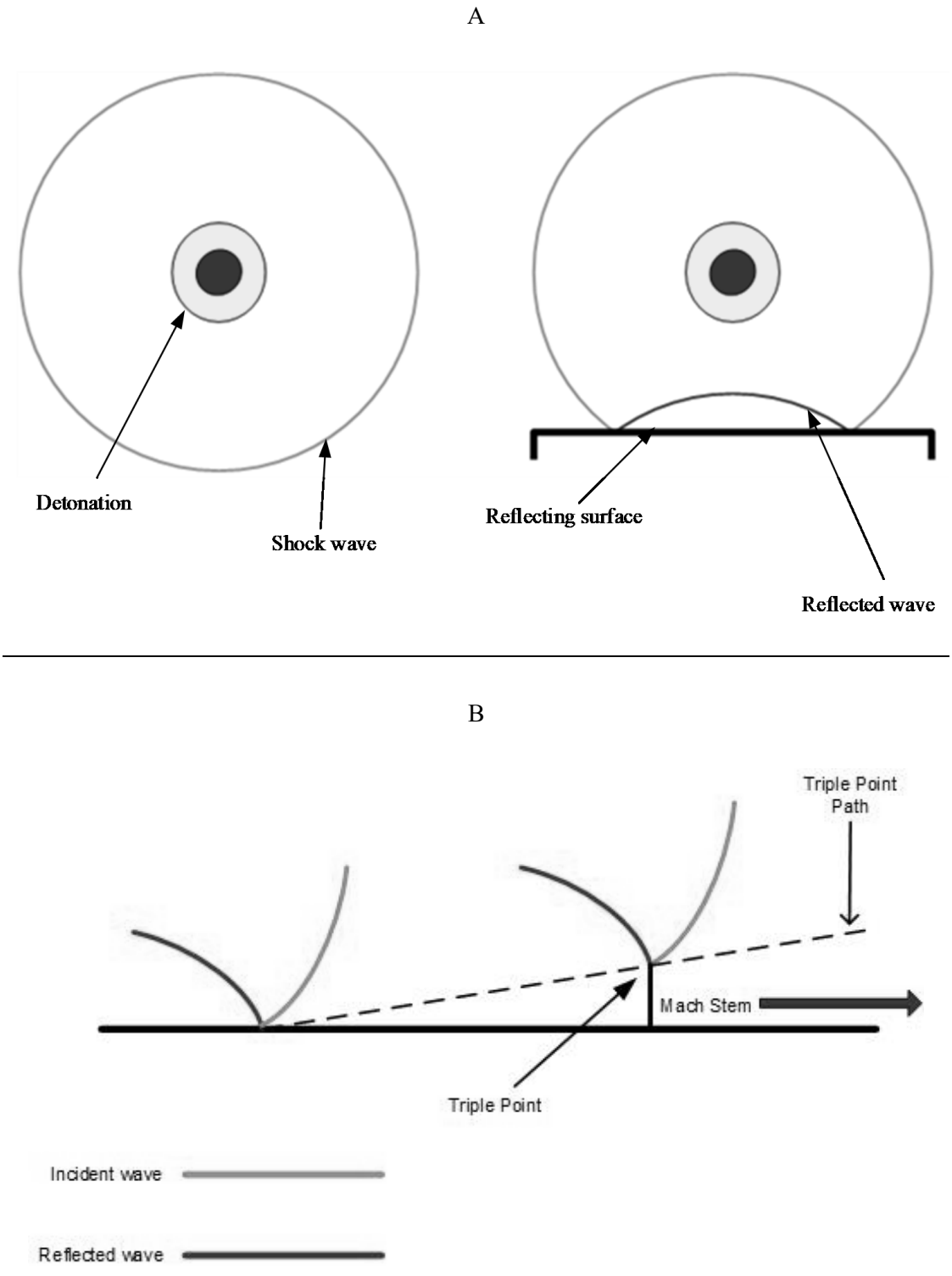

Figure 2.3 A) Explosion in open field vs explosion at ground level showing reflection of shock wave from ground. B) Formation of Mach stem due to interaction of incident and reflected wave. Adapted with permission from Edwards and Clasper (2016).

2.5 Weapon Types

The degree to which each of these explosive effects may be observed is dependent upon the weapon type and application. Modern explosive weapons vary widely in their composition, sophistication and application, but all utilise an "explosive train" system to deliver the desired effect. The train system requires the stimulus of a (relatively) small amount of a highly sensitive initiator material which produces heat or a shockwave with the intention of causing detonation of the (less sensitive but high energy) main charge (Proud, 2013b). Booster and delay charges may be intermediaries in the explosive train. The initial stimulus may be purely mechanical, or via activation of an electrical or magnetic switch.

The mostly commonly used explosive weapon and most common cause of battlefield death during recent coalition operations in Iraq and Afghanistan has been the Improvised Explosive Device (IED) (Holcomb *et al.*, 2007; Champion *et al.*, 2009a). US service deaths from IEDs in Afghanistan are shown in Figure 2.4.

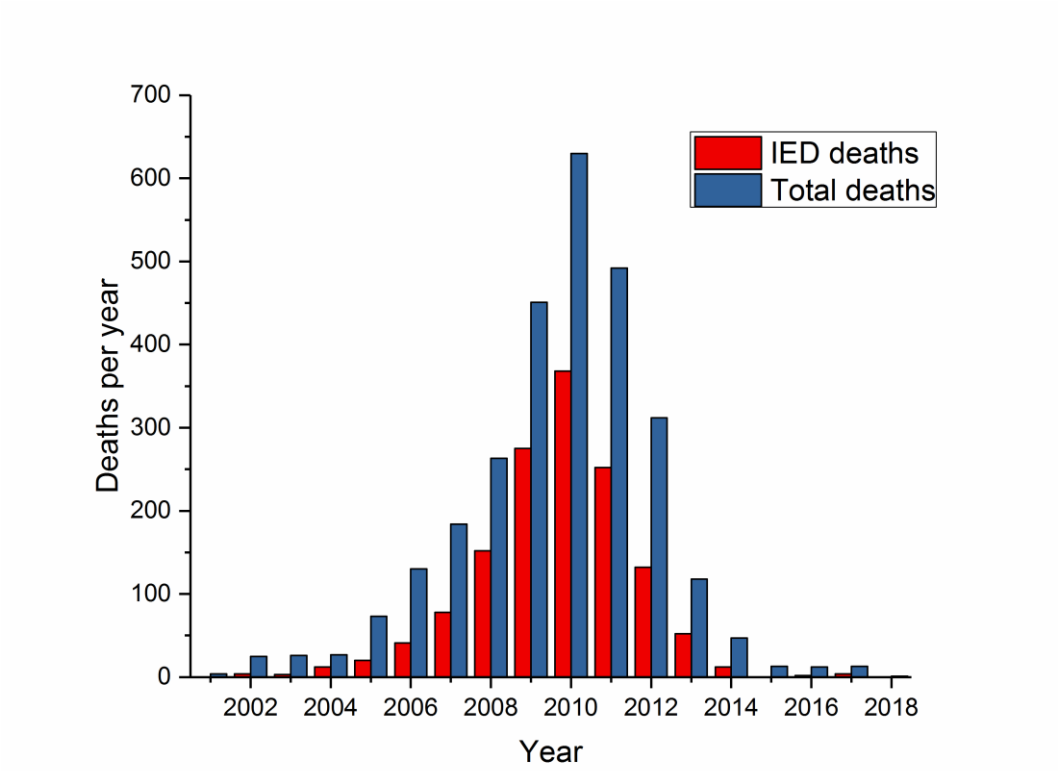

Figure 2.4: Numbers of death per year of US service personnel during military operations in Afghanistan. Total deaths and deaths from Improvised Explosive Devices are shown. Data from iCasualties.org accessed April 2018.

IED is an umbrella term which describes a wide range of weaponised explosive materials. They are often constructed from conventional materials such as artillery and mortar shells although not used for conventional military action. Although IEDs have been the signature weapon of insurgent groups in Afghanistan, they have been used historically across the globe in regions as geographically spread as Northern Ireland, Vietnam and Nigeria. The improvised nature of the weapons means that they are diverse in their construction, delivery, and trigger method. IEDs during recent Iraq and Afghanistan operations have included vehicle-borne, person-borne, and buried devices (Champion *et al.*, 2009b).

Buried or roadside IEDs were a feature of these recent coalition campaigns and responsible for a great number of injuries (Ramasamy *et al.*, 2008, 2009). These devices can be further separated on the basis of their intended application. Anti-personnel

devices tend to be smaller devices triggered by the action of the intended victim. Although similar effects are caused by anti-personnel landmines (which are pre-fabricated munitions), anti-personnel IEDs are often more severe (Smith *et al.*, 2017). This is probably because the size of the explosive charge is not constrained by a small pre-fabricated casing and the intention of conventional anti-personnel mines is to incapacitate, whereas that of IEDs is to kill

Anti-vehicular devices, (which do of course also injure personnel) tend to be larger devices which are often buried below the surface, deliberately positioned along roads and other transport thoroughfares. They may be triggered directly through pressure plates or remotely operated through the use of a command wire, mobile phone or radio transmission. They are designed specifically to destroy or incapacitate vehicles. Variations of anti-vehicular devices include the use of explosive formed projectiles in which the stress wave is used to shape and accelerate a metal disk into a "slug" able to penetrate armour. Such weapons were particularly common during UK operations during the 2003 and onwards Iraq conflict (Ramasamy *et al.*, 2008).

2.6 Classification of Blast Injury

Given the complexity and speed of an explosive event, the resultant injuries have classically been divided by the mechanism by which they occur (Horrocks, 2001). In reality, this separation is somewhat artificial as the injuries frequently occur together and defining the exact mechanism of each is difficult. This separation is important however as prevention, mitigation, or treatment of the injuries does require understanding of each injury process. Table 2.2 provides an overview of the conventional classification, where the first three are relevant to the subject matter of this thesis.

Blast Injury Type	Mechanism
Primary	Direct interaction of the blast wave with the body.
Secondary	Wounds caused by fragments and projectiles energised by the explosion.
Tertiary	Injury due to displacement of the body with subsequent impact or crush, including "solid blast" or "underbody blast".
Quaternary	Miscellaneous injuries including burns, inhalation of smoke or toxic substances, and psychological sequalae.
Quinary	Injury caused by exposure to deliberately added chemical, microbial or radiation elements of a device.

Table 2.2: Blast injury types and mechanisms.

2.6.1 Primary Blast Injury

Primary blast injuries refer to those injuries caused by the shockwave itself. To a degree, primary blast injuries the only ones unique to blast loading. Blast overpressure causes injury by interaction of the shockwave with susceptible tissues. Changes in stress propagation between materials of different densities means that injuries occur predominantly at interfaces between two tissues. The greatest density difference is at the tissue/air interface given that the density of air and any solid are approximately three orders of magnitude in difference. Although air containing organs are those most susceptible to primary blast loading, the precise physical mechanism which leads to injury remains uncertain. Early mechanical hypotheses of the primary blast mechanism by Schardin (1950) suggested that injury may be attributable to implosion, inertia, and spallation.

Spallation refers to throwing off of material (spalls) as a blast wave passes from a denser medium into a less dense medium. The effect can be observed in the water thrown up from the surface following an underwater explosion.

Implosion refers to the compression of less dense compartments. In physical tissues, this relates primarily to the air-filled cavities including the pulmonary alveoli, the ears and hollow organs of the gastrointestinal tract.

Inertial effects occur due to relative movement of tissues to one another. As previously discussed, the acceleration of biological tissues by stress waves is a function of the wave speed and tissue density in that material which is defined as the impedance of the material. As a consequence, different tissues are accelerated to different degrees by a shockwave. The interface between two tissues with different properties is subject to an acceleration differential which is most pronounced at the tissue/air interface. This opposing acceleration creates shear stress at the interface with potential injury of the tissue (Stuhmiller *et al.*, 1991a).

Primary blast lung injury (PBLI) is the most studied of the primary blast effects with incidence estimated at up to 11% of military blast casualties (McDonald Johnston and Ballard, 2015). The incidence may be considerably higher in those casualties who do not survive to receive medical treatment (Singleton, *et al.*, 2013). Interaction of the blast wave with the chest wall by the blast wave leads to disruption of the pulmonary tissues (through the three mechanisms outlined above). The mechanism of injury may be different in particular tissue types with the thin walled alveoli susceptible to implosion and spalling; and the tethered pleura and blood vessels injured by inertial effects (Sharpnack *et al.*, 1991). Whatever the causative mechanism, the most consistent finding of PBLI is pulmonary haemorrhage with bleeding occurring within the pleural space, lung parenchyma and in the areas surrounding the branching vascular and airway structures (Sharpnack *et al.*, 1991). Additional pulmonary injuries associated with primary blast loading including pleural rupture (with pneumothorax or haemothorax) and development of alveolovenous fistulae. Biomechanical considerations for PBLI will be considered in more detail in Chapter 6, it is important to appreciate that both likelihood and severity of PBLI increase with increasing blast overpressure and duration and are therefore related to the impulse (Stuhmiller *et al.*, 1991b). As discussed,

complex blast waves within an enclosed or partially enclosed area have a greater blast impulse and thus a greater propensity for causing primary blast injury.

The gastrointestinal (GI) tract also contains pockets of air which makes it susceptible to blast injury. Rapid compression and expansion of the GI lumen creates stress within the wall of the structure. This is manifested by haemorrhage within the intestinal or gastric wall with potential for perforation and subsequent peritonitis (Owers *et al.*, 2011). Those areas with the proportionally largest volume and potential for mural stress concentration, such as the ileocaecal junction are the most common sites of injury (Sharpnack *et al.*, 1991). Incidence of primary blast injury to the GI tract is uncertain but undoubtedly thought to be more common following exposure to underwater blast (Benzinger, 1950). Primary blast injury to the solid abdominal organs including the liver and spleen is likely due to rapid displacement of the organs and may manifest in either tearing of the surrounding capsules or rupture of the organs themselves with subsequent haemoperitoneum (Sharpnack *et al.*, 1991).

The auditory system is sensitive to primary blast injury at multiple sites. Perforation of the tympanic membrane (TM) is common although has now been shown to be a poor marker of primary blast injury with the absence of TM perforation not excluding other serious primary blast injuries (Harrison *et al.*, 2009). The ossicular chain of the middle ear may be damaged by direct displacement, which is often associated with TM rupture (Roberto *et al.*, 1989). The organ of Corti is the specialised epithelia layer of the cochlea which is sensitive to sound induced vibration. The abnormally intense vibrations from a blast wave may injure the sensitive membrane of the organ (Roberto *et al.*, 1989).

The mechanism by which primary blast causes traumatic brain injury (TBI) is still uncertain (Courtney and Courtney, 2015) but epidemiological studies consistently show the association of mild TBI with primary blast exposure (Bhattacharjee, 2008; Galarneau *et al.*, 2008; Rosenfeld and Ford, 2010). Brain injury may be caused by linear or rotational acceleration of the head, direct transmission of the overpressure to the brain through the skull or indirect pressure effects due to high rate thoracic displacement (Courtney and Courtney, 2009, 2015; Nakagawa *et al.*, 2011).

2.6.2 Secondary Blast Injury

Secondary blast injury describes penetrating injury due to energised fragments. These fragments may be part of the original device (primary fragments) or environmental objects (secondary objects) such as stones, soil, or glass which are energised by the shockwave or by the blast wind. Primary fragments may be either "natural" in that they are part of the device casing or either preformed (such as ball-bearings) or improvised (bolts, screws, stones). Biological material, including bone fragments, may well be energised and injurious following person-born IED (suicide bombing) (Breeze and Carr, 2016).

Secondary blast injury is not specific to any organ or system, given that the fragments can impact upon any area of the body. For most explosive weapons, death occurs from a combination of injury types and separating primary and secondary injury patterns is difficult. However, the wounding potential of a fragment is governed by its energy, which unlike the cubic decay of a primary blast wave, is inversely proportional to the square of the distance from the source. As a consequence, fragments are more likely than primary effects to contribute to the injury burden as the distance from the explosion increases (Figure 2.5). Those individuals who are injured, but not killed by explosions, are likely to have a lesser injury burden and discrimination of particular blast effects may be possible.

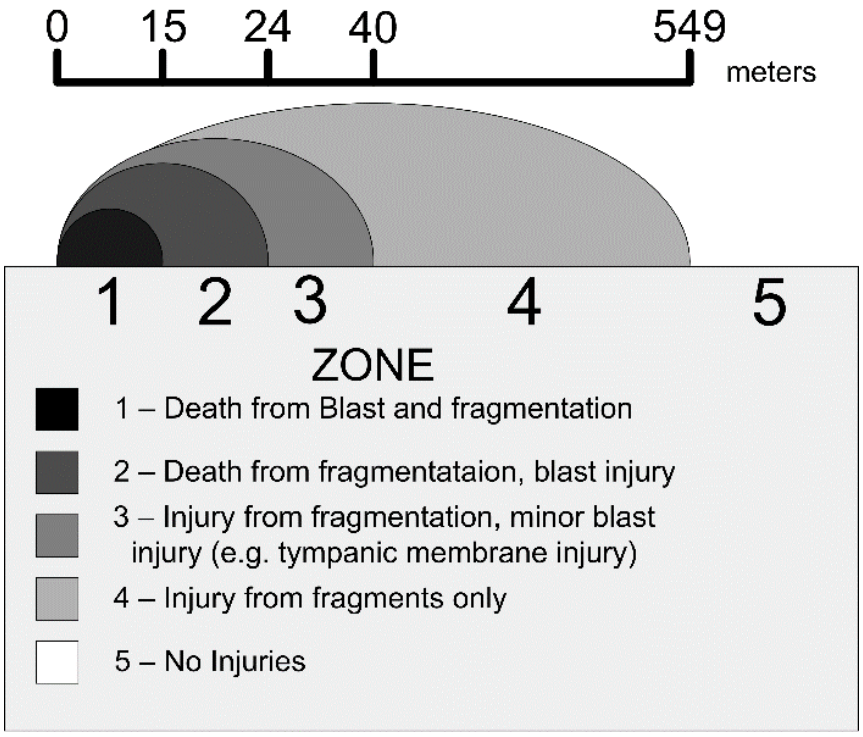

Figure 2.5: Injury zones from blast and fragmentation. Reproduced with permission from Champion *et al* (2009).

Given the propensity of primary blast injuries to be delayed in their presentation (Owers *et al.*, 2011; Aboudara *et al.*, 2014), penetrating fragments wounds are more likely to cause external injury and haemorrhage with requirement for immediate management.

2.6.3 Tertiary Blast Injury

Tertiary effects are due to the displacement of the body into solid objects (or vice versa) with subsequent blunt impact sufficient to cause injury. This displacement may be due to the blast wind effect although structural collapse with subsequent crush injuries have also been included within the group (Edwards and Clasper, 2016), and following bombings of large scale infrastructure, may be attributable for the majority of casualties. The broad range of injuries described by this definition is perhaps best broken down by more detailed mechanical descriptions of injuries. “Solid” blast is one such mechanism which describes the transmission of blast energy through a solid material. Although solid blast does describe the displacement of this solid material against a body, it may be separated from conventional blunt trauma by the high rate of displacement. The

direction of this transmission depends upon the location of an explosive device but was first recognised during the Second World War with the observation of lower limb injuries as a consequence of transmission of blast energy through a ship's hull ("…*the deck rose suddenly beneath the feet of those injured, and the force transmitted upwards through the skeleton produced a series of injuries including fractures of the os calcis, tibia and knee. Compression fractures of the lumbar and thoracic vertebral bodies sometimes occurred…*") (Keating, 1944). The contemporary analogue of this mechanism can be found in Under-Body Blast (UBB) which relates to the high rate vertical loading caused by detonation of an explosive device underneath a vehicle and which is the main focus of this thesis.

2.6.4 Under-Body Blast

Under-body blast may be caused by a variety of weapon types. Although buried and road-side IEDs were the most common device in Afghanistan, purpose built anti-vehicular mines have predominated in previous conflicts (Radonić *et al.*, 2004; Ramasamy *et al.*, 2009). The specific design of each device is beyond the scope of this thesis but the loading environment created by each of them is similar.

The effect of any buried explosive device depends primarily upon the size of the explosive charge and the way in which is buried.

Burying the device has a pronounced effect due to interaction of the explosive products with the surrounding soil. As for a free field explosion, detonation of the device and conversion of the explosive to extremely hot, highly pressurised gases results in transfer of heat to the soil adjacent to this gas bubble (Tremblay *et al.*, 1998). The shockwave itself propagates through the soil with resultant compression of the material. Upon reaching the soil-air interface, this shockwave is largely reflected back towards the explosion centre. A small proportion of the primary shockwave itself is propagated into the air above the soil cap while the reflected (tension) wave causes fracture of the soil cap (Grujicic *et al.*, 2008).

A

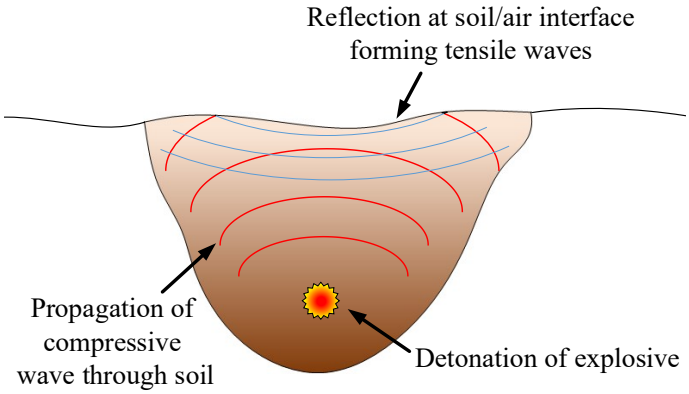

B

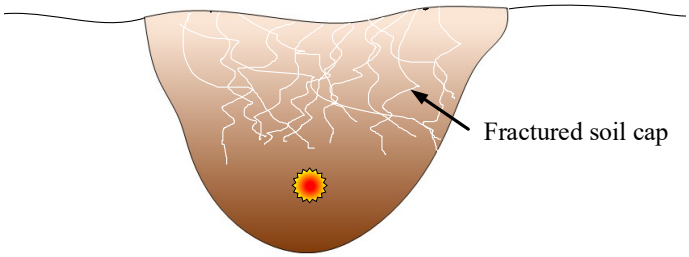

C

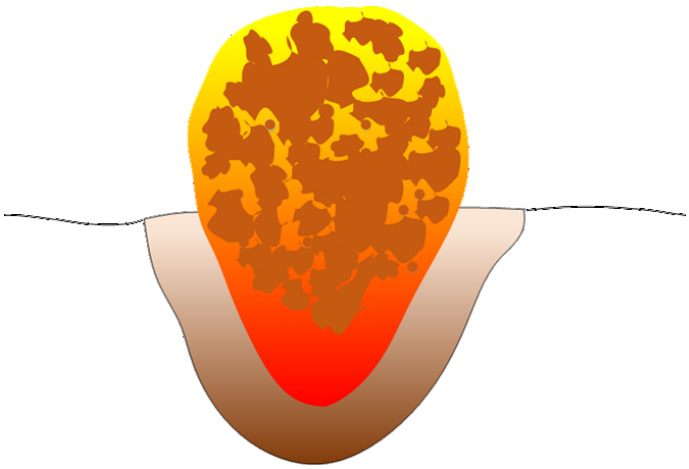

Figure 2.6 A) Propagation of compressive wave through soil following detonation of a device. Most of the resultant shockwave is reflected at the soil/air interface. B) Fracture of the soil results from the combined action of the compressive and tension waves. C) High velocity ejection of the soil cap.

Further collapse of the soil cap and expansion of the detonation products results in high velocity ejection of the soil plug. The direction and velocity of the ejecta is heavily dependent on the soil properties. Increased soil density and higher moisture content results in a more incompressible soil which directs more of the detonation products in a more vertical direction (Grujicic *et al.*, 2008)

The expansion of the detonation products and the physical momentum transfer from soil ejecta are the two primary load transfer mechanisms from a buried explosive device and occur at slightly different phases. The gas expansion occurs during the first 5-10 ms after detonation with the soil ejecta phase taking place shortly thereafter and lasting between 50 and 100 ms.

Any portion of the vehicle located in the expansion zone of the detonation products is exposed to a high pressure, transient, supersonic flow field. The transfer of momentum from the detonation products to the vehicle is governed by its gas dynamics characteristics which are influenced by the shape of the target (Ramasamy *et al.*, 2009). Objects which are perpendicular to the surface of the expansion (such as a flat vehicle hull) cause a rapid slow down and pressure concentration of the expanding gas with high energy transfer to the object in question. This loading causes rapid deformation of the floor of the vehicle and has been associated with distinctive injuries of the lower limb. The precise injury pattern is likely to depend upon the relative position of the floor deformation to the seat and occupant and will be examined further in Chapter 4 Deformation of the hull beyond its ultimate tensile strength may rupture with potential for expansion of gases and fragments into the vehicle.

The soil ejecta contains significantly more mass than the expanding gases and causes loading via transfer of momentum from the ejecta to the vehicle with resultant acceleration. The magnitude of the vertical displacement is dependent upon the relative masses of the soil and vehicle and the velocity of the soil. Asymmetric loading is likely to cause rotation of the vehicle round its centre of mass and is determined by the moment of inertia of the vehicle and moment caused by the ejecta.

What goes up must come down, and vertical displacement of the vehicle is followed by acceleration of the vehicle under gravity towards the ground whereby the hull and

occupants may sustain a “second hit”. The magnitude of this second impact is likely to be considerably less than the original acceleration but may worsen structural failure or injury.

The UBB phenomenon describes relates to the acceleration and deformation of the vehicle hull by the blast. It must also be clarified that the primary blast wave itself is not transmitted through the hull in the same way. Although it is conceivable that the interior of the vehicle is exposed to the blast wave (either due to open windows or in those vehicles with an open top), direct transmission of the blast wave is unlike as the vehicle hull is unlikely to deform quickly enough.

2.7 Conclusion

Blast injury refers to a spectrum of trauma sustained as a consequence of explosions. Prevention, mitigation, and treatment of these injuries requires a detailed understanding of the mechanism. This chapter has described the classes of mechanism and resultant injury. This thesis will focus entirely upon the vertical loading caused by underbody blast with a rig and experiments which aims to replicate this loading (in isolation from other primary and secondary blast effects).

Underbody blast is an important aspect of this spectrum and injuries from this relatively complex loading environment are the subject of this thesis. Previous work has concentrated on musculoskeletal injury following UBB with focus on lower limb injury (Henderson *et al.*, 2013; Bailey *et al.*, 2015; Danelson *et al.*, 2015). The clinical sequelae of these bony injuries are potentially severe with a proportion requiring amputation and many associated with long term medical and occupational consequences (Ramasamy *et al.*, 2008, 2011, 2013).

The well described lower limb injuries are unlikely, however, to result in death. This thesis aims to better characterise those soft tissue injuries associated with UBB which influence survivability. Quantification of injury burden and precise definition of survival and non-survivable injury is complex. The next chapter will address trauma

scoring systems and contemporary descriptions of survivability and demonstrate the challenges of linking death with this particular loading environment.

CHAPTER 3

DEFINING SURVIVABILITY IN THE BLAST ENVIRONMENT [1]

3.1 Scope of the chapter

Chapter 1 described increasing use of explosive weapons on the modern battlefield and discussed the effects of blast. This chapter will further describe the resultant changes in injury severity and will discuss contemporary methodologies for the description of combat casualty statistics. The chapter will focus on mortality from blast and will highlight the limited utility of currently used trauma scoring systems to define survivability within the complex blast environment. The work will stratify the combat casualty cohort by medical need and research focus and will demonstrate that a mitigative approach has great potential to improve blast survivability.

[1] This work was published in part as "Pearce, A. P., and Clasper, J. (2018). Improving survivability from blast injury: 'shifting the goalposts' and the need for interdisciplinary research. Journal of the Royal Army Medical Corps

3.2 The changing severity of war injury

As discussed in Chapter 1, blast injury is now the most common mechanism of wounding in modern warfare. There is no doubt that gunshot wounds (GSW) and other forms of penetrating trauma can be deadly. High velocity military rifles are capable of causing great tissue injury but explosive weapons carry with them a greater propensity for multi-system, multi-region, multi-casualty trauma than the more localised action of a bullet. The severe nature of blast injury is reflected in both the clinical manifestation of these injuries (such as dismounted complex blast injury) and greater burden of injury within the military injured casualty compared to a civilian cohort (Cannon *et al.*, 2016; Edwards *et al.*, 2016; Staruch *et al.*, 2016). The quantification of this injury burden is important and this chapter will explore the degree to which current systems may adequately describe injury and potential survivability due to battlefield and blast injury.

3.3 Contemporary descriptions of combat casualty survival

War is often reported to advance medical practice, particularly for the care of the injured but the retention of the skills and knowledge gained during conflict may be difficult during periods of relative military quiescence (Mabry and DeLorenzo, 2014; Berwick *et al.*, 2016). Maintenance of high standards of trauma care requires that a deployed military health system undergoes constant evaluation (Russell et al., 2010). A learning health system relies upon registry of injury and injury management data and upon a commitment to data-driven, performance improvement. It should be acknowledged that the clinical aspects of this thesis are only possibly because of the military's trauma system, its registry and performance improvement processes. The "denominator" of any trauma system is the volume and severity of injury for which it must care. This burden of injury is measured with the use of combat casualty statistics to determine effectiveness of the system, and to facilitate benchmarking against other military and civilian trauma systems (Smith *et al.*, 2007). Detailed analysis of injury patterns, severity, and outcomes enables ongoing assurance of standards despite changing threats and environments.

3.3.1 Injury Scoring

Scoring systems can be used to quantify injury burden and may be used to triage patients, prognosticate outcome, provide research focus, and to compare trauma systems. The broad range of uses requires a similarly broad range of scoring tools and a thorough understanding of the appropriate use of each. These systems can be divided based upon the parameters which they measure.

Physiological scores are based upon clinical findings. These scores include the Revised Trauma Score (RTS) (Champion *et al.*, 1989) which is based upon neurological function (as described by the Glasgow Coma Score - GCS), respiratory rate, and systolic blood pressure. These scores are used for both outcome prediction and triage.

Anatomical systems are based upon anatomical injuries without physiological measures. The most commonly used scoring tool is the Abbreviated Injury Scale (AIS). The tool was initially established in 1969 (Keller *et al.*, 1971) and has subsequently been maintained and updated by the Association for the Advancement of Automotive Medicine (Copes *et al.*, 1988). AIS is an anatomically based, consensus derived, global severity scoring system that classifies an individual injury by body region according to its relative severity on a 6 point scale (1=minor and 6=maximal). Given the consensus based nature of the AIS system, this number is based upon an agreed degree of severity rather than derived from outcome data.

Individual injury scores may be combined using different systems in order to give an overall burden of trauma. The most commonly used score is the Injury Severity Score (ISS), first described by Baker and O'Neill (1974). The ISS is made up from the three most severe injuries from three separate anatomical regions. The severity score (calculated using the AIS scale) of each of these injuries is squared and these are summed [3.1].

$$ISS = Max\ AIS_a{}^2 + Max\ AIS_b{}^2 + Max\ AIS_c{}^2 \qquad [3.1]$$

A major criticism of ISS has been in the use only of injuries from different regions (Copes *et al.*, 1990). Additional severe injuries from the same regions do not form part of the score even if the severity of these additional scores is higher than the most severe score from another region. This criticism led to the development of the New Injury Severity Score (NISS) (Copes *et al.*, 1990). In contrast to ISS, the three most severe injuries are used to make up the total score, irrespective of the region in which they occur. A further criticism of the ISS is on the weighting on injuries in that the same effect on survivability is to be expected from injuries of the same AIS severity from different regions and this patently cannot be true. The Anatomic Profile (AP) tool was developed by Champion with the aim of overcoming some of these limitations (Shuker, 2013). The AP tool divides up injuries into 4 body components (Head/Spinal cord, Thorax, Abdomen and Pelvis, and all other injuries). In contrast to ISS and NISS, the AP uses all injuries within each region to define the component score which is the square root of the sum of squares of all the AIS codes within that component. Each component score is therefore most affected by the highest AIS score within that region and decreasingly affected by subsequent lower scores. The score effectively measures the "Euclidian distance" that each injury component moves the casualty away from non-injury. A modification has been made to the AP which uses the maximum overall AIS injury as the 4^{th} component in place of "any other injuries". This modification was made on the basis that the single worst injury may be a more accurate predictor of death (Kilgo *et al.*, 2003).

Comparison of the different AIS utilising scoring systems has shown that modified AP (mAP) is the best predictor of survivability (with a higher Area under the Receiver Operating Curve (AUROC) compared to ISS and NISS). Despite this, mAP has been criticised for its relative complexity and difficulty in application given that it is made up of four different component scores and is rarely used as a control score for either research or governance.

The relatively recent International Classification of Diseases (ICD)-based Injury Severity Score is based upon ICD diagnostic codes (Osler *et al.*, 1996). These codes are routinely used for resourcing and billing purposes. Within a sufficiently large dataset, survival rates of each ICD code can be compiled to create an outcome prediction score which utilises the population-based survival rates for all injuries as coded. This score

has been shown to predict survival risk ratio as well as ISS within selected populations but has not been widely validated (Rutledge *et al.*, 1997; Tohira *et al.*, 2012).

Both ISS and NISS are calculated retrospectively based upon an extensive "AIS dictionary". Neither score is therefore of any utility within the acute setting. Other features limit the ability of the systems for describing survivability. Two injuries with the same score within the same region may have different outcomes. Given that the severity scores of each code are not based upon a quantifiable metric, they are non-linear in distribution. The difference in severity between a 1 and a 2 is not necessarily analogous to the difference between a 2 and a 3. This non-linearity is compounded when scores are squared for ISS or NISS.

The use of the scores as a predictor of survivability is further hampered by statistical features of the systems. Both ISS and NISS are formed by the combinations of between 1 and 3 squares, dependent upon the number of injuries. This method provides a range of scores between 1 and 75 for all injuries of 5 or less severity. Some scores are then formed more frequently as they can be formed from a greater number of score combinations. In contrast, some scores are impossible to score. The resultant distribution contains characteristic peaks and troughs and is not transformable to a Gaussian distribution by any conventional method (Stevenson *et al.*, 2001). Despite this, ISS and NISS are frequently used as a continuous variable despite neither being a continuous distribution nor is there a quantifiable relationship between score and tissue injury. Further evidence of a lack of established relationship between score and injury is in the discrepancy in outcomes for casualties with the same score formed from different injury combinations (Russell *et al.*, 2004; Aharonson-Daniel *et al.*, 2006).

The use of these scores is particularly problematic for analysis of survivability. Peaks of death or morbidity are associated with particular values due to the higher likelihood of these scores occurring. AIS 6 scores are given to those injuries that are deemed unsurvivable (by consensus). As a result, any casualty who sustains a grade 6 injury is automatically scored 75 by ISS/NISS. An ISS/NISS or 75 (achieved from either 3xAIS-5 or 1 or more AIS-6) is the maximum achievable score.

The Trauma and Injury Severity Score (TRISS) is a combined score which includes the ISS in addition to physiological data (the Revised Trauma Score - RTS) and age. The scores uses a logistic model [equation 3.2] to predict probability of survival (between 0 and 1) (Boyd *et al.*, 1987) .

$$P_S = \frac{1}{1 + e^{-b}} \qquad [3.2]$$

where $b = b_0 + b_1(RTS) + b_2(ISS) + b_3(Age)$

$b_{0..3}$ are coefficients based upon the population. Numerous revisions and modifications of the TRISS methodology have improved and refined performance. More recent models take account of mechanism, vary the physiological component (including only the GCS in place of the RTS) and include population specific coefficients (Bouamra *et al.*, 2006; Schluter *et al.*, 2010). It is important to emphasise that the anatomical component of these scores (the measure of trauma) is limited by use of ISS which fundamentally is the limitation of incorporating non-linear consensus derived data.

Dependent on the application of scores, great debate persists over the best trauma score to use (Chawda *et al.*, 2004; Harwood *et al.*, 2006; Tohira *et al.*, 2012; Miller *et al.*, 2017) and a pragmatic approach should be used for interpreting any such scores. Triage systems aside, other scores are based upon population level data and should be used with caution when examining injury data at either an individual or small cohort level. Scores with physiological components are clearly impractical when analysing deaths prior to medical treatments and will not be considered further.

Although there is sound rationale for using population level scores as a comparator of trauma system performance, their suitability for assessing survivability of severe injuries for the purposes of mitigation is less compelling. Paradoxically, the unsuitability of extant systems to define the “spectrum of unsurvivability” has been emphasised by improved survival in response to injury.

Advances in trauma healthcare have led to an increasing number of casualties surviving despite an ISS 75 injury burden. A recent examination of over 2800 >ISS75 US trauma admissions found that 48.6% were discharged alive (Peng *et al.*, 2015). In a military setting, Penn-Barwell *et al* (2015) have described sequential improvement in survival for a given battlefield injury burden. Although a testament to exceptional care and dedication to quality improvement, this data shows the degree to which a conventional scoring system inadequately predicts death in the face of good clinical care. More than 40 "unexpected survivors" (NISS>75) were treated during UK combat operations in Afghanistan (Penn-Barwell *et al.*, 2015). Probability of survival compared to injury burden is shown Figure 3.1.

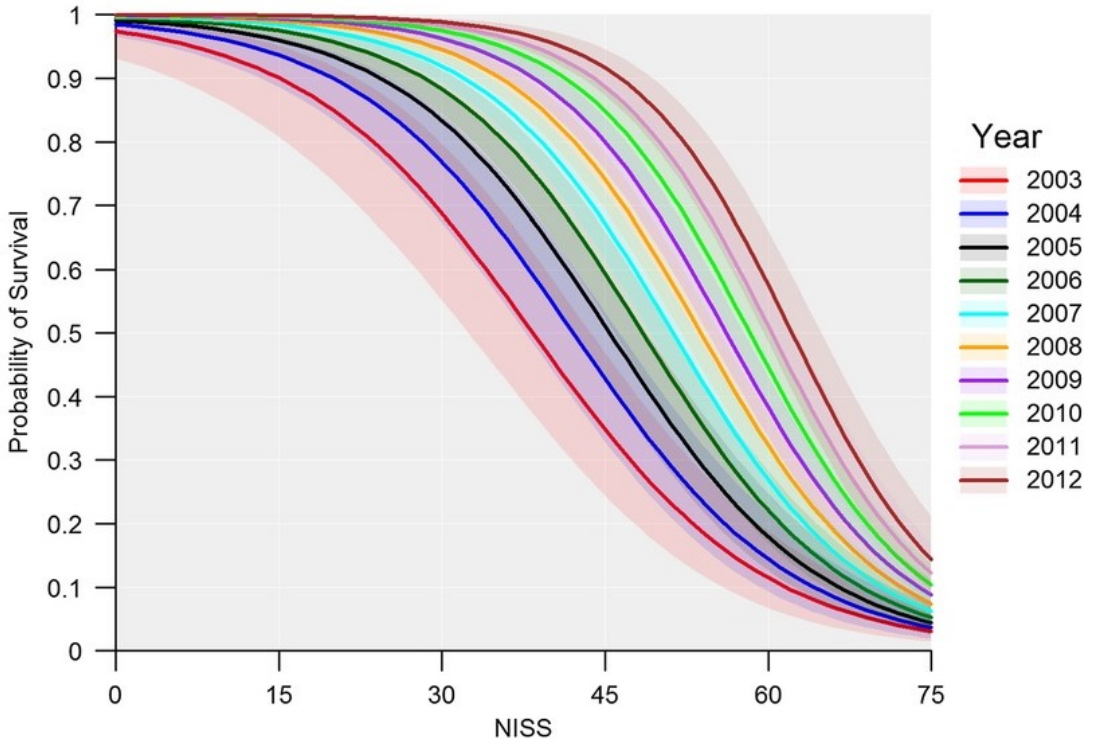

Figure 3.1: Plot of predicted probability of survival for a given NISS value for each year. Shaded regions indicate the 95% CIs for the predicted values. Reproduced with permission from Penn-Barwell *et al* (2015).

Although this data shows a laudable increase in the average probability for survival for a given injury burden as a result of clinical and systems improvement, it highlights the fallibility of injury scoring for assessing true survivability. If survivability scores are influenced by clinical ability, then no score will be truly accurate until the absolute limit

of medical advancement has been reached. The value of scoring systems may be in stratifying the needs of different casualty cohorts and identifying the future medical advances required. Therefore, there is an urgent need to develop a scoring system that does not score up to a current threshold of unsurvivability, but scores beyond that threshold and does so as a continuous variable.

3.4 Survivability

The premise of the unexpected survivor is a mathematical phenomenon but is suggestive of two important points:

1. If healthcare advances have now made the unsurvivable survivable, then the scoring system should be adjusted in order to maintain standards and improve further.
2. The scoring systems used are not adequate for defining an unsurvivable burden of injury.

The first point has already been alluded to. Ongoing evaluation of injury burden and resultant outcomes is essential for a trauma system but this should be accompanied by ongoing quality improvement and subsequent readjustments. Maintaining and improving upon such high clinical outcomes is of a concern to both the US and UK and must be achieved through innovation in both research and training in addition to synergy with domestic healthcare systems (Rasmussen *et al.*, 2013; Mabry and DeLorenzo, 2014; Rasmussen and Kellermann, 2016; Khan *et al.*, 2017).

The UK Defence Medical Services (DMS) have recognised the second point. The approach taken by the DMS to survivability is therefore to couple existing scoring systems to a peer review mortality panel (Russell *et al.*, 2014). This panel is made up on senior clinicians (including surgeons, anaesthetists, emergency physicians, and pathologists) and scientists and tasked with in depth review of all UK service deaths.

The approach of this panel was to first provide a consensus opinion of the salvageability of all UK deaths using the criteria given in Table 3.1Table 3.1: Categories of salvageability as used in the UK DMS peer review panel. Adapted with permission from Russell *et al* (2014). For each case, the question asked was: 'If these injuries had occurred five minutes from a Major Trauma Centre what is the likelihood that surgical intervention would be attempted for given injuries and what is the predicted likelihood of survival?'

Category	Definition
S1:	Salvageable: intervention would likely have influenced survival (probability of survival >95%).
S2:	Potentially salvageable: intervention would have been attempted and may have influenced survival (probability of survival 5%–95%).
S3:	Possibly salvageable: intervention would have been attempted but with a high probability of mortality (probability of death >95%).
S4:	Non-salvageable: intervention would not have led to survival.

Table 3.1: Categories of salvageability as used in the UK DMS peer review panel. Adapted with permission from Russell *et al* (2014).

No further analysis was conducted on S4 casualties although these were deemed to make up 91.1% of the fatalities. Tactical, clinical, and equipment factors were examined for S1-S3 fatalities. The UK DMS recognise that the true value of the peer review process may be in the further examining of mathematically unexpected outcomes which are the "flags" raised by conventional numerical scoring systems (Russell *et al.*, 2011). The

review panel noted that blast injury was the predominant mechanism of injury but did not specify mounted or dismounted loading environment. Focus upon the unexpected outcomes may be the most efficient method of identifying those cases from which lessons can be learnt.

A similar process has been undertaken in the US by Eastridge *et al*. (2012). Despite a similarly made up panel, this study estimated that only 75.7% of deaths were non survivable (NS). This difference may be explained by slightly different classification criteria but may be due to slightly different clinical opinion, suggesting that even consensus clinical opinion is inconsistent in predicting survivability; this is further evidence for the need for objective scoring methods. The US panel, when examining casualties with multiple wounds, evaluated each injury independently with respect to the potential for survivability. "The consensus was to err toward the maximal inclusion of these casualties as potentially survivable (PS) to be introspective and critical to further develop the paradigm of combat casualty care performance improvement and identify potential gaps requiring further research and development" (Eastridge *et al.*, 2012). Specific wounds deemed to be non-survivable prior to case review were physical dismemberment, catastrophic brain cervical cord transection, thoracic airway transection, cardiac injury, thoracic aorta injury, pulmonary artery, hepatic avulsion, and catastrophic abdominopelvic wounds. All other injuries were deemed to be medically PS without consideration of logistic, tactical, or equipment factors. The overall combination of injuries was not considered.

Eastridge examined the injury patterns of both the PS and NS groups and determined that pre-hospital NS death was most frequently caused by traumatic brain injury, heart and thoracic vessel, high spinal cord injury and destructive abdominopelvic injury. In contrast, the primary injury focus of PS acute mortality was associated with haemorrhage (90.9%) and airway compromise (8.0%). The most common site of PS haemorrhage was truncal (67.3%), followed by junctional (19.2%) and extremity (13.5%) haemorrhage.

Both UK and US systems of reviews conclusively find that the majority of combat deaths are unsurvivable. The focus of their clinical enquiry is those deaths which were survivable except for clinical, logistic, or system difficulties. This is certainly the correct

focus of the panel given that the panel is medical and it is in this group that clinical (medical) change would impact survivability. Given the large proportion of unsurvivable deaths, however, survivability could be more greatly influenced with improvements to injury mitigation or prevention. Such concepts are frequently beyond the mandate of the clinician and within that of the engineer, planner, or casualty themselves. Scoring systems typically do not incorporate these concepts, yet their inclusion (even if only to change the threshold for survivability, if not the score), would be a valued contribution.

Mitigation of unsurvivable injury such that a casualty sustains survivable trauma is possible only with a clear understanding of the relationship of injury burden to survival. This approach requires knowing how much "less injury" could significantly alter the possibility of survival. As already discussed, conventional scoring tools do not meaningfully describe this “mitigation gap”.

3.4.1 The next level of unexpected survivors

Singleton *et al* aimed to better understand the relationship between injury and death secondary to blast injury by examining likely cause of death amongst UK deployed blast casualties (Singleton *et al.*, 2013). The academic group, which included engineers and clinicians, conducted a retrospective analysis of all UK military personnel killed by IED blasts in Afghanistan from November 2007 to August 2010. Only those casualties with available post-mortem CT (computed tomography) imaging and relevant incident data were included. A cause of death analysis was performed by the group which acknowledged that determination of a single injury as the cause of death is not often possible in the face of severe polytrauma. The group instead used the AIS system and listed all AIS4+ injuries as potentially lethal. These lethal injuries were grouped into categories based upon mechanism of death. Haemorrhage was divided into extremity haemorrhage (from upper and lower limb), junctional haemorrhage (from neck, groin, or axilla) and intra-cavity haemorrhage (intra-thoracic or intra-abdominal).

The group compared the injury patterns between mounted (in-vehicle) and dismounted (on foot) blast casualties. Injury burden between the two groups was different with

mounted fatalities sustaining both significantly higher NISS and with injuries to significantly more AIS regions than the dismounted fatalities (Singleton *et al.*, 2013).

Junctional and extremity haemorrhage predominated as likely cause of death in the dismounted casualties. These injuries are described as part of the dismounted complex blast injury pattern that has been well described in the literature (Andersen *et al.*, 2012; Ficke *et al.*, 2012; Mamczak and Elster, 2012; Cannon *et al.*, 2016). Deaths in this group are more likely to fall within the PS injury class given that bleeding could potentially be controlled with tourniquets and direct pressure. Control strategies for junctional haemorrhage are somewhat more contentious. Although a number of junctional tourniquets and haemostatic devices exist, the degree to which a junctional injury is anatomically amenable to control by any particular device is uncertain (Walker *et al.*, 2014).

Death in the mounted blast cohort was most commonly attributed to head injury and "intra-cavity haemorrhage". Although supportive measures may reduce the effect of secondary injury (Carney *et al.*, 2016), outcome from severe head injury in this setting are unlikely to be influenced by any point of care intervention. Intra-cavity haemorrhage, or Non-Compressible Torso Haemorrhage (NCTH) has been extensively examined as a cause of battlefield death (Morrison *et al.*, 2013; Stannard *et al.*, 2013). Although NCTH is not a new concept, recent work has sought to define the injury complex and has included parenchymal lung injury, named torso vessel injury, solid organ injury, and complex pelvic fracture (Morrison and Rasmussen, 2012).

3.4.2 Death due to torso injury

By definition, NCTH is not amenable to external haemorrhage control. Bleeding control in this setting, regardless of the injury mechanism or pattern, is primarily dependent upon surgical haemostasis and cannot be achieved by point of care or pre-hospital intervention alone. As a consequence, NCTH has been identified as the most common causes of potentially survivable battlefield death (Eastridge *et al.*, 2012). The requirement for urgent surgery means that improvement to the casualty evacuation chain will improve outcome but such a change is difficult when it is highly dependent upon geography. Although the future operating environment is uncertain, it is considered

likely that transfer timelines will be longer in future operations with a requirement of prolonged field care (Smith and Withnall, 2017). Treatment of NCTH within such a setting may require novel technologies and changes to clinical practice.

One emerging technique for the treatment of NCTH is Resuscitative Endovascular Balloon Occlusion of the Aorta (REBOA). The principles REBOA uses are percutaneous insertion of an arterial catheter, followed by inflation of a balloon within the aorta above the zone of injury with the aim of reducing blood loss from the injury itself and increasing perfusion to the brain and heart (Stannard *et al.*, 2011). The precise role of REBOA, however, has yet to be established. Reduction of blood flow to target organs below the level of the balloon inevitably leads to time dependent ischaemia of these organs (Andres *et al.*, 2016). The role of REBOA as a bridge to definitive surgical or radiological control is likely to be most effective with very short timelines such as in the receiving area of the medical treatment facility and has been effectively used within the US civilian trauma setting (DuBose *et al.*, 2016). Ongoing work seeks to determine the tolerance of the body to prolonged periods of REBOA-induced ischaemia and to adapt REBOA techniques to prolong inflation time (Russo *et al.*, 2016). Morrison *et al* determined that use of REBOA may have changed outcomes in a proportion of severely injured UK combat troops and suggest that it may be a valuable deployed capability (Morrison *et al.*, 2014). Use of REBOA is limited to managing particular injury patterns and it is contra-indicated for the management of aortic or cardiac injuries.

Morrison *et al* examined the epidemiology of NCTH in UK deployed forces. They identified 296 casualties with NCTH and explored the effect of individual organ injuries upon overall survivability using a multivariable logistic regression model (Table 3.2). Mortality was most influenced by the presence of major vessel injury (Morrison *et al.*, 2013).

Injury Region	OR	95% Confidence Interval	*p*
Head	6.46	1.78–23.42	0.005
Neck	9.00	0.98–82.35	0.052
Major arterial	16.44	5.50–49.11	<0.001
Minor arterial	0.430	0.081–2.30	0.324
Pulmonary hilar	9.61	1.06–87.00	0.044
Liver	6.00	1.71–21.04	0.005
Spleen	3.78	0.73–19.58	0.114
Extremity	4.22	1.72–10.34	0.002

Hosmer-Lemeshow statistic, 3.448; $p = 0.841$; $df = 7$; area under the curve, 0.892.

Table 3.2: Odds Ratio of death in UK service personnel sustaining battlefield NCTH. Reproduced with permission from Morrison *et al* (2013).

Although Morrison examined battlefield injury, and showed that 68.6% of casualties were injured by blast, they did not compare relative lethality by injury mechanism and did not separate mounted from dismounted blast. Secondly, the paper was intended to highlight potentially survivable injury and thus excluded heart and great vessel injury.

In contrast, Singleton classified blast death by mounted or dismounted environment but did not further delineate the "intra-cavity" injury patterns and explore relative lethality of injuries (Singleton *et al*. 2013).

Singleton *et al* have further examined the torso response to UBB by describing the patterns of lung injury (Singleton *et al*. 2013). They found high rates of apparent "primary blast lung injury" seen at post-mortem CT of mounted blast casualties. They also showed higher rates of PBLI from all forms of blast exposure (79% of mounted and 32% of dismounted casualties) compared with 11% of those blast exposed casualties arriving for treatment at a role 3 medical facility (Aboudara *et al.*, 2014). This difference is likely due to high rates of mortality in those exposed to overpressures high enough to cause PBLI. Significant PBLI amongst mounted casualties had not previously been described.

3.5 Conclusion

A variety of scoring tools are used for the measurement of injury burden and estimation of survivability. These tools have been designed for the comparison of trauma systems and have statistical and pragmatic limitations. The tools are best applied for the stratification of casualties into those who would benefit from advanced treatment and those for whom only prevention would improve survival. Improvement in deployed military trauma care has led to previously unseen levels of survival amongst severely injured personnel. Challenges exist for both maintenance and improvement of this medical capability but significant improvements to blast survival should be made by prevention and mitigation of severe injury. Conventionally used scoring systems do not adequately quantify the "mitigation gap" required to shift a non-survivable injury burden to a potentially-survivable burden.

Morrison and Singleton have used battlefield data to highlight those injuries and injury complexes which have effect upon survivability. The next chapter will explore torso injury within the mounted environment in more detail and define those injuries which may be important markers of survivability within the mounted blast environment and which may inform future mitigative strategy.

CHAPTER 4

DEFINING THE PATTERN OF TORSO INJURY FROM UNDERBODY BLAST [1]

4.1 Scope of the chapter

Chapter 2 discussed contemporary methodologies for scoring trauma severity. The chapter highlighted the limitations of current tools for defining the limits of survivability in a modern battle-injured cohort and suggested a stratification in the casualty cohort for improving survivability. Chapter 2 also demonstrated the apparent importance of torso injury and non-compressible torso haemorrhage towards survivability but showed that previous models had not linked these injuries to a mounted blast environment. This chapter will demonstrate the pattern of torso injury which occurs subsequent to underbody blast events and discuss the statistical model used to link these injuries with mortality. The chapter will conclude by defining potential biomechanical targets for UBB injury research.

[1] This work was published in part as "Pearce, A. Phillip, Anthony MJ Bull, and Jonathon C. Clasper. "Mediastinal injury is the strongest predictor of mortality in mounted blast amongst UK deployed forces."" Injury 48, no. 9 (2017): 1900-1905.s

4.2 Introduction

The chest and abdomen contain the soft, vascularised organs of the body which are susceptible to injury from most trauma mechanisms. The clinical manifestation of torso injury is greatly dependent upon the organ injured and relevant severity but can be effectively divided into contamination, dysfunction, or haemorrhage.

Contamination is primarily a consequence of hollow viscus injury with exposure of a previously sterile cavity to the visceral contents. Bowel and gastric injury results in exposure of the peritoneal cavity to a large bacterial load, while injury to the oesophagus (or combined diaphragm/gastrointestinal injury) results in analogous injury to the chest or mediastinum. Injury to the pancreas or gallbladder may result in chemical contamination of the relevant space. Both chemical and microbial exposure may cause an inflammatory response with potential for severe clinical sequelae.

Organ dysfunction is most evident following injury to the lungs or heart, in that direct injury causes failure of ventilation due to lung injury or circulatory depression due to heart injury. Injury to other organs such as the kidney, liver, and pancreas may also result in organ dysfunction but the primary response to structural injury of these organs is likely to be haemorrhage or contamination. Organ dysfunction due to blast injury includes primary blast lung injury, lung contusion, and myocardial effects including stunning which may cause cardiovascular depression (Avidan *et al.*, 2005; Kirkman and Watts, 2011).

Haemorrhage results from injury from any vascular, or vascularised structure. Haemorrhage of any type may be classified as either compressible or non-compressible. Bleeding from the extremities may be controlled by either direct (application of pressure to the point of bleeding) or indirect (application of pressure to the relevant vessel "upstream" of the bleeding point") compression. Compressible haemorrhage on the battlefield may be caused by a variety of mechanisms but is commonly associated with limb amputation and dismounted complex blast injury (Mamczak and Elster, 2012). The compressibility of this bleeding type makes it amenable to point of care control and improved battlefield survival rates have been observed with judicious use of tourniquets (Kragh *et al.*, 2008, 2009). Junctional haemorrhage (from the neck, groins, and axillae)

poses more difficulty (Tai and Dickson, 2009). Application of sustained pressure to these wounds may be mechanically difficult and pragmatic combined use tourniquets, direct pressure, and topical haemostatics is advised (Kotwal *et al.*, 2013). A variety of junctional tourniquets have been developed but their role and effectiveness has yet to be defined (Kheirabadi *et al.*, 2013; Walker *et al.*, 2014).

As discussed in Chapter 3, NCTH are those injuries occurring within the internal cavities of the torso which are not amenable to direct or indirect compression. These injuries are a common cause of salvageable death and a major research focus for novel methods of bleeding control (Morrison and Rasmussen, 2012; Chang *et al.*, 2015; Andres *et al.*, 2016). These novel haemostatic methods may bridge the gap to definitive treatment; this bridge is essential given that survival from serious torso injury is time dependent with the death most commonly occurring within 30 minutes (Holcomb, 2018).

Treatment of even salvageable combat torso injuries relies not only upon effective treatment modalities but upon a robust evacuation system and point of care intervention. The extent to which such systems are sufficiently developed for any potential future operative environments is uncertain. Prevention of the injuries for a given threat would negate the need for treatment while mitigation would increase the timeline of survivability. Conversely, non-salvageable injuries have no potential treatment. Prevention and mitigation is the only strategy for such injuries.

Injury prevention can of course occur at a strategic or tactical level by avoidance of conflict or careful planning. The military and political discussions which underpin the deployment of troops in vehicles to areas of risk are well beyond the scope of this thesis. Instead, this work aims to identify those injuries which are important to survivability within the underbody blast environment and determine the extent to which they can be linked to (somewhat) predictable loading.

4.3 Methods

4.3.1 JTTR

The UK Joint Theatre Trauma Registry (JTTR) is a prospectively collected trauma database of every casualty admitted to a deployed UK medical facility or killed on deployed operations. Data on all injured casualties treated by the UK DMS (including UK military, coalition forces, detainees, and the civilian population) is collected. This data is subsequently returned to the Royal Centre for Defence Medicine (RCDM) in Birmingham (UK) where it is added to the JTTR. The JTTR is held and maintained by the Academic Department of Military Emergency Medicine (ADMEM) (Smith *et al.*, 2007). The JTTR hold continuous data on this battle injured cohort from 2003. Data is held electronically with hard copies accompanying patients to definitive care. The initial entry criterion for the JTTR was a casualty injured severely enough to trigger a deployed trauma team activation although this was expanded in 2007 to include any casualty returning to RCDM for definitive treatment (Smith *et al.*, 2007).

UK service deaths from trauma undergo a full *post mortem* examination following repatriation to the UK. This is carried out by a Home Office Pathologist. A military research nurse or other member of ADMEM attends each of these formal examinations. The findings are noted and compared to the formal report produced by the pathologist before entry on to the JTTR (Smith *et al.*, 2007).

In all cases, individual injuries (as detailed in clinical notes, imaging reports and post mortem examinations) are added using the AIS (Military) dictionary with additional free text detail (Smith *et al.*, 2007).

Access to this information is understandably protected and permission was obtained from the Medical Director (DMS) to examine the data for research purposes. A formal request was made via ADMEM and assistance provided by the Clinical Information Exploitation team.

A search of the dataset was made with the following inclusion criteria:

- operations in Iraq and Afghanistan 2003-2014;
- UK military personnel only; and
- explosive injury.

The resultant number of cases was reduced by excluding explosive mechanisms other than underbody IED or mine. Injury severity was used as a further exclusion criterion. Any cases with no injuries graded AIS 2 or above were excluded since this implies relatively minimal injury.

Both ISS and NISS were compared for each group. Both systems compile an overall score based upon the three most severe AIS coded injuries. The ISS is based on the three most severe injuries from different body regions, NISS allows these injuries to arise from the same region. Details of these systems (and their limitations) is discussed in Chapter 3.

The JTTR record was further interrogated for incident data, notably the location of each casualty. All in-vehicle casualties were grouped together as mounted, those on foot were described as dismounted. In-vehicle casualties were not separated by vehicle type or class for this study to avoid describing classified vehicle data.

The mounted group was split into two for the purpose of analysis, survivors and non-survivors. Non-survivors include both Killed in Actions (KIA), those who died in prior to reception at a medical treatment facility and Died of Wounds (DOW), those who died subsequent to admission.

4.3.2 Statistical Analysis

All statistical analysis was performed using SPSS for Windows (Version 24, IBM, New York, USA). Descriptive statistical analyses were performed upon demographic and basic injury data including age, gender, ISS, and injury number. In order to describe the effects of individual injuries upon outcome, all injuries were examined and placed within one of 49 organ specific injury categories based upon both the AIS code and free text data (where available). The prevalence of all torso injuries within outcome groups

were compared. Case Fatality Rate (CFR), a measure of injury lethality was calculated as shown in Equation 4.1.

$$Case\ Fatality\ Rate\ (CFR) = \frac{Number\ of\ Non-Survivors\ with\ Injury}{Total\ Number\ with\ Injury} \quad [4.1]$$

Categorical data was analysed using Pearson's χ^2 and Fisher's exact test depending on sample size. Mann-Whitney U tests were performed for non-parametric continuous data.

Measurement of CFR shows lethality of an injury but is likely to be confounded by the presence of multiple injuries. To account for polytrauma, a forward-entry binomial logistic regression model was constructed in which mortality was the dependent factor. The use of logistic regression is well established for the prediction of dichotomous outcomes (such as mortality) (Steyerberg *et al.*, 2004; Bouamra *et al.*, 2006). For the construction of this model, less common injuries, or injuries with only one outcome were grouped together. The mediastinal group includes aortic, cardiac, and other great vessel injuries. Injuries associated with non-compressible haemorrhage, organ dysfunction, and contamination were included. Presence or absence of each injury (or injury group) were listed as categorical independent factors.

In addition to torso injuries, head and pelvic injuries were also included given the previously recognised importance of these injuries to UBB mortality (Morrison and Rasmussen, 2012; Singleton *et al.*, 2013). Injuries to the chest wall (either rib or sternal fracture) was also included as an independent variable in an effort to better describe the loading pathway of these injuries.

The null hypothesis of the model states that there is no relationship between mortality and the presence of absence of each of the injuries.

The logistic regression model predicts probability of mortality based upon Equation 4.2.

$$p(mortality) = \frac{1}{1 + e^{-(\beta_0 + \beta_1 + \beta_{2\ldots n})}} \quad [4.2]$$

Where $p(mortality)$ is the expected probability of death, β_0 is the intercept of a graphical model and $\beta_{1,2\ldots n}$ are coefficients from each injury.

A β coefficient was generated for each of the independent predictors. The exponential of this coefficient was used to generate the odds ratio of mortality for each injury or injury group with 95% confidence intervals. An AUROC analysis was performed to show the ability of the model to correctly predict outcome. The Hosmer-Lemeshow test for goodness of fit was performed which compares the expected outcome generated by the model to the observed data. A small p-value for this test denotes a poor fit.

4.4 Results

1663 UK service blast casualties were identified in the time period. The exclusions and resultant sample are shown in Figure 4.1.

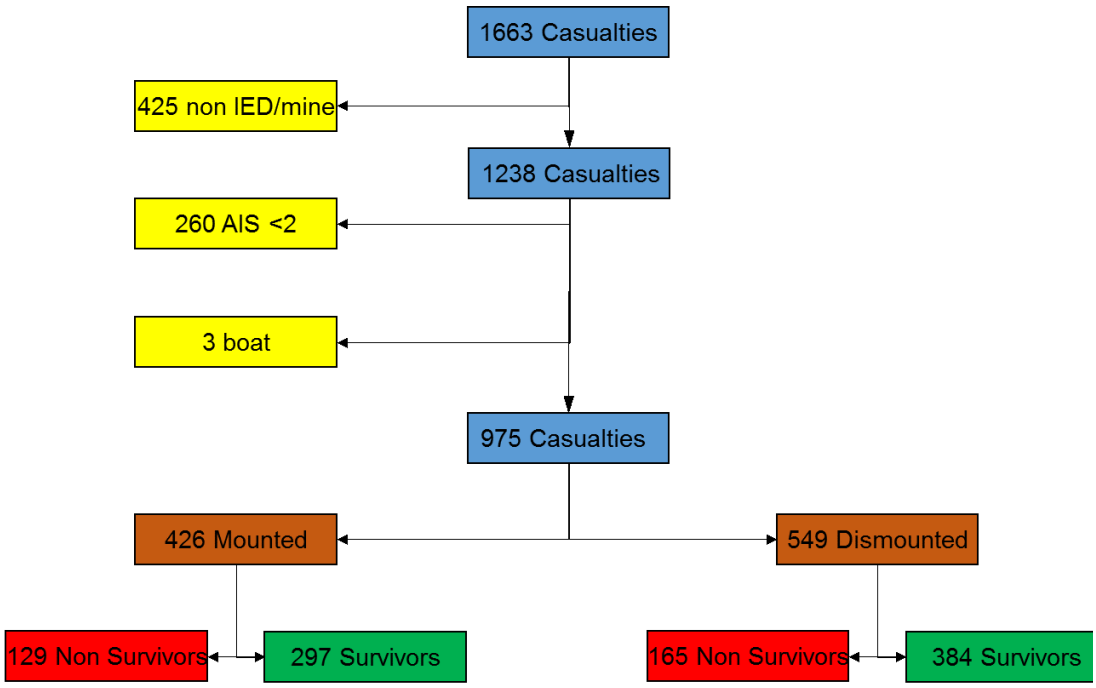

Figure 4.1: Search results of the Joint Theatre Trauma Registry for blast injured casualties resulting in a cohort of 426 for mounted blast.

Demographic data of the mounted blast is shown in Table 4.1. Descriptive statistics of the cohort demonstrated no significant difference in age between the survivor and non-survivor cohorts. Males accounted for the vast majority of casualties in both groups. A significant increase ($p<0.001$) was noted in the proportion of survivors between operations from Iraq and Afghanistan. As expected, differences are seen in both injury number and injury severity (expressed as ISS and NISS) of survivors and non-survivors.

		Survivor	Non-Survivor	p
n		297	129	
Male, n (%)		293 (98.7%)	126 (97.7%)	0.359
Operation	Iraq, n (%)	27 (44.3%)	34 (55.7%)	
	Afghanistan, n (%)	270 (74.0%)	95 (26.0%)	<0.001
Age		24 (21-29)	24 (21-29)	0.987
Injury Number, median (IQR)		4 (3-8)	14 (7-23)	<0.001
Injury Severity Score, median (IQR)		9 (5-17)	75 (75-75)	<0.001
New Injury Severity Score, median (IQR)		12 (8-22)	75 (75-75)	<0.001

Table 4.1: Demographic data of UK mounted blast injured cohort 2003-2014 focusing on differences between survivors and non-survivors. The p value for the operation denotes the significant difference in proportion of survivors between the two operations.

The distributions of injury scores between survivors and non-survivors is shown by Figure 4.2. The majority of non-survivors (105/129) sustained an NISS of 75. In contrast, the median NISS of the survivors is considerably lower. Neither NISS nor ISS is normally distributed (as expected based upon the statistical idiosyncrasies of these systems discussed in Chapter 2).

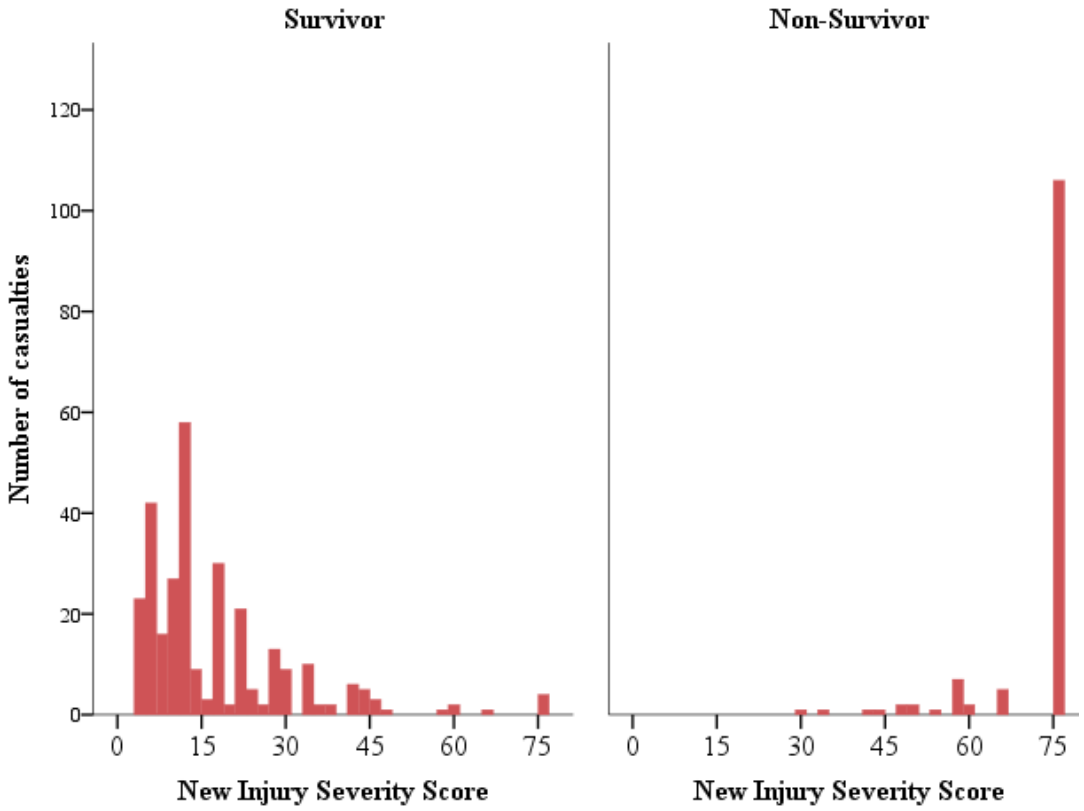

Figure 4.2: Frequency of New Injury Severity Scores sustained by both survivors and non-survivors of mounted blast injury.

Variation in the number of injuries occurred in both survivors and non-survivors with both a higher median number and wider distribution seen in the non-survivor group (Figure 4.3).

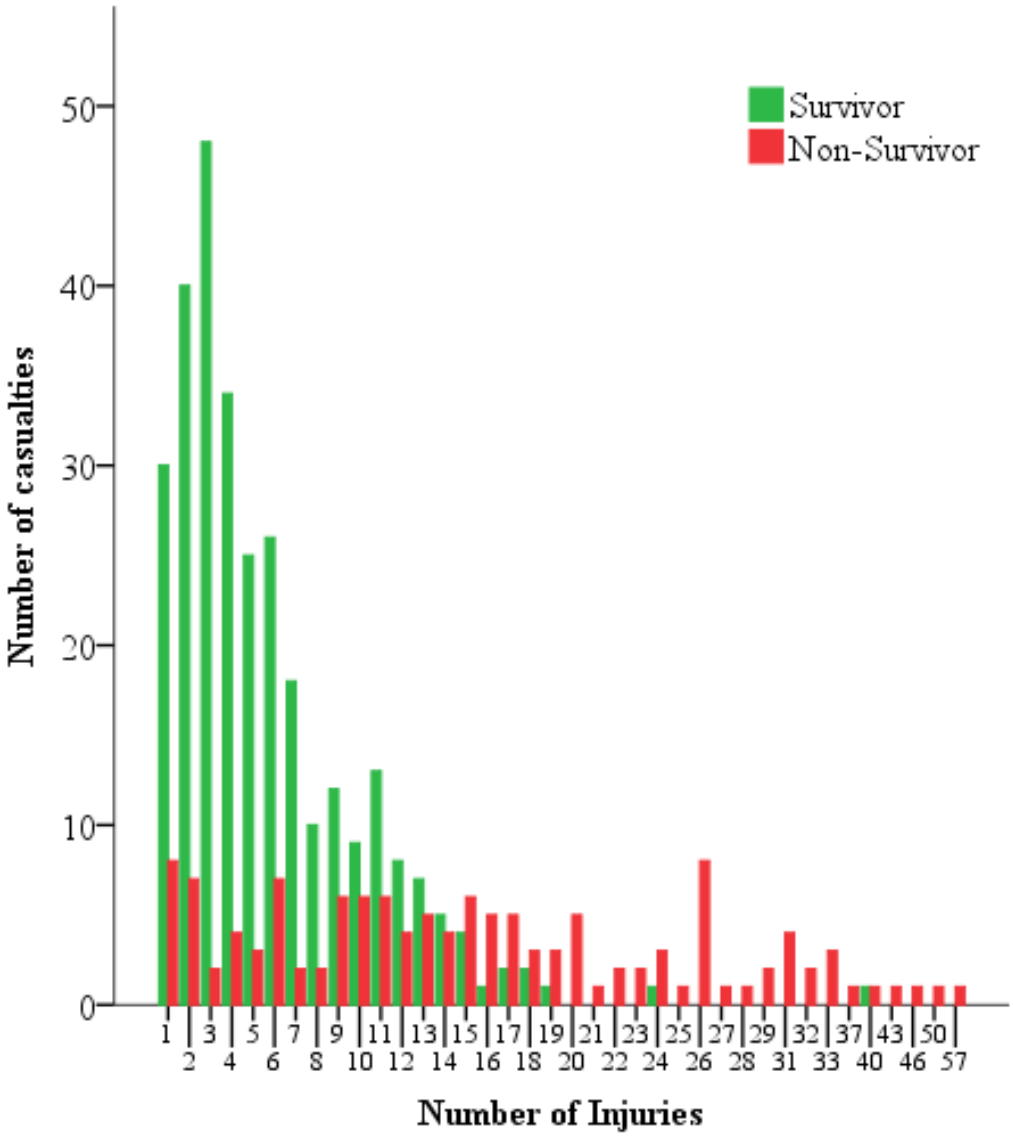

Figure 4.3: Number of injuries sustained by survivors and non-survivors of mounted blast injury.

A wide range of torso injuries was sustained. The incidence of each injury type (ordered from most to least common) along with CFR is shown in Table 4.2. Significance of the differences in incidence between survivors and non-survivors is demonstrated by the p value of the χ^2 test.

Injury Type	Survivor (n=297)	Non-Survivor (n=129)	Total	CFR	p
Splenic Injury	16 (5.4%)	47 (36.4%)	63	74.6%	<0.001
Liver Injury	6 (2%)	53 (41.1%)	59	89.8%	<0.001
Lung Contusion	20 (6.7%)	34 (36.4%)	54	63.0%	<0.001
GI Injury	8(2.7%)	33 (25.6%)	41	80.5%	<0.001
Haemothorax	8 (2.7%)	32 (24.8%	40	80.0%	<0.001
Kidney Injury	3 (1.0%)	35 (27.1%)	38	92.1%	<0.001
Cardiac Injury	1 (0.3%)	31 (24.0%)	32	96.9%	<0.001
Lung Laceration	2 (0.7%)	24 (18.6%)	26	92.3%	<0.001
Blast Lung	10 (3.4%)	13 (10.1%)	23	56.5%	0.006
Other Abdominal Vascular Injury	3 (1.0%)	19 (14.7%)	22	86.4%	<0.001
Thoracic aorta Injury	0	17 (13.2%)	17	100.0%	<0.001
Pneumothorax	11 (3.7%)	2 (1.6%)	13	15.4%	0.192
Other Thoracic Vascular Injury	1 (0.3%)	4 (3.1%)	5	80.0%	0.031
Pulmonary vein Injury	0	4 (3.1%)	4	100%	0.008
SVC injury	0	2 (1.6%)	2	100%	0.091
Abdominal Aorta Injury	0	2 (1.6%)	2	100%	0.091
IVC Injury	0	2 (1.6%)	2	100%	0.091
Pulmonary artery Injury	0	1 (0.8%)	1	100%	0.303

Table 4.2: Incidence of torso injuries from survivors and non-survivors of mounted blast injury. CFR- Case Fatality Rate. p value denotes significance of difference between survivors and non-survivors. Other abdominal vascular includes injuries to the renal, mesenteric, hepatic, and portal vessels. Other thoracic vascular included injuries to the azygous, subclavian, and intercostal vessels. IVC- Inferior Vena Cava, SVC- Superior Vena Cava.

Nearly all torso injuries are significantly more common in non-survivors than survivors. Injuries to the non-aortic great vessels had CFR of 100% but were uncommon. Thoracic aortic injuries were the most common injury (13%) with a 100% CFR. Spleen, liver, and lung injury were the most common injuries.

The effects of individual injuries were estimated using the multivariable logistic regression model. Odds ratio of mortality was calculated as the exponent of β, the regression coefficient. The results of this analysis are shown in Table 4.3.

					95% CI for OR	
Injury Type	**β**	**S.E.**	**p**	**OR**	**Lower**	**Upper**
Mediastinal	3.02	1.29	.019	20.38	1.63	254.60
Lung Laceration	2.43	0.98	.013	11.39	1.68	77.38
Head	1.96	0.33	.000	7.07	3.73	13.42
Rib/Sternal fractures	1.06	0.33	.002	2.89	1.50	5.56
Pelvic	1.04	0.43	.016	2.83	1.21	6.60
GI	1.02	0.67	.126	2.78	.75	10.32
Abdominal vascular	0.95	1.05	.365	2.58	.33	20.05
Kidney	0.84	0.74	.259	2.31	.54	9.92
Liver	0.83	0.65	.200	2.30	.64	8.24
Lower limb	0.45	0.32	.168	1.56	.83	2.94
Blast Lung	0.46	0.62	.456	1.58	.47	5.29
Spleen	0.19	0.63	.767	1.21	.35	4.15
Lung Contusion	0.11	0.44	.811	1.11	.47	2.63

Table 4.3: Multivariable logistic regression model predicting death from underbody blast injuries. B is the injury specific regression coefficient, SE is standard error, OR Odds Ratio of death. Hosmer-Lemeshow test 10.156, p=0.118, df=6, AUROC = 0.854.

All injuries analysed have odds ratios greater than 1 and are associated with mortality. Mediastinal (including heart, thoracic aorta, SVC, and pulmonary vessel) injuries are the strongest predictor of death. Of this group, heart and aortic injuries predominated in number. Head injury accounts for the largest proportion of deaths but remains a weaker predictor of mortality. The p value for the multivariable model was 0.118 which rejects the null hypothesis that death is not predicted by the presence of these injuries. The higher p values for individual injuries (within Table 4.3) suggests that the presence or absence of some injuries do not increase the ability of the model to predict death in the presence of polytrauma.

4.5 Discussion

This chapter describes in detail the pattern of torso injury due to mounted blast casualties and the influence of particular injuries upon survivability. Previous work has highlighted the importance of non-compressible torso haemorrhage but has not highlighted the importance of this injury complex due to a specific blast threat. Morrison *et al* (2012)

examined the incidence of NCTH within UK forces over a recent 10 year period and identified that 75% of those with this injury pattern were killed in action. While the majority of these injuries were attributed to explosions, there was no detailed study of the injury mechanism. The authors proposed that mitigation strategies for head injury are important, but mitigation and prevention of torso injuries were not considered. Morrison and Rasmussen (2012) included evidence of physiological compromise within their definition of NCTH but excluded mediastinal injuries. This approach may be valid when examining cases amenable to surgical intervention but less so for determining mechanism of injury and the potential for improving survivability of blast events.

Defining cause of death for service personnel killed in action is a difficult process and relies to some degree upon conjecture. The utility of the logistic regression model is to take into account all injuries sustained and the effect that a particular injury has upon likelihood of death. A Hosmer-Lemeshow test p value of greater than 0.118 and an AUROC of 0.854 suggest a reasonable fit for the model. Confidence intervals are wide, particularly for the effect of mediastinal and lung lacerations; these reflect the relative small numbers, particularly within the survival cohort. The sparse data bias caused by the use of a relatively small data set should be acknowledged. A logistic regression model is a relatively simplistic tool. More advanced methods of regression analysis, such as hierarchical Bayesian analysis have been suggested for predicting outcomes from multiple "exposures" but these models are still prone to over fitting and may not overcome the statistical issues arising from interactions across variables (Hamra *et al.*, 2014; Ayubi and Safiri, 2017).

4.5.1 Comparison with existing studies

While head injuries have been documented as the most common cause of death, they were not found to be the strongest predictor of mortality. The importance of head injuries to UBB mortality is known and reasonably well understood with direct head impact and severe brain injury (rather than cervical spine flexion/extension) attributed as the predominant mechanism (Stewart *et al.*, 2018). Physical and computational modelling of brain injury secondary to UBB are leading to ongoing research into protective strategies and novel helmet design (Fiskum and Fourney, 2014; Friedman *et al.*, 2016; Gibson *et al.*, 2017).

Thoracic aorta and heart injuries are the most statistically lethal injuries within this cohort. Cardiac and great vessel injuries are already known to have poor outcomes. They have been described as non-survivable within the battlefield cohort and excluded from some definitions of NCTH (Eastridge *et al.*, 2012; Morrison and Rasmussen, 2012).

In the civilian setting, aortic injuries are relatively rare following common blunt trauma (predominantly automotive collision) and although associated with a high mortality even when controlling for other polytrauma, are not untreatable (Demetriades *et al.*, 2008).

Treatment of blunt traumatic aortic injuries may be either endovascular or open. Endovascular treatment is preferred for those patients with multiple injuries with lower mortality seen in those patients with critical extra-thoracic injuries treated with endovascular stenting compared to those treated with open (Demetriades *et al.*, 2008). Clinical studies such as this are subject to an inherent survival bias as they include only those who survived to treatment. Post-mortem studies of automotive fatalities reveal a high rate of both thoracic aorta injuries and cardiac injuries with the majority of deaths (as in the military blast cohort) occurring at scene (Burkhart *et al.*, 2001; Teixeira *et al.*, 2011).

Chest wall injuries were also seen to be a significant indicator of mortality, although similar injuries have been noted within experimental models of underbody blast and are not necessarily indicative of direct torso trauma (Bailey *et al.*, 2015).

Blast lung and lung contusion are included separately within this model and appear to have different effects upon survivability. This separation reflects the description of the injuries within clinical and post-mortem JTTR data. Retrospective review of post-mortem CT imaging has suggested high incidence of blast lung within mounted fatalities of an overlapping cohort (Singleton *et al.*, 2013). The separation of the two entities within the mounted environment is somewhat arbitrary given that primary blast lung injury has been defined as “radiological and clinical evidence of acute lung injury occurring within 12 h of exposure and not due to secondary or tertiary injury” (Mackenzie *et al.*, 2013). The separation of blunt loading away from the blast is difficult

in any environment and particularly so following UBB which is characterised by axial blunt loading.

4.5.2 Limitations

There are limitations to this study which relate to the data itself and to the statistical analysis. Firstly, retrospective use of the dataset (even one that is prospectively maintained) is potentially hampered by recording error and bias.

The incident data has also been reviewed to ascertain blast conditions. The data was interrogated to only include underbody IED blasts events but there may be a variable amount of estimated vehicle flight and roll over between vehicle classes along with variation in explosive device. It is likely that the initial IED strike and axial load would have been the most energetic insult, yet it is difficult to discount the involvement of other forces as the cause of injury. Furthermore, this study has not separated out vehicles or vehicle classes (to avoid the military sensitivity). It is likely (and anecdotally true) that injury severity for a given loading varies with vehicle type and weapon type. Significant differences are seen between mortality rates in Iraq and Afghanistan. This may represent changes in vehicle use but may also be related to use of different weapons. The use of Explosive Formed Projectiles, designed with the intention of defeating armoured vehicles, were more prevalent during the Iraq conflict (Ramasamy *et al.*, 2009).

An assumption must be made that the primary loading from these insults is axial acceleration but this assumption, and the injury associations requires validation.

There are also statistical limitations of the study. The logistic regression model relies upon a reasonable sample size and sufficiently large variable groups. The addition of some injuries together as groups (cardiac and aortic injuries as mediastinal; IVC, abdominal aorta and others as abdominal vascular) increased the statistical power of the model for these individual groups but reduces the granularity of the model to describe the anatomical pattern of injury. The finally used model was a compromise of group size and injury number which does not provide robust proof of the individual injury

effect but is perhaps a better marker of those injuries and injury complexes which lie within the "mitigation gap".

Both ISS and NISS have limited utility in the description of injury severity above a prescribed severity, given that any non-survivable injury results in a maximum score. Saturation of the scale by an AIS 6 injury means that these scores are not descriptive of the overall injury burden and are poor discriminators of survivability. The statistical model used in this studyis useful in demonstrating the effects of individual injuries upon survival amongst a cohort who have sustained extensive polytrauma.

The results of this work demonstrate the range of severe torso injuries sustained during underbody blast events and that the presence of these injuries is an important influence upon survival. While all of the injuries within the analysis are potential targets for further study, mediastinal injuries are the most lethal and perhaps a suitable marker of absolute unsurvivability. Understanding the loading characteristics associated with these particular injuries will allow correlation between loading and survivability and enhance our ability to predict and influence "future unexpected survivors" (Singleton *et al.*, 2013)

4.6 Conclusion

Torso injury is clinically important within the context of mounted/under body blast. Mediastinal injuries are the strongest predictor of death but low numbers reduces the statistical confidence of this assertion. All torso injuries including those to the lung, liver, spleen, kidneys, and GI tract are considerably more common in non-survivors.

These injuries do not occur in isolation, with a significantly larger number of injuries sustained by non-survivors of underbody blast. The "all or nothing" phenomenon of under body blast injury and severe polytrauma is difficult to quantify using conventional injury scoring systems which rely upon arbitrary injury descriptions and which are "maxed out" by a single fatal injury. Devastating injuries such as mediastinal and massive head trauma may be used as surrogate markers of absolute survivability but it is important to remark that non-survivable injuries are not necessarily non-preventable.

As discussed in Chapter 3, improving survivability from UBB can be achieved by mitigating fatal injuries. Identification of future unexpected survivors requires quantification of the "mitigation gap" and the development of a quantitative relationship between loading characteristics and individual injuries within the complex underbody blast environment. Chapter 5 will describe the association of injuries in the UBB environment to better demonstrate the loading pathways attributable to torso trauma.

CHAPTER 5

DEFINING THE LOADING PATHWAY: INJURY ASSOCIATIONS WITHIN THE UNDERBODY BLAST ENVIRONMENT [1]

5.1 Scope of the chapter

Chapter 4 identified the pattern of torso injury resulting from underbody blast and the effect of these injuries upon survival. The aim of this chapter is to describe the relationship of torso injuries to musculoskeletal in order to understand the probable loading mechanism. This chapter will demonstrate the existence of two injury complexes which are likely the result of direct floor deformation and seat acceleration respectively.

[1] This chapter has been submitted as "Pearce et al, "Underbody blasts creates two distinct injury patterns, one of which is associated with mortality."

5.2 Introduction

UBB injury is dependent upon transmission of energy from the exploding device to the occupants of the vehicle above. As discussed in Chapters 3 and 4, death following UBB is commonly the result of head and torso injury (Singleton *et al.*, 2013; Pearce *et al.*, 2017) but the particular mechanism of torso injury has not been fully identified. In contrast, extensive research has determined the mechanism of some musculoskeletal injuries in response to UBB. An examples of a well understood injury is the "deck slap" fractures of the lower limb (Johnson and Strother, 1972; Ramasamy *et al.*, 20110.

As discussed in Chapter 2, the loading that occurs during UBB can be simplified into a) rapid deflection of the floor due to expansion of the gas products; and b) global vertical acceleration of the vehicle and seat due to transfer of momentum from energised soil ejecta (Ramasamy, *et al.*, 2009) (Figure 5.1).

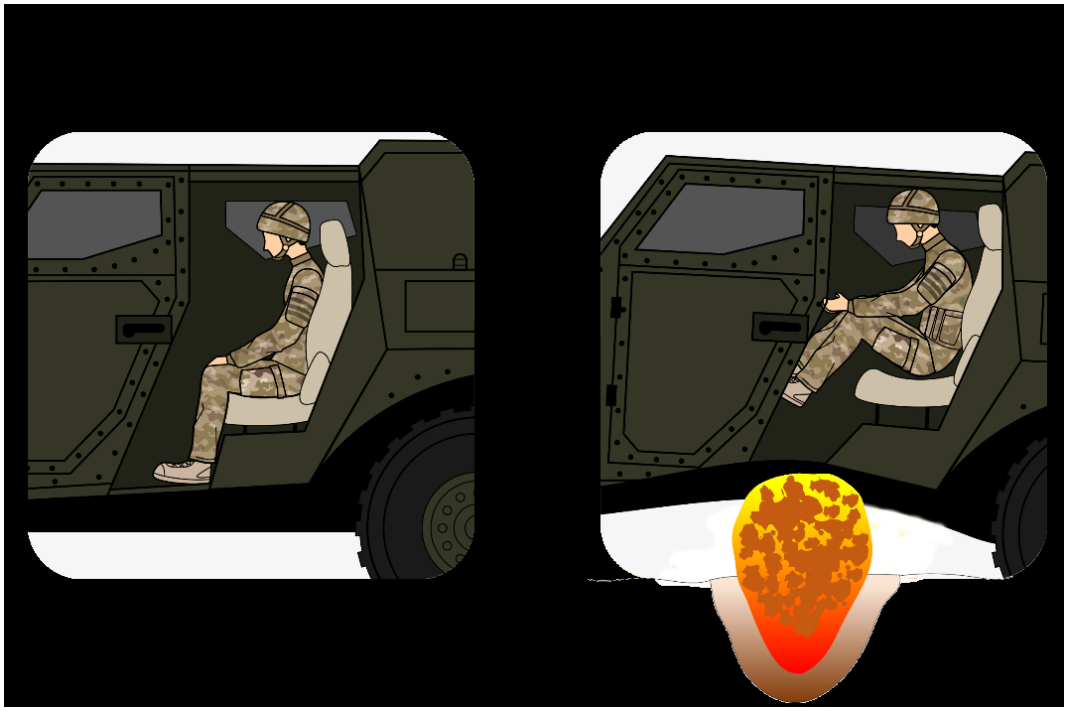

Figure 5.1: Explosion underneath a military vehicle with resultant deformation of the floor and axial acceleration of the seat.

Direct contact of the feet with the rapidly deforming floor has been confirmed as the cause of the classic "deck-slap" injury with physical models closely resembling corresponding battlefield injury (Masouros *et al.*, 2013).

The degree to which the different mechanisms of blast-to-vehicle energy transfer are attributable to other injury types remains uncertain although bony pelvic injury has been shown to relate to seat acceleration (Bailey *et al.*, 2015; Danelson *et al.*, 2015). Likewise, typical UBB injuries to the spine include characteristic burst fractures and are thought to result from pure axial load (Freedman *et al.*, 2014). The distribution of these spinal injuries is different to those seen following ejector seat activation, suggesting that both loading direction and rate affect the injury pattern (Spurrier *et al.*, 2015).

This chapter seeks to better understand the relevance of each injury mechanism by defining the relationship between anatomical injury regions and so quantify the association between injuries with previously identified mechanisms, and the association these have with high fatality rates. The classification of injury patterns with the mechanisms of injury will enhance efforts to design mitigative and preventative strategies.

5.3 Methods

The UK JTTR was interrogated for UK service personnel injured during deployed military operations.

As with the study described in Chapter 4, a search of the dataset was made with the following inclusion criteria:

- operations in Iraq and Afghanistan 2003-2014;
- UK military personnel only; and
- explosive injury.

The resultant number of cases was reduced by excluding explosive mechanisms other than underbody IED or mine. Injury severity was used as a further exclusion criterion. Any cases with no injuries graded AIS 2 or above were excluded since this implies relatively minimal injury.

Clinical data for each casualty were examined and presence or absence of particular injuries was noted. As the aim of the study was to identify mechanism of injury, fractures to the lower limb, and axial skeleton were selected on the basis of their known association with axial loading (Ramasamy *et al.*, 2011; Bailey *et al.*, 2015). Head and torso injuries were specifically studied on the basis of their importance to survivability following UBB events, as potential 'Future Unexpected Survivors' (Singleton *et al.*, 2013). Given the range of torso injuries described in Chapter 4, NCTH was used as a surrogate of the torso response. NCTH was defined as mediastinal injury, lung laceration, solid abdominal organ injury, or other named torso vessel. The injuries of interest were: calcaneus fracture, tibia fracture, femur fracture, pelvic fracture, spinal fracture, head injury, and NCTH.

5.3.1 Statistical analysis

All statistical analysis was performed using SPSS for Windows (Version 24, IBM, New York, USA). Casualty demographics of the cohort are described in Chapter 4. Presence or absence of each injury of interest was noted as a categorical variable. Pearson's χ^2 test was used to determine strength of association between any two injury combinations and performed for each possible combination. The association of each injury complex with mortality was also measured using the χ^2test. Asymptotic two-sided values were assessed and statistical significance defined as $p<0.05$.

5.4 Results

1663 casualties were identified as being injured by blast during the study period. Following exclusions, 426 mounted IED/landmine casualties were identified, and formed the study group. The search and inclusion process is illustrated in Figure 5.2.

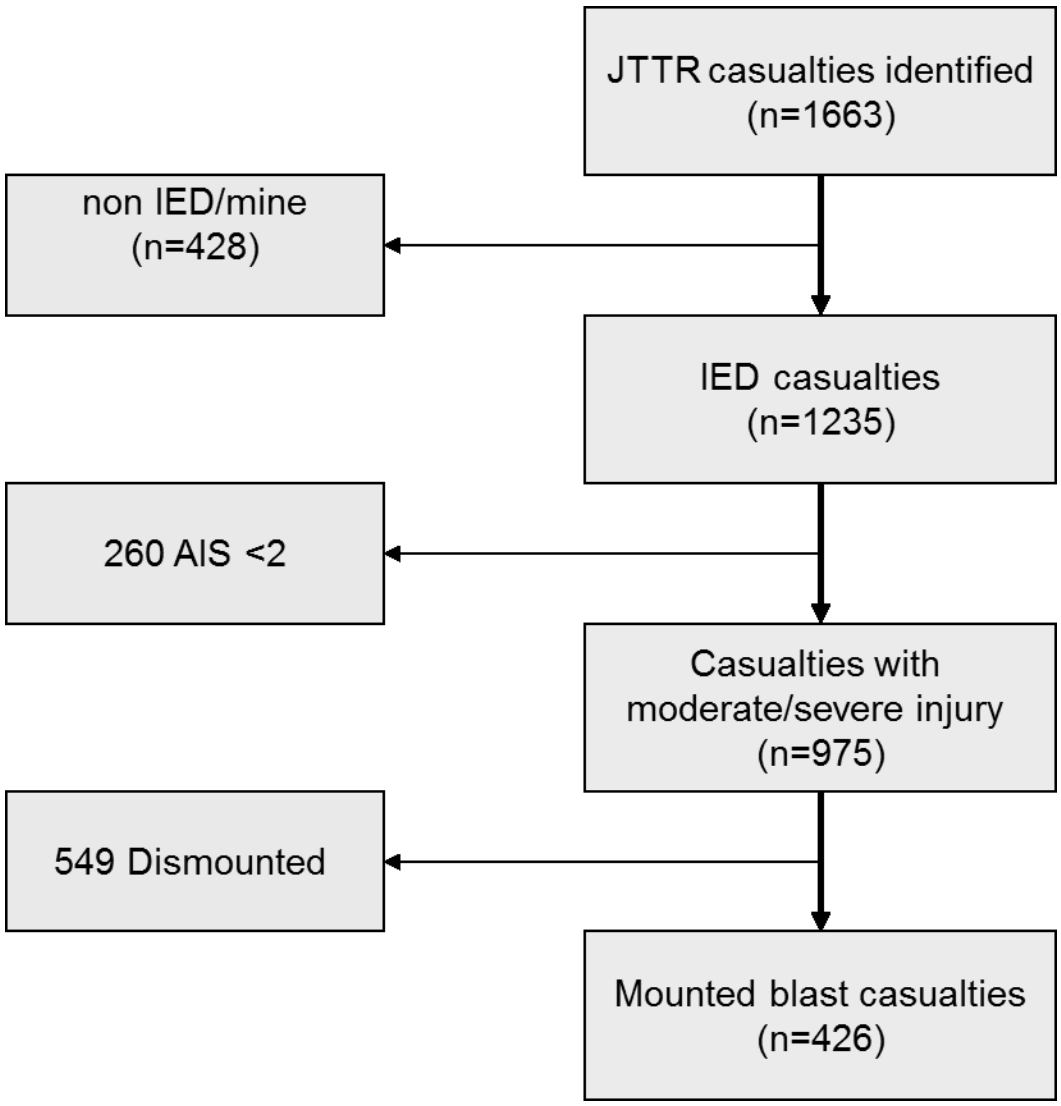

Figure 5.2: Flow chart summarising results of JTTR search for UK service blast casualties, exclusions and eventual mounted blast cohort of 426.

Of the 426 casualties, 297 (69.7%) were survivors and 129 (30.3%) were non-survivors. The median NISS of the total 426 cohort was 17 (range 4-75). As previously described, conventional scoring systems have limited utility in defining survivability within this

environment due to an apparent "all or nothing" distribution of death (Chapter 4). In keeping with similar combat studies, casualties were young (mean age 25.5 years) and mostly male 419/426 (98.4%). The incidence of the specified injury types is shown in Table 5.1

Injury region	Number of cases (% of total mounted)
Calcaneus	97 (23%)
Tibia	145(34%)
Femur	49 (12%)
Pelvis	85 (20%)
Spine	171 (40%)
NCTH	111 (26%)
Head	135 (32%)

Table 5.1: Incidence of injuries (by region) amongst mounted blast injured cohort.

Spinal fractures (of all types) were the most common injury followed by tibial injuries.

The association between each two-injury combination are shown in Table 5.2.

	Calcaneus					
Tibia	**<0.001**	Tibia				
Femur	0.079	**0.043**	Femur			
Pelvis	0.852	0.71	**<0.001**	Pelvis		
Spine	0.489	0.38	**0.001**	**<0.001**	Spine	
NCTH	0.099	0.605	**<0.001**	**<0.001**	**<0.001**	NCTH
Head	0.055	0.834	**0.006**	**<0.001**	**<0.001**	**<0.001**

Table 5.2: Statistical significance (two sided Pearson's χ^2) of associations between UBB injuries. Statistically significant associations ($p < 0.05$) are bold.

Table 5.2 demonstrates that injuries to the calcaneus were strongly associated with those to the tibia but not with any other injuries. In contrast, it can be seen that femoral, pelvic, spinal, head, and torso injuries were all associated with each other. These associations suggest two distinct injury complexes: the lower limb complex and the torso complex. There is also an association between tibial and femoral fractures that might suggest a cross-over between the two injury mechanisms.

Presence of any of the lower limb-complex injuries (calcaneus, tibia, and femur) was not associated with mortality ($p = 0.09$). However, the presence of any of the torso injuries (pelvis, spine, NCTH, or head) was significantly associated with mortality ($p < 0.0001$), adding further evidence that these are two distinct injury complexes.

5.5 Discussion

This chapter describes the anatomical injury associations following UBB events. The results demonstrate that the UBB loading environment causes two distinct injury patterns. Calcaneal and tibial fractures are related to rapid floor deflection (Ramasamy *et al.*, 2011). These injuries have been demonstrated with validated physical models reflecting battlefield injury morphologies (Masouros *et al.*, 2013; Grigoriadis *et al.*, 2017). In contrast, this study leads to the hypothesis that injuries to the pelvis, spine, torso, and head are due to a different and common loading mechanism through the seat. Rapid seat acceleration could be due to localised hull deformation at the point of seat mounting, internal vehicle dynamics secondary to hull deformation, or to global axial acceleration of the vehicle. The precise mechanism of load transfer through the seat is dependent upon vehicle and seat type, and requires further study, to help identify successful current, or design new mitigation strategies.

Of interest is the lack of significant association between injuries of the lower limb complexes and death. This may be a statistical phenomenon based on a relatively small sample size but differences in mortality between the two complexes may suggest an "either/or" phenomenon with death far more likely when the loading is localised to the seat.

5.5.1 Comparison with existing studies

This chapter has not examined the incidence of every injury but has focused on those injuries which are known to affect survival or for which the injury mechanism is most understood. The attribution of pelvic and foot injuries to direct loading has previously been described through experimental studies (Ramasamy *et al.*, 2011; Bailey *et al.*, 2015). Clinical studies of UBB-related spinal injuries add further evidence to the role of direct loading. In examining the pattern of spinal burst fractures, Freedman *et al* (2014) describe the frequency of "first contact fractures" to either the foot or pelvis following UBB before axial transmission of the load through the spine. 23 of the 42 (55%) casualties in their cohort sustained a first contact fracture, of which 18 occurred within the lower limb, 12 in the pelvis and 7 in both. This study has demonstrated with

a larger sample size that spinal injuries (although not uniquely burst fractures) are more strongly associated with pelvic injuries.

Injuries to the femur are of interest as they are associated with both lower limb and torso injury complexes. They may represent a junctional area in terms of mechanism of injury, or there could be two different injury patterns within the femur. Femoral fractures were not described in full body cadaveric UBB experiments (Bailey *et al.*, 2015; Danelson *et al.*, 2015), but it is known that bending and torsional loading can cause femoral fracture (Viano and Stalnaker, 1980). Within the UBB environment, the femur is effectively the lever between the two complexes and it is reasonable to assume that a large axial force acting upon either injury complex would cause a significant bending moment to the femur. Additionally, bending of the femur could feasibly occur in response to direct impact of the seat to the posterior femoral surface. Association of the femoral fracture with superior injuries and not with calcaneal injuries suggests that the seat loading is the mechanism of injury within this battlefield UBB cohort, although the association with the tibia suggests some crossover.

Figure 5.3: Injury complexes from UBB with light shading denoting the floor-lower limb complex and dark shading denoting the seat-torso complex. The femur is evidently the lever between the two complexes.

The absence of femoral injuries within cadaveric testing suggests discrepancy between experimental conditions and battlefield blast exposure. This discrepancy could be in the magnitude of loading, different posture, the wearing of personal protective equipment, or an environmental or anatomical constraint (such as impaction of the femur upon a vehicle part) which is not captured experimentally.

5.5.2 Limitations

As with the study described in Chapter 4, there are both data based and statistical limitations to this study. As previously discussed, although the JTTR is prospectively maintained, this analysis was performed retrospectively and is subject to potential error based on data quality. As with the logistic regression model of Chapter 4, the statistical power is increased by the combination of all injuries of a particular type together. Additional work could examine precise fracture patterns in order to more thoroughly understand the response of each injury region (as has been done for the calcaneus) (Ramasamy *et al.*, 2011). Each injury type includes a broad range of either fractures or internal organ injuries. More detailed work on the biomechanical response of bony and soft tissues to this form of loading is available (Spurrier *et al.*, 2016; Grigoriadis *et al.*, 2017; Pearce *et al.*, 2017). The following chapter will examine the relevant biomechanics of the internal organs in response to high rate loading.

5.5.3 Vehicle Type

Although only in-vehicle IED/landmine exposure has been included, it remains somewhat heterogeneous, as several different vehicle classes were included. The loading conditions between different vehicles will differ. As previously discussed, seat type and vehicle characteristics are likely to affect the energy transfer between explosion and occupant. Seats may be attached to the floor or suspended from the walls or ceiling of the vehicle and may be "energy absorbing" using either a readily deformable component or sliding mechanism to offset some vertical acceleration. Description of particular injury characteristics amongst occupants of specific vehicle classes would be a worthwhile exercise that could elucidate injury mechanisms and associations specific

to a vehicle type, therefore allowing for informed, targeted improvements in protection from explosive threats.

Just as tibial injuries occur in response to direct loading to the foot, injuries to the head, torso, and spine are likely coupled to blast loading through the pelvis and buttocks. The importance of whole body testing at high rates for the purposes of "mass recruitment", where mass recruitment refers to the effect of the input loading recruiting the entirety of the involved mass has previously been established (Bailey *et al.*, 2015). This is particularly the case for the seat-loaded complex in which the group of injuries is multifaceted with likely interaction between various body segments, restraint systems, and personal protective equipment.

5.6 Conclusion

This chapter has identified two discrete injury complexes in UBB that are likely associated with separate mechanisms: lower limb injury due to floor deformation and pelvis-torso-head injuries due to seat loading. Although much work has previously focused on high fidelity models of the lower extremity, mortality in UBB is related to the pelvis-torso-head complex. The independence of these injuries from the lower limbs suggests that high rate loading of the seat or vehicle should be examined in greater detail, including consideration of the 'second hit' due to gross vehicle deceleration after having been initially accelerated vertically Discrepancies in injury severity between battlefield data and physical models may mean that loading conditions within experimental conditions do not adequately replicate real-world scenarios.

The strong association of injuries to the pelvic-torso-head complex and the mortality associated with this apparently seat loaded pattern suggests that mitigative strategies to address this form of loading are the most likely to improve UBB survivability.

Mitigation of torso injuries is reliant upon an understanding of the relationship between loading and injury. Chapter 6 will review the literature regarding the relevant anatomy, and multi-scale biomechanical response of the torso to impact with emphasis upon the response to high rate axial loading. The chapter will define the current understanding of

the response of the torso to high rate vertical loading and will emphasise the limited ability of current the numerical criteria to quantify this relationship.

1

CHAPTER 6

BIOMECHANICAL CONSIDERATIONS FOR TORSO INJURY FOLLOWING UNDERBODY BLAST

6.1 Scope of the chapter

Chapter 3 described the pattern of torso injury sustained from underbody blast and the effect of these injuries upon survival, while Chapter 4 demonstrated the association of torso haemorrhage with musculoskeletal injures and proposed high rate seat loading as a causative mechanism. This chapter will review the relevant literature for torso injury in response to impact and high rate loading. Relevant anatomy, principles of injury mechanisms, and component level biomechanics will be discussed. The chapter will then focus upon impact and whole body accelerative loading scenarios including historical and existing models before critically examining currently used injury criteria.

The chapter concludes by discussing the need for a novel model and better understanding of the relationship between axial loading and torso injuries.

6.2 Introduction

Injury biomechanics is the study of the tolerance to impact and extreme accelerative loading and aims to describe and quantify the extent to which mechanical loading causes deformation of tissue beyond its failure limit. This tissue failure may result in anatomical disruption or physiological dysfunction.

Chapter 3 described the resultant anatomical and physiological disruption that occurs within the torso in response to UBB. This chapter will explore the susceptibility of the torso to injury in response to different loading scenarios and examine contemporary and historic literature for relevant torso injury biomechanics. The injuries and injury patterns identified in Chapters 4 and 5 are not unique to underbody blast and have been examined within other injury domains. This chapter will examine these domains and discuss the extent to which existing literature is relevant, translatable, and of potential use in describing the relationship between UBB loading parameters and torso injury.

All injuries are the result of either intentional or unintentional application of force against the body. Injury biomechanics research has historically focused upon unintentional injuries on the premise that they are more preventable. Given that automotive collisions are the most common cause of unintentional trauma (Office for National Statistics, 2016), injuries from crashes are at the forefront of injury biomechanics.

Although suicide and self-harm are more common causes of death and injury in the UK (Office for National Statistics, 2016), intentional violence inflicted against oneself (or another person) may take so many forms that the ability to experimentally replicate these conditions is limited and prevention of these injuries can be best achieved by reducing suicidal intent.

Given that UBB events typically produce high rate blunt loading, review of relevant automotive injury research is appropriate. In this context, impact injury research may be divided into anatomical regions or specified organs. The principles of injury biomechanics are to identify injury mechanisms, quantify the mechanical response of the body to loading, determine risk of injury from this response, and develop mitigative strategies (Viano *et al.*, 1989).

The aims of this chapter are therefore to demonstrate potentially translatable knowledge from existing work in these other injurious environments. The chapter will provide an overview of relevant anatomy and injury grading before exploring known and postulated injury mechanisms. Experimental and numerical models with potential application to UBB loading will be explored and current used injury criteria discussed.

6.3 Anatomy of Torso Injury

The torso comprises the thorax and abdomen. The vertical direction of UBB may cause complex injury mechanisms involving both regions but the majority of impact biomechanics research considers the regions separately and hence a separate description of the relevant anatomy is appropriate.

6.3.1 Thoracic anatomy

The thorax is the upper region of the torso. It is bounded superiorly by the neck and shoulders and inferiorly by the diaphragm. The thorax is comprised of the rib cage and the soft tissues within. The human rib cage is made up of 12 pairs of ribs connected anteriorly at the sternum and posteriorly at the thoracic vertebrae (Figure 6.1).

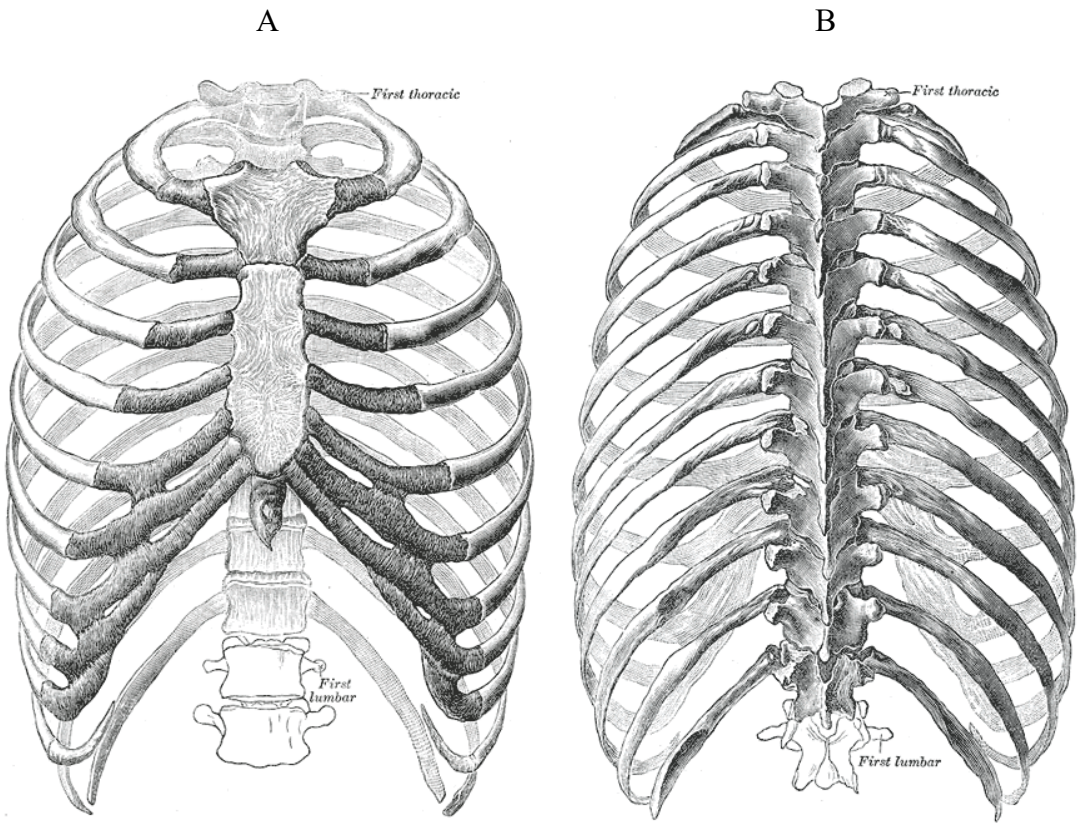

Figure 6.1 A) Anterior view of the rib cage B) posterior view of the rib cage. From Gray *et al.* (1918)

The rib cage contains the lungs, mediastinum, pleura, heart, and great vessels. The left lung is made up of upper and lower lobes whilst the right comprises the upper, middle, and lower lobes. Both are invested by the visceral pleura with the parietal pleura lining the inner surface of the chest wall, and covering the diaphragm. The potential space between the two pleural membranes is the pleural cavity but is only apparent when containing air or fluid. The reflections of the pleura which contains the hilum of the lung is the pulmonary ligament (Figure 6.2). This pleural fold retains the lower pole in position by preventing rotation about the axis of the hilum. The pulmonary artery, pulmonary veins, bronchial arteries and veins, lymphatic vessels and bronchus form this hilum which connects these structures with the heart and trachea. The right hilum lies behind the superior vena cava and right atrium. The left hilum passes beneath the arch of the aorta and in front of the descending aorta.

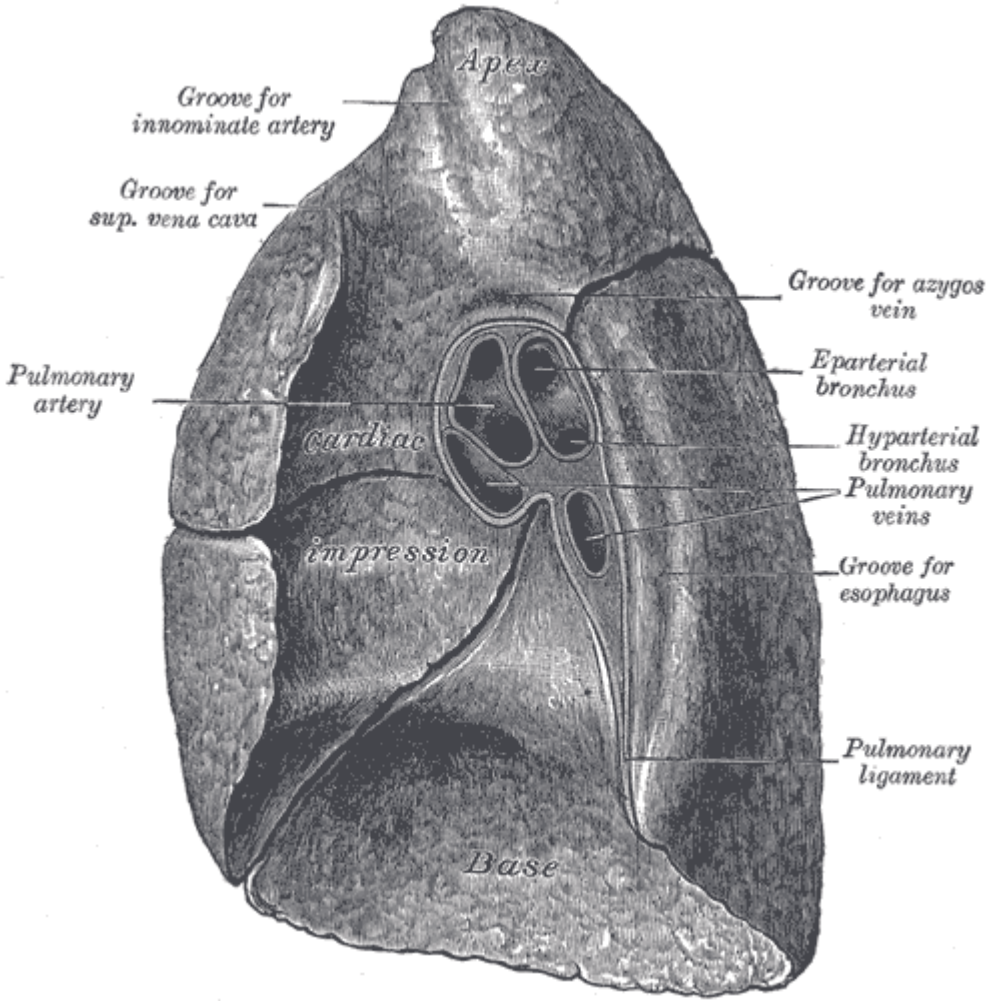

Figure 6.2: Medial view of the right lung showing the hilar structures as they enter the lung and the formation of the pulmonary ligament from the pleural reflections. From Gray *et al.* (1918)

The concave bases of the lungs rest upon the convex surface of the diaphragm. The medial surface of the lungs border the mediastinum, the central region of the thoracic cavity. Within the visceral pleura, the lungs are formed from sub-serous areolar tissue, the bronchial tree and parenchyma. After branching from the trachea, the bronchi enter the lungs at the hila and divide and subdivide within the parenchyma. The smallest subdivisions are the respiratory bronchioles which themselves divide into a several alveolar ducts from which a variable number of alveolar sacs connect. Each alveolar sac bears alveoli on their circumference.

This parenchyma is formed of distinct secondary lobules connected together by areolar tissues. Each secondary lobule is composed of several primary lobules which are the anatomical units of the lung and formed from alveolar ducts, alveolar sacs, and alveoli. Acini refer to the functional units of the lung. They are larger than primary lobules, being made up of respiratory bronchiole with associated alveolar ducts and sacs.

The right lung is heavier than the left although the absolute weight of both varies between individuals. Table 6.1 shows the post mortem organ masses of young (18-35 year old) healthy men and women who had died sudden from trauma (Molina and DiMaio, 2012a, 2015). Although lung mass was significantly greater in men than women, mass was poorly correlated with total body mass, body length, and Body Mass Index. Variation in post mortem lung mass is related to the fluid content of the lung with lighter lungs in those dying from haemorrhage and heavier lungs in those with visceral congestion (Molina and DiMaio, 2012a).

		Male	Female
Right lung mass (g)	Mean	445	340
	SD	159	123
	Range	185-967	142-835
Left lung mass (g)	Mean	395	299
	SD	147	117
	Range	186-885	108-736

Table 6.1: Lung masses of otherwise healthy 18-35 year old men and women dying from trauma. SD - Standard Deviation. Data from Molina and DiMaio (2012a, 2015)

The mediastinum lies between the right and left pleura and from the sternum anteriorly to the vertebral column posteriorly. It is divided into an upper and lower division at the level of the sternal angle. The superior mediastinum, which is bounded superiorly by the thoracic inlet, contains the aortic arch, innominate artery, the thoracic portions of the left common carotid and left subclavian artery, part of the superior vena cava, the trachea, oesophagus, thoracic duct, thymic remnant, and vagus, cardiac, phrenic, and left recurrent laryngeal nerves.

The inferior mediastinum is divided into three regions (anterior, middle, and posterior) relative to the pericardium. The anterior mediastinum exists only on the left and contains loose connective tissue, lymphatics and small branches of the internal mammary artery. The middle mediastinum contains the heart, ascending aorta, lower portion of the superior vena cava, the bifurcation of the trachea, and pulmonary veins. The posterior mediastinum contains the thoracic descending aorta, azygos and hemi-azygos veins, oesophagus, thoracic duct, and vagus and splanchnic nerves (Figure 6.3).

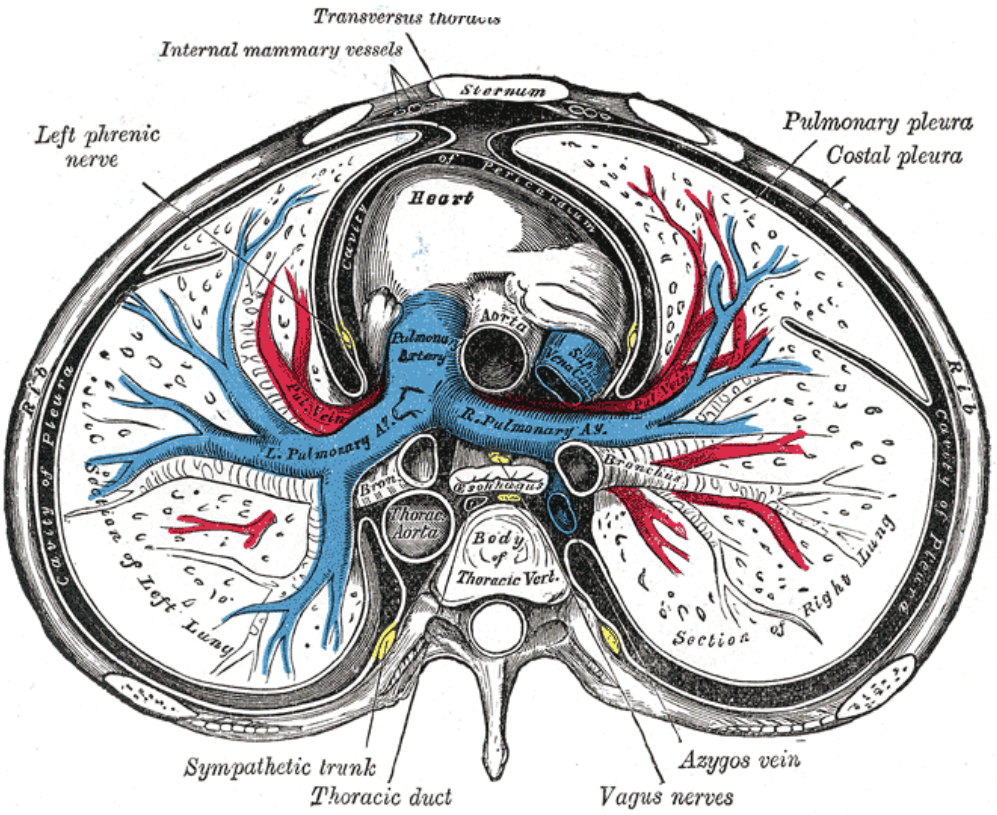

Figure 6.3: Axial section of the thorax showing the contents of the middle and posterior mediastinum. From Gray *et al*. (1918)

The heart is a hollow, muscular organ which sits within the pericardium in the mediastinum and is divided into four chambers, the left and right atria, and left and right ventricles. The great vessels are those veins and arteries which carry blood to and from the heart. The left atrium and ventricle receive oxygenated blood from the lungs and pump it to the rest of the body, via the aorta. The right atrium and ventricle receive blood

from the rest of the body and pump it, via the pulmonary artery, to the lungs. The inflow tracts to the left and right side of the heart and the pulmonary veins, and superior and inferior vena cava respectively. The anterior view of the heart is shown in Figure 6.4.

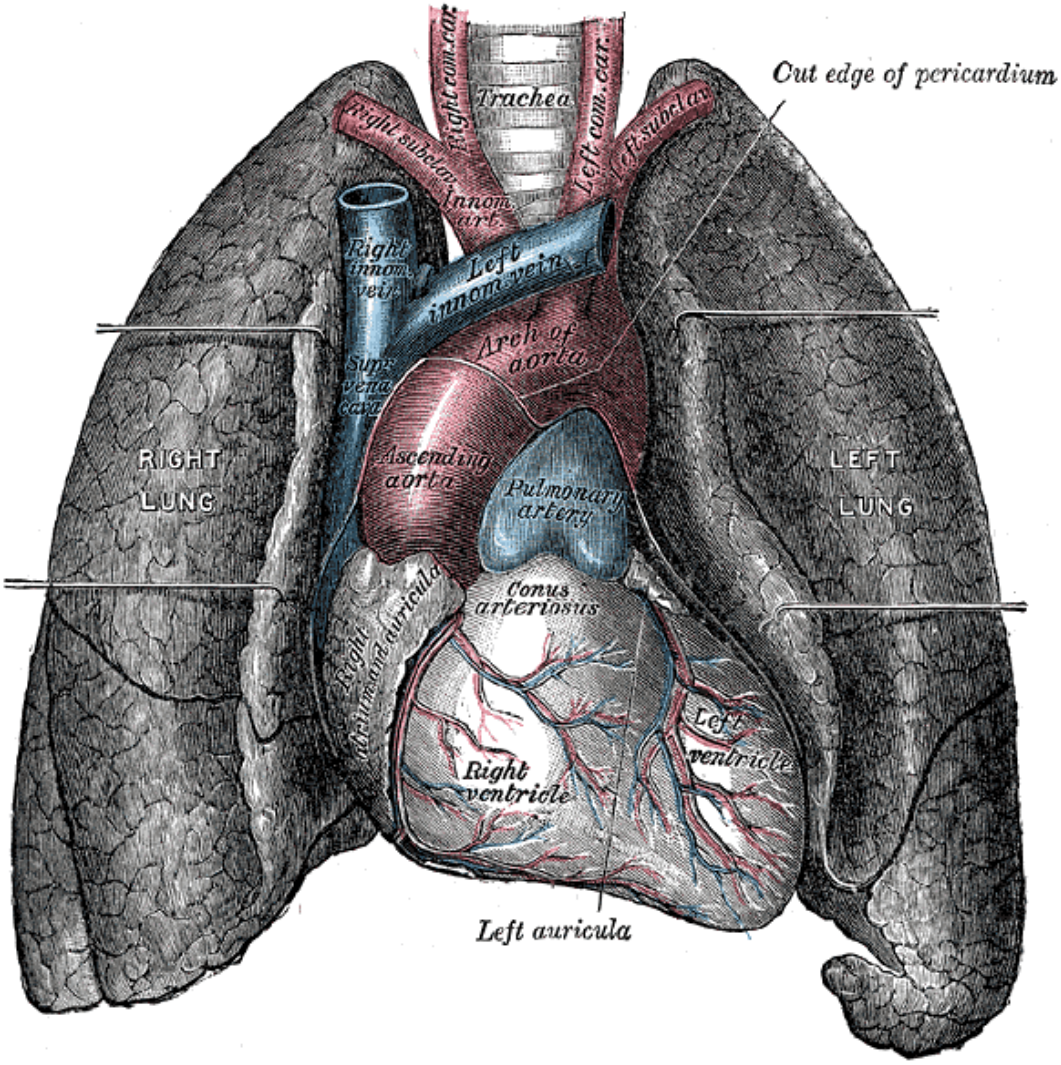

Figure 6.4: Anterior view of the heart. From Gray *et al* (1918).

The heart is related anteriorly to the pericardium, and then to the internal surface of the sternocostal chest wall. Inferiorly, the heart is related to the central tendon of the diaphragm which is continuous with the pericardium. The heart is attached to the pericardium only at the roots of the vessels which emerge through it and is otherwise able to move freely within it, as is necessitated by the dynamic nature of its action. Like the lungs, the mass of the heart correlates poorly with body size but is significantly

different in men (mean 331g SD – 56.7g) and women (mean 245g SD – 52g) (Molina and DiMaio, 2012b).

The aorta is the main outflow tract from the heart and conveys oxygenated blood to the tissues of the body. It begins in the left ventricle, ascending for a short distance before arching posteriorly and towards the left side, over the left pulmonary hilum (Figure 6.5). The aorta then descends within the thorax on the left side of the vertebral column before passing through the aortic hiatus in the diaphragm and into the abdomen.

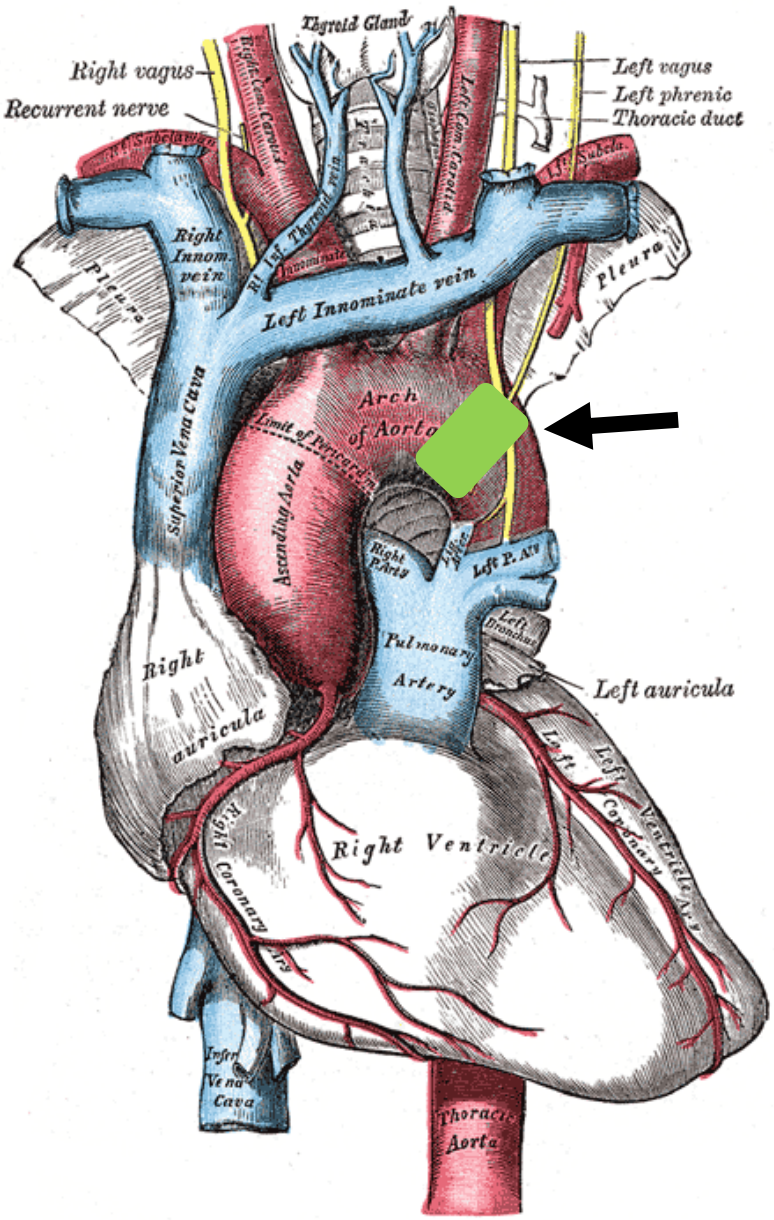

Figure 6.5: The ascending and arch of the aorta with branches. The aortic isthmus, between the origin of the left subclavian artery and the ligamentum arteriosum is shaded green. Adapted from Gray *et al* (1918).

The ascending aorta is initially enclosed by the pericardium, along with the pulmonary artery and gives off only the two main coronary arteries. The arch of the aorta begins at the level of the second sternocostal joint on the right side and before passing backwards and to the left in contact with the left lung and pleura. Arising from the convexity of the arch are the brachiocephalic (or innominate), left common carotid, and left subclavian

arteries. The ligamentum arteriosum, the remnant of an embryological vessel, connects the commencement of the left pulmonary artery to the aortic arch. Just distal to the origin of the left subclavian artery and proximal to the ligamentum arteriosum is the aortic isthmus, a slight narrowing of the aorta.

The descending thoracic aorta commences from the isthmus and runs inferiorly along the left lateral surfaces of the vertebral column. The left lung and pleura overlie it and constrain it anteriorly (Figure 6.6). It gives off both visceral (pericardial, bronchial, oesophageal, and mediastinal) and parietal (intercostal, subcostal, superior phrenic) branches along its course though the chest.

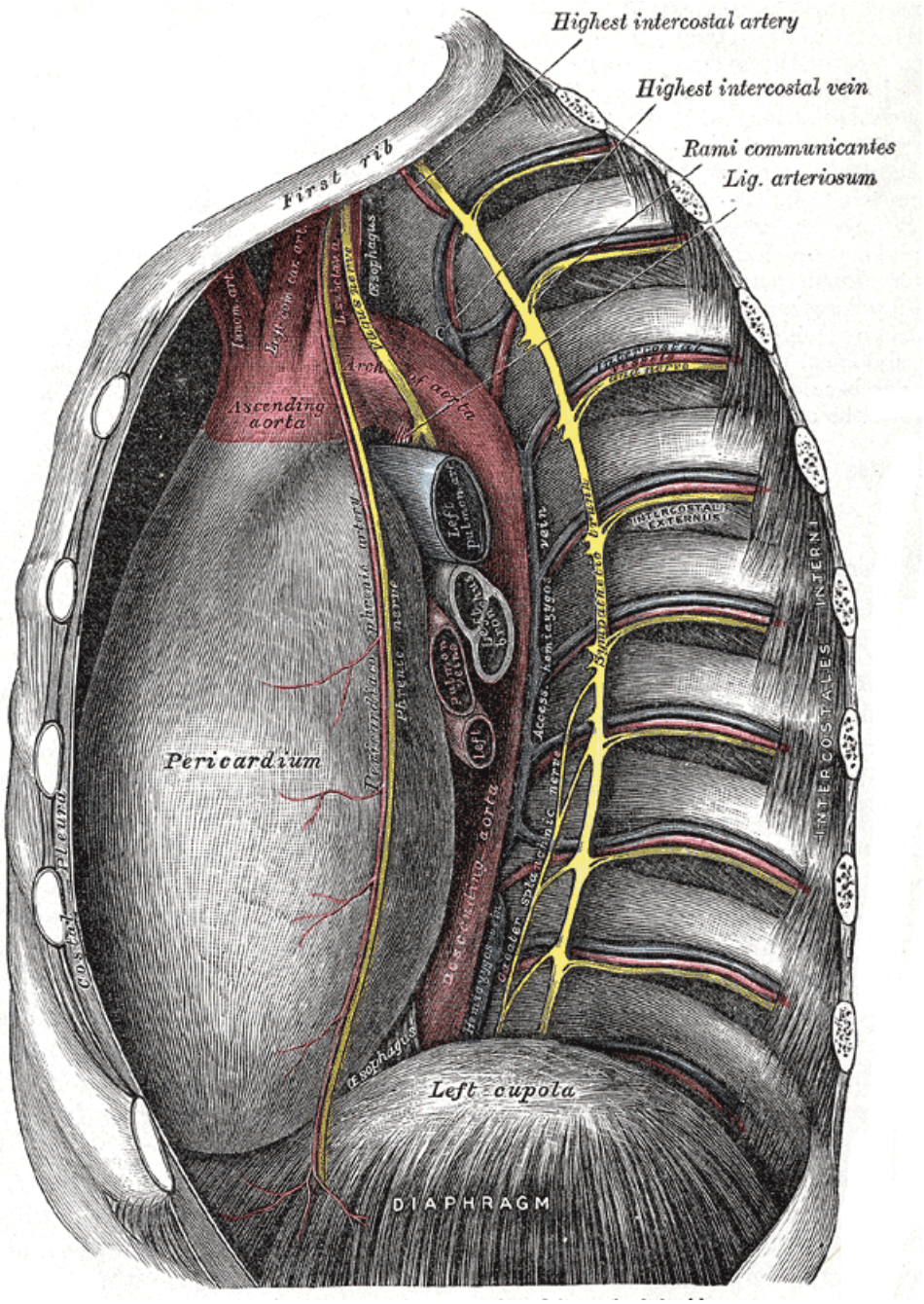

Figure 6.6: The thoracic aorta, as viewed from the left side with left lung, left pulmonary vessels, and pleura removed. From Gray *et al.* (1918).

Separating the thorax from the abdomen is the diaphragm. This is a dome-like structure forming the floor of the chest and roof of the abdomen. The peripheral portion of the diaphragm is formed of muscular fibres which originate from the lower ribs, sternum, and lumbar vertebrae of the thoracic outlet and converge into a central tendon. This

central tendon is a thin fibrous structure which blends superiorly with the pericardium. The diaphragm is pierced by several openings which allow passage of structures including the aorta, IVC, oesophagus, thoracic duct and various nerves.

6.3.2 Abdominal anatomy

The abdomen is the lower section of the torso. It is bounded superiorly by the diaphragm and extends into the pelvis. Given the upward convexity of the diaphragm into the chest, the upper portion of the abdomen is afforded some protection by the lower ribs. Beneath this level, the anterolateral wall of the abdomen comprises peritoneum, fascia, varying thickness of musculature, subcutaneous tissue, and skin. The posterior abdominal wall is comprised of similar structures but organised around the spinal column and thoraco-lumbar fascia.

The peritoneum, like the pleura in the chest is a serous membrane which lines the internal surface of the abdominal wall (parietal peritoneum) and reflects up to encase the internal organs (visceral peritoneum). Rotation and translation of organs during embryological development results in double layers of peritoneum and mesentery, which extend between certain organs, transmitting vascular connections and permitting relative movement of some organs.

The liver is the largest internal organ in the body and occupies the right upper quadrant of the abdomen. Post mortem examination of young adult liver mass reveals differences between gender with mean of 1288g (SD 330g) in women and 1561g (SD 317g) in men (Molina and DiMaio, 2012a, 2015). There is a poor positive correlation with changes in body weight and BMI. Liver mass was found to significantly decrease in the setting of haemorrhagic injury.

The liver has three surfaces, superior, inferior, and posterior. The superior surface is attached to the diaphragm and anterior abdominal wall by a triangular fold of peritoneum, the falciform ligament. The line of the falciform divides the liver into left and right lobes. The coronary ligament is a wide tethering of the liver to diaphragm formed from the left and right triangular ligaments, which are reflections of the peritoneum from the upper margin of the bare area of the liver to the under surface of

the diaphragm. The coronary ligament is continuous with the right layer of the falciform ligament. The right lobe is much larger than the left with fossae on the inferior surface separating its medial part into two smaller lobes (the quadrate and caudate lobes) (Figure 6.7).

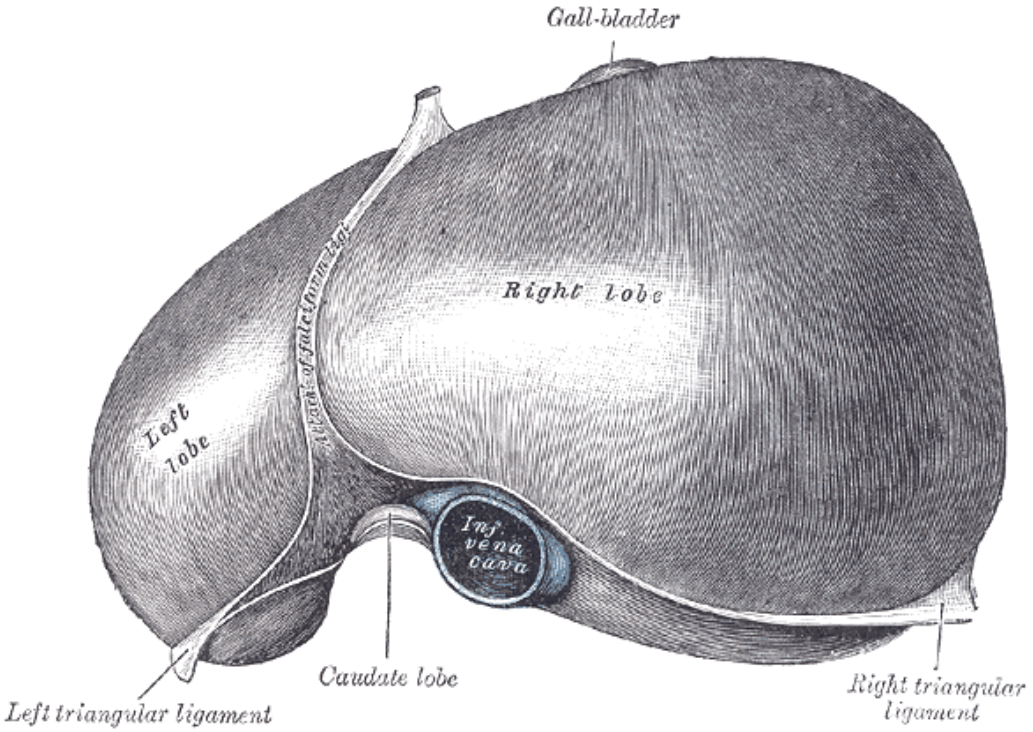

Figure 6.7: The superior surface of the liver as viewed from above. Separation of the left and right lobe by the falciform ligament can be seen. From Gray *et al* (1918).

The inferior surface is uneven, concave, and almost completely covered by peritoneum (Figure 6.8). The gallbladder attaches to the liver here within the gallbladder fossa while the porta hepatis is a mesentery like wrap of peritoneum which encases the portal vein, hepatic artery and bile ducts as they enter and emerge from the liver. The posterior surface is rounded and presents a broad concavity which moulds against the vertebral column. The IVC runs within a fossa on this posterior surface, at which point the hepatic veins drain directly in to it, before it passes through the central tendon of the diaphragm, through the pericardium, and into the right atrium of the heart.

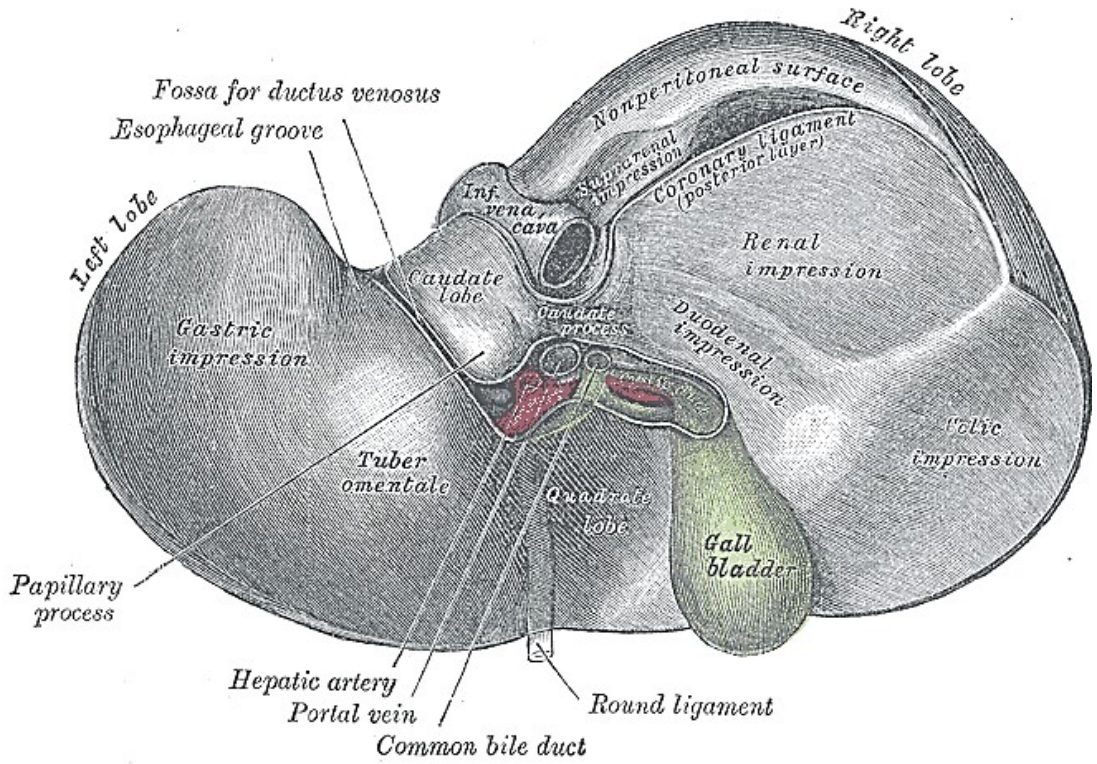

Figure 6.8: Posterior and inferior surfaces of the liver showing gallbladder, porta hepatis, and IVC. From Gray et al (1918).

The anatomical features of the liver resist relative motion; this may be important when considering large relative motion that could be included by UBB. Attachments of the liver to the diaphragm by coronary and triangular ligaments, along with the close relationship to the IVC constrains movement of the posterior liver. The close approximation of the superior surface, combined with intra-thoracic pressure constrains movement in the axial plane (Gray *et al.*, 1918).

The liver parenchyma is composed of lobules bound together by areola tissues which invest the portal vein, hepatic ducts, hepatic artery (and branches) and hepatic veins. A fibrous capsule covers the surface of the entire organ. The function of the liver (including detoxification of metabolites, synthesis or proteins, breakdown of red cells and production of digestive compounds requires a large blood supply. 75% of this blood comes from the portal system, venous blood drained from the spleen and GI tract. The remaining supply is from the hepatic arteries which arise, via the coeliac trunk, from the abdominal aorta.

The spleen is part of the lymphatic system and responsible for both breakdown of red blood cells and provision of immunity against encapsulated bacteria. This highly vascular organ sits in the left upper quadrant, adjacent to the left upper flexure (splenic flexure) of the colon. The spleen has both a diaphragmatic surface which is smooth and convex against the surface of the diaphragm which separates it from the ninth, tenth, and eleventh rib of the left side. The inferior visceral surface faces the stomach and left kidney and is divided by a ridge into corresponding gastric and renal portions (Figure 6.9).

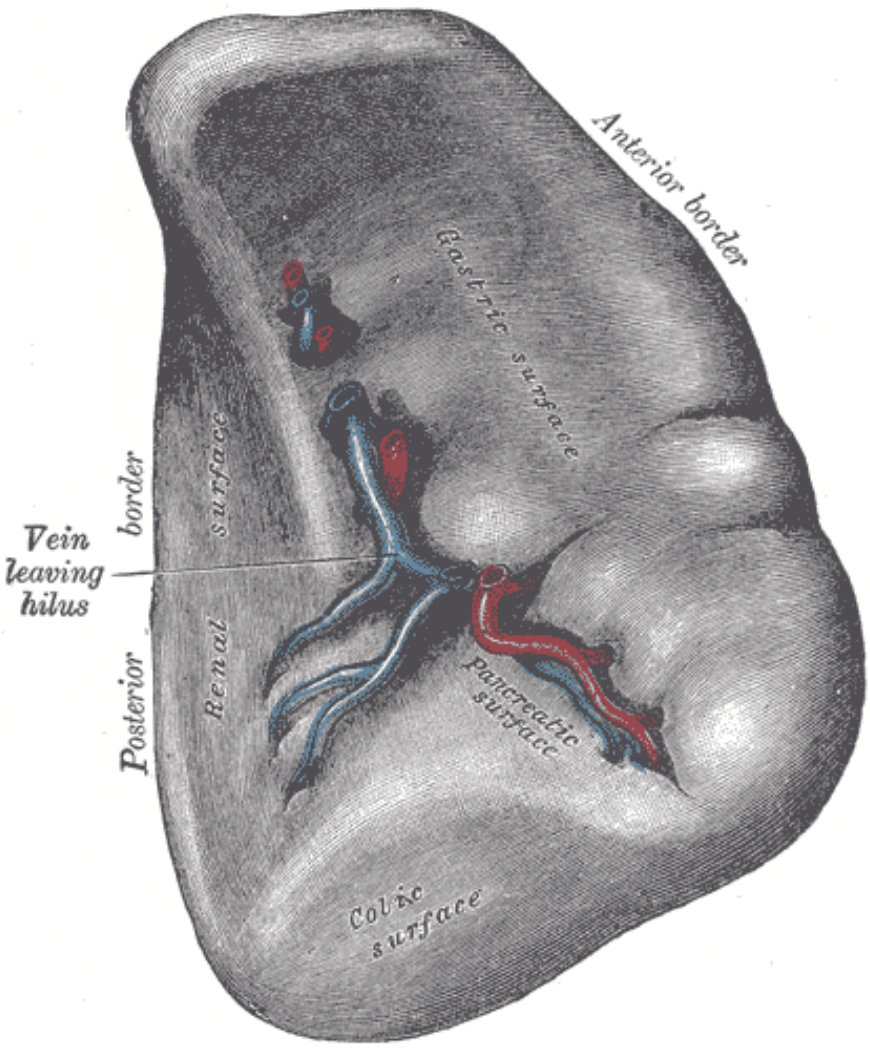

Figure 6.9: Visceral surface of the spleen showing the anterior (gastric) and posterior (renal) portions separated by a ridge. The splenic veins and arteries can be seen entering and emerging from the hilum. From Gray *et al.* (1918).

The spleen is surrounded by peritoneum and held in position by two peritoneal folds, the lienorenal ligament which attaches to the left kidney, and the gastrosplenic ligament which attaches it to the greater curvature of the stomach. The hilum, at the centre of the visceral surface contains the large splenic artery, itself a branch of the coeliac trunk, and the splenic vein which is a main tributary of the portal vein. Like the liver, the mass of the spleen differs significantly between sexes. The mean adult female spleen has a mass of 115g (SD - 51g), while the mean male mass is 139g (SD - 58g) (Molina and DiMaio, 2012a, 2015).

The kidneys, primarily responsible for filtration of the blood and production of urine, sit posteriorly in the abdomen, in the retroperitoneal fat. They are encased in perinephric fat which may offer some protection from impact (Hardy *et al.*, 2015). The right kidney is positioned lower than the left due to the liver above. The renal artery, vein, and ureter enter each kidney at the hilum with the arteries and veins coming directly from the abdominal aorta and IVC respectively. Due to the side by side-nature of the aorta and the IVC, the right renal artery is longer than the left, and the opposite is true of the renal veins (Figure 6.10).

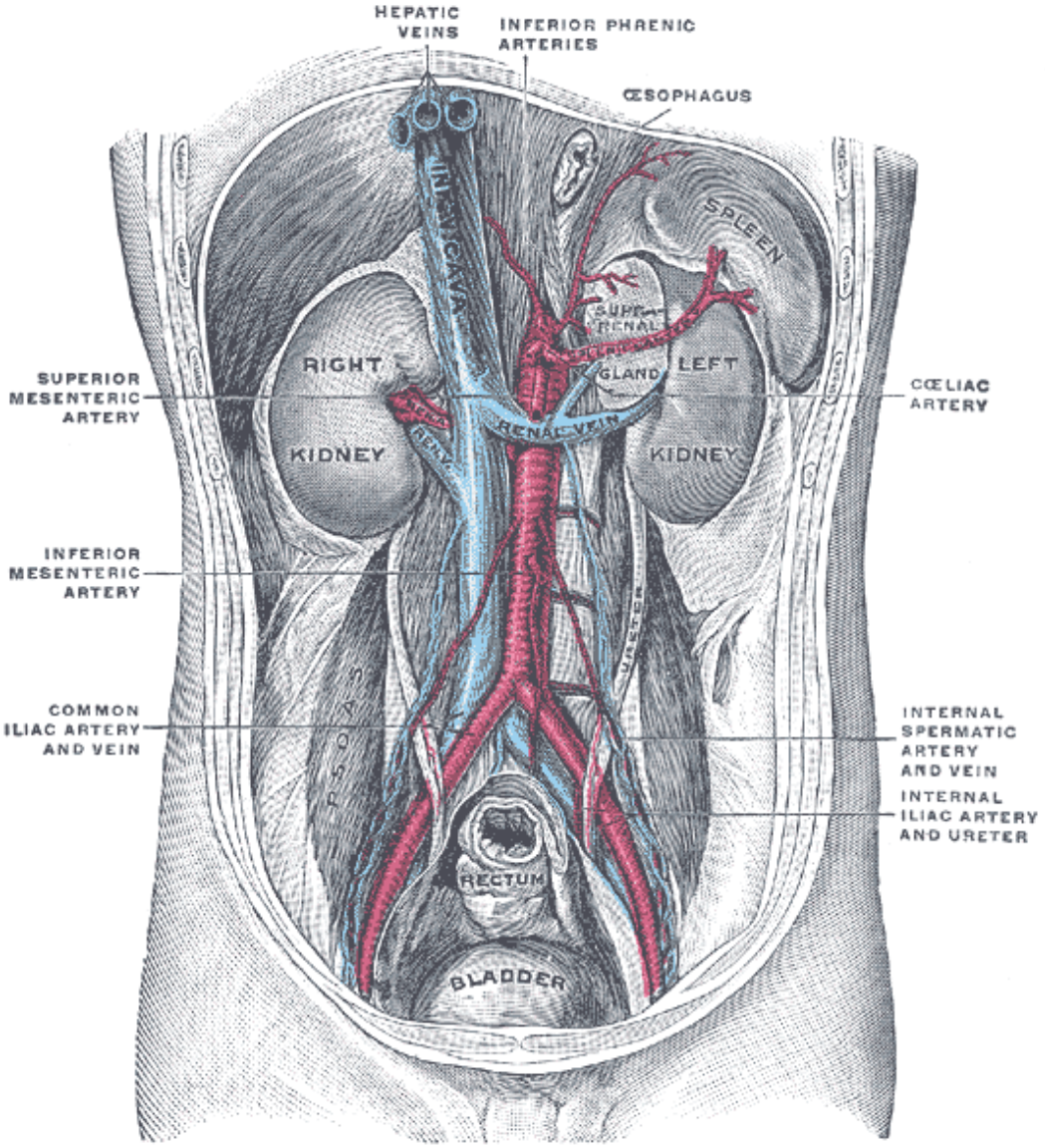

Figure 6.10: The retroperitoneal space showing relative positions of the kidneys and large vessels. From Gray *et al* (1918) .

As with other organs, the masses of the kidneys is higher in men than women. Although left kidneys were consistently heavier than the right, Molina and DiMaio found this to be statistically significant only in men (Molina and DiMaio, 2012a) (Table 6.2).

		Male	Female
Right kidney mass (g)	Mean	129*	108
	SD	26	27
	Range	79-223	67-261
Left kidney mass (g)	Mean	137*	116
	SD	28	32
	Range	74-235	55-274

Table 6.2: Post-mortem masses of young adult kidneys. * denotes a significant difference ($p<0.05$). Data from (Molina and DiMaio (2012a, 2015).

The pancreas is also situated within the retroperitoneal space between the spleen and the duodenum. The pancreas is closely associated with large blood vessels; its uncinated process wraps around the inferior mesenteric artery and the splenic artery runs along the inferior pancreatic border.

The hollow abdominal organs include the stomach, small intestine, large intestine, urinary bladder and gall bladder. The digestive tract is formed from the oesophagus, stomach, small intestine, and large intestine. Within the abdomen, this tract takes a circuitous route from the oesophageal hiatus in the diaphragm to the anus (Figure 6.11).

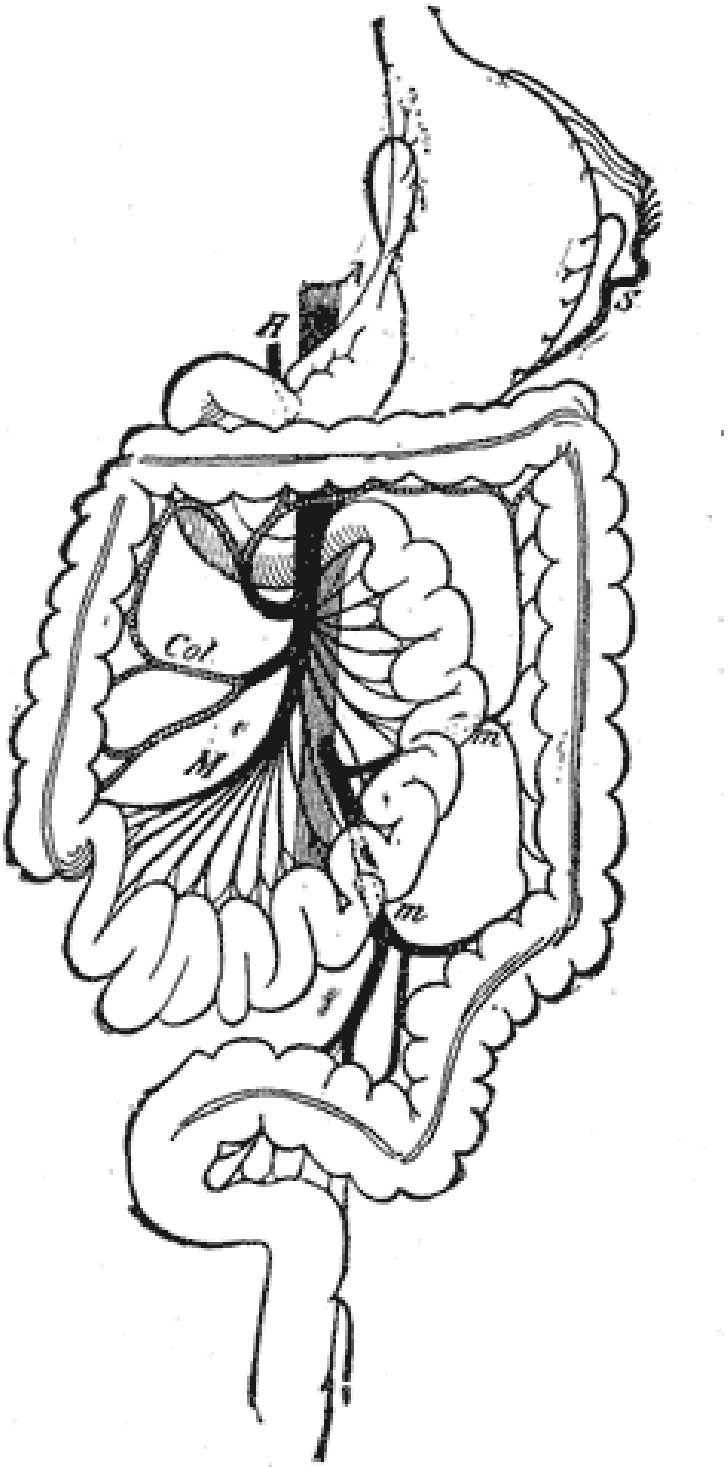

Figure 6.11: Route and position of the gastrointestinal tract from lower oesophagus to rectum with arterial supplies shown. A - Aorta, H - Hepatic artery, M and Col - Ileocolic and right colic branches of the superior mesenteric artery, m - branches of the inferior mesenteric artery. S-Splenic artery. From Gray *et al.* (1918).

The walls of this tract vary somewhat along its length but have a consistently layered structure throughout with (from outside in), a serosa or adventitia, muscularis propria, sub mucosa, and mucosa. Mobility of these organs depends on their peritoneal attachments. With the exception of the duodenum (the majority of which is retroperitoneal), the small intestine is tethered by a long mesentery and therefore very mobile within the abdomen. The large abdomen is similarly split; the ascending and descending portions are retroperitoneal, while the transverse and sigmoid colon are (depending on length) relatively free to move upon their mesenteries.

The internal organs of the abdomen are supplied with blood from branches of the aorta which bifurcates into the left and right common iliac arteries (Figure 6.10). The venous anatomy follows a similar pattern with the common iliac veins forming the IVC although blood from the GI tract and spleen drains predominantly into the portal vein before flowing through the liver.

6.4 Generalities of torso injury mechanisms

Injuries to the internal organs of the thorax and abdomen occur by a variety of mechanisms. Penetrating injuries, as caused by sharp implements, ballistics, or blast-energised fragments (secondary blast injuries) clearly have a separate mechanism from blunt injury in that energy transfer is direct to the organ and does not require propagation through the wall of the torso and subsequent tissue layers. Penetrating injuries will not be discussed in any further details.

6.4.1 Tissue deformation

An injury mechanism is “a description of the mechanical and physiological changes that result in anatomical and function damage” (Viano *et al*. 1989). Understanding these mechanisms provides the basis for determining the response and tolerance for a particular form of loading. Injury is caused by deformation of biological tissues beyond a recoverable limit with damage to structure or alteration in function. Impact from non-penetrating injury generates force due to the inertial resistance of the body tissues and the elastic/plastic (deformation related) and viscous (rate related) compliance of body

structures (Viano *et al*. 1989). This force leads to deformation of tissue which may cause injury.

Deformation of tissues due to blunt loading is measured in strain, the change in any given dimension as a proportion of the original dimension. The ability of any tissue to resist a distorting force is termed elasticity. Moduli of elasticity are the inherent measures of a particular material's ability to resist strain under a specified load (measured as stress, the force per cross sectional area). Strain is a tensor, which means that it acts in all directions. This is typically separated into tensile/compressive strain (stretching of the tissue along with elongation of length or crushing of tissue; this causes a change in size, not shape) or shear (opposing forces acting across a tissue in opposite direction; this causes a change in shape, not a change in size). The moduli of elasticity are also tensors and are partitioned into Young's modulus - the tensile modulus of elasticity, and shear modulus - the shear modulus of elasticity.

Each of these strain types may cause injury to organs including laceration (tearing of the structure) and contusion (internal injury to the structure without tearing of the exterior) (Viano *et al*. 1989). Human tissue, like all biological tissue has viscoelastic properties, meaning that the tissue response is influenced by both degree of deformation, and the rate at which this loading is applied; it is a time-dependent effect. The consequence of this viscoelasticity is a reduced tolerance to a given stress when the load is applied at a high rate. Compressive strain of a soft organ can absorbed if applied slowly but if applied quickly, the organ cannot deform and absorb the applied energy quickly enough with injury occurring prior to change of shape (Viano *et al*. 1989). These viscoelastic properties are of particular relevance with regard to blast injuries. Figure 6.12 demonstrates schematically the effect of this viscoelasticity on the tolerable degree of chest compression for a given rate.

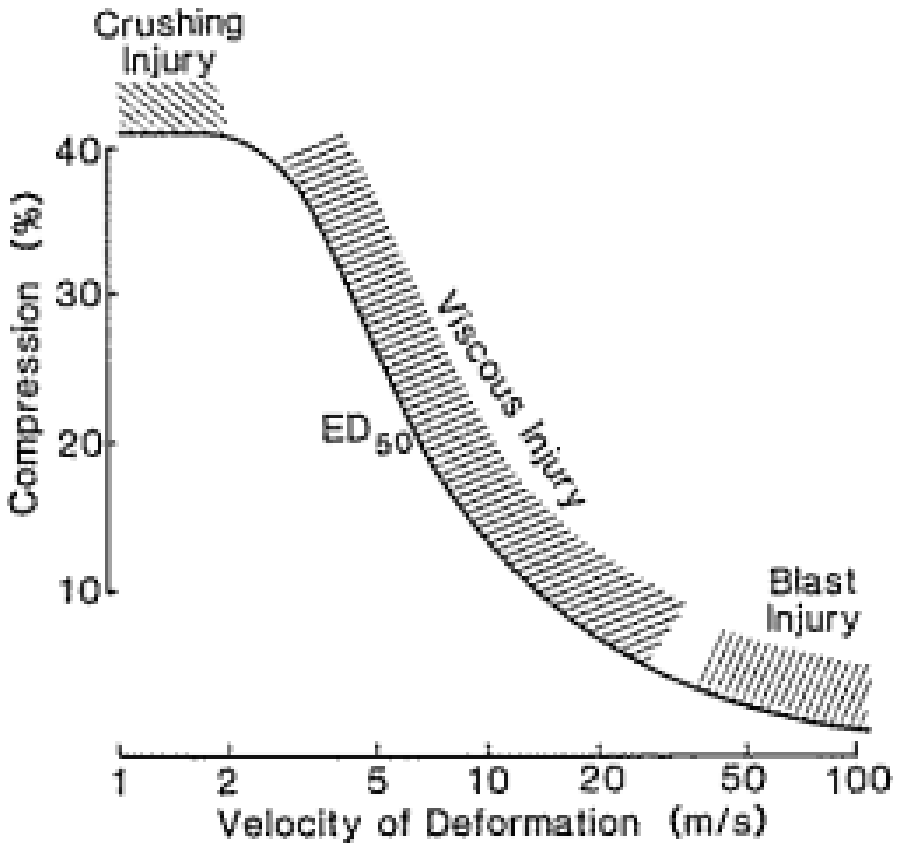

Figure 6.12: Tolerance (of chest injury) showing the effect of low-rate, moderate-rate, and high-rate. With permission from Lau and Viano (1986). ED_{50} is the "effective dose" at which point 50% of exposed samples would sustain injury.

The effect of such rate change is evident in other soft tissues in regard to blast. As an example, work by Bonner *et al* (2015), demonstrates an increase in tensile elastic modulus of knee ligaments in response to increasing strain rate with a plateau beyond a certain limit (Figure 6.13).

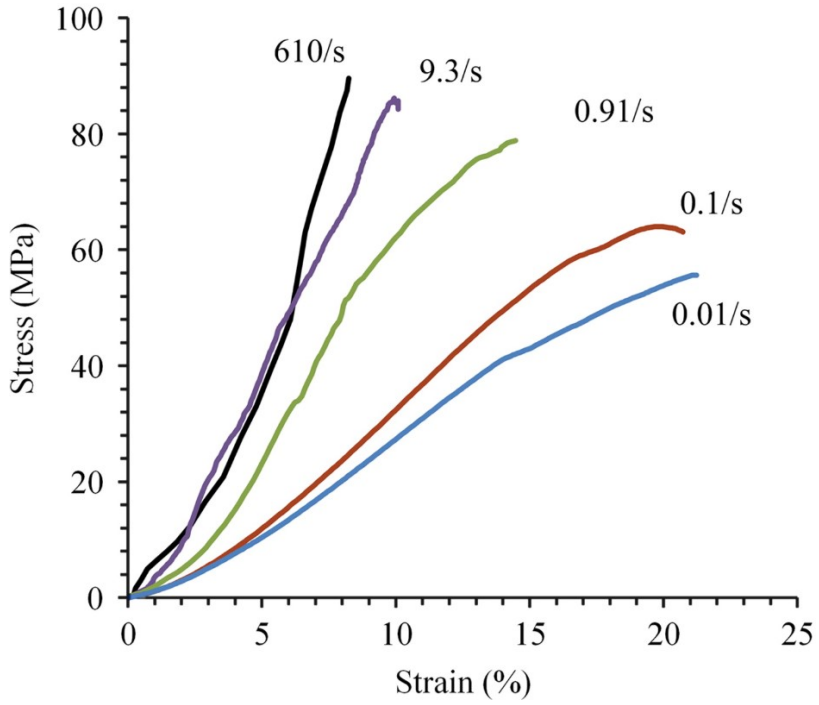

Figure 6.13: Stress strain curves for lateral collateral ligaments of the knee exposed to tensile testing at 5 different magnitudes of strain rate. In this case, statistically significant increases in elastic modulus are encountered up until around $1s^{-1}$ strain rate. With permission from Bonner *et al* (2015).

The importance of this relationship will be explored later in the chapter in regards to injury criteria.

6.4.2 Wave phenomena

Some have attributed the response of the body to high rate loading as being due to wave phenomena (von Gierke *et al.*, 1952; Cooper and Taylor, 1989; Cooper *et al.*, 1991). Cooper and Taylor attributed internal injury from impact to four mechanisms:

Crush– injury occurring due to deformation beyond the elastic limit of the tissue and more dependent upon degree of displacement rather than speed. As described above, the elastic properties of soft tissue change with rate and thus injury itself is to some degree rate dependent.

Stress waves – longitudinal pressure waves travelling at or faster than the speed of sound in the tissue and with considerably greater amplitude than sound waves. Stress waves cause small but rapid tissue distortions and cause injury at a microscopic level rather than macroscopic laceration. Their action is focused at tissue interfaces where the speed velocity of the wave is altered. Stress waves may cause indirect injuries (away from the site of impact) due to reflection, interaction, and reinforcement of the waves producing concentration of the stress at distant sites (Cooper and Taylor, 1989). The magnitude of the stress wave generated is determined by the velocity of the body wall impacted rather than by the magnitude of the deformation.

Shock waves- a form of stress wave characterised by an effectively instantaneous wave front propagated through the tissue at a supersonic velocity. The speed of a shockwave is therefore dependent upon the speed of sound within the medium of transfer. In most soft tissues, this speed is 1300-1500m/s which precludes the generation of shockwaves from most impacts. The speed of sound in lung tissue, however, is only 15-40m/s for lung tissue (Cooper and Taylor, 1989) allowing the generation of true shockwave by some impacts. The transmission of shockwaves and reliance upon tissue impedance has already been discussed in Chapter 1 with regards to primary blast injury. Cooper and Taylor assert that equivalent rates of transfer may also occur from blunt impact if the impacting surface has a high enough velocity.

Shear wave – long duration shear waves of relative low velocity which produce gross distortion of tissue and tissue interfaces. Displacement of the body wall may cause local shear to those organs adjacent to the body wall but also cause indirect injury to more distant sites due to:

I. differential motion of connecting structures,
II. generation of tensile stress at attachment points, and
III. collisions of the organs with stiffer structures.

In contrast to the velocity dependent nature of stress and shock wave generation, the incidence of shear-wave injuries is determined by both the maximum displacement of the body wall and the time taken to attain this displacement (Cooper and Taylor, 1989).

The combination of crush, stress (and shock) wave, and shear wave mechanism perhaps explains the apparent viscoelastic behaviour of the body in response to a variety of traumatic loading. The degree to which any particular mechanism causes injury is more difficult to ascertain but is likely most dependent upon the velocity of that loading and resultant body wall velocity. The majority of "civilian impacts" (including falls, and traffic collisions) are relatively slow and shear wave injury is likely to predominate (Cooper and Taylor, 1989). Conversely, dismounted blast injury is very high rate with stress and shockwave propagation. What remains uncertain is the contribution of these injurious mechanisms to those loading scenarios, such as Underbody Blast, which sit in the middle of this loading rate spectrum. Understanding of this relationship is not merely an academic exercise but has real world application given that protective strategies for low rate transfer (such as a rubber mat) may increase injuries caused by stress wave propagation by reducing the difference in impedance between the impacting and impacted objects (Cooper *et al.*, 1991).

6.5 Grading of torso injuries

Although a large variety of injuries may occur both on and off the battlefield, many of these injuries can be grouped together for the purposes of understanding the underlying mechanism. The following section will firstly discuss the grading of injuries before exploring the component level biomechanics of thoracic and abdominal injuries.

In addition to variation in injury type, the severity of injury varies greatly. The most common method for grading individual injury severity is AIS. Limitations of the use of this scale for predicting survival and statistical problems of combining injury level scores into injury burdens (such as ISS and NISS) have also been discussed previously. The severity of each AIS level equate to:

1. Mild Injury,
2. Moderate Injury,
3. Serious Injury,
4. Severe Injury,
5. Critical Injury,
6. Maximum Injury.

The AIS system was created to code injuries and not as an outcome measure (Petrucelli *et al.*, 1981). The subjectivity of the severity of the levels described above is apparent and yet AIS is routinely used an as outcome measure for both clinical and biomechanical studies. More grading systems for soft tissue injuries have been formed for both prognostic and clinical utility and which map to the AIS system. These systems are validated against clinical datasets and are continually revised as the prognostic value of each system changes with clinical care (Moore *et al.*, 1989, 1990; Tinkoff *et al.*, 2008). Many of these contemporary grading systems are based upon quantitative measurements of CT imaging which improves reproducibility although reduces translation of the same system to cadaveric or computational models, or in situations where imaging is not feasible.

Regardless of limitations to the AIS, the ubiquity of the system for description of injury is apparent. AIS-1 injuries (the "ouch level" - Yoganandan *et al.*, 2014) is used when testing human volunteers. AIS-3—4 level injuries are frequently used as the outcome of biomechanical studies in both cadaveric and animal models. In these cases, that level of injury is used to determine clinical significance. Given that the outcome of any one injury with a specified injury grade may be very different to a different but similarly graded injury, a pragmatic "clinically significant or not" approach may be more appropriate for many biomechanical studies.

6.6 Thoracic Injuries

6.6.1 Rib Fracture

Injuries within the chest can be separated anatomically and by injury type. Rib fractures are the most common clinically significant chest injury in response to frontal and lateral impact and are associated with injury to internal organs; increasing organ injury severity is predicted by an increasing number of rib fractures (Sırmalı *et al.*, 2003). The shape, stiffness, and homogeneity of ribs (and other bones) makes the biomechanics of their failure somewhat more predictable than soft tissue. Ribs fail from bending with failure (fracture), occurring initially at the surface of the rib under tensile stress. With regards to those mechanisms discussed above, maximum chest compression rather than velocity is the predictor of fracture (Melvin *et al.*, 1975), suggesting that viscoelastic effects are less important than strain effects. Melvin *et al* reviewed rib injury data for a variety of studies and concluded that rib fractures were likely with anterior-posterior chest deflection greater than 3 inches and rare with less than 2.3 inches of deflection.

A flail chest describes chest wall injuries in which more than one consecutive rib is fractured in more than position such that there is a "floating piece" of chest wall which moves paradoxically with breathing when compared to the rest of the chest. Flail chest is associated with worse morbidity and mortality than non-flail chest wall injuries which likely related to the severity of underlying lung injury (Dehghan *et al.*, 2014). Although rib-level differences in fracture characteristics of individual ribs have been observed

under anterior-posterior compression (Kindig *et al.*, 2010), the complexity of the rib cage structure makes isolated component testing difficult and perhaps inappropriate.

Rib fractures are not unique to non-penetrating chest impact with fractures also observed from vertical acceleration and blast (Christensen and Smith, 2013; Bailey *et al.*, 2015).

6.6.2 Lung contusion

Lung or pulmonary contusion describes injury to the parenchyma of the lung. Contusion most commonly refers to that tissue injury directly caused by the loading and is characterised histologically by alveolar haemorrhage with subsequent neutrophil infiltration (Figure 6.14).

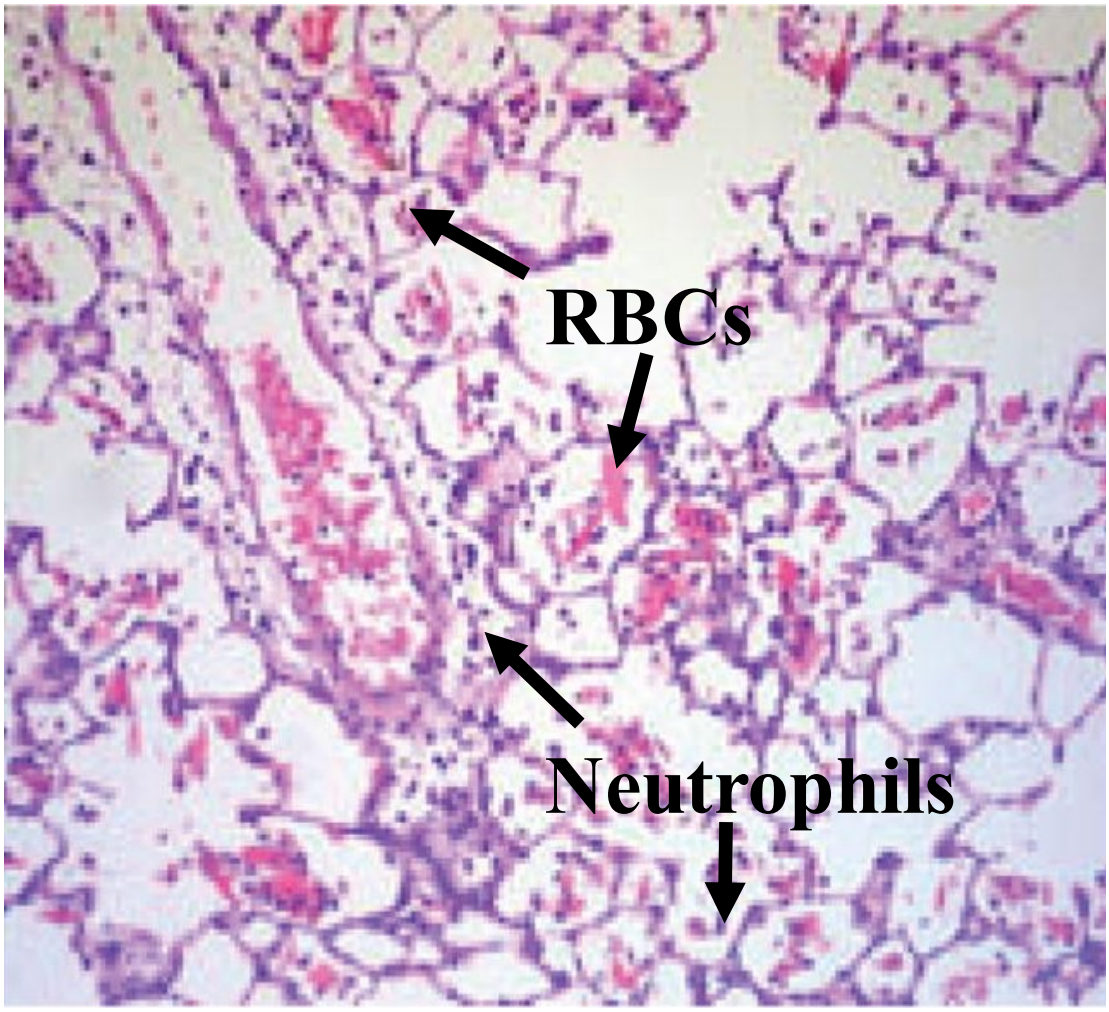

Figure 6.14: 10x Lung tissue section at 24hr post contusion with haematoxylin-eosin staining showing neutrophils, and red blood cells (RBCs) within the air spaces. Reproduced with permission from Raghavendran *et al* (2009).

Macroscopically, the contusion is seen as darkening of the lung with patchy haemorrhage seen on the lung surface (Figure 6.15). These changes have historically been referred to "hepatisation" of the lung (Hooker, 1924).

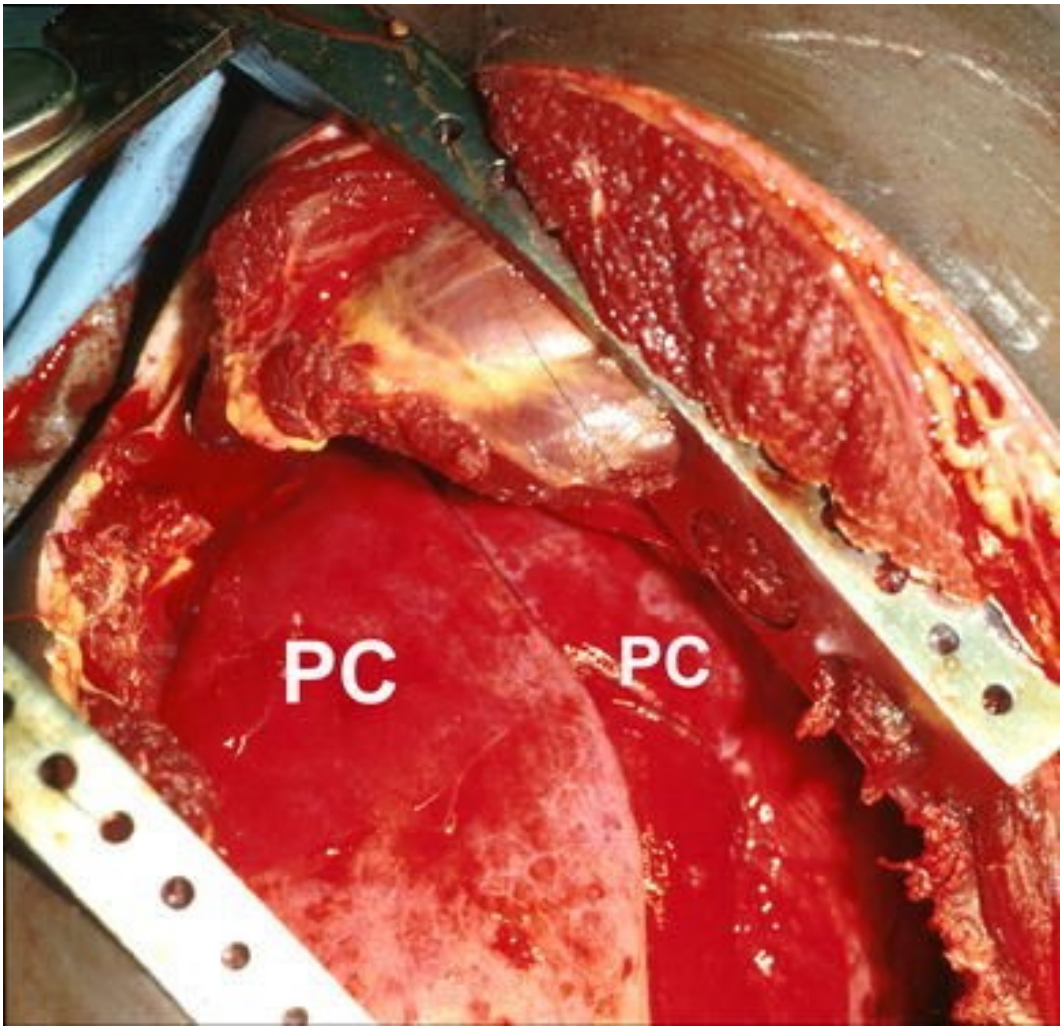

Figure 6.15: Left hemithorax during an emergency thoracotomy showing pulmonary contusion (PC) involving multiple lobes of the lung. Reproduced with permission from Cohn and DuBose (2010).

This contusion may be complicated by Acute Lung Injury which is the intense inflammatory response in the lungs and which may be induced by both traumatic and non-traumatic insults (Raghavendran *et al.*, 2009). Clinical data shows that lung contusion is common from all forms of blunt trauma, occurring in 10-17% of admissions, and particularly common following automotive collisions (Weaver *et al.*, 2009; Rodriguez *et al.*, 2016). Lung tissue contrasts greatly with ribs and other bones in that the lung is able to undergo large scale deformation without injury. Injury to the lung parenchyma is therefore not determined by magnitude of compression but by the speed of this compression (Fung and Yen, 1984). Rib fracture is commonly associated with lung contusion (55.8% of contusion patients had rib fractures) but chest wall injury is

by no means ubiquitous with lung injuries which is further evidence of the disparate injury mechanisms (Rodriguez *et al.*, 2016). The sparing of the ribs is more likely in younger patients in whom the chest wall itself is more elastic or ductile and able to undergo large deformation without fracture (Cohn and DuBose, 2010)

As described above, lung injury likely results from the propagation of stress and/or shockwaves through the lung. Impact experiments on excised rabbit lung showed worsening of injury when the lung was supported on a rigid plate rather than a net. This worsening was explained by reflection of the compressive wave by the rigid boundary condition, and thought to confirm the wave mechanism of this injury (Fung *et al.*, 1988).

In further contrast to rib injury, physical models of lung contusion use live animal tissue. A variety of small and large animal models have been used to study lung contusion with the majority aiming to better characterise the pathophysiology and cellular mechanisms of pulmonary contusion (Raghavendran *et al.*, 2009). Although large animals have been used, they are limited by high cost and low sample number (Davis *et al.*, 2000). Rodent models of lung contusion are well established for examination of the cellular mechanisms of lung contusion and associated with higher sample numbers and lower cost (Raghavendran *et al.*, 2009).

In addition to describing the pathological and immunological response to lung contusion, rodents have also been used to describe the relationship between impact loading and injury (Hoth *et al.*, 2006; Gayzik *et al.*, 2007). Gayzik *et al* directly impacted the lungs of anaesthetised Sprague Dawley rats through an open thoracotomy. They collected force and deflection data and following recovery of the animals, followed them up with serial CT imaging. The CT changes and force data were used to create a computational model of lung injury which showed that maximum injury was predicted by the product of maximum principle strain and strain rate, thus demonstrating that there is a viscoelastic component of failure that should be borne in mind.

Although lung contusion can be complicated by acute lung injury and acute respiratory distress syndrome, the injury itself likely occurs as a broad spectrum. The imaging based study by Rodriguez *et al* suggests that increased used of CT imaging has increased diagnosis of pulmonary contusion including a significant proportion which is not

clinically significant. They suggest that contusion should be viewed as part of a thoracic injury complex (Rodriguez *et al.*, 2016).

6.6.3 Lung laceration and pleural injury

Lung contusion refers to microscopic scale lung injury, but impact and accelerative loading also causes large scale lung injury. Laceration of the lung refers to tearing of the lung parenchyma. Unlike lung contusion, laceration is likely a consequence of shear stress within the lung tissue rather than compressive stress waves (Wagner *et al.*, 1988). Alternatively, injury to the lung can be caused by direct impact with a fractured rib end and is therefore dependent upon chest wall deflection (Wagner *et al.*, 1988). Lacerations are associated with high energy impacts and as a consequence are more frequently found alongside a significant polytrauma burden (Hollister *et al.*, 1995). The lung laceration itself may cause large volume haemorrhage into the parenchyma of the lung or the pleural space and may cause haemodynamic instability and death (Masuda *et al.*, 2007; Pearce *et al.*, 2017). Lung lacerations may be categorised based on their site and mechanism and are frequently associated with pneumothorax and haemothorax (Hollister *et al.*, 1995).

Pneumothorax and haemothorax describe collection of air and blood within the pleural cavity. Pneumothoraces may be caused either by disruption of the parietal pleura by a rib fracture or by primary rupture of the visceral pleura with flow of air into the pleural space from the lung. Haemothorax may be caused by lung laceration, or by bleeding from the heart, great vessels or intercostal vessels. Both haemothorax and pneumothorax may be observed in the absence of rib fracture (Shorr *et al.*, 1987). Although these injuries are well documented in *in vivo* impact and accelerative loading experiments (which will be discussed later in the chapter), the complex mechanism of injury (which is likely a combination of shear wave, stress wave, and crush) and necessary boundary conditions are difficult to replicate at a component level.

6.6.4 Heart Injury

Blunt traumatic cardiac rupture is associated with a high mortality rate and death at scene (Brathwaite *et al.*, 1990; Alanezi *et al.*, 2002; Teixeira *et al.*, 2009) . The spectrum

of cardiac injury is broad although the right side of the heart is more commonly injured (Teixeira *et al.*, 2009). The heart may be both contused and lacerated. The former is likely a result of high velocity compression and the latter due to gross deformation by the posterior aspect of the sternum (Cavanaugh and Yoganandan, 2015). The function of the heart may also be affected in the absence of anatomical injury such that the electromechanical rhythm is disturbed. *Commotio cordis* (Latin: "disturbance of the heart") may result in sudden death without morphological damage to the heart (Kohl *et al.*, 2001). Dysrhythmias from blunt impact are diverse and may include transient alterations which indicate ischaemia as well ventricular fibrillation (Cooper *et al.*, 1982). This phenomenon (whilst fascinating), without structural heart injury is unlikely to be of particular significance within the high rate accelerative loading scenario given that it seems to require transient impact at a specific time within the cardiac cycle and with force applied to the specific point upon the heart (Cooper *et al.*, 1982; Kohl *et al.*, 2001; Link *et al.*, 2001).

6.6.5 Great Vessel Injury

Injury to the thoracic great vessels is associated with high mortality with the majority of deaths occurring at scene in both civilian and military settings (Mattox, 1988; Eastridge *et al.*, 2012). Although all vessels are susceptible to injury, injuries to the venae cava, azygous systems, and pulmonary vessels are less common and as a result less characterised (Kudsk *et al.*, 1984; Collins and Robinson, 1989; Sharma and Rawitscher, 1999; Ambrose *et al.*, 2000; Lim *et al.*, 2013).

6.6.6 Thoracic Aortic Injury

In contrast to other great vessels, blunt injury to the thoracic aorta has been well studied clinically and biomechanically. Although most commonly observed following motor vehicle collision, Blunt Traumatic Aortic Rupture (BTAR) has been recognised for a long time with reports that Vesalius was amongst the first to document it as far back as 1557 (Parmley *et al.*, 1958). Interest in the injury is driven by the effect it has upon mortality. A major US study reported that injury of the aorta occurs in less than 1% of collisions but is responsible for 16% of deaths with 80% dying prior to admission at

hospital (Neschis *et al.*, 2008). Similarly, Richens *et al* reported BTAR in 21% of UK road traffic deaths (Richens *et al.*, 2003). Despite this clinical interest, the precise mechanism by which BTAR occurs is greatly contested. The most consistent finding, from both clinical and post-mortem studies is of a transverse laceration at the level of the aortic isthmus just distal to the origin of the left subclavian artery (Figure 6.5), which is observed in over 90% of cases. Smaller number of injuries occur at the root, ascending, or arch portions of the aorta (Fabian *et al.*, 1997; Teixeira *et al.*, 2011). Injuries may vary in severity from limited intimal tears to complete transection with free haemorrhage into the chest or mediastinum. The tear is thought to originate on the intimal surface (Viano, 1983). BTAR is more common following lateral impact with risk of injury not eliminated by the use of seat belts or air bags (Richens *et al.*, 2003).

The tissue properties of the thoracic aorta have been well characterised. The stress-strain response of the vessel wall has been shown to be non-linear with stiffening of the tissue with elongation beyond the physiological level (Viano, 1983). Differences in tissue properties are observed at different portions of the aorta. Lundevall found the strength of the isthmus and descending aorta to be 63% and 80%, respectively, of the ascending aorta (Lundevall, 1964).

The tissue is both strain rate sensitive and anisotropic, exhibiting different material properties based upon the direction of loading. Mohan and Melvin conducted material testing of samples of the descending thoracic aorta using both uniaxial and biaxial testing devices and at both quasi-static (~0.01s^{-1}) and dynamic rates (~20 s^{-1}) (Mohan and Melvin, 1982, 1983). They demonstrated strain rate sensitivity of the aorta with stiffness increasing by 1.8 times for the dynamic tests over the static. This strain rate sensitivity was consistent in both circumferential and longitudinal directions. The samples consistently failed in a direction perpendicular to the long axis of the vessel, consistent with injuries described clinically (Mohan and Melvin, 1983). Mason *et al* developed a new biaxial testing device able to consistently hold small samples of aortic wall and subject them to very high rate loading in both longitudinal and transverse directions (Mason *et al.*, 2005). High rate testing using this device did not show significant strain rate sensitivity when varying between strain rates over ~75s^{-1} (Shah *et al.*, 2006). This group also performed whole aorta component level testing and

concluded that the aorta fails in the transverse direction with complete transection occurring from 92 N of axial tension and 0.221 of axial strain.

Three putative mechanisms have been proposed as the cause of BTAR (Cavanaugh and Yoganandan, 2015):

- crushing of the vessel against the vertebral column during anterior-posterior compression;
- traction of the vessel between relatively mobile portions and points of fixation; and
- rapid intraluminal pressure increase.

Crushing of the vessel between the chest wall and vertebrae has been proposed based on physical models using excised canine aorta (Crass *et al.*, 1990). This "osseous pinch" theory has been criticised as simplistic given that it neglects the influence of other mediastinal structures.

Traction of the vessel due to relative motion is the most widely held mechanism of BTAR (Sevitt, 1977; Viano, 1983).The descending aorta remains relatively fixed at the posterior thoracic wall by the intercostal arteries and pleura while the heart and ascending aorta are able to displace, causing strain at attachment points). Displacement of the heart may be caused by direct impact although it is thought that inertial loads from a blood filled heart may also cause sufficient displacement under certain conditions (Viano 1983).

The contribution of intraluminal pressure increases to BTAR remains uncertain. Strassman (1947) proposed that either compression of the heart due to the hydrodynamic affect of acceleration increased aortic pressure enough to burst the vessel. Stresses in a cylindrical model inflated by internal pressure are predominantly circumferential and would cause longitudinal tears unless the transverse strength is more than twice the longitudinal strength if the thin cylindrical pressure theory holds true under these conditions (Viano, 1983). Such a substantial difference in strength has been demonstrated but only at high rates (Mohan and Melvin, 1983). Mohan and Melvin

hypothesised that high intraluminal pressure could induce instability and ballooning in the vessel wall and predispose the creation of a transverse tear (Mohan and Melvin, 1983). Experimental data on the hydrodynamic pressure caused by blunt impact has been compared to the pressure required to burst the aorta in component testing (Lundevall, 1964; Viano and Warner, 1976). The pressure increase caused by the impact amounted to only around 20% of that required to lacerate the vessel in the ex vivo experiment (Viano, 1983), suggesting that intraluminal pressure alone is insufficient to cause clinically relevant injury.

It is thought that the actual mechanism of aortic rupture is multivariate, involving both hydrodynamic and displacement-induced tension (Viano, 1983; Richens *et al.*, 2002). Maximum displacement of the heart during frontal impact occurs at the same time as peak hydrodynamic pressure (Viano *et al.*, 1978a). Voigt and Wilfert described a shovelling effect in response to superiorly directed frontal loading (Voigt and Wilfert, 1969). This mechanism proposed that impact to the chest and upper abdomen displaces the mediastinum upwards ("shovelling"). The resultant compression of the heart would squeeze blood into the aorta with resultant pressure rise while also displacing the heart and aortic arch cranially. This displacement would create tension at the isthmus which would act in combination with raised intraluminal pressure to create a transverse tear (Richens *et al.*, 2002). Direction of the impact to the chest and the resultant deformation is likely important as to defining the exact mechanism of BTAR. Impact acting right to left predominates in clinical data which is perhaps more likely to force the heart and aortic arch posteriorly and cranially with stretch at the isthmus (Gotzen *et al.*, 1980).

Recreating these mechanisms experimentally has proven challenging. Aortic injuries have been created in both small and large animal of models of frontal impact(Viano and Warner, 1976; Culver *et al.*, 1977; Viano *et al.*, 1978a). Reproducing these injuries in post-mortem human surrogates (PMHS) has not been as succesful. Viano (2011) impacted the chests of eleven unenbalmed, repressurised cadavers with a 24-34kg mass at 8.6-14.9ms^{-1}. Autopsy showed severe chest injury with multiple rib fractures and four cases of heart laceration. One cadaver sustained a rupture of the ascending aorta but no isthmus injury was generated. Viano did not publish his results at the time and only in retrospect suggested that the organ positions within an upright cadaver were not representative of a living subject.

Hardy *et al* (2006) investigated BTAR mechanisms in several quasistatic and dynamic tests in which the heart and aortic arch were directly displaced, with resultant isthmus injury. Their results indicated that neither intraluminal pressure nor whole body acceleration were required. Hardy *et al* (2008) conducted impact tests with a variety of loading scenarios upon 8 unenbalmed PMHS. These tests used a 32 kg impactor and crucially placed the cadavers in an inverted position. High speed cineradiography observed aortic motion. BTAR was induced in seven of the eight cadavers. Transverse failure occurred at the isthmus. Peak strain of 0.208 was similar to that seen in component level testing performed by Shah *et al* (Shah and Mason, 2005; Hardy *et al.*, 2008). This longitudinal stretch was found to be the principle component of injury causation. Thoracic deformation (at least in the context of frontal impact) was required for injury generation.

6.7 Abdominal Injuries

As with thoracic blunt trauma, the majority of abdominal blunt injury (in both children and adults) is caused by road traffic accidents (Yoganandan *et al.*, 2000a; Karamercan *et al.*, 2008; Poplin *et al.*, 2015). Patterns of abdominal injury are influenced by loading scenario and direction but the liver and spleen are most frequently injured in road collisions (Yoganandan *et al.*, 2000b). A description of the injury mechanism for each organ includes understanding of the material properties of theses organs under loading. These tests cannot recreate the complex mechanisms generate by impact or acceleration but demonstrate the material level response of the tissues. Testing methodologies vary but most subject small samples of the relevant tissue to tension or compression in one or more directions with measurement of the resultant stress and strain.

6.7.1 Liver Injury

The anatomy of the liver has already been discussed. Its large size and soft parenchyma make it vulnerable to impact injury (Melvin *et al.*, 1973). Injuries to the liver vary in both type and severity. Mild injuries include subcapsular haematoma while severe injury types include burst-like injuries with tearing of the capsule; and hepatic avulsion (Tinkoff *et al.*, 2008). Both the liver and spleen are at more risk of injury than the hollow

organs as they are essentially incompressible (Hardy *et al.*, 2015). Although somewhat protected by the lower ribs, they are still vulnerable to direct impact. The relatively large masses of these organs and points of fixed attachment also predispose them to inertial strain due to whole body acceleration. The material properties of the liver have been evaluated using both animal and recently deceased human specimens (Santago *et al.*, 2009; Brunon *et al.*, 2010; Kemper *et al.*, 2012). Changes in temperature and the use of freezing changed the material properties of the tissues which makes human cadaveric component level testing difficult. Comparison of human to porcine tissues demonstrated higher failure stresses in porcine tissue. No difference was seen between human and bovine tissue (Kemper *et al.*, 2010). Kemper *et al* also demonstrated that the human liver parenchyma has non-linear and rate dependent material properties in tensile testing with failure strain significantly decreased with higher loading rates (Kemper *et al.*, 2010). Further work by Kemper *et al* (2013) demonstrated similar properties of human liver parenchyma in compression.

6.7.2 Spleen Injury

As with the liver, the spleen is partly shielded from impact by the lower ribs. Although splenic injury frequently occurs alongside rib fracture, isolated splenic injuries are also common and the number of rib fractures is not predictive of splenic injury severity (Boris *et al.*, 2014; Rostas *et al.*, 2017). Splenic injuries are graded by injury severity and vary from small sub capsular haematoma to a completely shattered or devitalised spleen (Tinkoff *et al.*, 2008). Far fewer studies of splenic material properties have been conducted than of liver but similar trends are seen across the two tissues (Hardy *et al.*, 2015). Splenic samples (including parenchyma and capsule/parenchyma) specimens exhibited non-linear rate dependent properties in both tension and compression with decreased failure strain and increased failure stress at higher loading rates (Kemper *et al.*, 2012).

6.8 Impact testing

Although material properties derived from mechanical testing are important data for the development of computational models and for comparison of different tissues, they

provide little information as to how this stress is generated during an impact or accelerative event. Injury to the tissues and organs of the chest and abdomen is highly dependent upon the anatomical constraints and attachment of these tissues. These attachments are not replicated for material testing. Instead, in-situ impact and accelerative tests must be performed. These tests may be conducted upon animals or PMHS depending upon the application or injury of interest.

In each case, the test aims to recreate some form of loading scenario under laboratory conditions. Biomechanical response (which may include deformation, acceleration, force, or pressure) is measured and recorded. Resultant injury is obtained from physical examination and/or imaging (Cavanaugh and Yoganandan, 2015).

This in situ testing can be divided into those tests that replicate focal loading tests and those that replicate whole body accelerations. In reality, any high rate loading scenario (either automotive, aeronautic, or UBB) is likely a combination of these effects.

6.8.1 Frontal impacts

Frontal impact tests use a variety of impactors to simulate interactions of the vehicle occupant with different components of the vehicle interior. Rigid bars and disks may be used to simulate the effect of a steering wheel or column upon the torso. Initial studies of impacts to the thorax used a six inch pendulum which impacted upon the sternum of unembalmed PMHS (Lobdell *et al.*, 1973; Kroell *et al.*, 1974; Nahum *et al.*, 1975). Each measured the resultant deflection against impact force (as measured at the impact surface) under slightly different scenarios (Cavanaugh and Yoganandan, 2015). The responses of these tests can be divided into a loading and unloading phase (Melvin, 1985). Initially, there is a rapid rise in force with minimal deflection (high initial stiffness) followed by a force plateau until the point of maximum deflection. The unloading phase followed the non-linear loading which would be seen in quasi-static tests of the thorax (Melvin, 1985).

Injuries produced during these frontal chest impacts included lacerations of the heart, liver, and spleen (Kroell *et al.*, 1974). The comparability of the visceral response during PMHS testing to real life loading is uncertain. As has already been discussed, difficulty

in experimental recreation of aortic injuries led to the use of inverted positioning in an attempt to approximate living anatomy (Hardy *et al.*, 2008; Viano, 2011). Similarly, using impact force as the "dose" of trauma has limited utility given that the relationship quantifies only the risk of injury given a very specific point of impact (and with a specific point of measurement).

The soft tissue limitations of PMHS may be complemented by the use of animal models of frontal impact. Lau and Viano subjected rabbits to sternal impact and found that both bronchial injury and pulmonary contusion could be predicted by a combination of chest wall displacement and impact velocity (Lau and Viano, 1981a). Culver *et al* caused reproducible aortic injury from frontal impact of rabbits and suggested the use of high speed radiography as a methodology for assessing internal organ response (Culver *et al.*, 1977). Frontal impact upon the porcine thorax may cause heart, aortic, lung, and liver injury (Viano *et al.*, 1978a). The position of the impact (high, mid, or low sternum) was shown to change the injury pattern.

Frontal impacts of the abdomen most commonly reproduce steering wheel loading using some form of rigid bar. Hardy *et al* examined and reanalysed the existing body of rigid bar abdominal impact data in 2001 (Hardy *et al.*, 2001). This data was drawn from PMHS, porcine, and primate testing (Stalnaker and Ulman, 1985; Cavanaugh *et al.*, 1986; Viano *et al.*, 1989; Nusholtz and Kaiker, 1994). Their data showed rate sensitivity of injury to impact with greater rate dependence occurring in those tests in which the impactor/subject mass ratio was high. Hardy *et al* performed their own PMHS tests which confirmed this rate dependence and found it to be more pronounced in free back tests (the PMHS is not fixed to the back of the seat and therefore subject to whole body acceleration) which they propose is due to additional inertial loading (Hardy *et al.*, 2001).

Following on from their work examining aortic injury within inverted PMHS, Howes *et al.* (2013) used a similar model to best approximate living torso anatomy for PMHS study of abdominal loading. They compared the anatomical geometry of the thoraco-abdominal contents in this position to magnetic resonance images of living subjects and found it to be a better representation than conventional PMHS positioning. Howes *et al* concluded that this phenomenon could explain previous experimental discrepancies for

torso injury and that differences between PHMS and living subject organ position should be a consideration for future research.

As with thoracic loading, some of this discrepancy may be overcome by the use of anaesthetised animals. Abdominal impact testing has been performed on a variety of animal subjects (including rabbits, pigs, and primates) with emphasis typically placed upon the generation of liver injuries (Mcelhaney *et al.*, 1971; Melvin *et al.*, 1973; Lau and Viano, 1981b; Rouhana *et al.*, 1985). As with thoracic loading, differences in size and anatomy must be acknowledged and where possible, accounted for.

6.8.2 Additional impact scenarios

Given that frontal impacts are the most common cause of automotive injury (Viano *et al.*, 1989) evaluation of frontal impact testing is a suitable way to explore historical and contemporary knowledge of the torso response to impact. For the purposes of automotive impact, a variety of additional impact modes have been tested. These include lateral and oblique impact testing in addition to the contribution of seat belt and air bags to injury (Cavanaugh and Yoganandan, 2015; Hardy *et al.*, 2015). Although the injury patterns and loading parameters for each of these scenarios may be slightly different, the detail of each is beyond the scope of this thesis. Importantly, clinical data and automotive data demonstrates that the direction of loading may influence the likelihood of injury(Siegel *et al.*, 2004). Given that the component level properties of the tissues remain consistent, these differences in patterns must relate to orientation of the organs to loading and the resultant differences in tethering and boundary conditions. These differences require that separate injury criteria may be required for different loading pathways.

6.9 Whole-body acceleration

The test scenarios outlined above replicate focal loading to the chest and abdomen using pendulums, impactors, and bars. The aim of these experiments is to reproduce impact from a particular part of a vehicle interior (such as the steering wheel, steering column, or door post). These experiments are important but are directed at very particular

environments and therefore of limited translatability to the mounted blast environment. Whole body testing examines the tolerance of the internal organs when the torso is subjected to a well-distributed load which may not grossly deform the cavity. In this case, the organs are accelerated through their attachment to their surroundings and by the contact forces developed between the organs and the internal thoracic wall (Mertz and Gadd, 1971).

Understanding the results of rapid acceleration is essential in building a working knowledge of the force and tolerance limits of the body. Determining the tolerance of the body to pure acceleration indicates the degree to which environmental and structural effects are the cause of injury; and determines the extent to which mitigating and preventative design may be of use. Although change in velocity is estimated to be the strongest predictor of torso injury and death following automotive collision, the extreme tolerance of the body to these accelerations is difficult to obtain from field data as estimation of collision, or blast velocity is not always possible (Siegel *et al.*, 2002, 2010).

Estimations of the tolerance to acceleration have thus been made using descriptions of falls, human volunteers, anesthetised animals, and PMHS subjects.

6.9.1 Falls from height

Falls are the major cause of trauma in England and Wales (Kehoe *et al.*, 2015). However, the majority of these falls are from standing or low level and cause injury in elderly and frail patients. Exploring the tolerance of a body to extreme acceleration requires a high rate of change in velocity, which in the case of falls requires that a great enough velocity is first reached before impact with the ground.

Resultant velocity (v) can be calculated from initial velocity (u) if both acceleration (a) and displacement (s) are known and the effects of drag (or wind speed) are negligible [Equation 6.1):

$$v^2 = u^2 + 2as \quad [6.1]$$

For the purposes of a fall from height, the initial velocity is zero, the acceleration is that due to gravity, and this displacement is the height of the fall [Equation 6.2]. This assumes that terminal velocity due to drag is not reached prior to impact. Calculation of terminal velocity requires

$$v = \sqrt{2gh} \quad [6.2]$$

Of course, neither an acceleration of 1g nor a velocity alone will cause injury. The negative acceleration caused at impact is a function of the resultant velocity prior to impact (from Equation 6.2) and the stopping distance. This deceleration distance is determined by the stiffness of the impact material and the compliance of the human body (including the tissues of the body, but also, importantly, the position and compliance at the joints).

De Haven (1942) used these characteristics to examine the tolerance to acceleration based on survivor accounts of falls from between 50 and 150 feet. In each case, the height of the fall was exactly known but estimating the impact acceleration was difficult as the apparent deceleration distance varied between body parts. De Haven concluded from these cases (which were all sustained in a predominant frontal, or G_x, direction) that the human body could tolerate 200g for brief intervals without sustaining significant injury.

Injury records of fatal falls from height have also been examined. Heart, aortic, and liver injuries are well described in post mortem evaluations of both accidental and suicidal falls from height (Atanasijevic *et al.*, 2009; Casali *et al.*, 2014). Casali *et al* described over 300 suicidal falls from height and reported high incidence of rib (92%), lungs (76%), heart (53%), liver (58%) and aorta (43%) injuries (Casali *et al.*, 2014). Incidence of the visceral injury (but not of rib or head injury) was statistically related to the height of the fall suggesting a greater dependence of these injuries upon change in velocity.

Inference of the absolute response to acceleration can be made by comparing survivors and non-survivors of falls from height. Risser *et al* (1996) reported no survivors of falls from greater than 18m in a series of 41 patients while Lapostolle *et al* (2005) studied the records of 287 patients and concluded that both height of fall and point of bodily contact were independent predictors of death. The latter finding suggests the importance of direction of loading to both injury pattern and severity. They concluded that those who experience purely vertical loading (G_z) landed feet first and sustained severe lower limb injury (Lapostolle *et al.*, 2005). This injury pattern is not quite analogous to seated underbody blast loading as the lower limb itself acts as a "crumple zone" during a fall and increases the deceleration distance to the thorax.

Attempts have been made to correlate risk of death with height. Smith *et al* have suggested an LD_{50} (the height at which 50% of those falling would die) of between 14.8 and 20.1m (M. R. Smith *et al.*, 2017). Discrepancy in their data arises from uncertainty on the exact fall height and normalisation of the number of floors fallen to either 3 or 4m. Their data suggested the LD_{50} had increased over recent decades (perhaps due to improved clinical care) but that 24m represented the maximum fall height tolerable (Smith *et al.*, 2017).

Calculations of terminal velocity was not considered in these cases. Terminal velocity (the point at which acceleration due to gravity is equalled by air resistance from below) may be calculated based upon an assumed cross-sectional area, constant air density and drag coefficient. Terminal velocity of a human in free fall is approximately 55m/s and likely to occur following around 12s of free fall during which time the person would have fallen ~500m (Warner and Demling, 1986). This distance is so much greater than the likely survivable height that terminal velocity does not pragmatically need to be considered.

More precise measurements of the thoracic tolerance to falls from height have been generated using human volunteer tests. Mertz and Gadd conducted sixteen tests upon a professional high diver from between 8.3m and 17.4m (Mertz and Gadd, 1971). He was instrumented and landed supine upon a soft foam. They calculated a peak acceleration of 49.2g with a duration of 100ms. No injuries were sustained nor discomfort

experienced. They subsequently recommended that an anterior-posterior chest acceleration of 100ms be the tolerance limit (Mertz and Gadd, 1971).

6.9.2 Vertical acceleration

Injury and death from falls provides a rough estimate of the tolerance of the body from vertical loading. The variation in fall height and orientation in clinical data restricts the use of this data for the inference of precise tolerances. Equally, understanding injury tolerance to falls has clinical importance but prevention of these injuries relies more upon the prevention of the fall itself.

As the study of impact injury has been driven by the automotive advances, understanding the response to vertical acceleration and the requirement for protection from this form of loading has been driven by aeronautic advances (Chandler, 1988).

Vertical accelerative loading has applications both to crash worthiness and ejection seat tolerances. Research into this domain began during and after WWII (Chandler, 1988). Eiband summarised the war time and immediate post war research and made it apparent that the tolerance to impact was dependent upon four primary factors (Eiband, 1959):

- the direction of the acceleration;
- the magnitude of the acceleration;
- the duration of the acceleration; and
- how the occupant body is supported during the acceleration.

Eiband combined the available data at this time and developed tolerance curves for acceleration in different directions (Eiband, 1959). Research analogous to UBB was described as “headward” acceleration. The injury patterns most commonly described were bony spinal injuries. Human volunteer studies (using catapults) were analysed and a tolerance limit of 16g for up to 0.04 seconds described. Given the use of volunteers, this tolerance described the border of non-injury to minor injury. Tolerance to severe spinal injury was described using animal data with tolerance of 110g for 0.002 seconds without injuries seen in pigs and 42g for 0.048 seconds in chimpanzees (Eiband, 1959).

The use of animal testing for defining human tolerance to injury has been described as a limitation of Eiband's work (Franklyn and Lee, 2017). Despite this, animal models have frequently been used for other impact scenarios (as described above) and although caution should be used when interpreting absolute values, these tests are fundamental for the understanding of injury mechanism and development of injury criteria. Animal models are of particular relevance to severe injury when human volunteers are not appropriate.

The pattern of human torso injury in response to UBB (as described in Chapters 4 and 5) has not previously been described although similar injuries have been shown following air-crashes. The direction of occupant loading during such a crash may be complex with both frontal, side, and vertical forces. A review of crashes and resultant injuries described frontal impact as the principal force in most cases (Wallace *et al.*, 1971). Wallace *et al* also describes a particular case in which an aircraft was subject to purely vertical impact having following entanglement with power lines. In this instance, all six occupants died from internal injuries despite no evidence of external trauma. Wallace suggested that the protective features of an aircraft seat were ill equipped to prevent injuries when vertical impact was predominant (Wallace *et al.*, 1971). This might represent a similar scenario to UBB.

Experiments which determine the tolerance of these internal organs to vertical loading cannot be performed with human volunteers and instead, with the caveats outlined above, are reliant upon animals or computational simulations. Historically, these experiments were performed using rocket powered sleds in a programme initiated by John Stapp which used both human volunteers and animals (Stapp, 1957; Snyder, 1970). Animals were anaesthetised and restrained in a sitting position with backs against the floor of the sled. A stopping mechanism enabled reasonable control of both duration and magnitude of the deceleration. Stapp demonstrated visceral haemorrhage in pigs exposed to around 80g for 30ms in a $+G_z$ (upwards) direction (Stapp, 1957). Cook and Mosely performed similar experiments upon 8 black bears at varying accelerations and durations (Cook and Mosely, 1960). They described the occurrence of cardiac injury, mediastinum haemorrhage (without aortic rupture), along with lung haemorrhage and liver injury. Internal injuries were associated with fractures of the vertebral column and ribs. Severe internal injuries were seen in two bears who underwent accelerations of

~130g for around 15ms (Cook and Mosely, 1960). Cook and Mosely suggested traction of these structures in response to relative inertia as the cause of injury.

Hanson used a canine model to investigate mediastinal injury in response to G_z acceleration (Hanson, 1967). 2/7 subjects (those exposed to >35g for around 30ms) sustained injury to the aortic arch with avulsion of the brachiocephalic artery. Hanson suggested an inertial mechanism of injury due to relative motion of the cardiac mass. A radiographic system was used to show the relative position of the heart and diaphragm during different phases of the acceleration (Figure 6.16).

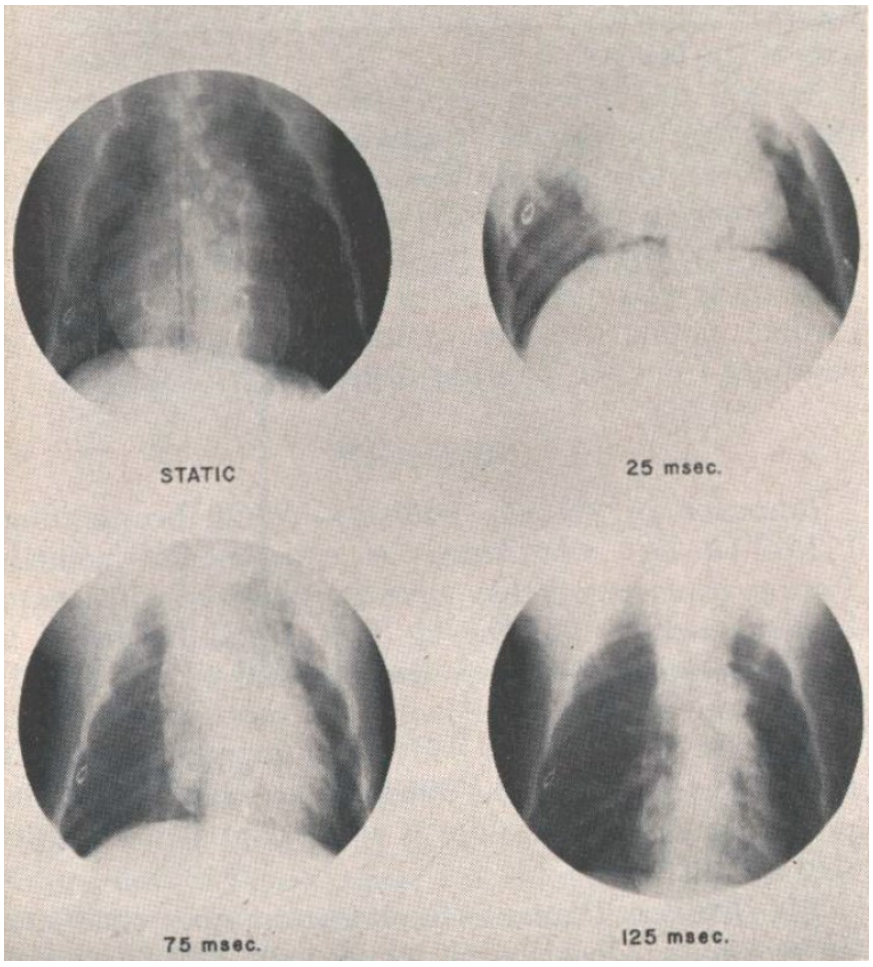

Figure 6.16: Thoracic radiographs showing relative motion of the heart and diaphragm during G_z acceleration. From Hanson (1967).

Hanson asserted that injuries sustained to the aorta were caused by tensile strain generated in the aorta by the cranial and caudal displacement of the heart described by Figure 6.16. He suggested that tension exerted on the descending aorta is stretched by diaphragmatic and visceral attachments and further increased by acceleration of the heart (Figure 6.17). As with the aortic experiments described above, greatest stress is likely to have occurred at the classically susceptible points, the root and isthmus.

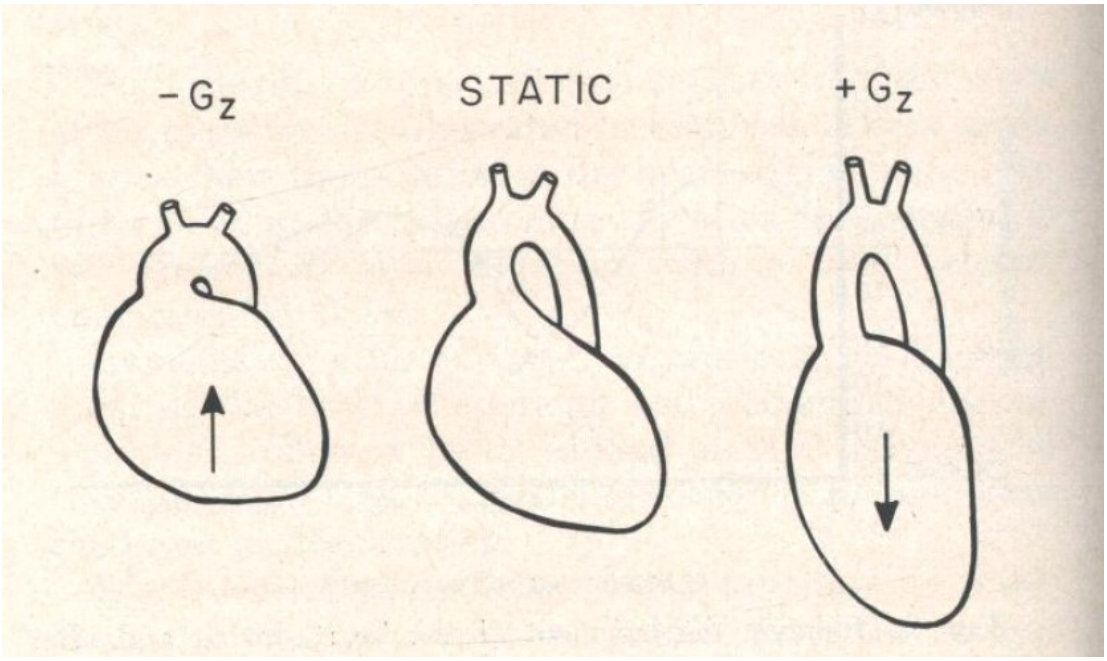

Figure 6.17: Relative movement of the heart in response to Gz loading. Reproduced with permission from Hanson (1967).

The description of the heart mass as a spring mass system is comparable with other mechanical analogues of the thorax and abdomen. Understanding of the body as a mechanical transmission system allows the calculation of forces and resulting displacement between organs and tissues. The theory of such models is that they allow a quantitative understanding of the observed biological phenomena. These models may range in complexity but are formed from masses, springs and dampers (such as Figure 6.18).

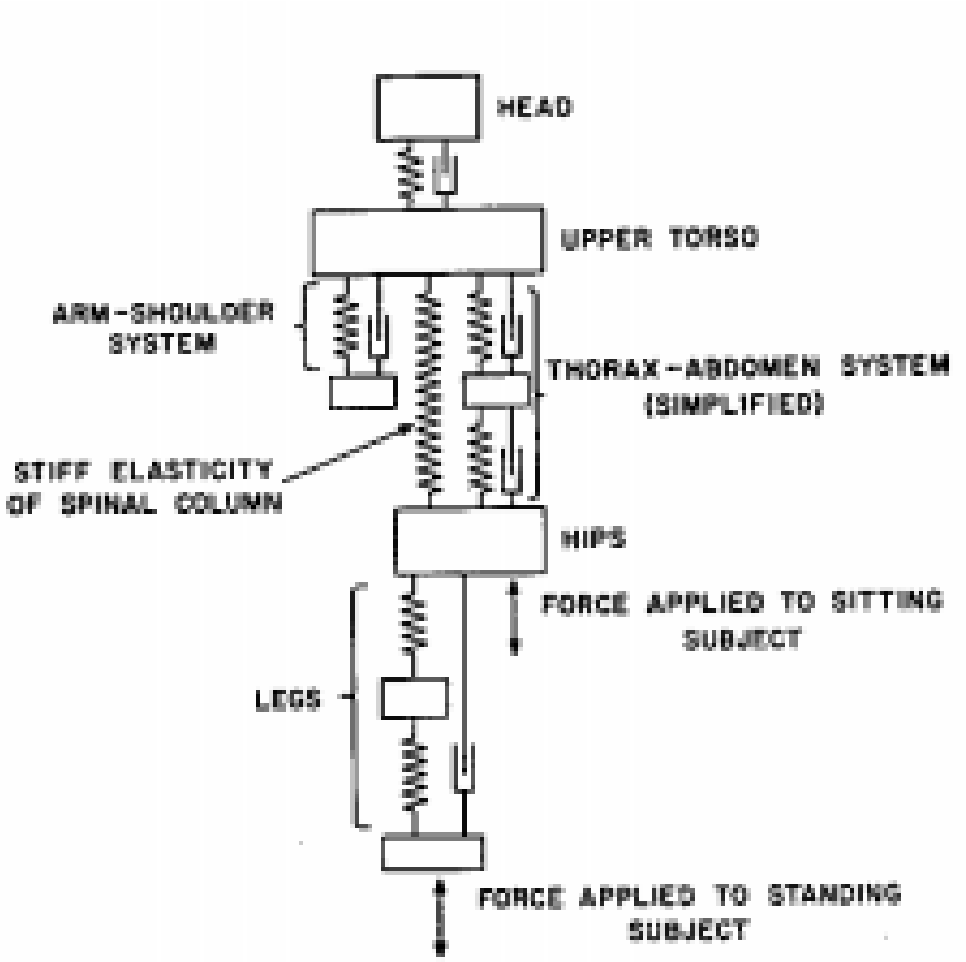

Figure 6.18: Mechanical analogue of the human body exposed to longitudinal vibration or impact. The greatest influence on the impedance of the system is the spring and dampers of the spine and torso. Reproduced with permission from Coermann *et al.* (1960).

The main concern with the use of a mechanical analogue is the failure of the system to take into account the non-linear response of tissues which occur in the force ranges of interest (Coermann *et al.*, 1960). Similarly, the models themselves may have no way of detecting injury; the injurious response to the calculated imposed force may not be known. It is for these reasons that experimental study of the loading is required.

Kazarian investigated the use of primates for G_z loading (Kazarian, 1975). In contrast to the rocket sleds used by other researchers, Kazarian used a drop tower rig in order to evaluate the spinal response of chimpanzees, rhesus monkeys, and baboons. Impact

velocity was determined by the drop height with deceleration profile altered using a crushable aluminium honeycomb (Figure 6.19)

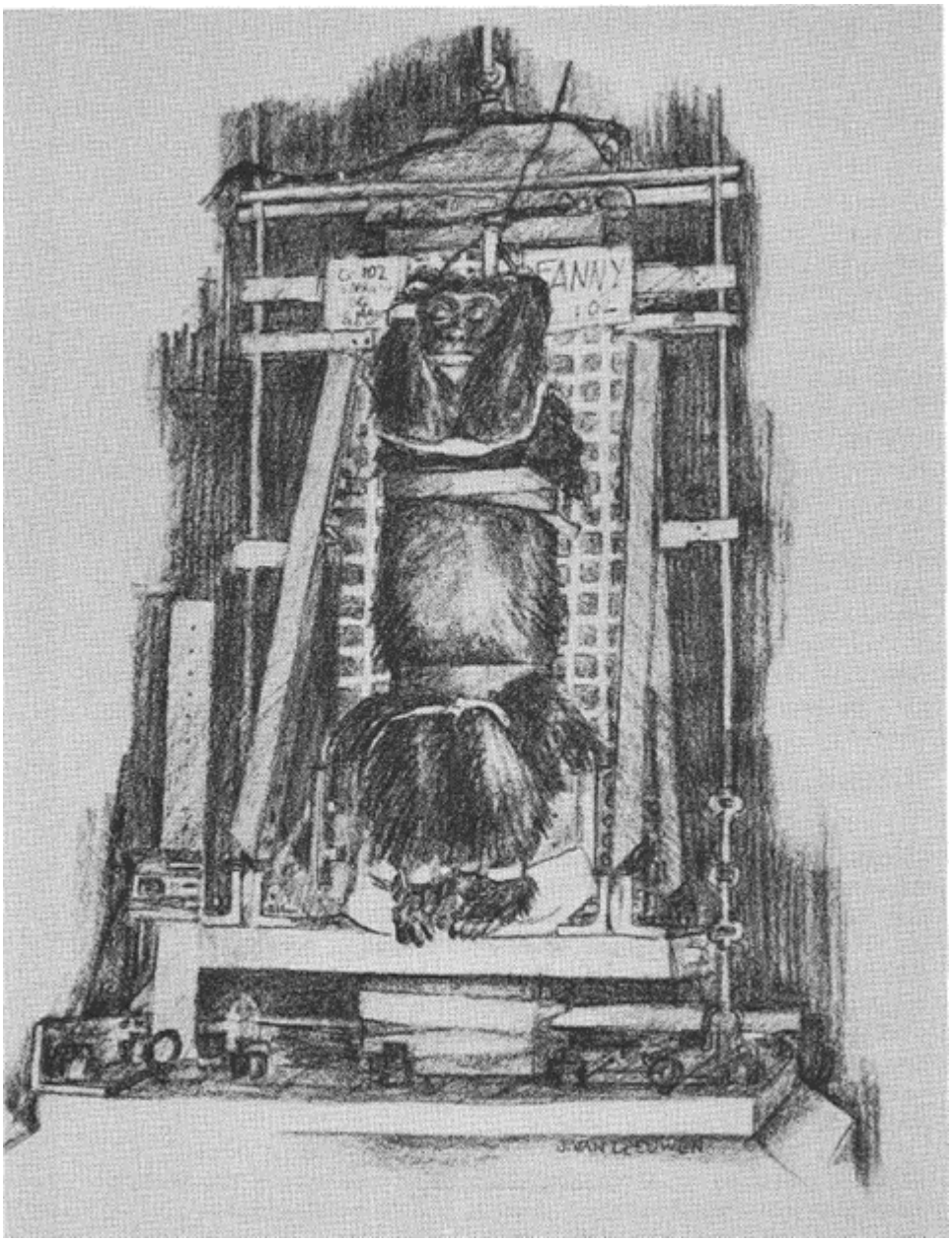

Figure 6.19: Chimpanzee restrained upon a drop tower for Gz loading. Reproduced with permission from Kazarian *et al.* (1969).

Although the primary aim of Kazarian's work was to describe spinal injury in response to G_z impact, he also noted internal injuries. A series of experiments using the above impact vehicle was performed upon Rhesus monkeys undergoing $+G_z$ accelerations between 25-900g (with durations 2-22ms) (Kazarian *et al.*, 1970). Injuries were observed in the liver, lungs, and heart.

Kazarian remarked upon the contrast in understanding of bony spinal injuries and soft tissue torso injuries: "*Although additional modes of injury to the various internal organs are known to occur, quantitative information on internal organ dynamics and injury probability, along with clinical dysfunction and symptomatology, is almost non-existent. Consequently, the mechanisms of injury to the various components within the torso are not understood in enough detail to be quantitatively compared with the injury predictions resulting from the use of higher degree of freedom mathematical models*" (Kazarian *et al.*, 1970). Although mathematical models may facilitate the understanding of load transfer and the inference of injury mechanisms, they are very limited in their ability to predict injury.

Kazarian observed haemorrhagic injuries in five organ systems: lungs, liver, heart and great vessels, gastrointestinal tract, and central nervous system. Haemorrhage into the lungs was sub pleural and distributed along the base of all the lobes at short acceleration time histories. As the total time duration and G level increased, haemorrhage into the lungs was complicated by superficial irregular lacerations at the roots of the lungs, or at the base of the heart (or both) and resulted in a haemothorax in 15% of all experiments. Contusion and laceration in the base of the lungs over the area in contact with the dome of the diaphragm extending 2-5 mm into the lung parenchyma were common (Kazarian *et al.*, 1970). Rupture of the aorta just distal to the aortic root was observed in 5 of 104 cases although the loading threshold for these injuries is not described. Myocardial contusion and rupture were relatively common at accelerations greater than 40ft/second.

Injuries to the diaphragm ranged from haemorrhage into the musculature (which was occasionally observed), to tearing at the marginal points of attachment, and, in four cases to extrusion of abdominal viscera into the thorax.

Haemorrhages of the liver measuring 0.5-2.0 cm were present in 89% of all cases. Subcapsular hematomas in the diaphragmatic surface of the liver and ragged lacerations lateral to the falciform ligament were observed. Occasional lacerations at the periphery of the superior convex surface of the right lobe involved the capsule and underlying hepatic parenchyma. Moderately large 1-3 cm areas of haemorrhage into the soft tissue of the porta hepatitis were observed in all animals exposed to acceleration levels greater than 130 G. In 24% of these experiments, deep parenchyma lacerations radiating from the large hepatic veins near the terminations in the inferior vena cava were observed. Injuries to the spleen, pancreas, and kidneys were uncommon.

Kazarian related the internal organ injuries to the acceleration and time duration of the impact and showed that lung injury was the primary mode on injury before vertebral body fracture, liver injury, and heart injury (Figure 6.20).

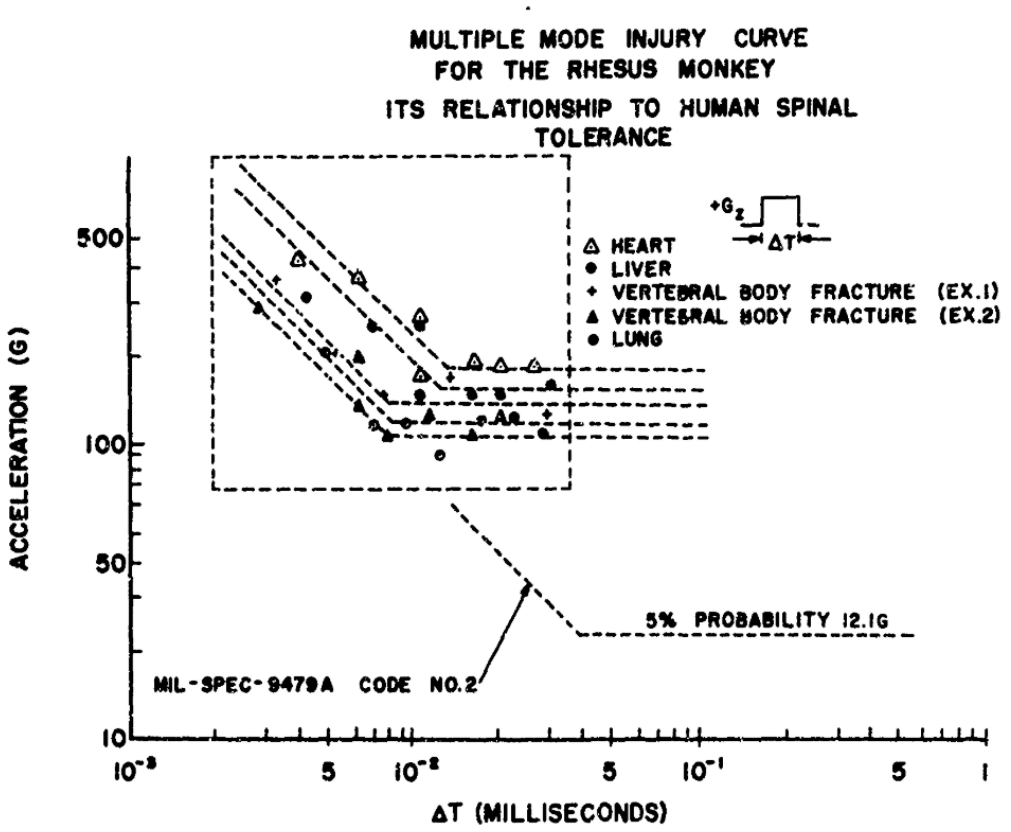

Figure 6.20: Spinal and organ injuries in rhesus monkeys in response to +Gz impact. Injury occurrence at particular accelerations and durations are shown. Reproduced with permission from Kazarian *et al.* (1970).

As with Hanson, Kazarian also described the organs in reference to a mass spring system and stated that the degree of excitation of an individual organ is a function of its location, mass, physical dimensions, and elastic limits of suspensory, and accessory attachments along with the point and method of attachment to the surrounding structures. At certain critical frequencies, the relatively unsupported organs within torso were observed to move as a semi-viscoelastic mass and oscillate within various cavities. These hydrodynamic characteristics were observed on film and described in several stages:

- a free-fall stage - The organs respond to the drop fall in their individual manner, but in general are forced upward against the respiratory diaphragm with stretching of the intestines and mesentery. This stage pre-supposes an initial $-G_z$ accelerative stage which is relevant to crash testing but not to UBB. This freefall stage may preload the suspensory attachments and modify the transmission of loading;
- an impact stage - At the instant of impact, the pelvis, sacrum, and vertebral column act as the prime load-bearing, load- transmitting structures surrounded anteriorly by tissue onto which the rate dependent organs are anchored. These structures are unable to respond immediately to the impact deceleration and exhibit a complex mechanical behaviour. Following impact, a time varying mechanical and volumetric distortion occurs with the entire torso compressing under decelerative loading. As it arrives at a level of maximum compressive deformation, a fullness develops under the surface of the skin which Kazarian described as the surface wave; and
- an expansion phase – this surface wave is seen to propagate up the animal with complex reflections and attenuation before apparent rebound causes expansion of the body with reversal of the initial deformation.

Kazarian inferred that this compression and expansive behaviour observed at the surface was associated with similar distortions of the torso organs with injury occurring when the strain-time relationship of this deformation was outside of the elastic limits of the relevant organs (Kazarian *et al.*, 1970). The group did not measure the precise mechanical behaviour of the torso itself and believed that a novel methodology would be required in order to describe the relationship of this torso deformation to organ injury.

Weiss and Mohr described internal organ movement of human volunteers in response to (considerably lower) accelerations (Weis and Mohr, 1967). Volunteers experienced up to 65G for around 7.5ms. The tolerance level was the discomfort described by the volunteers. Cineradiography was used to describe the movements of the organs. In apparent concordance with the kinematic characteristics described by Kazarian, Weis

and Mohr observed a wave of relative radiolucency passing up the volunteers and being most pronounced within the abdomen. The motion of the liver was seen to coincide with this wave.

Weiss and Mohr took their findings to concur with those of Kornhauser and von Gierke who had postulated a critical velocity for short duration loading (von Gierke *et al.*, 1952; Kornhauser and Lawton, 1961; von Gierke, 1968). These models assumed for short duration loading below the critical frequency of the observed system, the overall velocity change must be sufficient to induce the necessary physical response. What remained unsure was the level of physical response required to cause sufficient strain, and therefore injury, within each system.

More recent linear sled testing upon anaesthetised swine has also shown torso injuries subsequent to $+G_z$ loading (Guan *et al.*, 2018). Guan *et al* demonstrated increasing injury severity with increased impact velocity and hence deceleration. The swine subjects sustained lung, heart, spleen and spine injuries although no liver or great vessel injuries. Test subjects exhibited torso compression although the group didn't explore the relationship of this deformation to injury although they did quantify the degree of spinal flexion.

Lung haemorrhage is also described in small animal models of impact loading (Richmond *et al.*, 1961; Fiskum and Fourney, 2014). A recent rodent model of UBB (developed primarily to investigate brain injury) demonstrated lung haemorrhage to be the primary cause of death in animals accelerated beyond 2000g (Fiskum and Fourney, 2014). Although this model is one of very few to reproduce pure whole body vertical acceleration without prior free fall stage, the animals themselves were positioned prone and acceleration was therefore directed perpendicular to the axis of the spine. Furthermore, the animals were enclosed with no way to record their biomechanical response.

The response of the human torso to vertical loading has been evaluated using cadavers. Danelson *et al* compared the response of PMHS to Anthropomorphic Test Devices (ATD), using a whole body explosive driven blast buck (Danelson *et al.*, 2015). These tests are were performed to show the biofidelity of these devices and investigate skeletal

injury in response to UBB. As such, the cadavers were not ventilated or perfused and internal organ injury not described. The biomechanical response of the torso was noted, however, with up to 20% compression of the torso height in response to the loading. Importantly, the ability of the torso to compress is not a feature of contemporary ATDs (Danelson *et al.*, 2015).

6.10 Injury Mechanisms for UBB

What then is the likely injury mechanism of the internal organs in response to UBB? Prediction of these injuries requires a mechanical hypothesis. Firstly, it is assumed from the clinical data presented in Chapters 4 and 5 that injuries occur in response to vertical loading applied through the seat. This load is transferred through the pelvis. Injury to the organs likely occurs as a result of two mechanisms: direct compression of the organs in the axial direction, or by relative movement of the organs causing tears at points of attachments. Individual organs may be injured be either or both mechanisms depending upon anatomical factors. Compression of the liver and other abdominal organs due to displacement against each other, the diaphragm, or the lower ribs may cause laceration at point of compression. Tensile strain at the ligamentous and peritoneal attachments of the organs due to inertial effects may cause injuries to these tethering points. Further shear may be generated at the vascular insertions given that the IVC and hepatic veins are fixed to the liver. This mechanism, as it applies to the liver is shown in Figure 6.21.

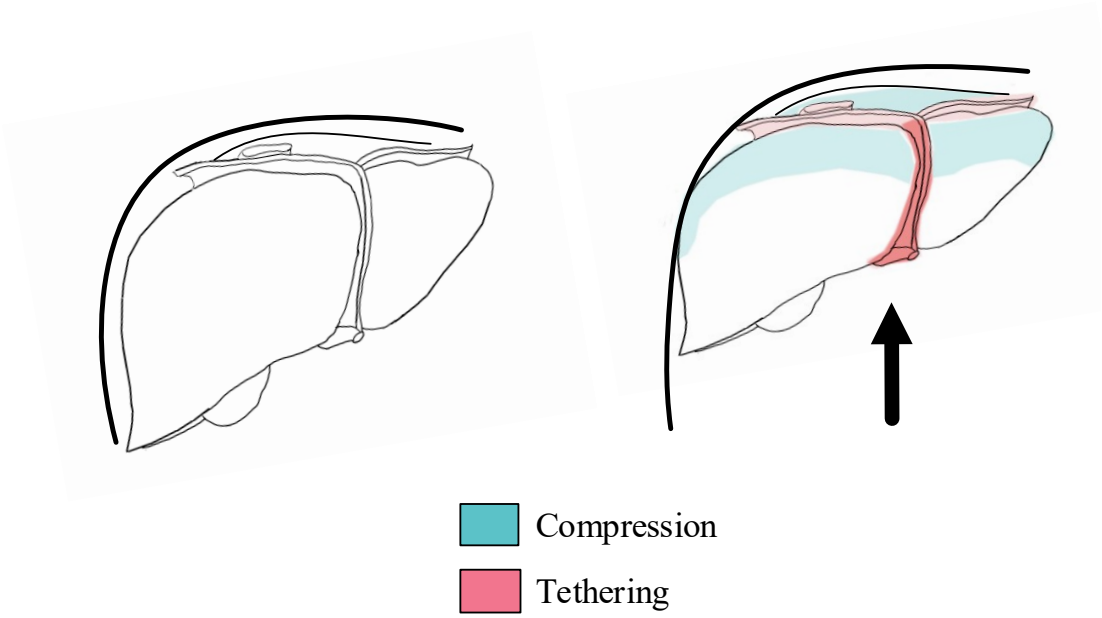

Figure 6.21: Proposed injury mechanism for the liver following UBB loading. Craniad displacement of the viscera causes direction compression against the diaphragm and adjacent organs. Tethering of the organ by peritoneal attachments (particularly those orientated parallel to the direction of loading) would result in shear strain at these points.

This craniad displacement of the abdominal contents and diaphragm would cause direct compression of the lungs (both at point of impact and at distant interfaces. This direct compression may cause parenchymal injury similar to that described as primary blast lung in mounted blast (Singleton *et al.*, 2013). Gross disruption of the lungs, including laceration, and injuries to the great vessels and mediastinum are more likely caused by relative movement of these organs, with tethering most pronounced around the pulmonary ligament (Figure 6.22).

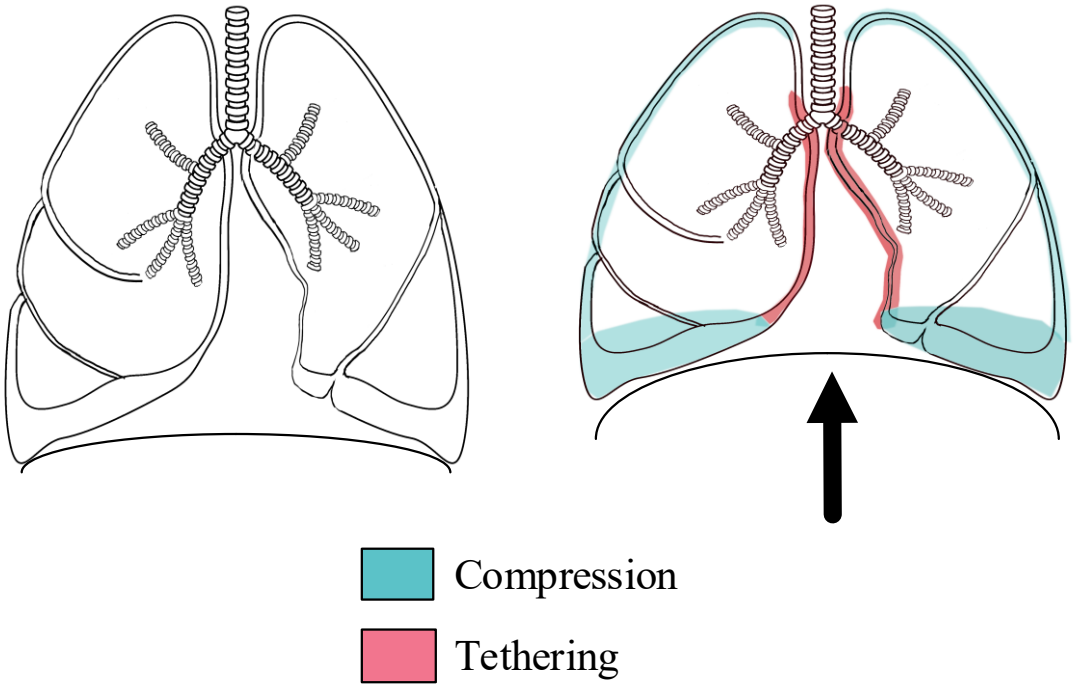

Figure 6.22: Proposed injury mechanism for the lungs following UBB loading. Craniad displacement of the viscera and diaphragm compresses the lungs and generates shear at the points of tethering.

Injuries to the heart and aorta could also arise from craniad displacement of the abdominal contents causing direct compression of the heart. As the heart is displaced vertically, the relatively mobile aortic arch is also displaced with strain generated at the aortic tetherings (including vessels and the commencement of the retro-pleural descending aorta. The overall effect would resemble the shovelling mechanism proposed by Voigt and Wilfert (1969) and is depicted in Figure 6.23.

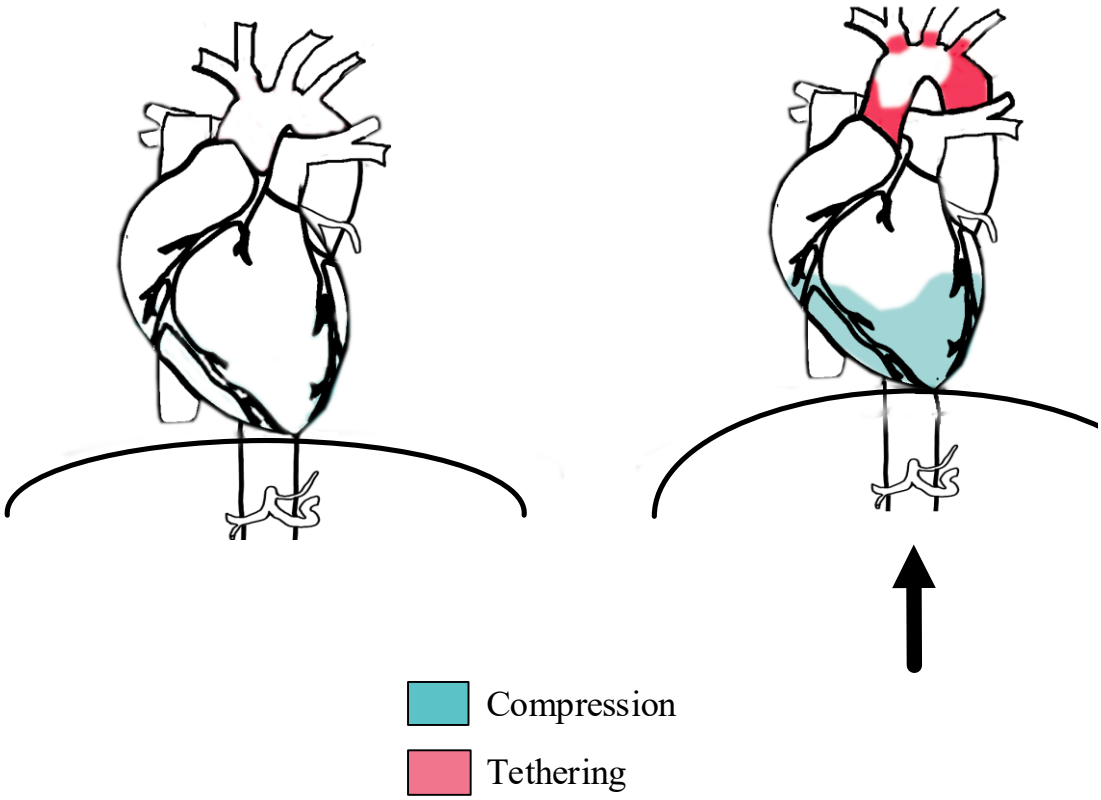

Figure 6.23: Proposed injury mechanism of the heart and aorta following UBB loading. The pericardium is not shown.

What is clear from these proposed mechanisms is that axial displacement of the organs (either together or separately) is required. The rate of loading is important given that firstly, individual organs are known to be rate dependent with higher stiffness and therefore greater strain at higher rates; and secondly because the rate of impact is likely to affect the degree of displacement of the organ assuming that each may be somewhat described by a mass-spring system.

Previous research is not able to satisfactorily predict injury in response to this loading. Mechanical analogues, whilst explaining the injuries, are unable to predict injury given the need to make broad assumptions about the non-linear nature of the soft tissues. The dynamic response index (DRI, based upon such a mechanical analogue and assuming shock loading (based upon the natural resonance of the system) has already been shown to be inaccurate for prediction of spinal injury in UBB (Spurrier *et al.*, 2015). This discrepancy is likely because the DRI assumes a single spinal spring and does not

account for changes at different levels. The boundary conditions of the soft tissue organs relative to one another are even more complex, and the relationship of the input loading, physical response of the torso, and resultant injury have not been established. An important aim of injury biomechanics research is not only to describe this mechanism but to accurately predict its occurrence and therefore allow the implementation of mitigation systems. The following section will explore currently used injury criteria for both conventional and UBB loading.

6.11 Injury Criteria

Although a wide variety of animal, human volunteer, and cadaveric studies are used, the common goal by researchers is to correlate injury outcomes to some form of biomechanical parameter. These parameters, injury criteria, may then be used to predict the risk of a particular injury. Risk curves may be generated for particular injuries and injury criteria using survival analysis or non-linear regression approaches (Hardy *et al.*, 2015). Statistical considerations for the generation of these curves will be considered further in Chapter 9.

Different physical parameters have been investigated and developed in order to predict chest and abdominal injuries in response to impact. This section will discuss some of these parameters including those currently used for the assessment of UBB.

6.11.1 Acceleration

The acceleration criterion is known for application in whole body response studies and for the assessment of chest injury following frontal impact (Lau and Viano, 1986; Hardy *et al.*, 2015). Acceleration data can only meaningfully be measured on bony structures and so is typically based upon the acceleration of a particular point on the spine (Lau and Viano, 1986). Human tolerance for chest injury is often stated as the peak spinal acceleration not to exceed 60g for longer than 3ms (Cavanaugh and Yoganandan, 2015). This is based on the previously mentioned work of Stapp, Mertz, and Gadd who used human volunteers (Stapp, 1957; Mertz and Gadd, 1971). As a consequence, this tolerance limit applies only to frontal acceleration and is a discriminator of non-injury

vs minor injury rather than of severe injury or survivability and so is not relevant to the subject of this thesis.

Eppinger developed the Thoracic Trauma Index (TTI) as a predictive criterion for chest injury in response to lateral impact (Eppinger *et al.*, 1984). The TTI uses maximum side rib acceleration. Further work by Cavanaugh *et al* developed the criterion using average spine acceleration which was shown to have better predictive value than TTI in sled testing (Cavanaugh *et al.*, 1993). Both tools were specific for lateral impact testing. Eppinger also demonstrated a limited ability of the TTI to predict upper abdominal organ injury from side impact although this did not apply to middle or lower organs.

Later, Horsch *et al* reported no correlation between abdominal injury and lower spinal acceleration measured directly opposite to the impact site (Horsch *et al.*, 1985). This was unsurprising given the location of the accelerometer away from the site of frontal impact loading although both Viano *et al* and Brun-Cassan *et al* have also described the limitations of using acceleration as an abdominal injury criterion (Viano *et al*. 1989; Brun-Cassan *et al*. 1987).

Despite these limitations, the acceleration criterion is the most reported for animal models of $+G_z$ loading. Both early work by Stapp, Cook, and Hanson; and more recent studies by Fiskum and Guan have used the acceleration criterion as the primary physical biomechanical parameter (Stapp, 1957; Cook and Mosely, 1960; Hanson, 1967; Fiskum and Fourney, 2014; Guan *et al.*, 2018). The utility of an accelerative criterion for UBB torso injury is further limited by the need to position the sensors some distance from the organ in question (upon either a bony prominence or impact device). No injury curve for torso injury has been developed based upon $+G_z$ acceleration values.

6.11.2 Compression

As with acceleration, compression criteria have only been applied to the frontal and side directions. Kroell *et al* showed that maximum chest compression correlated better with AIS than maximum force (Kroell *et al.*, 1981). In 5-7m/s frontal impacts to the chest, 20% anterior-poster compression caused rib fracture with 40% causing flail chest (Nahum *et al.*, 1975). The skeletal response to compression is understandable based

upon the elastic nature of the ribcage (Paragraph 6.6.1). Viano also demonstrated that thoracic organ damage occurred at a maximal compression (C_{MAX}) of 40% and recommended a C_{MAX} of 32% top maintain sufficient rib cage integrity to protect the organs (Viano, 1978). This assumption is thus only relevant in the frontal/side impact environment where the rib cage is likely to be between the impact and the organs.

Compression of the abdominal organs may be independent of any rib cage deformation. Impact may cause crushing of the abdominal organs between the impact surface and the spine or other surface.

Previous studies of frontal and lateral abdominal impact experiments have contrasting findings as to the predictive ability of the compression criterion. Stalnaker *et al.*(1973) found that abdominal compression was related to abdominal injury severity in human and primate cadavers with different injury tolerances for left and right sides. In contrast, Viano *et al* (1989) demonstrated poor correlation between compression and abdominal injury for lateral pendulum impacts of abdominal cadavers. A study by Miller (1989) demonstrated that compression correlated well with the severity of injury in seatbelt loading of anaesthetised pigs.

The applicability of a compression criterion is likely dependent upon the behaviour of the material and organ in question. Compression is likely a better predictor of injury at low rates when a rate related mechanism is less important (Lau and Viano 1986). Given this, purely compression based criteria are likely to be limited for a high rate UBB application.

6.11.3 Viscous Criterion

The viscoelastic nature of the internal organs and the rate dependence of injury to these organs has already been discussed. The importance of this property was initially investigated by Lau and Viano who sought to improve upon existing soft tissue injury criteria (Lau and Viano 1986). They recognised that soft tissue injury is caused by excessive deformation and is sensitive to loading rate. Although compressive criteria address the deformation aspect, they additionally included rate sensitivity in their new criterion.

They demonstrated rate sensitivity to compression using anesthetised rabbits. Impact to the liver, to a constant compression, caused a variety of injury severity dependent upon the impact velocity (5-20 m/s) (Lau and Viano, 1981b). They found that no injury was caused at 16% compression below 8m/s but that the same level of compression caused critical injury with 20m/s impact. A similar interdependence between velocity and compression was observed for lung injury following direct chest impact (Lau and Viano, 1981a).

Lau and Viano proposed measuring the viscous tolerance of an organ system and developed the viscous criterion. They defined a viscous criterion as "*any generic biomechanical index of injury potential for soft tissue defined by rate sensitive torso compression*" (Lau and Viano 1986). They specifically defined the viscous response (VC) as a time function formed by the product of the velocity of deformation V_t and the instantaneous compression C_t .

$$VC = V_t \,.\, C_t \qquad [6.3]$$

Where V_t is the velocity of deformation:

$$V_t = \frac{d(D_t)}{dt} \qquad [6.4]$$

and D_t is the instantaneous deformation along the direction of the impact to the torso:

$$C_t = D_t / \text{ Initial Torso Thickness} \qquad [6.5]$$

The viscous tolerance is therefore the risk of soft tissue injury associated with a specific induced VC with maximum risk occurring at VC_{max}.

Other experiments by the group demonstrated the range of impact velocity (3 to 30ms) over which the viscous criterion was valid (Kroell *et al.*, 1981; Horsch *et al.*, 1985). At low velocities, (below 1m/s), the criterion is predominantly a function of compression and at high velocities (>30m/s) the influence of the compression becomes secondary as blast like wave phenomena occur (Lau and Viano 1986) (as previously shown in Figure 6.12). Given that C_t is a dimensionless number, VC has the same unit as V_t which is m/s.

The viscous response was found to be a superior predictor of heart injury in response to frontal impact upon anesthetised pigs with a *VC* of 2m/s predicting a 50% chance of cardiac rupture (Kroell *et al.*, 1981). Similarly, a *VC* of 1.4 was found to be predictive of 50% chance of severe liver laceration when applied to abdominal impact.

A further viscous criterion has also been developed. The Abdominal Injury Criterion (AIC) is the product of maximum impact velocity and maximum compression (Rouhana *et al.*, 1985). The AIC was also found to correlate well with abdominal injury in anaesthetised rabbits. The time varying nature of the VC is likely important as the rate of deformation and degree of deformation may not peak at the same time. As such, the VC_{max} is likely to occur before the maximum compression (Lau and Viano 1986).

Although the two criteria are clearly related, the time varying VC is considered the more desirable parameter to measure as it may discriminate the time of injury which could help in the design of countermeasures (Lau and Viano, 1986).

It is important to note that neither viscous criterion has been applied in the G_z direction with all previous experimental data based only upon frontal and lateral impact.

6.11.4 Pressure

Pressure has been investigated as a potential injury criterion and as a way to account for impact surfaces of differing size and shape (Hardy *et al.*, 2015). Experiments using isolated cadaveric organs by Fazekas *et al* demonstrated that surface pressure of 168.5kPa was necessary to cause superficial laceration of the liver with multiple injuries occurring beyond 320kPa. Superficial splenic injury was observed with surface pressure of 44kPa (Fazekas *et al.*, 1971).

Internal organ pressure has also been used as a criterion. Prasad and Daniel used aortic pressure change as an indicator of abdominal compression for impact tests upon anaesthetised pigs and found no serious injuries with peak aortic pressure below 53 kPa (Prasad and Daniel, 1984). Both Mays and Stein *et al* have asserted that rapid increases in internal pressure could be important to injury of solid abdominal organs (Mays, 1966; Stein *et al.*, 1983). Sparks performed drop tests upon isolated perfused livers and found that tissue pressure alone was a good predictor of injury severity. Interestingly, injury was best predicted by the product of peak tissue pressure and peak rate of tissue pressure increase, suggesting that rate sensitivity should be taken into account if pressure is to be used as an injury criterion (Sparks *et al.*, 2007a). A rapid rise in intra-abdominal pressure is feasible following UBB assuming sufficient deformation of the torso. Such a rise in pressure has been suggested as a cause of surrounding fascial and skeletal injury in this environment (Newell *et al.*, 2018).

6.12 Injury Criteria for UBB

Injury criteria are used to predict probability of a particular injury in response to a particular impact scenario. The primary application of injury criteria for UBB is in the development of protective materials and vehicles. Injury criteria allow standardisation of testing methodologies and the quantification of the protection offered by a platform in response to UBB insults.

Internationally, this information has been collated by the Research and Technology Organisation of the North Atlantic Treaty Organisation (NATO). The particular NATO group tasked with the investigation of UBB has been HFM 148 (NATO Research and Technology Organisation, 2012). The goal of HFM 148 has been to *"analyse injury loading mechanisms, investigate injury assessment criteria, define test methods and measurement tools to assess vehicles (and protection systems) against the mine and IED threat. Injury criteria were defined, and the pass/fail (tolerance) levels established for the body regions are considered to represent low risk of life-threatening and disabling injuries"* (NATO Research and Technology Organisation, 2012).

The group explores available injury criteria for all bodily regions. In each case, these criteria are applied for use with one of several ATDs for both live fire and simulation testing. Tolerances are described according to each criterion such that each test results in a pass or fail for each criterion.

As discussed above, the criteria for torso injury available to the group do not include any which have been designed or validated for vertical loading. The recommendation of HFM 148 for thoracic injury criteria is the use of Compression Criterion (C) in conjunction with the Viscous Criterion (VC) for both frontal/rear/vertical loadings (with the Hybrid III ATD) and lateral loading (with the ES-2re ATD).

Threshold values recommended for pass/fail standards by the group are shown in Table 6.3.

Loading	ATD	Compression Criteria	VC
Frontal/Rear/Vertical	Hybrid III	30mm (10% risk of AIS3+)	0.7m/s (10% risk of AIS 4+)
Lateral	ES-2re	28mm (10% risk of AIS 3+	0.58m/s (10% risk of AIS 3+)

Table 6.3: Tolerance values for thoracic loading in response to UBB testing as recommended by NATO Research and Technology Organisation (2012).

Although frontal, rear, and lateral loading may play some part in injury following UBB (following rolling or tipping of the vehicle), the physics of UBB (as discussed in Chapter 2) suggests that the primary loading pathway is vertical. Similarly, the severe torso injuries described in Chapter 4 may, in part, be caused by anterior-posterior or lateral impact but the associations described in Chapter 5 suggest vertical loading through the seat. Previous work in this chapter has demonstrated that torso injuries are

observed following pure vertical loading in animals and which do not require frontal chest compression. Measuring conventional compression and VC though the Hybrid III is facilitated by chest deflection sensors on the ATD (NATO Research and Technology Organisation, 2012). These ATDs do not currently have the ability to undergo axial torso compression.

The limitations of these ATDs is further evidenced by the HFM 148 recommendations for abdominal injury risk. The group recommends the use Abdominal Peak Force (APF) measured with the ES-2re ATD for prediction of risk in cases of lateral loading. This criterion was based on localised pendulum tests causing liver injury in the anterior direction in PMHS (Walfisch *et al*. 1980; Viano *et al*. 1989).

There are important limitations with the current injury criteria recommendations. Firstly, APF does not have any rate sensitivity, which has been described as an important factor in abdominal injuries (Lau and Viano, 1981b). Secondly, although there may (for some blast events) be a degree of lateral loading, vertical loading is the likely to predominate. The limitations to the criteria are in part due to currently used ATDs. Due to lack of measurement capabilities in the Hybrid III ATD, there is actually no recommended abdominal injury criterion for frontal/rear/vertical loadings (NATO Research and Technology Organisation, 2012).

Injury criteria should be based upon both predominant physical loading (high rate vertical acceleration), the known material and anatomical properties of the tissues (rate dependent with tethering structures aligned in the vertical direction), and a proposed injury mechanism. The injury mechanisms postulated above take these first points into account and are an appropriate mechanical approach. They fit with previously observed measures of vertical torso deformation (as described in both anaesthetised animals and human cadavers).

Current UBB test methodology does not address these points and as a consequence may not be accurately predicting the risk of torso injury in response to UBB.

6.13 Conclusion

This chapter has illustrated both the relevant anatomy and injury mechanisms of the organs of the torso in response to impact. Organs may sustain injury either within the parenchyma or at sites of attachment. Injury mechanism are likely to vary between organs but depend upon some degree of deformation. Impact is likely to cause injury through either stress wave propagation causing high rate, low deformation injury or shear wave propagation with relative movement of organs generating strain at attachment points.

Existing data for impact testing has focussed upon frontal and lateral impact with direct contact of the chest and abdomen. Component level testing demonstrates rate sensitivity of the internal organs to injury. Whole body accelerative testing has demonstrated torso injury within anaesthetised animals exposed to vertical loading although these tests have not demonstrated a clear relationship between established biomechanical parameters and torso injury.

A variety of injury criteria have been established for investigation torso injury. Viscous response has shown to be a good measure of both abdominal and pelvic injury risk, reflecting the viscoelastic nature of these organs. No vertically orientated injury criteria for the thorax or abdomen have yet to be developed or validated.

Chapters 4 and 5 have demonstrated the importance of torso injuries to survivability following UBB. Protection against such injuries depends upon clear understanding of the risk of injury for given UBB load but current testing methodologies for UBB use frontal or lateral criteria to assess risk of chest injury and have criteria only to assess lateral impact of the abdomen.

Both cadaveric and animal studies of vertical loading demonstrate axial compression of the torso rather than anterior-posterior deflection. Cadaveric studies are limited in their ability to replicate visceral injury with inversion of the torso required in order to replicate *in vivo* conditions. Although immediate translation of data from animal studies is complicated by anatomical, physiological, and scaling considerations, such studies have previously led to the development of injury criteria for severe visceral injury.

The injury mechanism of internal organs in response to short duration vertical loading is likely to be displacement of the organs with compression of the tissues and tension of the attachments. This displacement has been visualised in animals and at low rate in humans and is associated with torso compression and surface wave phenomena. Movement of the organs can be partly explained using mechanical models but to date these fail to take into account non-linear properties and require assumptions as to the damping and elastic properties of the organs and attachment.

Currently injury criteria for assessment of UBB thorax and abdominal injury risk are based solely on automotive data and designed to determine injury risk from frontal and lateral loading.

Prediction of injury risk, and possibility of prevention requires thorough characterisation of both the mechanical response to UBB analogous vertical loading and the relevance of this response to injury. Any criteria should be mechanically appropriate for the form of loading and response of the animal. The criteria should include rate and deformation dependence. Purely physical measurements such as acceleration or velocity are difficult to translate between tests and platforms as they do not adequately couple the loading to injury.

Survivability of UBB injury is affected by the occurrence of severe and lethal injuries. Replicating these injuries in cadaveric models poorly represents the *in vivo* physiological and anatomic sequalae of these injuries. Describing the relationship between loading and severe visceral injury therefore requires the development of an *in vivo* animal model of high rate loading which demonstrates the role of rate and deformation for torso trauma. The following chapters will describe the development of a novel experimental platform (Chapter 7) and a series of rodent experiments (Chapter 8) which will enable the quantification of this injury risk.

CHAPTER 7

DESIGN, CONSTRUCTION, AND CHARACTERISATION OF THE RIG FOR *IN VIVO* UNDERBODY LOADING (RIVUL)[1]

7.1 Scope of the chapter

Chapter 6 described existing historical and contemporary work in impact biomechanics with an emphasis upon the relevant anatomy and response of the internal organs to conventional impact. The chapter highlighted the limitations of both existing models and existing injury criteria to examine visceral injury in response to the high rate vertical loading caused by underbody blast. The chapter concluded by stating the need for a new *in vivo* model of this loading which will enable to quantification of this relationship. This chapter will describe the design, instrumentation, and characterisation of a new

[1] This chapter has been part published as Nguyen, Thuy-Tien, A. P. Pearce, D. Carpanen, D. Sory, G. Grigoriadis, N. Newell, J. Clasper, A. Bull, W. G. Proud, and S. D. Masouros. "Experimental platforms to study blast injury." Journal of the Royal Army Medical Corps (2018):

device for in-vivo axial loading. Although this device will not use explosives, it will employ a pneumatic mechanism in order to replicate the same loading effect.

7.2 Introduction

As discussed in Chapter 6, assessment of visceral injury in response to high rate axial loading cannot be sufficiently performed using existing human cadaveric models. Assessing this form of injury requires live tissue in order to reduce post mortem changes in both tissue properties and relative organ positioning (Hardy *et al.*, 2008; Crandall *et al.*, 2011; Viano, 2011). Although the use of animals for such research also has limitations (as discussed further in Chapter 7), animals provide the only viable surrogate to study the pathophysiological response to impact injury (Crandall *et al.*, 2011). The use of a small animals facilitates the development of injury criteria as a large sample population, and therefore study power, is enabled by low cost and simple infrastructure requirements.

An injury simulator for small animal use will be, by necessity, different to existing rigs used to measure cadaveric and ATD responses to under-vehicle blast. These devices aim to accurately reproduce the response of a human to UBB and as such are large and tuned to produce human range injury parameters. The chapter will discuss the specification, design, construction, instrumentation, and characterisation of this device.

7.3 Specification

Specifying the desired loading parameters of a device are difficult for two reasons. Firstly, security sensitivities necessitate that defence organisations do not publish live blast test data and therefore they cannot be reviewed here. There is no published data which specifically characterises the behaviour of a military vehicle during under-vehicle explosions. Although a number of papers make references to similarity of their tests to live blast data, these tests relate to lower limb injury with the physical parameters reflecting that of the floorplate (Wang *et al.*, 2001; McKay and Bir, 2009).

Loading data for the seat, and therefore of the torso has been described to a lesser degree. Bailey *et al* have reproduced some of this live fire data from military sources although the vehicles and charge size used are unknown (Benesch, 2011; Bailey *et al.*, 2015). Examples of the seat loading from this data are shown in Figure 7.1. These data suggest seat accelerations of around 500G (around 6000m/s^2) occurring at less than 5ms with a peak velocity of around 9ms occurring at around 5ms. Not only are charge size, composition, and vehicle specifics unknown but no attempt was made during these tests to correlate these parameters with injury.

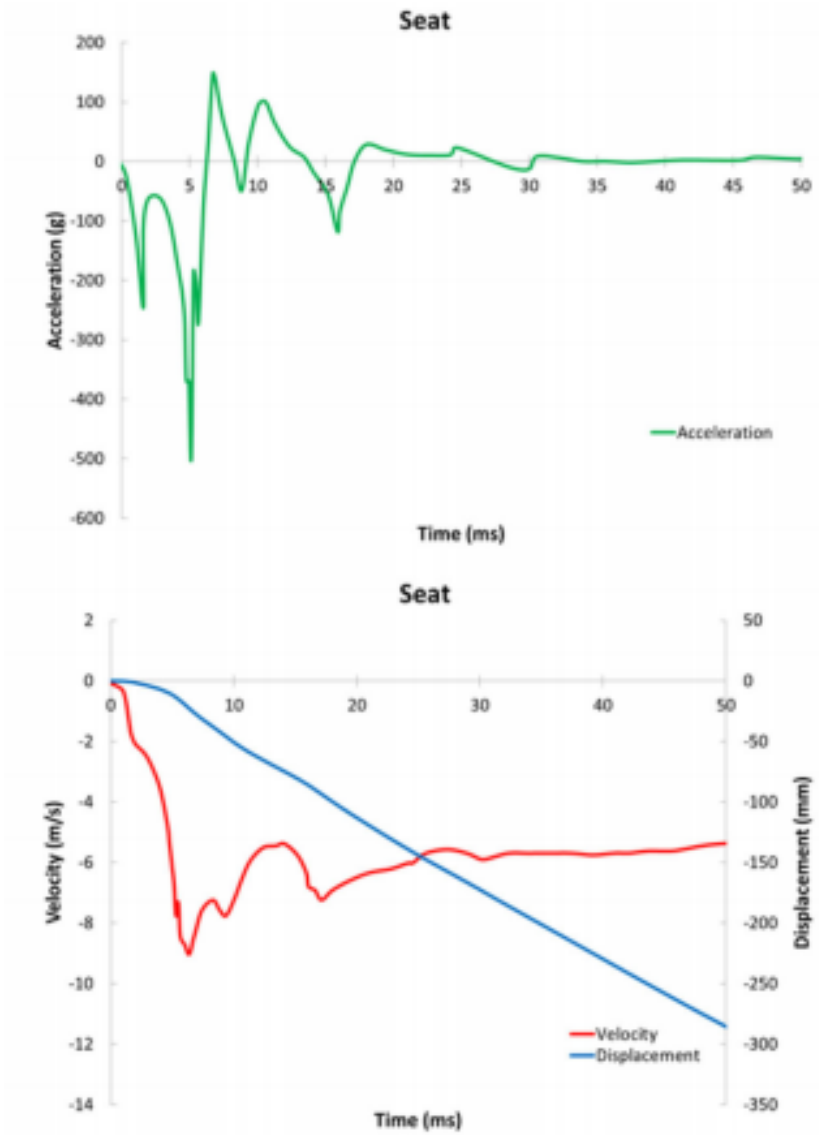

Figure 7.1: Seat pan loading data from live fire testing showing acceleration (above), and velocity/displacement (below). Reproduced from Bailey *et al*., (2015) with data from Benesch, (2011).

A further difficulty in determining the specifications for an *in vivo* device is that the physical parameters required to reproduce visceral injuries in response to axial loading are uncertain, particularly when comparing across scales and varying anatomy. Experiments designed to specifically replicate underbody blast have in the most part been aimed at reproducing skeletal injuries (Henderson *et al.*, 2013; Bailey *et al.*, 2015). Animal experiments of axial loading have varied greatly in their methodology (as

described in Chapter 6) but torso injuries have been shown to occur at around 100-150g (with around 10-20ms duration) for large animals and 1500-2500G (around 0.5ms duration) for rodents (Cook and Mosely, 1960; Hanson, 1967; Kazarian *et al.*, 1970; Fiskum and Fourney, 2014). The rodent models used by Fiskum did not truly approximate axial loading (as the animal was prone) and so the true tolerance may be different (Proctor *et al.*, 2014).

The scaling of both input and response will be discussed further in Chapter 9 but linear mechanics (assuming similar geometry) suggests that scaling of acceleration can be done by examine the ratio of lengths of the two systems in question (Panzer *et al.*, 2014). For the purposes of scaling the acceleration of established live fire data shown in Figure 7.1 for device specification, one can assume that the ratio of rat to human torso lengths (around 7-10) should be applied to greatest magnitude acceleration described (i.e. 10 times 500) to provide an upper target of 5000G.

Despite these differences, some aspects of the design will be similar to existing traumatic injury simulators. The common mechanism for these devices is to replicate an impact event by accelerating a mass to a target velocity in a given time before rapid and controlled deceleration. Examples of existing human sized impact rigs are described in Chapter 6. These rigs vary in their ability to affect whole body acceleration or localised impact. Within the modern era of UBB research, only one experimental system has been constructed to study the in-vivo effect of UBB upon a small animal model (Fiskum and Fourney, 2014). This system utilises a small explosive charge detonated within a water tank to drive parallel steel plates. The rat is restrained within a cylindrical tube attached to the upper plate. Acceleration of the plate was linearly related to the mass of the charge detonated. Although designed with the intent of studying traumatic brain injury, animals in this experiment sustained “lung haemorrhage” above an acceleration threshold of ~2500g. These accelerations were achieved within 1ms, which is a reasonable measure for shock loading (as opposed to gradual acceleration) in a rodent model (Kornhauser and Lawton, 1961).

There are several problems with this design that should be improved upon with a novel rig. The use of explosive material is not a fundamental problem but requires the acquisition of suitable licenses and modification of infrastructure. Tuning of a system

utilising high explosive is possible (by changing the amount of explosive) and may be subject to small variations in explosive composition.

The positioning of the animal in the "Fiskum model" is laid prone and restrained within a cylinder. A new model of torso injury should instead align the torso in the axial plane to replicate a human seated position for the purposes of the inertial response of organs. Secondary movement should be allowed although controlled in a similar manner to that of a typical vehicle restraint system. As with the Fiskum model, secondary impact should be reduced or limited such that injuries to the torso may be causes only by axial load. Whilst previous rigs have been custom produced by external contractors, the size and scale of the new device lends itself to in-house fabrication. Given the above considerations, the design of this *in vivo* loading device should meet the following specifications:

a) fit within existing Centre for Blast Injury (CBIS) infrastructure and where possible, use existing CBIS technology;
b) allow adequate restraint of a rat or surrogate in an upright posture analogous to a sitting human;
c) be capable of causing whole body axial acceleration of a small animal to the magnitude of 5000G within a 1ms;
d) rapidly decelerate the animal in order to simulate vehicle seat deceleration and avoid secondary impact; and
e) be instrumented to allow accurate measurement of input dose (seat velocity and acceleration) alongside output biomechanical response (high speed video).

7.4 Design and construction

The wish that the new rig be based upon existing CBIS technology and infrastructure, and not to utilise explosives required that the axial loading of the device be achieved with a pneumatic system. CBIS already has expertise with pneumatic systems, currently employing them within a shock tube, Split-Hopkinson Pressure Bar, 32mm Gas Gun,

and the Anti-vehicle Underbody Blast Injury Simulator (AnUBIS). Each of these systems utilises high pressure gas which is released onto a target actuator using some form of controlled failure.

The AnUBIS system is a large scale device design to replicate the effect of high rate floor deformation upon the lower extremity (Masouros *et al.*, 2013) . Compressed gas is forced into a chamber and applied against a steel plate (the surrogate floor). Movement of the floor occurs following failure of a shear pin. Variation of the pin material and size determines resultant floor velocity.

Both shock tube and gas gun also utilise compressed air with release determined by controlled rupture of a thin mylar diaphragm. The shock tube relies upon interaction of the high pressure air (driver section) released by the rupture with atmospheric gas in the subsequent (driven) section to produce a shock front. In contrast, the high pressure gas within the gas gun acts directly upon a projectile which is forced at high velocity along a honed barrel following diaphragm rupture. In both cases, output (either overpressure or projectile velocity) is controlled by varying the diaphragm thickness. The linear relationship between diaphragm thickness and burst pressure has been characterised and described (Nguyen *et al.*, 2014).

The initial design of the new rig was of a modified gas gun system. The design included a double diaphragm to allow rapid acceleration of a projectile along the length of a suitable honed barrel. The projectile would be shaped such that the shoulders of it would stopped by the top “collar” flange attached to the barrel while allowing the head to strike a target plate. A schematic of the initial design is shown in Figure 7.2:

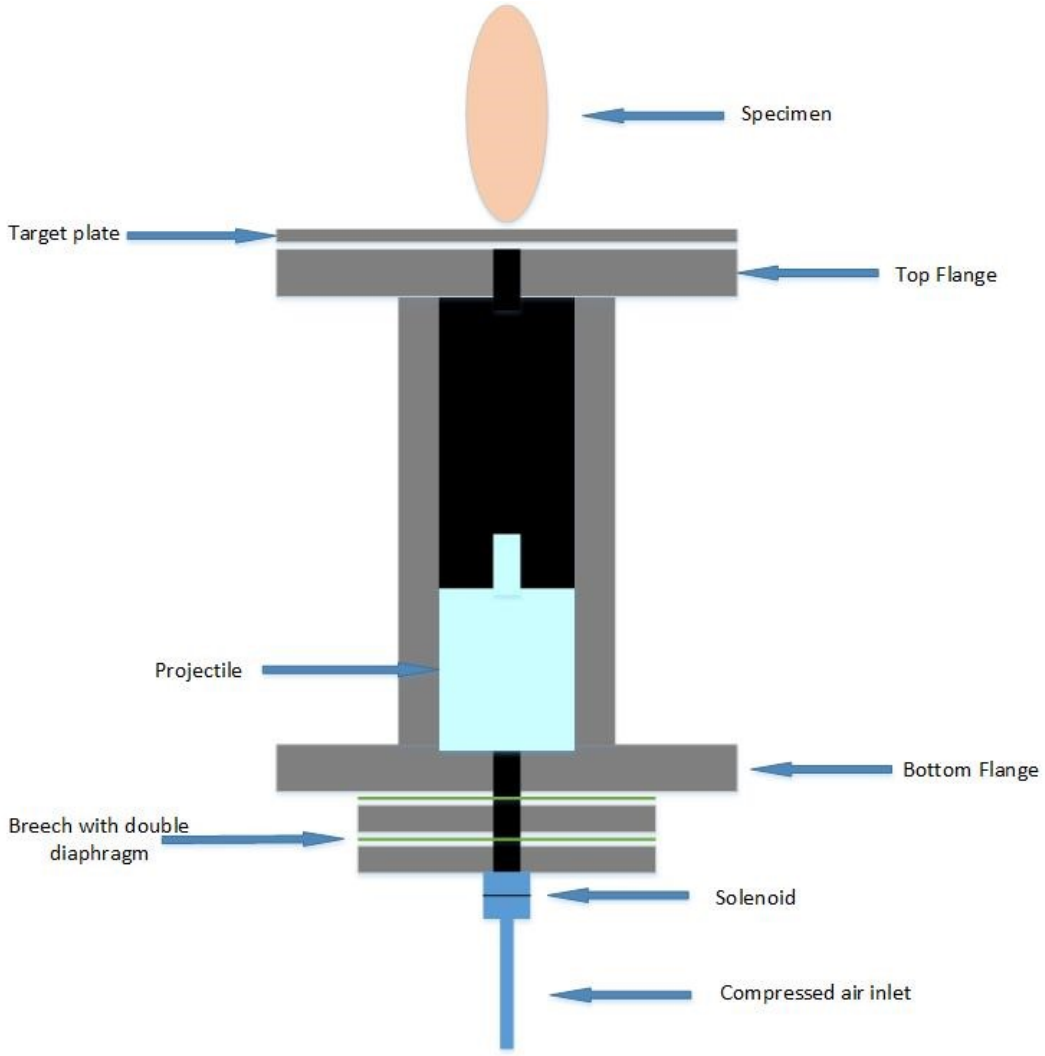

Figure 7.2: Initial design for the *in vivo* rig.

A specimen would be secured to the top of the target plate. Upward movement of the projectile along the barrel would result in extrusion of the projectile head beyond the top of the top flange with resultant impact and acceleration of the target plate and specimen. Given that previous work had characterised the burst pressure of a given thickness of mylar (Nguyen *et al.*, 2014), projectile velocity could be altered by changing mylar thickness. Assuming a closed system, subsequent velocity of the projectile could be calculated by estimating the pressure acting upon the base of the projectile as the burst pressure of the diaphragm.

Given that pressure is

$$P_B = \frac{F}{A} \quad [6.1]$$

where P_B is the burst pressure, A is the cross sectional area of the projectile acted upon and F is the resultant force. Using Newton's second law, acceleration of the projectile is derived

$$F = P_B A = ma \quad [6.1]$$

which rearranges to

$$a = \frac{P_B A}{m} \quad [6.2]$$

where α is acceleration and m is the mass of the projectile. Subsequent velocity of the projectile can be estimated using equations of motion.

$$v^2 = u^2 + 2as \quad [6.3]$$

where v is the resultant velocity, u is the initial velocity (which would be 0) and s is the displacement (barrel length).

Combination of equations 6.2 and 6.3 gives:

$$v^2 = \frac{2P_B AS}{m}, \quad [6.4]$$

Which may be rearranged to:

$$v = \sqrt{\frac{2P_B AS}{m}} \quad [6.5]$$

These equations assume a constant acceleration which is directly proportional to the burst pressure of the diaphragm. In reality, the driver pressure behind a projectile is likely to differ from the initial burst pressure for several reasons:

1) the driving pressure will constantly fall in relation to the expansion of volume behind the projectile as it is accelerated;
2) there is likely to be some leakage of pressure in the system; and
3) drag effects of the air (not considered within the equations of motion) and of the fluid "boundary layer" effects between the projectile, wall, and gas.

The resultant acceleration will vary as a function of the varying pressure. Given that mass, cross sectional area, and barrel length will be constant, final velocity will therefore depend upon the average pressure along the length of the barrel. Simple numerical estimation of this average pressure is difficult and likely to be flawed. Computational simulation of the system would allow higher fidelity estimation of resultant velocity by iteratively solving the changes in pressure and acceleration. However, even a (computationally demanding) simulation would not take into account a variety of unknown factors such as projectile friction, and adherence of the system to ideal gas laws.

Of similar uncertainty is the resultant acceleration and velocity of the target plate and mounted specimen following impact. Given that the target plate will be stationary, any

movement will be a consequence of momentum transfer from the upward moving projectile. In an idealised elastic collision, the momentum of the projectile would be entirely transferred to the plate such that:

$$m_{p1}v_{p1} = m_t v_t + m_{p2}v_{p2} \quad [6.6]$$

where m_{p1} and v_{p1} are the initial mass and velocity of the projectile, m_{p2} and v_{p2} are the resultant mass and velocity of the projectile, and m_t and v_t are the resultant mass and velocity of target plate. The mass of both projectile and plate will be known but no collision is truly elastic. Energy will be lost to friction of the plate resisting motion and to deformation of both objects. In an ideally elastic collision, acceleration of the target would be instantaneous such that the resultant velocity would be achieved immediately and the entire momentum of the projectile would be transferred to the plate. Acceleration following a realistic collision would depend upon a variety of unknown factors within both the materials and the boundary conditions.

An experimental approach was therefore decided upon in that the rig would be built, tested, and iteratively improved upon in order to achieve the desired effect. In order to satisfy the specifications outlined above, the following features were included at all stages of the design and construction:

a) a 1.2m barrel which would provide a suitable displacement for acceleration whilst optimising use of space within the intended laboratory;
b) a target plate of 180mm diameter. This would be sufficient to accommodate the specimen and any instrumentation without affecting vertical movement of the plate. The material must be stiff enough to resist excessive deformation;
c) a projectile mass which approximates that of the target such that the velocity of the projectile would approximate that of the target. This was estimated at around 500g;

d) an internal diameter of 70mm within the barrel. This size barrel would be large enough to accommodate this projectile and fit onto an existing breach with minimal modification;
e) the thickness of the barrel wall would be sufficient that that it would withstand the maximal operating pressure of the system;
f) both ends of the barrel would be threaded to fit similarly threaded flanges. These flanges would allow fitting of the rig to a mounting structure at the bottom surface and attachment of the linear movement system at the top;
g) the target plate will be coupled to the top flange with a linear bearing system. Rails will be mounted to the top flange. Bearings should be used which minimise friction in the vertical direction. The rails will minimise the 'tipping' (out of plane motion) of the target plate after impact. A stopping mechanism will allow variation over the degree of upwards displacement of the plate;
h) the projectile should be of suitable mass, stiffness, and fatigue strength to provide the required momentum, resist deformation, and not break under repeated loading; and
i) input pressure to the breech of the system would be provided by the existing gas gun or shock tube control panel.

The Computer Aided Design (CAD) of the rig was performed using Fusion 360 (Autodesk Inc, USA). The honed barrel was sought from Apperley Honing (Cheltenham, UK). It consisted of an ultrasound honed welded stainless steel tube with an internal diameter of 70mm and external diameter of 80mm. The tube itself is pressure rated to 280bar. The ends of the barrel were threaded to allow fitting of custom made flanges (*Figure 7.3*).

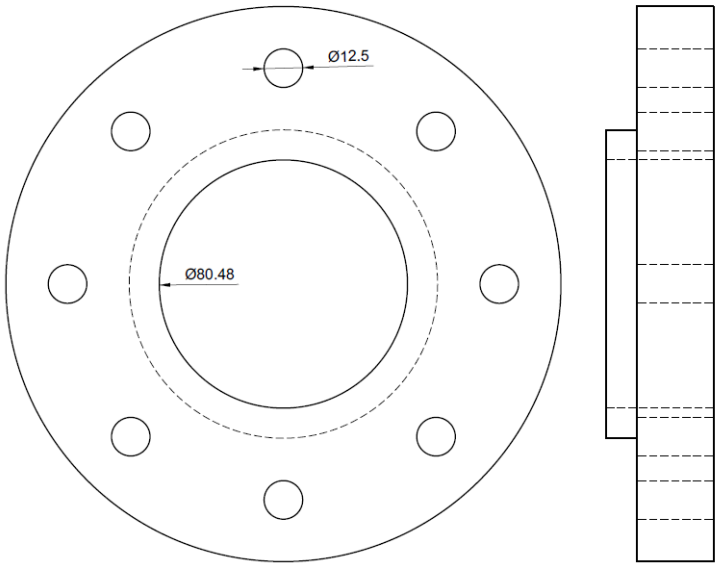

Figure 7.3: Flange (for fitting to the top and bottom of barrel)

The existing shock-tube breach had a 15mm output so an adaptor plate was constructed which fixed to the bottom of the lower flanged to reduce the inlet to 15mm. Each plate was secured to another using stainless steels screws and nuts. Nitrile o-rings acted as pressure tight seals between components. The CAD of the lower breach section is shown in Figure 7.4.

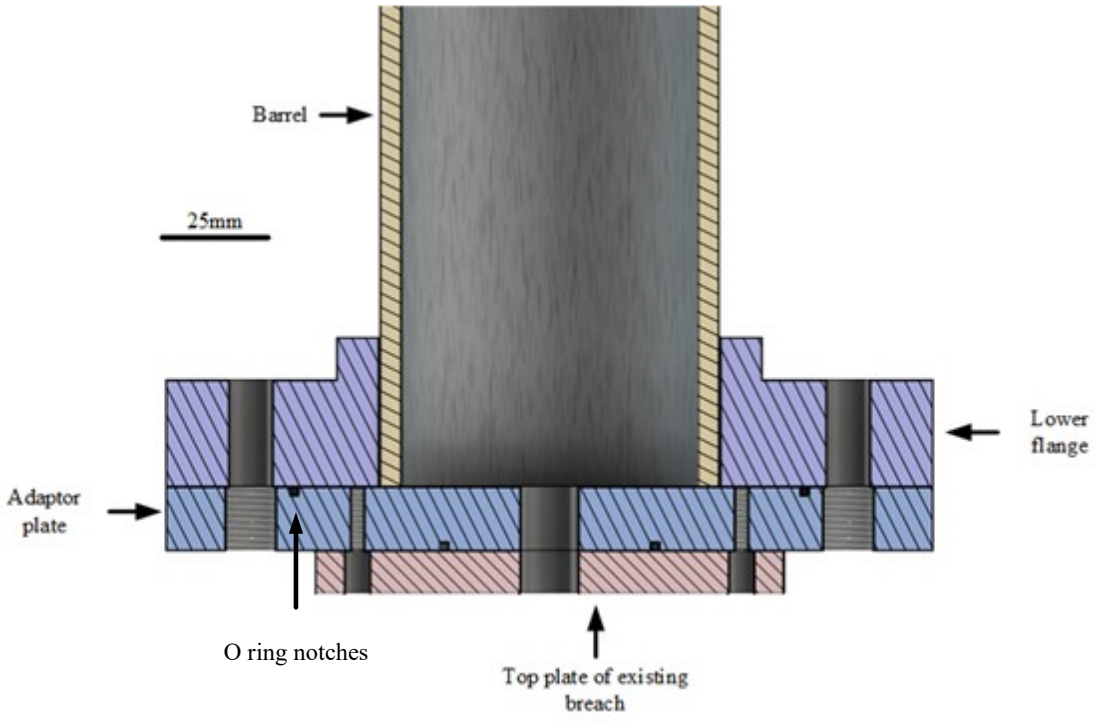

Figure 7.4: Cross section CAD view through the centre of the lower aspect of the RivUL showing relative position of the barrel, flange, adaptor plate, and existing breach inlet. O-ring notches are seen in the adaptor plate. Fixing bolts (m12 and m8) are not shown.

Although the initial design called for the stopping collar to be fixed to the upper flange, this would not have allowed for release of the projectile and therefore of barrel pressure venting. Consideration was given to placing holes in the upper segment of the barrel but the flow rate required to adequately vent the barrel would have necessitated around 40% of the area of the segment to be cut away. This would have caused deformation of the barrel and loss of honing effect. Instead, the stopping collar was raised above the top flange such that the projectile would undergo a period of free flight prior to striking the

target plate. The linear rail mounting of the stopping collar and target plate would act as a cage to prevent egress of the projectile outside of the rig. The opening of the top collar was cut large enough to accommodate any tumbling of the projectile during the free flight period. 10mm thick neoprene rubber sheet was affixed to the lower surface of the steel stopping collar to slow the projectile following plate impact. The CAD of the upper section is shown in Figure 7.5

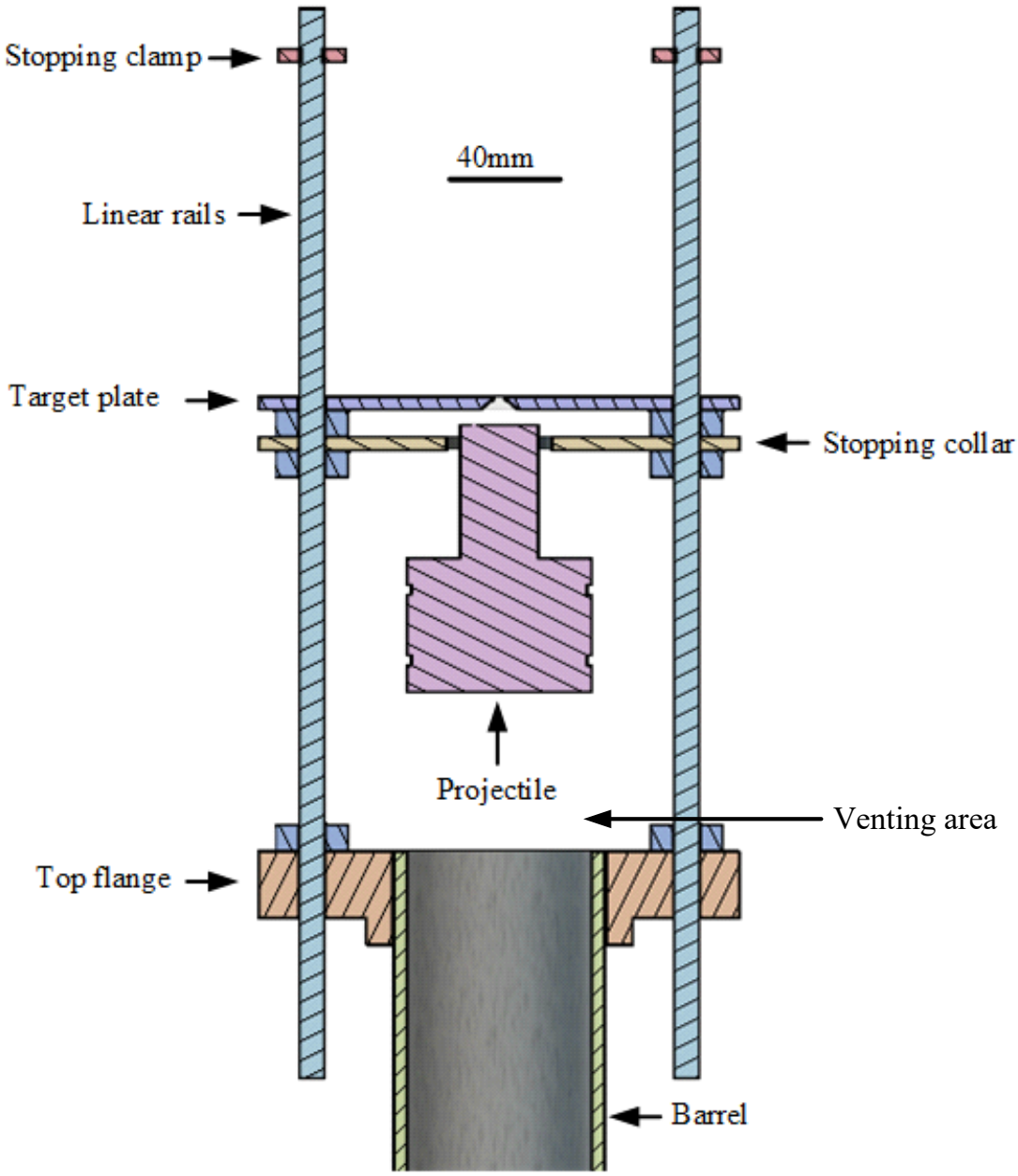

Figure 7.5: Cross section CAD view through the centre of the upper aspect of the rig. The projectile is shown in the free flight period prior to striking the target plate and stopping collar.

The initial design for the device was to utilise a single or double breach diaphragm system in order to allow very rapid exposure of the projectile to the driving pressure. Following initial testing, the need for very high rate pressure exposure of the projectile was found to be unnecessary and the diaphragm was taken out of the circuit. As a consequence, the input pressure to the device was based upon the input pressure (as controlled via flow from the control panel (Swagelok, OH, USA) (*Figure 7.6*).

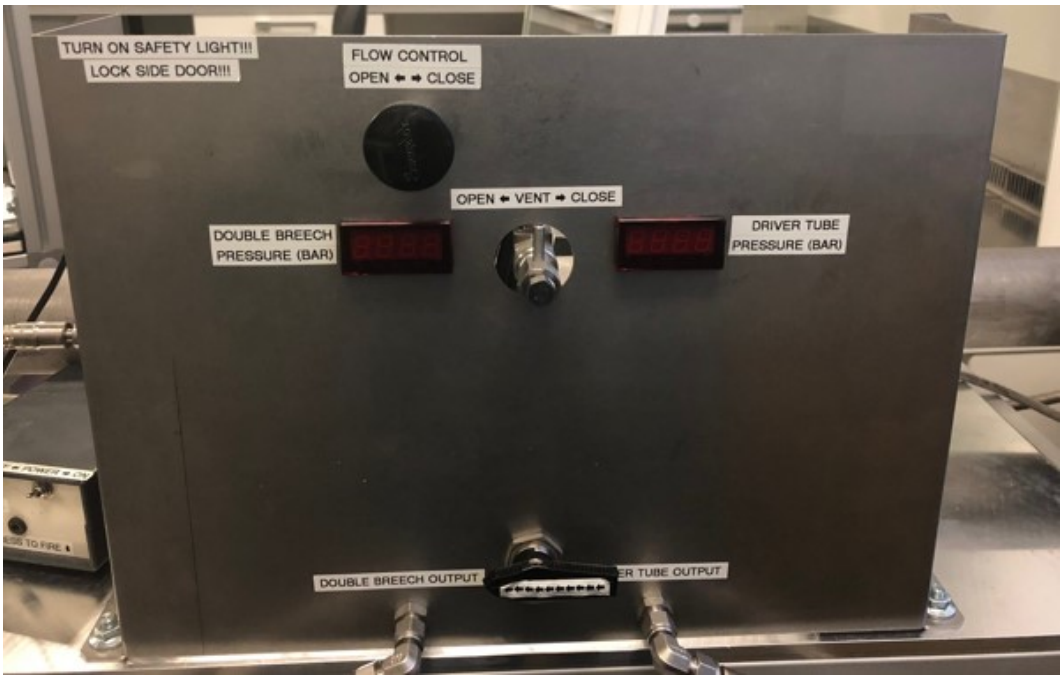

Figure 7.6: Shock tube control panel used to control input pressure of compressed air. Only one of the lower outputs is utilised.

Compressed air was fed into the control panel which directed the suitable pressure into a 2l reservoir. This reservoir was connected via a solenoid valve and then wide necked high flow hose into the lower breach. The solenoid valve was opened using a direct current input from a firing switch. Omitting the diaphragm leads to a likely reduction in resultant driving pressure but speeds up experimental throughput by eliminating the need for changing of the diaphragm between tests. The operational schematic of the device is shown in Figure 7.7.

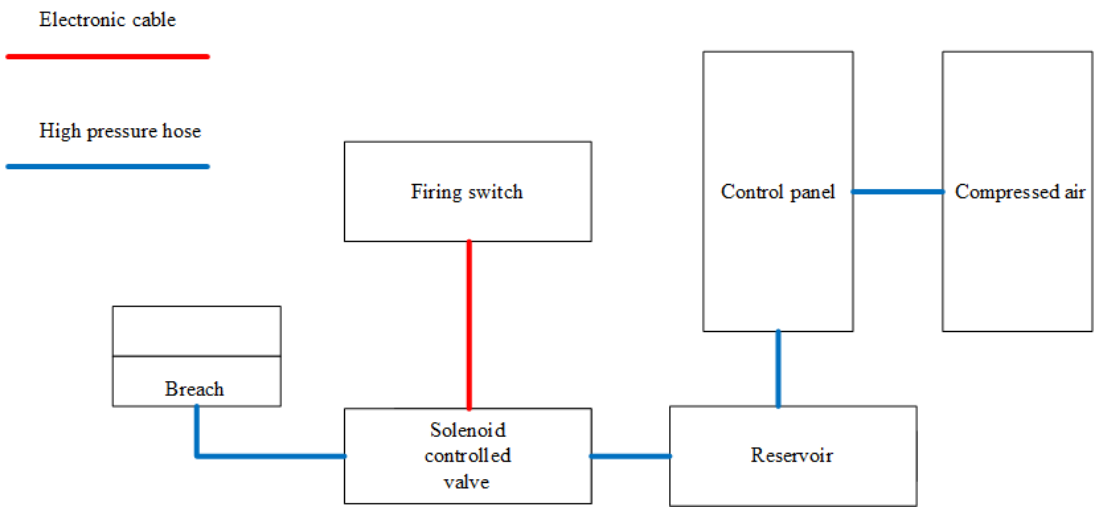

Figure 7.7: Operating schematic of the device breach.

The loading component of the rig is provided by the impact of the projectile with the target plate. The impact plate needed to be light enough such that the projectile could cause it to accelerate quickly enough and stiff enough to resist deformation from the impact. An initial plate was made from 5mm thick polyethylene. Testing with these disks showed high acceleration but significant bending with "wobbling" of the plate as it moved vertically.

A simple two dimensional finite element model of the mechanism was created in MSC.Marc (MSC.Software, CA, USA) with the assistance of Dr Nic Newell to compare the behaviour of the disc under loading given different materials and thicknesses. The model was subjected to a linear ramp displacement (up to 100mm in 5ms) of the lower 15mm to replicate the impact of a projectile at the plate centre..

The model demonstrates that increases to the thickness of the disc reduces the plate deformation (Figure 7.8).

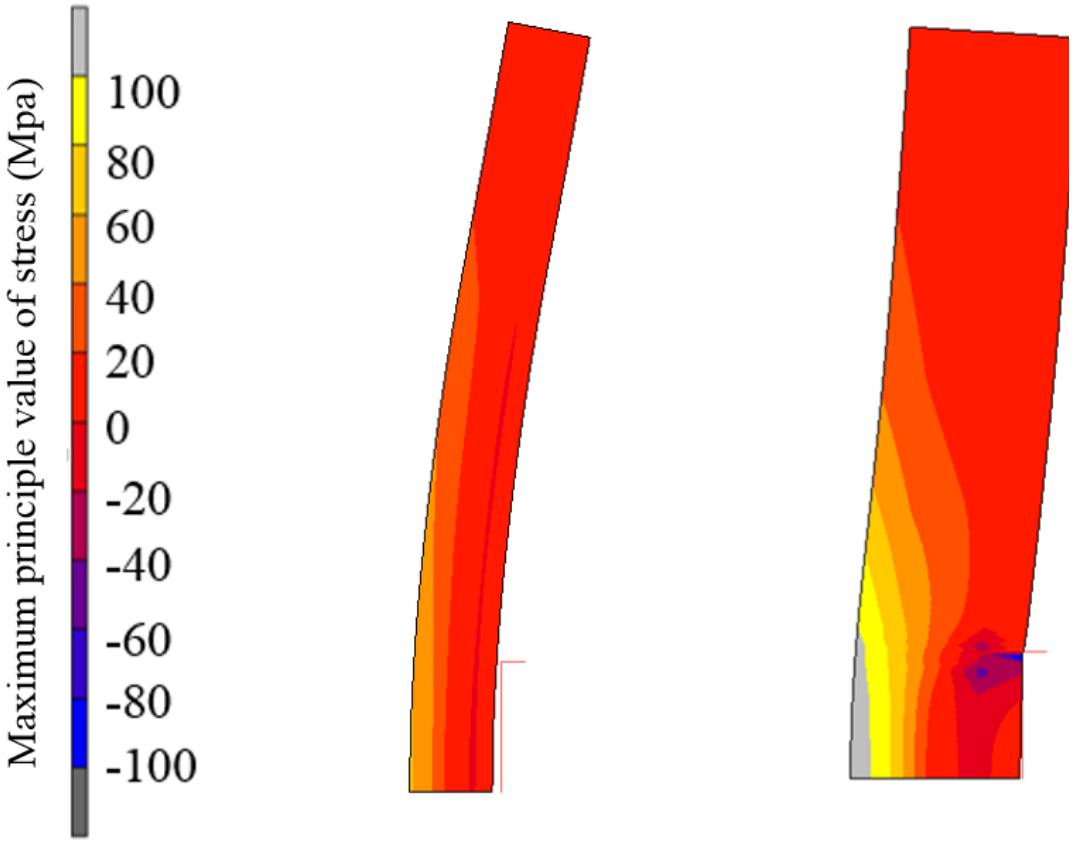

Figure 7.8: Two-Dimensional finite element model of a 10mm (left) and 20mm (right) thick polycarbonate plate following impact at the central 15mm of the 90mm radius shown. Colours show maximal principal stress. Greater deformation of the thinner disc with less stress is demonstrated.

Data analysis of the predicted response of the disc showed that maximum deformation occurs at the centre of the disc with oscillations in velocity less pronounced at the edge and halfway along the radius of the disc (Figure 7.9 to Figure 7.11)

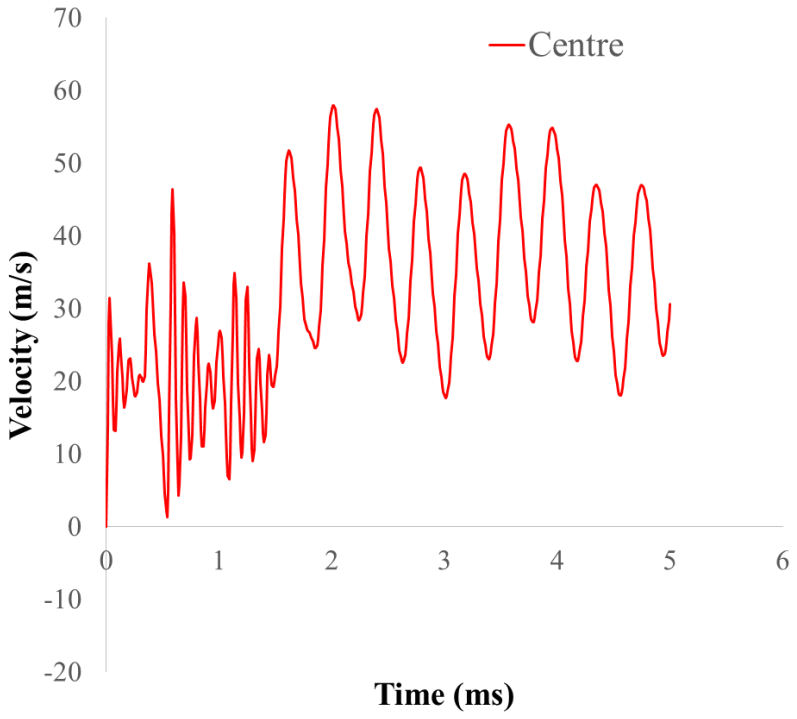

Figure 7.9: Velocity at centre of the plate following projectile impact, as predicted by a 2D finite element model of a 10mm thick polycarbonate disc.

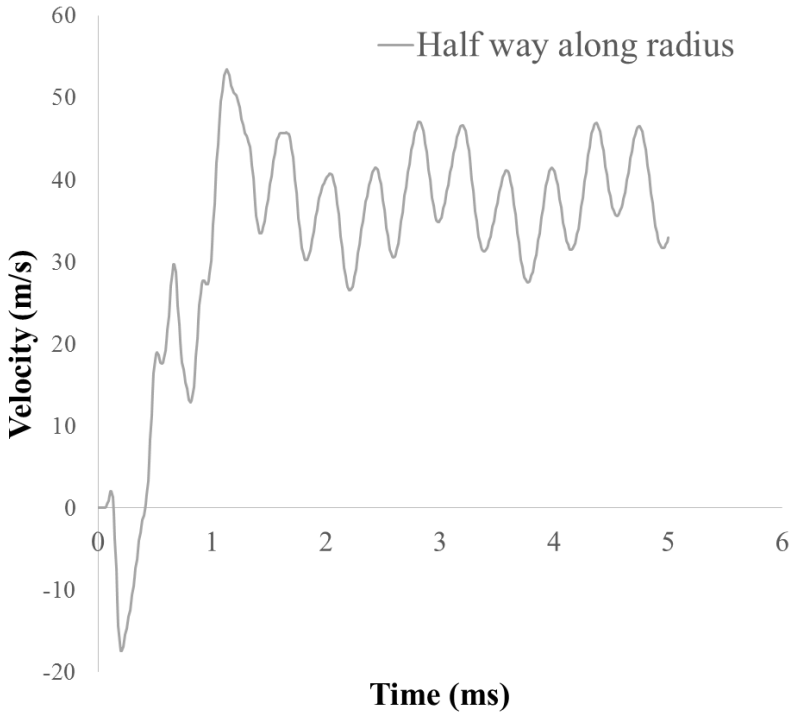

Figure 7.10: Velocity at a point halfway along the plate following projectile impact, as predicted by a 2D finite element model of a 10mm thick polycarbonate disc.

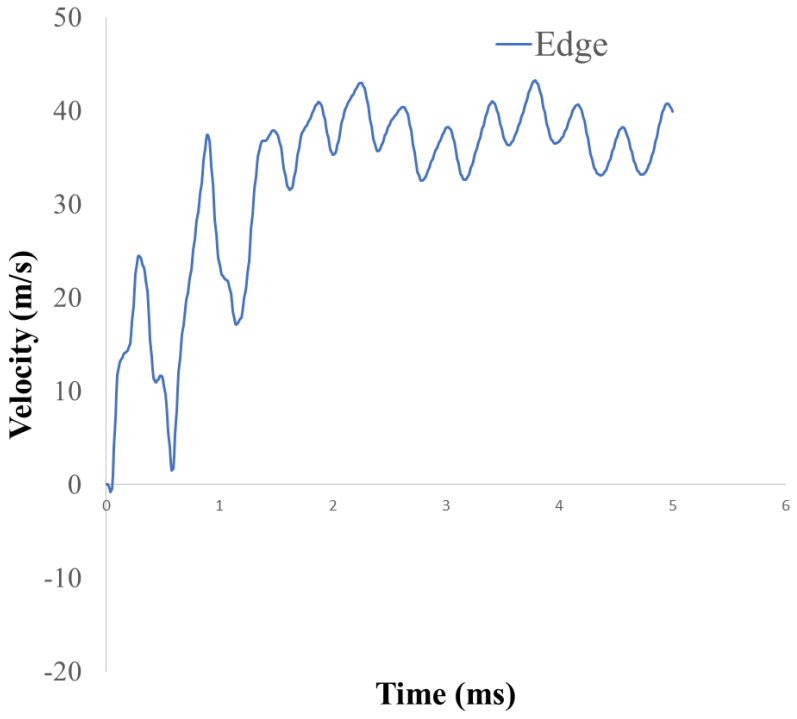

Figure 7.11: Velocity at edge of the plate following projectile impact, as predicted by a 2D finite element model of a 10mm thick polycarbonate disc.

Although aluminium or steel would be even stiffer, any benefit would be lost due to the greater mass and therefore slower final velocity (as predicted by Equation 6.6). Steel although stiffer, is around 6 times denser than polycarbonate and would require an enormously high pressure to accelerate the projectile sufficiently to induce the required velocity change. 12mm polycarbonate was found to be a suitable compromise. High density polycarbonate was selected for both projectile and target plate given that it has relatively low density (1.2g/cm^3), high yield strength (~60MPa) and high impact strength (20kJ/m^2) In both cases, custom milled high density polycarbonate (Sustunat ® PC) was milled into the required shape (by Engineering and Design Plastics Ltd, Cambs, UK). The projectile was cut to ensure a 4 mm total gap within the barrel. O ring grooves cut into the projectile and fitted nitrile o rings provided a pressure fit seal along the honed barrel. The projectile was designed such that the "head" would extrude past the collar and impact the target plate prior to the "shoulders" of the projectile impacting the stopping collar. Addition of further neoprene rubber sheeting to the lower surface of the collar would reduce the extrusion distance, and hence the impact time of the projectile. The projectile is shown in Figure 7.12.

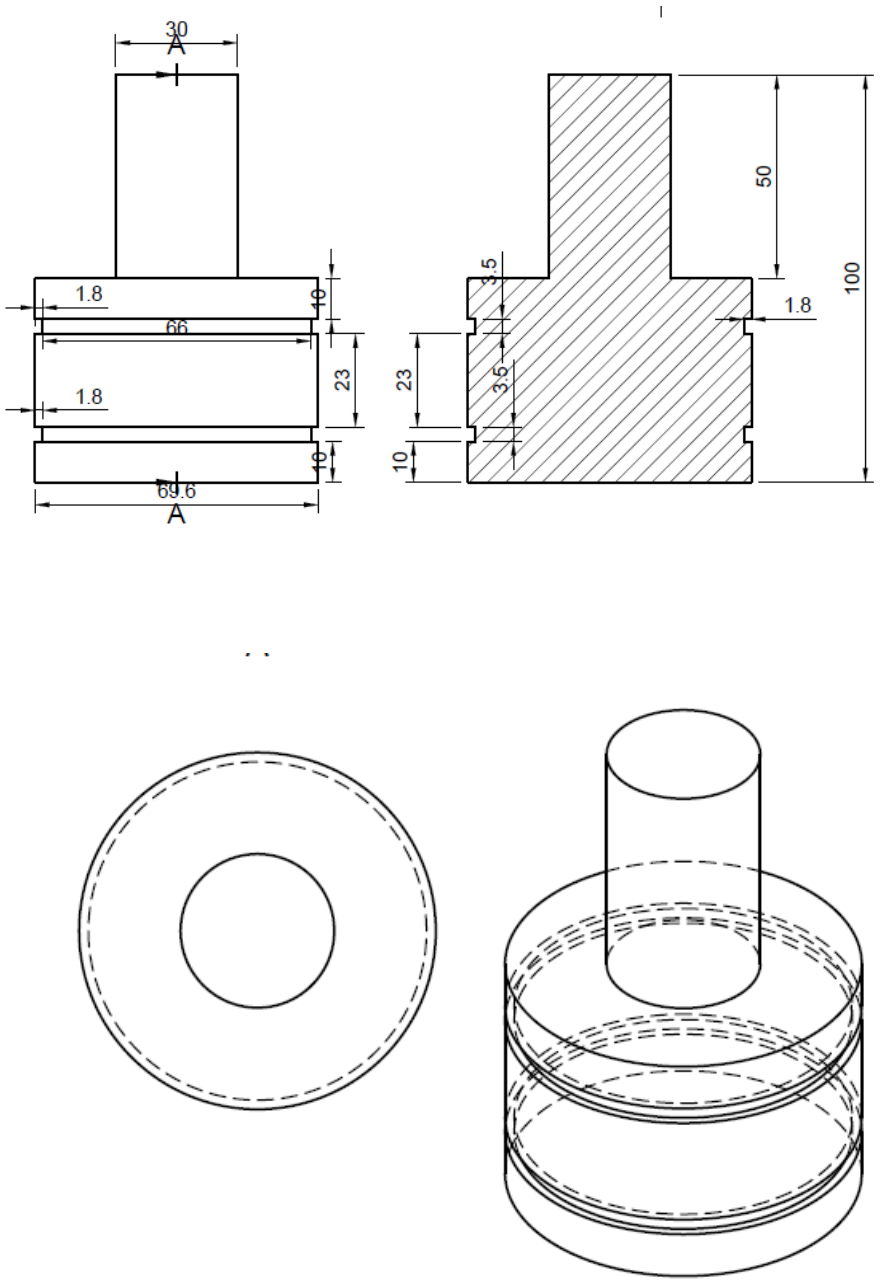

Figure 7.12: CAD views of the polycarbonate projectile.

Linear guide rails were bolted to the upper flange and the target plate mounted to the rails using linear bearings. Stoppage of the plate was determined by the placement of padded collar clamps higher up the linear bearings such that the stroke of the seat plate could be easily changed.

Furthermore, a conically shaped aluminium spreader was added beneath the target plate (and above the stopping collar) in order to spread the impact load over the area of the target plate.

The seat for the device was custom made from aluminium. Although twice as heavy as polycarbonate, aluminium was used as it easily machined and allows precision fitting of threaded instrumentation. The seat was designed to allow upright positioning of the animal with direct loading from below. Slots in the seat allow placement of soft webbing straps to approximate a 4 or 5-point harness (Figure 7.13). In house manufacturing of the seat was conducted with assistance from Mr Satpal Sangha.

Figure 7.13: Aluminium seat with harness (lower strap not attached).

As guided by the model, the seat was bolted to the polycarbonate plate halfway from the centre to the rim in order to minimise oscillation. Counter sunk bolts were used such that the lower surface of the plate sits directly upon the stopping collar or conical spreader.

For logistical reasons, the rig was mounted in two separate locations for the different experimental phases. For the latter animal experiments (as detailed in Chapter 8), the rig was mounted using a free standing frame. This frame was constructed from a steel tubing, and fixed to the floor using anchor bolts. An aluminium plate was fixed to the

frame to which the lower flange of the rig was bolted. This mount is shown in Figure 7.14 .

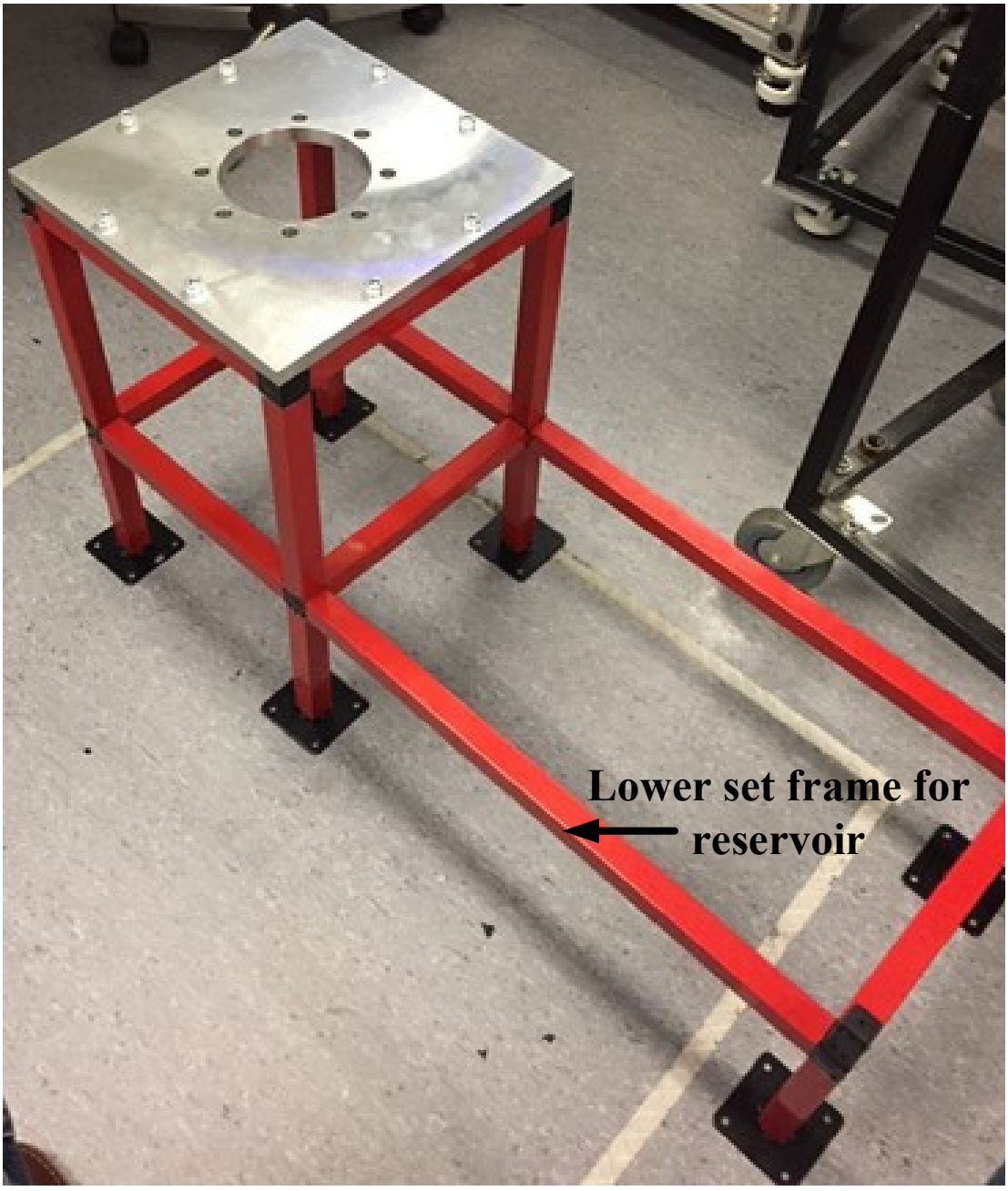

Figure 7.14: Free standing rig mount for animal experiments. The lower set portion of the frame allows positioning of the reservoir and solenoid valve.

For the purposes of characterisation, the rig was wall mounted using interconnect aluminium plates. A CAD of the mounted rig (without free flight segment), and in-situ photograph of RivUL are shown in Figure 7.15.

Figure 7.15: CAD of the rig in wall mount (left) with photograph of the rig in wall mount (right). The projectile is seen upon the top plate on the right (seat not pictured).

7.5 Instrumentation

The previous sections have described the specification, design, and construction of the RivUL but of equal importance is the acquisition of accurate, reliable data. The specifications and expected performance of the device require that information be gathered at a high rate and in a short period of time (within only a few ms). Information gathered during the tests are required to understand firstly the behaviour of the rig itself, and secondly of the specimen or animal.

An understanding of the rig behaviour can be obtained by measuring the resultant acceleration of the target. The accelerometer used for RivUL (350D02, PCB Piezotronics Depew, NY, USA) has a frequency response of 10 kHz allowing a rise time of 0.025 ms. The rise time of the acceleration of the plate is expected to be greater than this ensuring that this accelerometer is appropriate for this application. The accelerometer is uniaxial and has a measurement range up to 50000G and an overload limit of 150000G, and is therefore unlikely to be damaged by the experiments. The accelerometer includes a small threaded mounted stud. A threaded hole to fit this stud was cut into the base of the aluminium seat. The sensor was then mounted with its axis of measurement aligned with the vertical axis of the seat using an additional anti-vibration washer. Data from the accelerometer were recorded at 25 kHz through a PXIe data acquisition system (National Instruments, Newbury, Berkshire, UK). This acquisition rate is the maximum for the system and allows a data point every 0.04ms, sufficient for the expected experimental duration. The accelerometer module of the PXIe includes a digital and analogue filter to attenuate signals outside of the sampling rate and reduce noise.

The mechanical behaviour of the target or animal can be observed using high speed video. The Phantom v210 high speed camera (Vision Research Inc, USA) was placed on a tripod facing the target plate. Marks placed upon the floor ensured consistent positioning. The camera was set to record at 10000 fps, which was found to be suitably fast and provide good video fidelity. The high speed video has built in memory which can be accessed through specialised computer software (Phantom Camera Control Version 10, Vision Research Inc, USA).

The short duration and high rate of the experiments require that the sensors and rig operating system be synchronised. The system was configured such that a common trigger could be used to activate recording by the PXIe and the high speed camera whilst also opening the solenoid valve Figure 7.16.

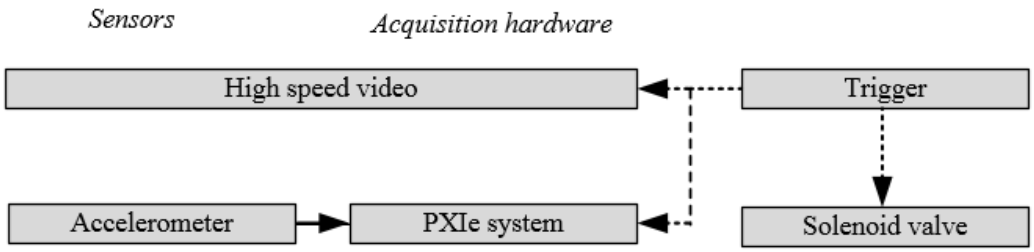

Figure 7.16: Trigger configuration for both data acquisition and firing activation.

7.6 Characterisation

7.6.1 Introduction

In order to assess the suitability of the axial loading rig for *in vivo* testing, a series of characterisation tests were performed without any animal samples. The purpose of these tests was to determine whether or not the behaviour of the rig meets the specifications described earlier in this chapter.

7.6.2 Methods

RivUL was constructed and configured as described in the sections above. A 300g rubber puck was strapped to the seat in an upright position. This mass is similar to the anticipated mass of the rats to be used in the *in vivo* protocol. At each test, the system was charged and the output of the control panel adjust to provide the expected driving pressure. The safety limit of the control panel is 19 bar and 18 bar was used as the

maximum test value. 3 bar was found to be the minimum required to accelerate the projectile sufficiently to strike the target plate.

It was instrumented with the shock accelerometer with data acquired using PXIe system described in the section above. LabView (National Instruments, Austin, Texas, USA), a graphical programming software developed to enable coupling of electronics with computer resources, was used to control the acquisition of data for further analysis. This analysis was performed using MATLAB (2017, MathWorks, USA). A low-pass Butterworth filter was used to filter the acceleration measurements. The cut off frequency (4 kHz) was selected based on the frequency analysis of the signal and was greater than the CFC1000 filter suggested by Society of Automotive Engineers for impact testing (Society of Automotive Engineers, 1995). The LabView programming was conducted with the assistance of Dr Grigorios Grigoriadis, Dr Nic Newell, and Dr Dilen Carpanen. The resultant axial velocity of the seat was derived after integrating the acceleration signal. High speed video was used to ensure correct functioning of the system and to ensure a straight trajectory of the projectile during the free flight period.

7.6.3 Results

Twelve tests were successfully completed (including full data acquisition). In each of them, the high speed video confirmed impact of the projectile with the plate. As expected, increasing pressure increased the acceleration and velocity of the plate and seat.

In each test, there was a peak of positive Gz acceleration at point of projectile impact followed by a smaller negative acceleration as the plate movement was arrested by the stopping clamps. The resultant acceleration profiles are shown in Figure 7.17.

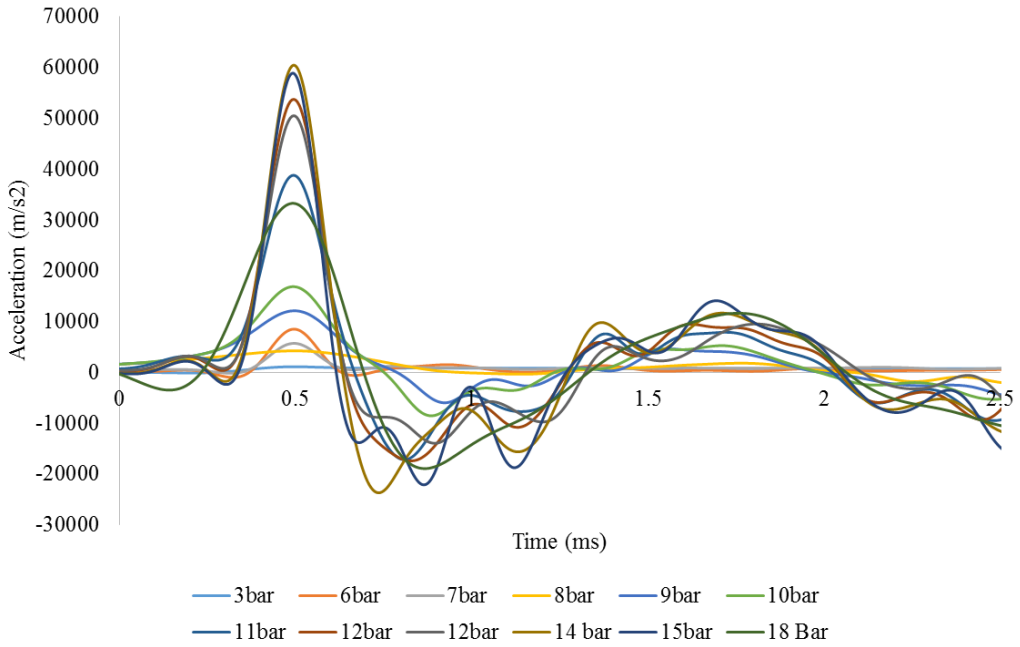

Figure 7.17: Acceleration profile of seat/plate following projectile impact. The driving pressure behind each curve is illustrated.

In each case, peak acceleration of the seat is achieved within 1 ms. The peak acceleration and peak integrated vertical velocity are shown in Table 7.1 with the corresponding curves shown in Figure 7.18.

Test #	Pressure (bar)	Peak Acceleration (m/s^2)	Peak Velocity (m/s)
1	3	1114	0.69
2	6	8514	1.79
3	7	5726	2.26
4	8	4244	3.08
5	9	12136	4.65
6	10	16885	5.44
7	11	38817	8.32
8	12	53780	9.75
9	12	50552	7.92
10	14	60490	10.03
11	15	58887	9.00
12	18	33290	8.45

Table 7.1: Peak acceleration and velocity characteristics of the rig with varying input pressure.

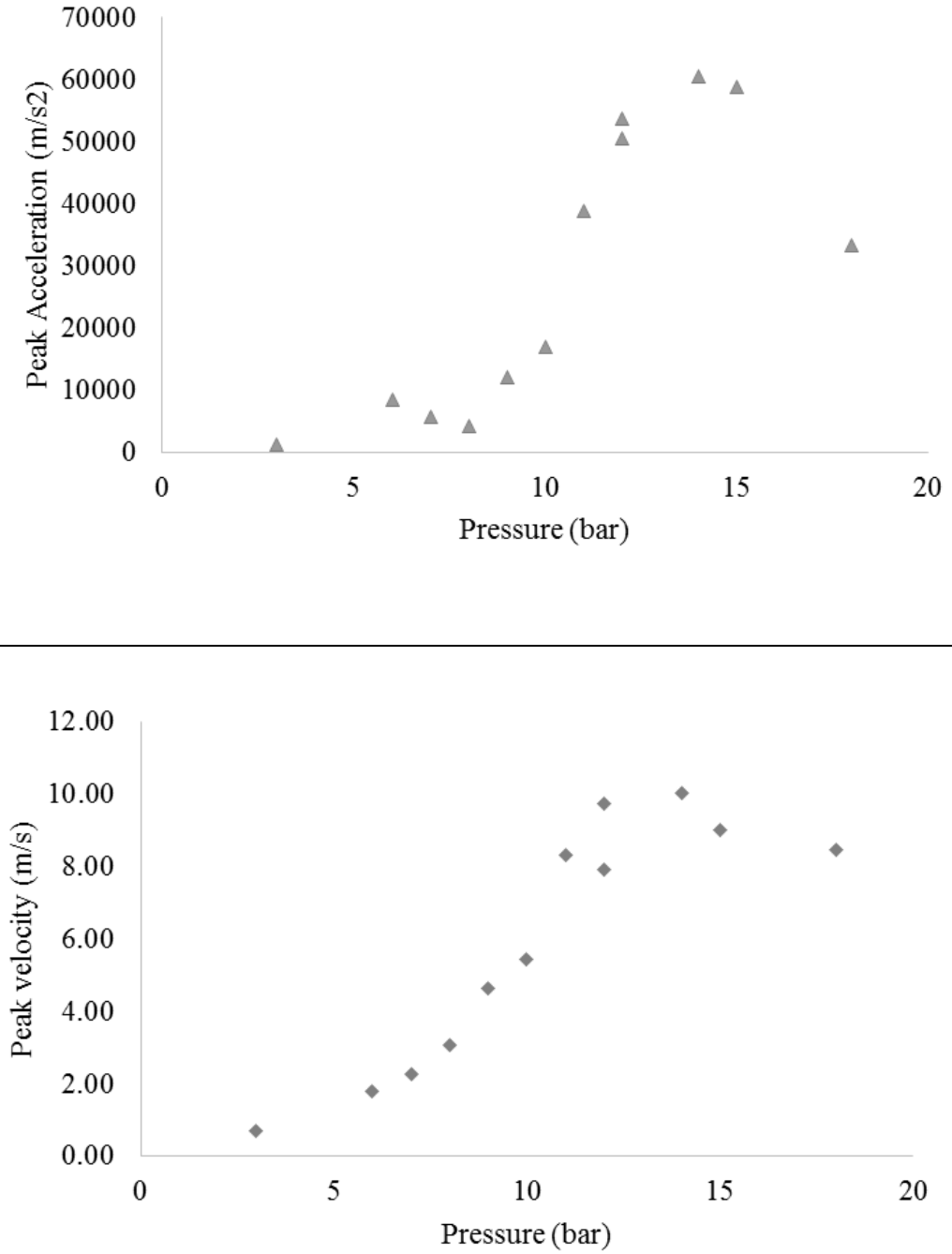

Figure 7.18: Peak acceleration (above) and peak velocity (below) of the seat and plate in response to varying input pressure.

7.6.4 Discussion

Although limited in number, the characterisation tests demonstrate that the accelerative capabilities of RivUL meet the specifications outlined earlier in the chapter. The acceleration profile of the device includes a steep relatively linear portion prior to a relative plateau. This pattern fits with the initial mathematical assumption [Equation 7.5] that final volume would be proportional to the square root of the input pressure. Importantly, the specified 5000g (identified as a maximum requirement) is within this linear region. The acceleration occurred over a sufficiently long duration that predicted UBB velocities were also achieved, albeit at rates likely more appropriate for small animal scaling. Although an increased sample number may have better characterised the behaviour of the rig, several tests were conducted but not included in this chapter due to data loss.

The fall in acceleration and velocity at 18 bar may be due the proximity of the pressure to the failure limit of the control panel which represents a true limit to this system. This failure limit represents an inherent property of a pneumatically driven system. Gravity driven drop towers have a well characterised linear relationship between impact velocity and height but do not realistically approximate underbody loading (due to the initial freefall state).

7.7 Conclusion

This chapter has discussed the specifications, design, and construction of RivUL. The initial characterisation of the device had demonstrated that it meets the expected maximum acceleration and velocity limits within an appropriate period. The mechanical action of the system functions as designed with resultant plate acceleration and velocity varying as a function of the input pressure up to a limit. The triggering and data acquisition system enabled precision recording of accelerative data while the high speed video will enable the measurement of biomechanical parameters.

A significant unknown is the required axial loading which causes torso injury in the small animal model. The specified 5000g is thought to be a reasonable maximum limit.

A major benefit of RivUL is the ease of varying the loading up to and past this point by simple manipulation of the pressure input.

Having demonstrated the accelerative range of the system, the next chapter will discuss the use of this range with a series of small animal experiments. The primary purpose of these experiments will be to determine the biomechanical behaviour of the torso in response to high rate axial loading and explore the relationship between loading and injury tolerance. The larger number of experiments required to describe the relationship will also be used to better describe the behaviour of the rig itself.

CHAPTER 8

INVESTIGATING TORSO INJURY IN AN *IN VIVO* RODENT MODEL OF UNDERBODY BLAST

8.1 Scope of the chapter

Chapter 6 described existing historical and contemporary work in impact biomechanics and discussed the limitations of existing cadaveric and *in vivo* models of underbody blast. The chapter concluded by highlighting the need for a new *in vivo* model to demonstrate severe injury. Chapter 7 discussed the design, construction, and initial characterisation of a new device with which to cause high rate axial loading of a rodent model. This chapter will expand upon the experimental rationale of such an experiment before detailing the experimental protocol and results of an *in vivo* rat model of underbody blast using the new apparatus.

8.2 Introduction

As discussed in Chapter 6, investigation of human injury tolerance to particular mechanical insult requires either human volunteers or the development of an experimental (computational or physical) surrogate. Volunteer studies are suited only to low level discomfort or very mild injury. In contrast, cadaveric studies have been used to great effect for severe skeletal injury but the use of PMHS for soft tissue injury testing is limited by post mortem changes in soft tissue structure, positioning, and pressurisation. Anthropomorphic tests devices and computational studies are widely used for contemporary assessment of injury risk but both depend upon experimental data for validation and accuracy of boundary conditions and biofidelity. Computational models of torso injury have been developed for direct frontal and lateral loading (Shah *et al.*, 2001; Richens *et al.*, 2004; Cooper and Taylor, 2015), but none have been developed or validated for axial load. This may be due to the complex boundary conditions and uncertainty of injury mechanisms in the vertical direction.

Replication of torso injury severe enough to affect survivability may be best achieved using an *in vivo* animal model. Given the stated need to better understand the relationship between underbody loading and torso injury, this model must combine:

a) loading conditions similar to UBB;
b) an animal torso with anatomy and positioning analogous to that of the seated vehicle occupant; and
c) experimental numbers great enough to adequately demonstrate the relationship between loading and injury.

Chapter 7 detailed the development of a rig capable of replicating the high rate axial loading of UBB. The aims of this chapter are to describe the development of an *in vivo* rat model of UBB and to demonstrate the relationship between clinically relevant torso injury and high rate vertical loading.

8.3 Rationale

The choice of animal model is based upon the consideration of two main factors:

a) relative similarity to the human in regards to anatomy and tolerance and
b) the ability to acquire and utilise the animal model in a suitable experiment.

These two factors are somewhat opposing in that those animals with most similarity to humans (such as sub-human primates) are difficult to acquire and subject to a great deal of ethical controversy. Although historical experiments used a large number of primates (and other large mammals such as bears), such experiments are associated with great expense (Cook and Mosely, 1960; Kazarian *et al.*, 1970; Kazarian, 1975). Similarly, smaller "large animals" such as swine and dogs may be closer in size to humans but are more anatomically distinct than primates and still likely to incur greater experimental difficulty than rodents (Huelke *et al.*, 1986).

Rat models of high rate loading are well described. The so called "Bowen Curves", originally derived by researchers of the Lovelace foundation in 1968, are still used for the assessment of primary blast lung injury risk (Bowen *et al.*, 1968). These injury curves estimated the risk of primary blast lung injury to the human based on extrapolation of experiments conducted upon a range of animals (including rats). Scaling for these experiments were primarily based upon body mass which was found to be the only variable needed to predict the duration of blast tolerance (although the absolute pressure tolerance was found to relate to other variables including lung density and relative lung mass). These scaling considerations will be examined in further detail in Chapter 9. The same group had previously investigated whole body impact injury using mice, rats, guinea, pigs and rabbits dropped from various heights (Richmond *et al.*, 1961). Precise injuries were not described but similar injury thresholds (in terms of impact velocity) were seen among the animals despite a large mass variation. Richmond *et al* mathematically predicted a fatal impact velocity for humans of 6.4m/s compared to 7.3m/s threshold of a rat obtained experimentally. The reason for these values being so close to each other despite orders of magnitude of difference in body mass will be discussed in Chapter 9.

More recently, the rat has been used to as a model for direct impact pulmonary contusion (Hoth *et al.*, 2006). This experimental series was used to generate a finite element model which accurately predicted the occurrence and location of pulmonary contusion in response to the loading (Gayzik *et al.*, 2007). The group validated the model against sequential micro CT.

The rationale for using such a model is based upon mechanical properties. A simple mechanical analogue of any living body in response to loading may be developed assuming similar geometry and tissue properties (von Gierke, 1968). Although the application of these analogues to scaling, and the translation of injury potential the human will be discussed further in Chapter 9, it is important to discuss to what degree the anatomy could be considered similar. Although relative anatomical similarity is shared by all mammals, there is organ specific geometric variation which must be explored in order to determine the extent to which any mechanical assumptions can be made.

8.3.1 Comparative anatomy

This section will discuss fundamental anatomical similarities and differences between the rat and human with focus upon the relevant torso anatomy explored in Chapter 5. Of course, some gross anatomical similarities and differences which are apparent at whole animal scale. The rat is a quadruped, with a relatively long tail. Accordingly, the rat has a greater number of coccygeal vertebrae than the human. The rat has a similar number of cervical (7), thoracic (13), lumbar (6) and sacral (4) vertebrae. The bone histology between the two species is similar (Treuting *et al*., 2018).The mass of a rat varies with strain and gender; the average adult mass of the adult Sprague-Dawley rate is 250-300g (female) and 300-400g (male) (Treuting *et al*., 2018) compared to 75-85kg in humans. The implications of this difference in mass will be discussed in greater detail in Chapter 9.

8.3.2 Thorax

As in the human, the visceral cavities of the rat are lined with serosa. The thorax is lined with pleura, with a parietal pleural lining the lungs. As in the human, the mediastinum is enclosed between the left and right pleural cavities and filled with the great vessels, heart, oesophagus, trachea, and pericardium (Figure 8.1).

A

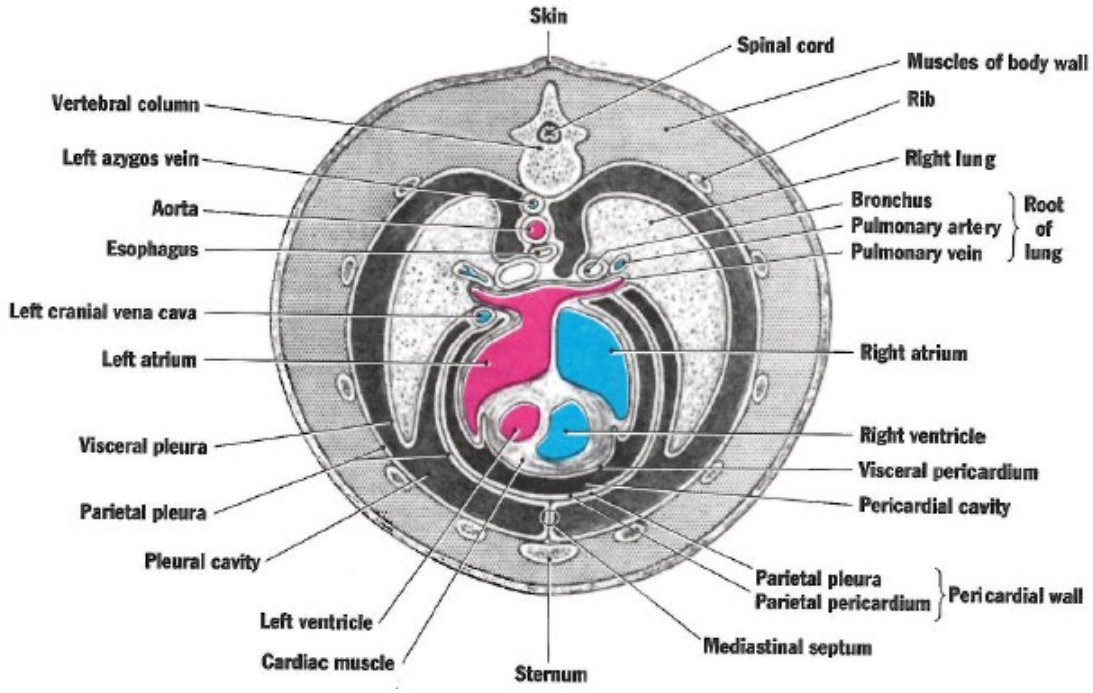

B

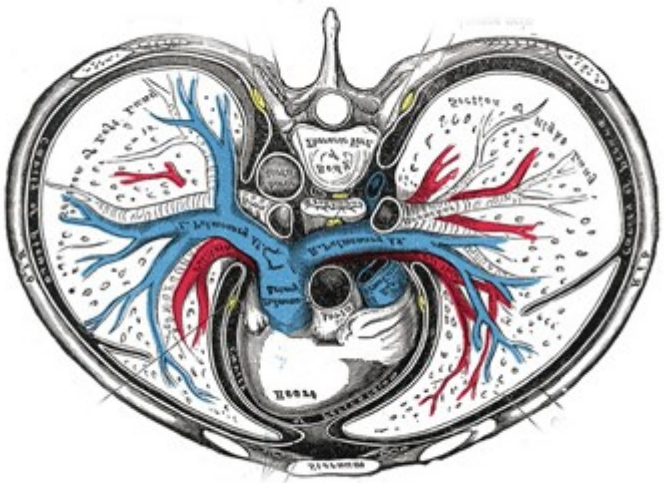

Figure 8.1: A: Diagrammatic cross section through the thorax of a rat at a level near the cranial end of the heart showing the relationships of the pleura and pericardial cavities and their serosae to the thoracic viscera. The serosa is depicted thicker than it is in reality to demonstrate its continuity and anatomical relationships. With permission from Walker and Homberger (1997). B: Analogous cross section from a human torso shows similarly arranged structures. With permission from Gray *et al* (1918).

Although human lungs are divided into three lobes (upper, middle, and lower) on the right and two (upper and lower) on the left, the lungs of the rat are divided into four lobes (cranial, middle, caudal, and accessory) on the right with only one lobe on the left. The accessory lobe of the left lung passes dorsal to the caudal (inferior) vena cava to enter a pocket of the right pleural cavity. In both species, pleura wrapped lower portions of the lungs rest directly upon the diaphragm. As in humans, the pleura condenses over the hila of the lungs to form the inferior pulmonary ligament (Rajab, 2018) which may be a potential tether point in response to axial motion .

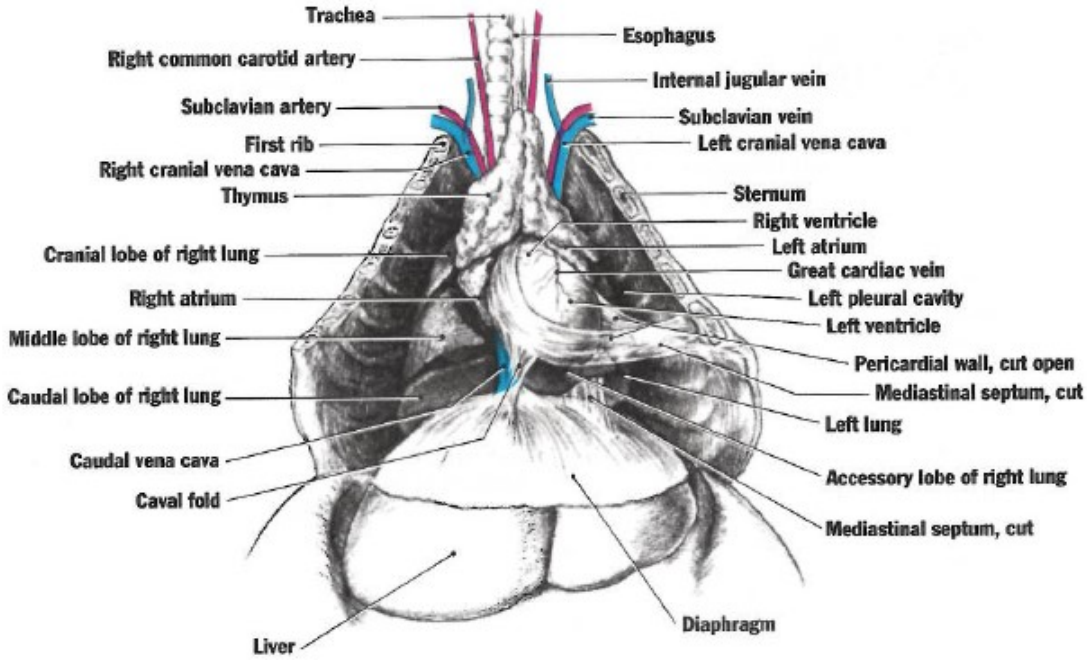

Figure 8.2: Ventral view of the thoracic cavity showing lobar segmentation of the right lung and mediastinum. Reproduced with permission from Walker and Homberger (1997).

As in humans, the trachea bifurcates at the carina into two extra pulmonary bronchi which enter the left and right lobes. There are differences in epithelial cell thickness and cell type composition with non-ciliated cells predominating over ciliated cells in the rodent proximal airways (Treuting *et al.*, 2018). Within the respiratory zone of the pulmonary parenchyma, the rat lung resembles the human histologically although rodents lack well developed respiratory bronchioles. Both species possess alveolar ducts and alveoli as the functional component of the respiratory zone. The structure of the alveolus is similar across the two species but the size is proportional to body mass, and

thus inherently scaled for the rat (Treuting *et al.*, 2018). The overall mass of the lung (~1.5g for a Sprague Dawley rat of experimental size) equates to around 0.6% of the overall body mass. Measured human lung mass is dependent upon cause of death but has recently been estimated at between 185 and 967 g with a mean of 445g for the right lung and 395g for the left lung. The total lung mass thus equates to around 1.1% of overall body mass (Molina and DiMaio, 2012a).

The structure and organisation of the rat and human cardiovascular systems are generally similar (Treuting *et al.*, 2018). As is true in all mammals, both species have four chambered hearts. Although the rodent heart is far smaller than the human heart, the mass of the heart relative to the whole body is very similar across the two species (3-4% of overall body mass), as are the relative thicknesses of the right and left ventricular walls. In both species, the heart is overlaid anteriorly by the sternum, ribs, and intercostal muscles, and laterally by the lungs. The descending aorta and oesophagus lie posteriorly. Although the rat is a quadruped, the long axis of the heart, from apex to base lies in a very similar direction to that of the human although the overall shape of the heart is rounder than the human (Figure 8.3).

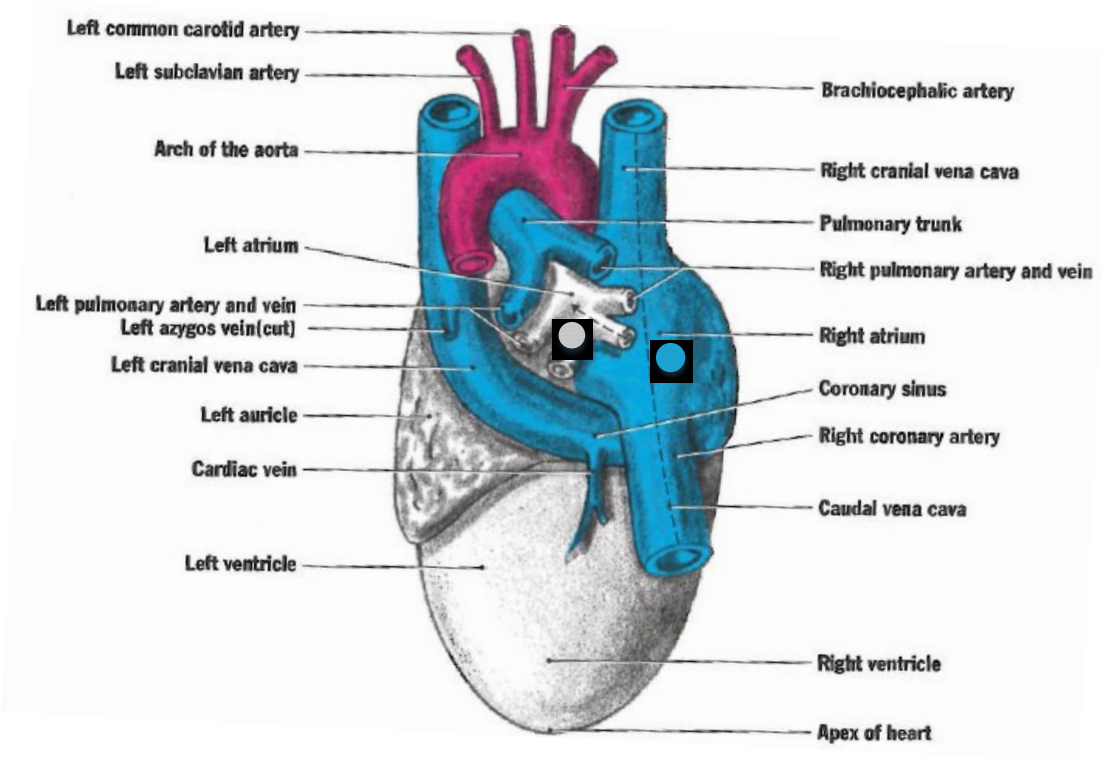

Figure 8.3: Dorsal view of the rat heart. Reproduced with permission from Walker and Homberger (1997)

The organisation of the rat great vessels are very similar to those in the human although there are both left and right cranial (superior) vena cavae, each formed from the confluence of the respective subclavian and internal jugular veins.

The branches of the aortic arch are analogous to the human with brachiocephalic trunk, left common carotid and left subclavian arising directly from the arch. Subsequent thoracic branches are also similar with intercostal arteries arising from the descending aorta. An analogous pulmonary trunk directs de-oxygenated blood away from the right ventricle.

The basic structure of the circulation, as demonstrated in Figure 8.4, can be seen to closely resemble that of the human.

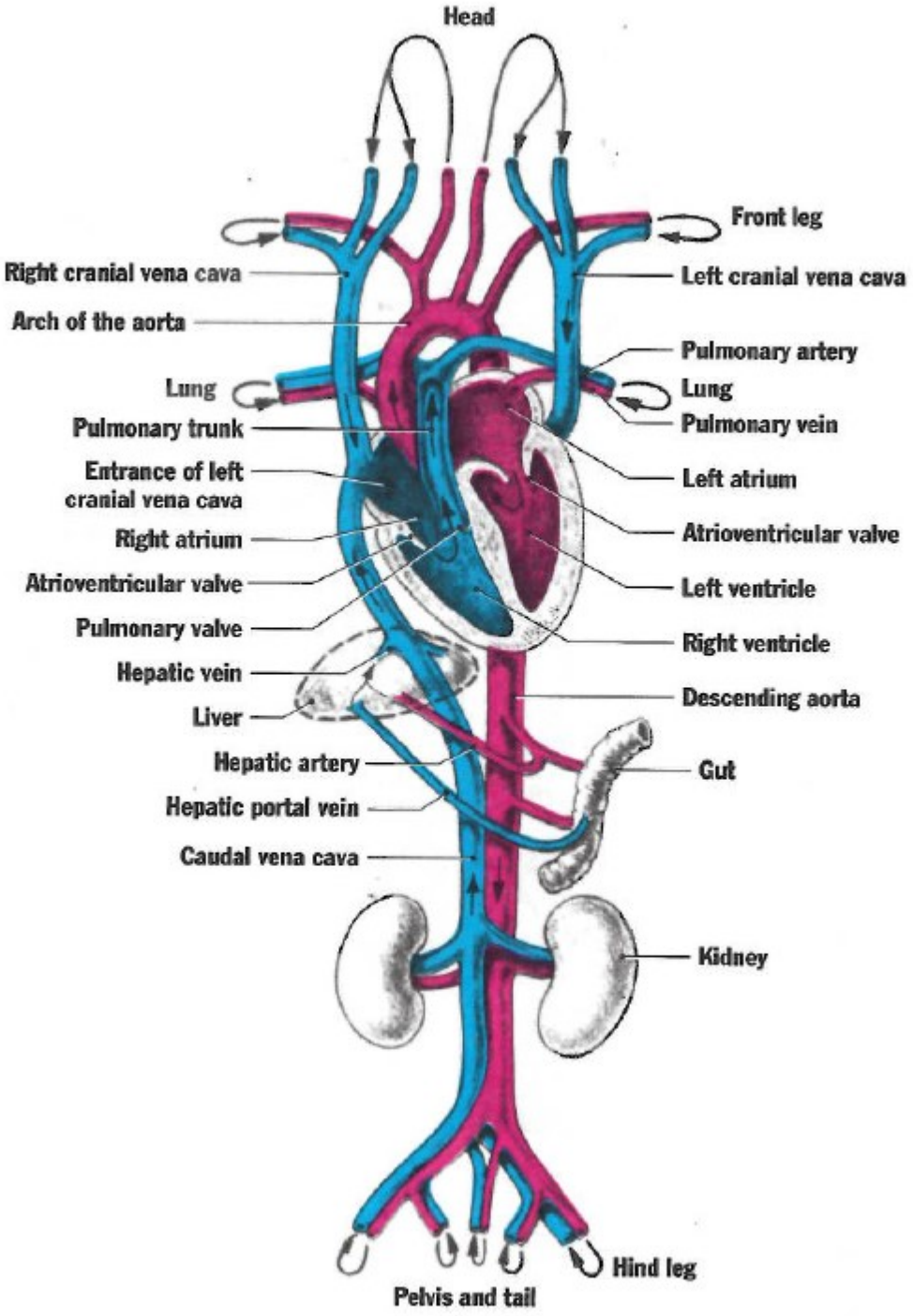

Figure 8.4: Diagram of the adult rat circulatory system. Reproduced with permission from Walker and Homberger (1997)

Histologically, the structure of the rat vasculature is generally similar to that of the human. The vessel wall components are the same with arteries formed from tunica intima, tunica media, and tunica adventitia. In rodents, the sub endothelial connective

tissue is virtually non-existent with the endothelium resting upon the internal elastic lamina. This connective tissue layer in humans varies with artery, size, age, and disease state.

The gross morphology of the major vessels are similar with attachments of the descending rat aorta behind the pleura and relative freedom of the aortic arch. Like humans, rats have a well-defined aortic isthmus at the base of the left subclavian artery (Wang *et al.*, 2015) .

8.3.3 Abdomen

As shown by Figure 8.4, the arterial and venous system in the rat and human are similar in their basic distribution with branching and bifurcation occurring at analogous points. The abdominal viscera, hind legs, and tail are supplied by branches of the descending aorta and drained ultimately by the caudal (inferior) cava. The hepatic portal system is the main blood supply to the liver and, as in the human, is formed from the superior mesenteric and splenic veins.

In rats, the liver mass represents approximately 5% of the total body mass, while in adult humans it represents 2.5%. In rats weighing between 250 and 300 g, the liver mean mass was 13.6 g and the liver transverse diameter measured from 7.5 to 8.0 cm (Martins and Neuhaus, 2007). While the human liver is predominantly confined to the upper right sub-diaphragmatic region, the rat liver spans most of the sub-diaphragmatic region. The superior (parietal) surface comprises a part of the left lateral and medial lobes, and, as a whole, is convex, and fits under the vault of the diaphragm. It is completely covered by the peritoneum, except along the line of attachment of the falciform ligament.

The line of attachment of the falciform ligament divides the liver into two parts, termed the right and left lobes. Different from human livers, in which the right lobe is much larger than the left one, the rat left and right liver have approximately the same volume. The inferior (visceral) surface is uneven, concave and is in relation to the stomach, duodenum, right colic flexure, superior part of the pancreas, right kidney and suprarenal gland. The rat liver inferior surface does not have the fossae in the shape of the letter H as in humans. This surface is almost completely invested by the peritoneum. Through

the porta (transverse fissure) goes the portal vein, hepatic artery and nerves, the hepatic duct and lymphatics. Liver impressions (colic, renal, duodenal and suprarenal) are not as evident as in human livers. The posterior surface is not covered by the peritoneum over some part of its extent, and is in direct contact with the diaphragm. It extends obliquely between the caudate lobe (CL) and the bare area of the liver. The inferior vena cava is completely intrahepatic (Martins and Neuhaus, 2007).

The rat liver lobes, like the human liver, are named after the portal branches that supply them, as among mammals, the portal system is the most constant anatomical reference The middle or median lobe (ML) is the largest, accounting for approximately 38% of the liver weight. It has a trapezoidal shape and is fixed in the diaphragm and abdominal wall by the falciform ligament. It is in continuity with the left lateral lobe (LLL) and is subdivided by the umbilical fissure into a large right medial lobe and a smaller left medial lobe.

The right lobe (RL) is located on the right of the vena cava and is almost completely covered by the medial lobe. It comprises about 22% of the liver weight and is divided by a horizontal fissure into two pyramidal-shaped lobules: the superior right lobe (SRL) and inferior right lobe (IRL). The left lateral lobe (LLL) has a rhomboid shape, is flattened and situated in the epigastric and left hypochondriac regions over the anterior aspect of the stomach. Its medial portion is covered by the left part of the medial lobe. The CL is situated behind the LLL and on the left of the vena porta and inferior cava vein. It may be further divided into the anterior (AC) and posterior caudate (PCL) lobes. The in situ positions of these lobes are shown in Figure 8.5.

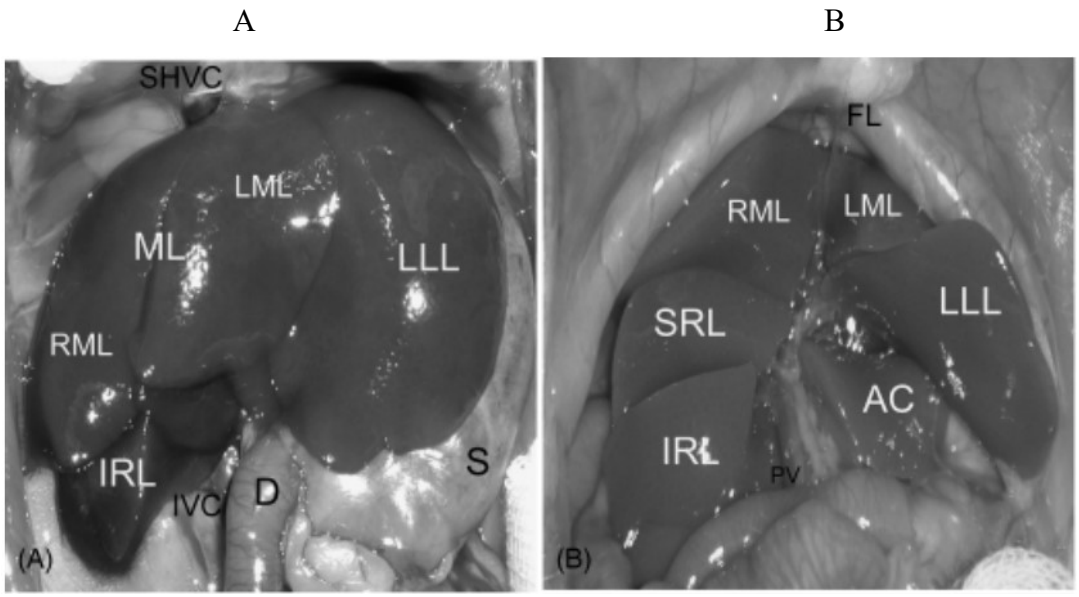

Figure 8.5: Anterior (A) and Separated (B) view of the rat liver showing relative positions of the lobes of the liver (Inferior right lobe –IRL; right medial lobe- RML; medial lobe - ML, left medial lobe-LML; left lateral lobe -LLL; superior right lobe- SRL; anterior caudate lobe AC) in addition to the duodenum (D), IVC, portal vein (PV) and supra-hepatic vena cava (SHVC). Reproduced with permission from Martins and Neuhaus (2007).

Similar to the human liver, the rat liver is connected to the under surface of the diaphragm and to the anterior wall of the abdomen by five ligaments: the falciform, the coronary, and the two lateral are peritoneal folds; the fifth, the round ligament, is a fibrous cord, the obliterated umbilical vein. The liver is also attached to the lesser curvature of the stomach by the hepatogastric ligament, and to the duodenum by the hepatoduodenal ligament. The falciform ligament is a thin peritoneal fold and it is attached to the under surface of the diaphragm and the posterior surface of the right rectus abdominal muscle at the level of the umbilicus.

The triangular ligaments are divided into the right and left ligaments. The right triangular ligament is situated at the right extremity of the SRL, and is a small fold that passes to the diaphragm, being formed by the apposition of the upper and lower layers of the coronary ligament. The left triangular ligament is a fold that connects the posterior part of the upper surface of the left lobe to the diaphragm. The caudate process is attached to the dorsal diaphragm by thin ligaments. The IRL is also attached to the diaphragm and has another ligament to the anterior part of the infra hepatic vena cava.

The round ligament is a fibrous cord resulting from the obliteration of the umbilical vein. It ascends from the umbilicus, in the free margin of the falciform ligament, to the umbilical notch of the liver.

The histological structure of the liver is common across both species with blood and bile flow occurring in opposite direction across the hepatic lobules.

Inferior to liver, the main vessels of the abdomen run within the retroperitoneal space (Figure 8.6). The relative positions of the kidneys differ in that the left rodent kidney is closely adjacent to the liver and lies superiorly to the right; the opposite is true in the human.

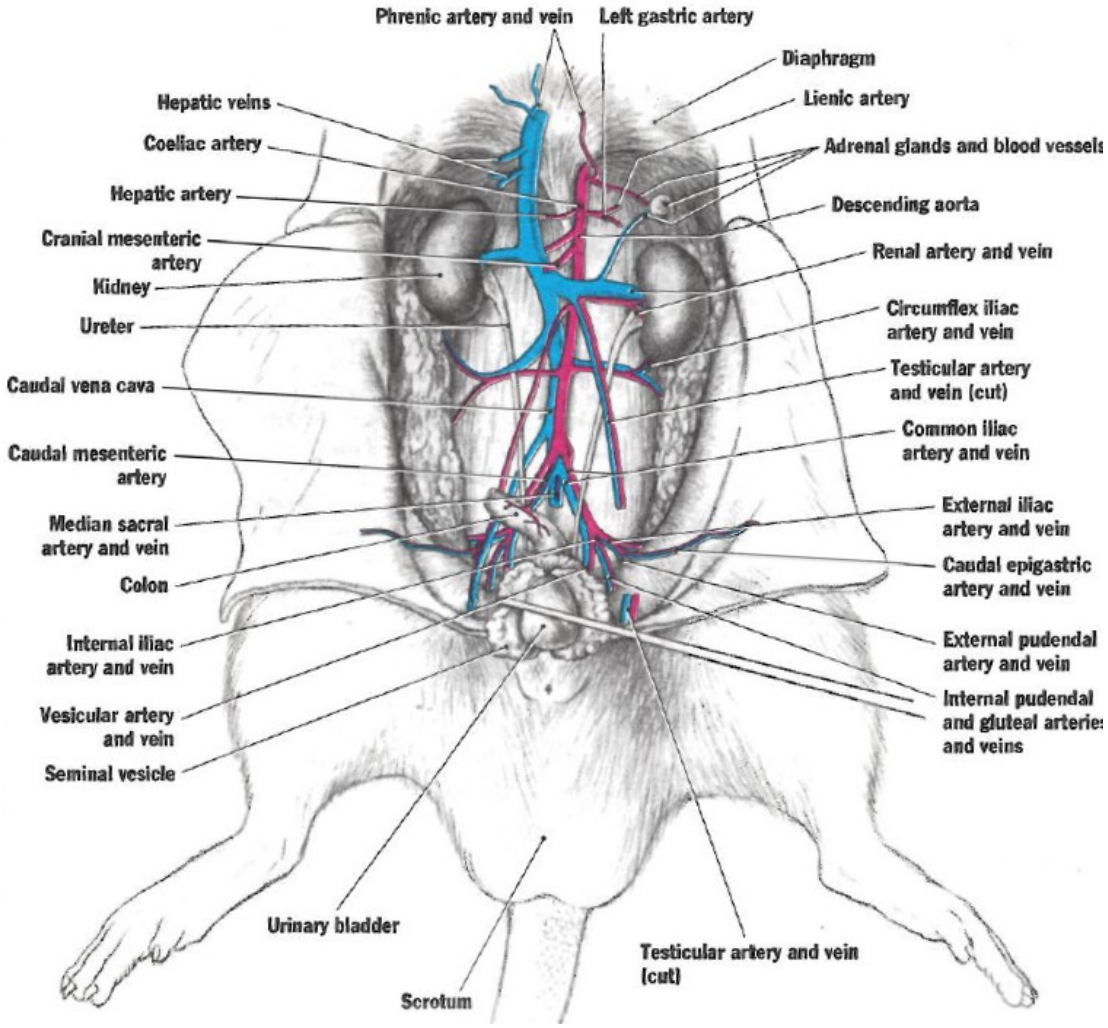

Figure 8.6: Anterior view of the retroperitoneal compartment of the male adult rat with other abdominal organs removed. Reproduced with permission from Walker and Homberger (1997).

The basic structure of the GI tract in rodents is similar to that of humans. The rodent possesses a non-glandular forestomach. The rodent duodenum is proportionally shorter although both species have a similar small bowel mesentery. The large bowel is less similar with the caecum, a curved blind sac representing one third of the large bowel in the rat. The rodent pancreas is locally dispersed throughout the mesentery adjacent to the duodenum although the function, cell distribution, and duct structure are similar.

The spleen of both species is located in the upper left abdominal quadrant although the rat spleen is considerably more elongated. The rat spleen is around 500-750mg in an

adult rat, compared to ~150 g in the human, equating to around 0.3% of total body mass in both species (Treuting *et al.*, 2018). The organ is supplied by splenic vessels to a hilum in both species.

8.3.4 Conclusions

Although there are a great many differences in the torso anatomy of the rat and human, there are probably more similarities. The basic histological structure of each of the organs is very similar, suggesting similar scaled material properties. The relative size and masses of the organs to the overall body size and mass are also similar to the respective human organs with the liver being an exception. Organs are in general, similarly located throughout the torso with the analogous peritoneal, pleural, and ligamentous attachments. It is possible that these attachments generate similar boundary conditions and tethering in response to loading.

These anatomical and structural similarities are unlikely to allow direct translation of absolute injury risk values but may be combined with appropriate scaling to demonstrate the relationship of UBB to severe injury. More compelling are the benefits offered by the use of small animal model: ease of acquisition, housing, and ability to use the small scale device will facilitate a larger number of experiments with sufficient power to demonstrate the desired relationship.

8.4 Methods

8.4.1 Ethics

Ethical approval for animal experiments was obtained at both an institutional and national level. The experimental protocol was submitted to the Imperial College Animal Welfare and Ethical Review Board (AWERB). The AWERB includes members who are vets, animal care staff and lay people (some of whom are independent of the College), and scrutinises all project proposals for scientific and ethical justification of animal use. Following AWERB approval, the amended project license (P5B192285) was submitted to and approved by the UK Home Office in align with the Animals (Scientific

Procedures) Act 1986 (ASPA). The ASPA is a rigorous piece of legislation which regulates any experimental procedure applied to a protected animal that may have the effect of causing that animal pain, suffering, distress or lasting harm (a regulated procedure). The overall purpose of both local and nationally boards is the widest possible application of the 3Rs: Replacement (of animals with non-sentient alternatives), Reduction (in animal numbers) and Refinement (of techniques to minimise pain and suffering).

8.4.2 Study Design

The primary outcome of these experiments were the presence or absence of torso injuries in response to varying high rate loading. As with existing animal models of blunt injury, lung injury was the primary chest injury outcome and liver injury was the primary abdominal injury outcome. The variable for the experiment was loading provided by the RivUL system. The input of the system will be varied by the changing of the driving pressure, although acceleration and resultant velocity of the seat will be used to describe the loading.

Given the intuitive absence of injury in the absence of loading, no control group is required but a range of input loading was required in order to adequately describe the relationship of loading to injury. Although 2800g was shown to be an approximate chest and abdominal injury threshold in work by Fiskum and Fourney (2014) , these experiments were carried out upon prone rats. The effect size required to accurately predict a required sample number is therefore uncertain. Instead, a pragmatic approach was used whereby the data was progressively examined to determine the need for additional tests.

8.4.3 Animals and environment

Female Sprague-Dawley rats (Charles River, UK) of between 250-300g were maintained under a controlled environment with an ambient temperature of 23 ± 2°C, a 12 hr light/dark cycle, and continuous free access to food and water. Female rats were chosen as the large scrotal sacs of male rats may have impeded the ability to sit them

upright. 60 animals were obtained in total with some animals used for development of the loading, restraint, and imaging protocols.

8.4.4 Animal restraint and positioning

Animals were restrained to the RivUL seat using soft webbing straps. These straps were custom made using adjustable clips to allow tightening and loosening behind the animal. Three straps fastened such that the torso straps crossed over and threaded through the holes of the seat behind. An additional "lap strap" was threaded over the top of the rat pelvis so that the overall configuration approximated the restraint provided by a "five-point" harness with the animal positioned so that the torso was aligned parallel to the upright seat back in an effort to replicate the posture of a seated soldier (Reed, 2014). The legs of the animal were allowed to fall to either side of the seat so that the pelvis was in direct contact with the seat bottom. The upper portions of the straps were passed over the shoulders of the animals with a crossing point over the mid chest. The straps were tightened sufficiently to maintain this posture and prevent egress of the animal during loading without causing unnecessary anterior posterior compression of the animal, defined as visible sagittal compression of the chest. Consistency of positioning was checked using video footage from a high speed camera, set up 1 m away from the upper portion of the rig.

Cadaveric animals were initially used to develop this restraint technique that was designed to simulate military in vehicle harnessing. The strap positioning and seat itself were modified following an initial series of *in vivo* tests in which both the seat and straps were found not to be positioned high enough upon the animal torso. This first series of tests created extensive liver injuries in response to relatively low seat loading. Examination of the high speed video for these tests noting that crossing of the torso straps across the lower chest from the sides resulted in inferior movement of the straps upon loading with resultant flexion of the animal torso around this cross over point. Modification of the seat and raiding the straps to pass medially over the shoulders eliminated this torso flexion and "seat belt injury". The modified seat and resultant position are shown in Figure 8.7.

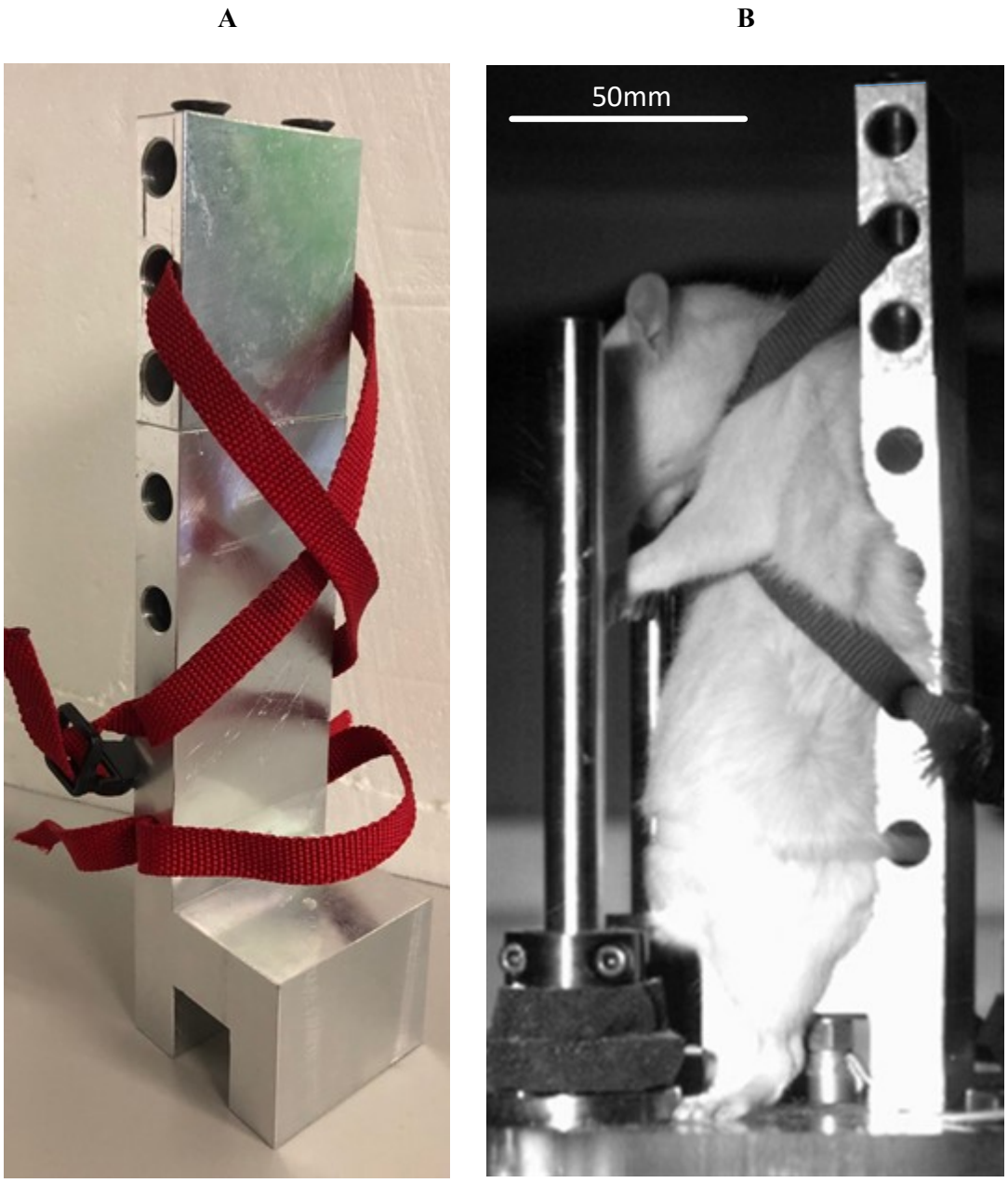

Figure 8.7: A) Seat following height modification with adjustable straps in situ. B) Animal in situ with restraint straps over shoulders. The legs can be seen at the side of the seat.

8.4.5 Exposure of rats to high rate vertical loading

Each animal was individually weighed and anaesthetised with ketamine (100mg/kg) and xylazine (15mg/kg) administered via an intra peritoneal injection. Suitable depth of anaesthesia was confirmed by assessing the withdrawal response to a paw grasp. Once suitably anaesthetised, each animal was restrained to the RivUL seat as described above. Following the necessary safety protocols, the system was charged to the requisite input pressure. The system was triggered with simultaneous activation of the high speed video capture, accelerometer data acquisition, and RivUL projectile.

Following loading, the seats straps were loosened and the animal removed from the seat. The animal was moved to a warming pad and observed for up to 5 minutes. This observation time was used to assess the apparent immediate lethality of the loading. An external examination was undertaken at this point to determine the extent of any surface injuries. Signs of life were observed at 5 minutes at which point the animal was euthanised either by injection of intraperitoneal sodium pentobarbital (100mg/kg) or by perfusion with intravenous contrast medium (further details described in imaging section below).

Death was confirmed in those animals not undergoing imaging studies by transection of the femoral vein and observation of cessation of bleeding. These animals underwent immediate necropsy to include laparotomy and thoracotomy. Each procedure was carried out carefully to avoid iatrogenic injury. The presence of free blood within the peritoneum, pleura, or mediastinum was first noted. Injuries to any organ were initially noted in situ. All organs were removed to allow full evaluation of injury. Lung injury was defined as macroscopically visible parenchymal lung haemorrhage or contusion whilst liver injury was defined as laceration to the liver sufficient to cause a free haemoperitoneum on the basis that such injuries are analogous to “clinically significant” injury.

Injured and non-injured organs from a range of loading input were taken and fixed for histological examination (further details are described in the histology section below).

8.4.6 Micro CT

Of those animals subjected to loading, a proportion underwent CT imaging rather than necropsy. The aim of this CT imaging was to demonstrate torso injuries using a diagnostic method analogous to clinical CT. The secondary aim of scanning was to attempt more detailed quantification of torso injury. Although micro CT has been well established for the assessment of skeletal anatomy and injury in small animal models, its utility for assessing soft tissue injury is limited by similarity in radio density of adjacent tissues and fluids (Clark and Badea, 2014; Polfer *et al.*, 2015). Imaging of the vasculature and vascularised soft tissues (which includes those organs of interest) requires the addition of an intravascular contrast agent. A variety of such products exist to cover a variety of applications (Grabherr *et al.*, 2008; Schambach *et al.*, 2010). The use of most of these products was prohibited either by cost (as was the case with heavy metal nano-particle based agents) or the need to perform pump based CT angiography at the time of imaging (similar to a clinical CT and unfeasible given the logistics of the scanner availability and location).

BriteVu (Scarlet Imaging, UT, USA) was selected as the contrast agent. This barium based agent has been designed specifically for post-mortem vascular and soft tissue imaging of both small and large animals although not previously used within a model of traumatic injury. The protocol advised by Scarlet Imaging included exsanguination of the terminally anaesthetised animal with flushing of a heparinised saline solution through a large vein following by slow perfusion of the agent. Discussion with the designer of the agent advised that this procedure be carried out immediately following loading.

Initial use of this protocol upon euthanised non-injured rats was successful and generated detailed images of the arterial and venous systems. Use of this protocol following loading was found to be problematic; the saline solution did not flush the vasculature but accumulated within both body cavities (from bleeding sites) and within tissues. This accumulation was not improved with an increasing concentration of heparin. In light of this, the perfusion protocol was changed with omission of the exsanguination stage and immediate infusion of a smaller (30ml) and more concentrated volume of the BriteVu solution. Although trial perfusion of non-injured was

successfully performed through the lateral saphenous vein, cannulation of this vessel following loading was found to be extremely difficult and further cannulations were performed through a cut down onto the femoral vein.

Following loading, and then perfusion, animals were mounted within a cardboard cylinder and packed with polystyrene microbeads. The carefully mounted sample was left to rest for 30mins to 1 hour before scanning, allowing the sample to stabilise and minimise sample movement during image acquisition. The sample was scanned using a Nikon Metrology HMX ST 225 scanner with a tungsten reflection target at the Natural History Museum, London, UK. Each sample was imaged by acquiring 3142 projections (2 frame average) during a single 360 degree rotation. X-ray conditions were as follows; 150kV, 150uA, 0.5 second exposure time, filtered with 0.5mm of copper. The overall scan time was around 50 minutes per sample. The rat samples varied slightly in size (across the target area) affecting the magnification range and thus the final resolution. All scans achieved a resolution of 30 to 40 microns per voxel. All scans were reconstructed using a filtered back projection algorithm. Image analysis and reconstruction was performed using Image J (National Institutes of Health, US) and Mimics (Materialise, Belgium). Scans were performed with the assistance of Dr Amin Garbout and Mr Brett Clark..

Lung injury was defined as the presence of high density concentrations within the lung parenchyma and liver injury was defined as laceration of the liver associated with free peritoneal contrast.

8.4.7 Histology

In those animals undergoing necropsy, a sample of livers and lungs across the range of loading was processed for histological examination. Organs were initially fixed in 10% formalin for 48 hours at 4^{o}C and then transferred for storage in 70% ethanol until processing. At processing, the organs were fully dehydrated in increasing concentrations of alcohol, cleared using xylene, and embedded in paraffin wax. Slices were taken at 4 μm thickness and stained with haematoxylin and eosin stain (H and E stain) prior to light microscopy.

8.4.8 Data acquisition

As with the rig characterisation discussed in Chapter 7, accelerometer data was acquired at 25 kHz from the point of triggering. This data was integrated with respect to time to calculate velocity and filtered through a low pass Butterworth filter (4 kHz cut off). Peak acceleration and peak velocity of each test were recorded.

8.4.9 Kinematics

The high speed video camera was set up 1m away from the rig and used to film the movement of the seat, plate, and rat throughout the loading. The video was captured at 10,000 fps, a rate which allowed both sufficient resolution (256x704) and accurate recording of the animal motion. Tracker, an open source motion analysis software (version 5, Open Source Physics) was used to determine the kinematics of the animal during the loading phase.

All movement was measured in respect to a co-ordinate system dictated by the long axis of the seat (z). The lowest point of the torso (defined as the rear point of the pelvis which is initially in contact with the seat bottom.) and uppermost point of the torso (defined as the rear uppermost point bounded by the shoulder strap) were used to define torso length in each test. Separate "tracks" were made of each point recording their motion during the loading. Torso compression was defined as the change in torso length (L_c) normalised by the initial length (L). Additionally, the velocity of compression at each step along the track was measured using a moving average system over the previous and subsequent 5 data points (i.e. over the surrounding 1ms). Examples of the measurements used are shown in Figure 8.8.

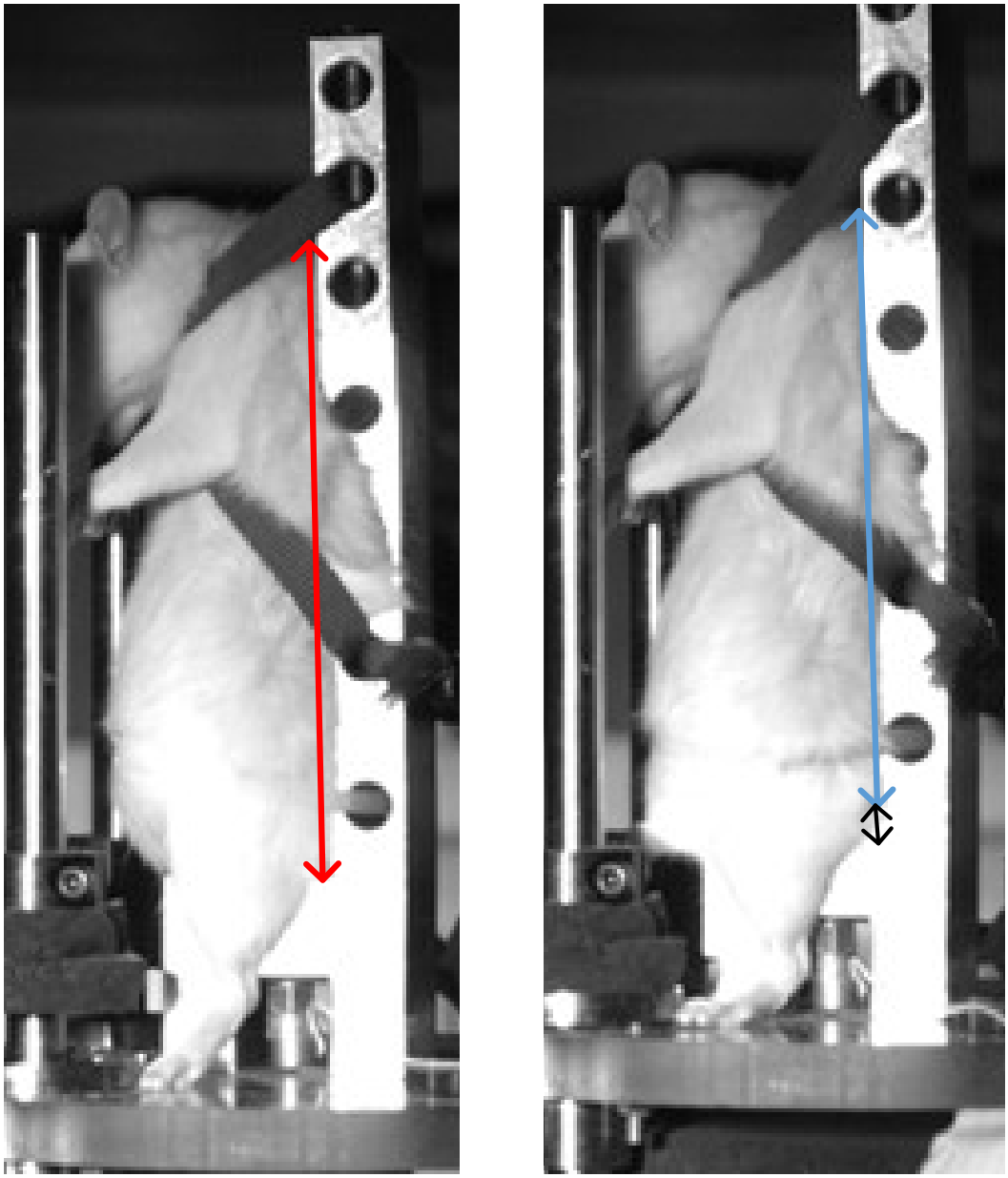

Figure 8.8: Measurement of torso length in high speed video. The red arrow denotes the initial torso length (L). The blue arrow denotes the changed torso length and the black arrow denotes the resultant compression (L_c) calculated as the difference between the two.

These measurements were used to define additional biomechanical criteria, based upon existing viscous and compression criteria for frontal loading as described in Chapter 6, to take into account the rate effect of loading.

Compression rate (the first derivative of the degree of compression with respect to time) was defined as:

$$Compression\ rate\ (CR) = \frac{L_c/L}{t} \quad [7.1]$$

Where L_c is compressive length, L is initial length and t is the time taken. This measurement is effectively the axial strain rate of the animal torso and has no unit.

The viscous criterion has proven utility for predicting both abdominal and chest organ injury in response to frontal loading (Viano and Lau, 1988). The criterion was adapted for the vertical direction using the measurements of compression and velocity discussed above.

The axial Viscous Response (the time varying product of compression and velocity) was therefore defined as:

$$VC_a = \frac{L_{c(t)}}{L} . \frac{L_{c(t)}}{dt} \quad [7.2]$$

where the time varying velocity is measured using the moving average of displacement over the 1ms time period as discussed above. Given that the degree of compression is unitless, the viscous response is measured in m/s.

8.5 Results

In total, 60 rats were used for development of the protocols and experimental series. The flow chart for the use of animals is shown in Figure 8.9.

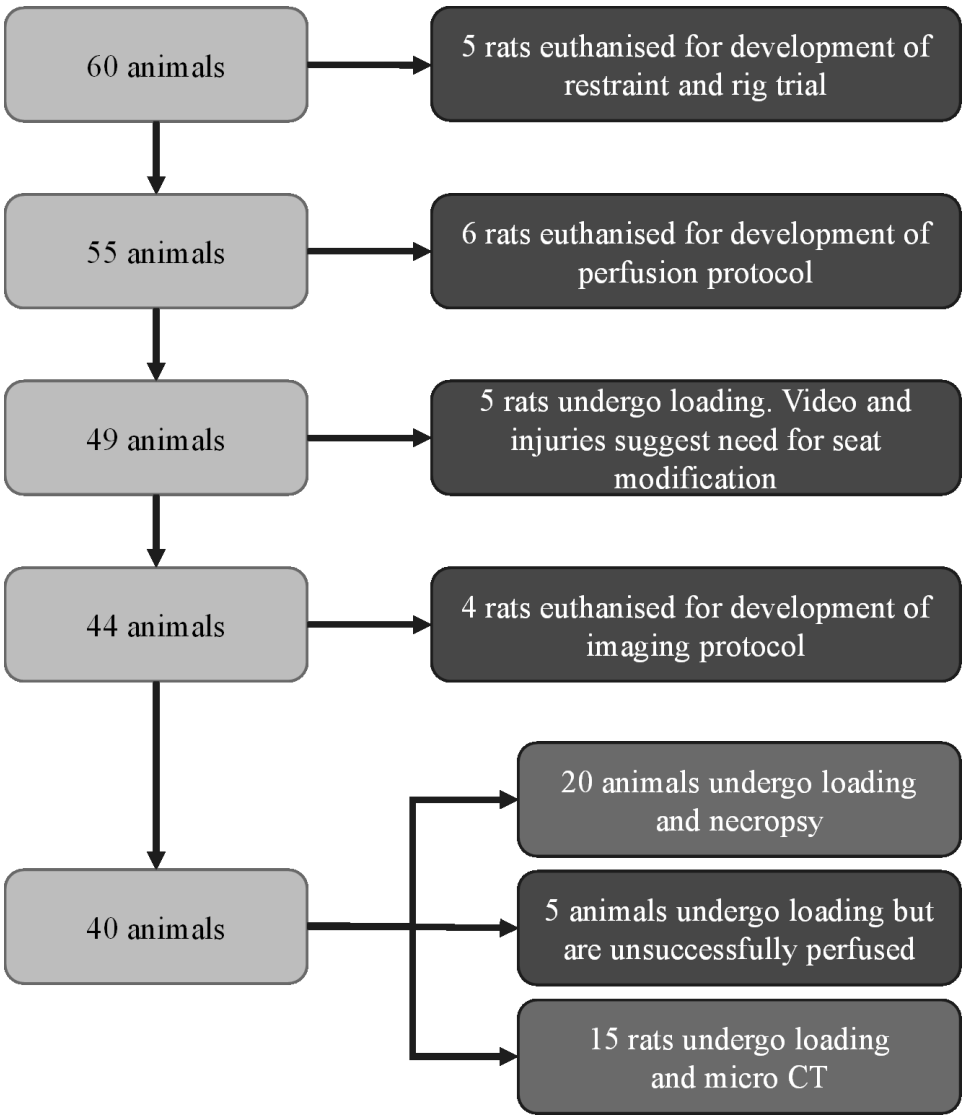

Figure 8.9: Flowchart showing outcome of animals used during procedural development and experiments.

The test matrix, showing input pressure, peak acceleration and velocity of seat, time to peak of velocity, presence or absence of lung and liver injury, and 5 minute mortality of the resultant 35 animals are shown in Table 8.1.

Sample Number	Body mass (g)	Diagnostic modality	Input Pressure (bar)	Peak Acceleration ($m/s^{2)}$	Peak Velocity (m/s)	TTP (ms)	Liver Injury	Lung Injury	5-minute mortality
1	263	CT	6	447.0	2.06	3.76	Yes	No	Alive
2	265	CT	7	731.1	2.77	3.22	No	No	Alive
3	262	CT	8	No trigger	No trigger	n/a	Yes	No	Dead
4	260	CT	8	1211.4	3.45	2.9	No	No	Dead
5	271	CT	9	2099.2	5.88	1.2	Yes	Yes	Dead
6	268	CT	10	2221.0	5.95	1.2	No	No	Alive
7	260	CT	11	2298.9	7.23	1.32	Yes	No	Alive
8	276	CT	12	4342.1	8.16	1.12	Yes	No	Alive
9	282	CT	14	5529.6	9.43	1.04	Yes	Inadequate	Dead
10	277	CT	15	No trigger	No trigger	n/a	Yes	Inadequate	Dead
11	282	CT	15	No trigger	No trigger	n/a	Yes	Inadequate	Dead
12	271	CT	18	5965.8	10.30	1.16	Yes	No	Alive
13	275	CT	13	No trigger	No trigger	n/a	Yes	Yes	Dead
14	274	CT	17	4283.2	7.31	1.16	Yes	Yes	Dead
15	290	CT	17	No trigger	No trigger	n/a	Yes	Yes	Dead
16	262	Necropsy	5	100.4	1.98	3.56	No	No	Alive
17	273	Necropsy	6	145.0	2.29	3.18	No	No	Alive
18	280	Necropsy	7	276.9	2.61	3.44	No	No	Alive
19	256	Necropsy	8	707.6	3.55	3.4	No	No	Alive
20	312	Necropsy	9	886.8	4.46	2.96	No	No	Alive
21	287	Necropsy	10	2022.6	6.06	1.28	No	No	Alive
22	306	Necropsy	11	2099.0	7.18	0.96	No	No	Dead
23	277	Necropsy	12	3225.7	8.05	1.16	Yes	No	Alive
24	299	Necropsy	13	5709.0	9.64	0.92	Yes	Yes	Dead
25	255	Necropsy	14	4315.3	9.75	1.04	No	Yes	Dead
26	284	Necropsy	15	6177.0	10.13	0.96	Yes	No	Dead
27	275	Necropsy	16	6503.2	10.45	0.96	Yes	Yes	Dead
28	263	Necropsy	17	No trigger	No trigger	n/a	Yes	Yes	Dead
29	280	Necropsy	18	6843.7	11.01	0.92	No	Yes	Alive
30	260	Necropsy	13	5492.9	9.65	1.16	No	No	Alive
31	281	Necropsy	14.5	6563.3	10.94	1.12	Yes	No	Dead
32	295	Necropsy	14	4623.9	9.15	1.16	No	Yes	Alive
33	256	Necropsy	15	6901.0	11.35	1.16	Yes	Yes	Dead
34	293	Necropsy	19	6653.4	10.25	0.88	Yes	Yes	Dead
35	293	Necropsy	19	7475.8	12.06	0.8	Yes	Yes	Dead

Table 8.1: Test matrix of *in vivo* UBB blast test showing input pressure, mechanical seat parameters, and injury outcome.

Of note, the accelerometer system failed to correctly trigger on 6 of these tests. The time to peak of the test decreases beyond a threshold of around 8 bar input pressure (Figure 8.10).

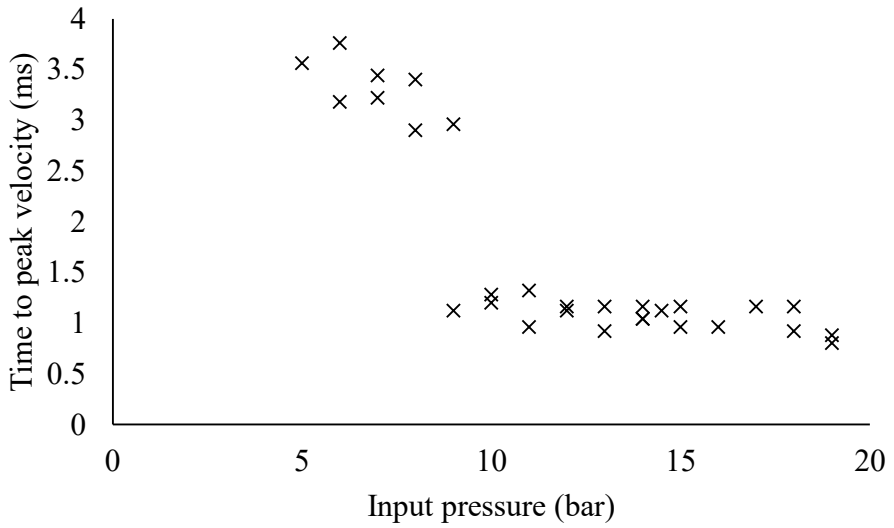

Figure 8.10: Time to peak velocity of the seat in response to changing pressure.

This threshold may be due to the projectile causing maximum compression of the stopping collar foam at a certain velocity such that the effect of the foam in damping the impact is saturated beyond this point. As a consequence, the time to peak of all higher loading tests was reasonably constant at around 1ms. Even when taking the slightly slower tests into account, there is a linear relationship between acceleration and velocity of the seat (Figure 8.11).

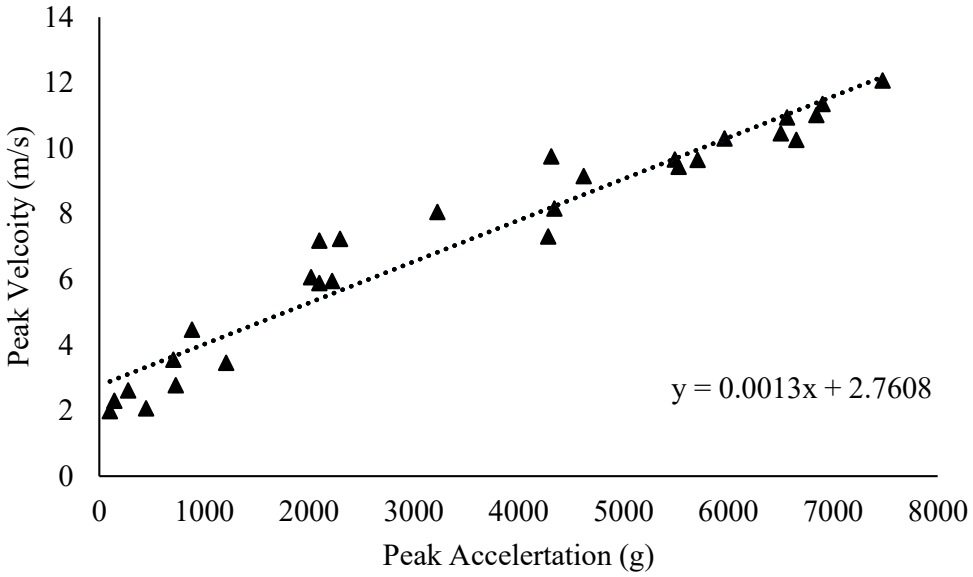

Figure 8.11: The relationship between peak velocity and peak acceleration which due to a consistent time to peak, is linear with an R^2 regression coefficient of 0.94.

8.5.1 Necropsy findings

Parenchymal lung injuries and liver injuries were the most commonly noted internal organ injuries. Only injuries thought to be of clinical significance (visible lung haemorrhage or haemoperitoneum) were documented to have an injurious outcome. Although these injuries were not numerically graded, the severity of these observed injuries did vary with increasingly severe injuries noted at higher loading. Although all liver injuries were sufficient to cause haemoperitoneum, these injuries ranged from isolated laceration of a single lobe to avulsion of the liver from the IVC. Injuries to the liver were most commonly seen centrally with lacerations occurring on the inferior surfaces of the lobes adjacent to lobar attachments (Figure 8.12 and Figure 8.13).

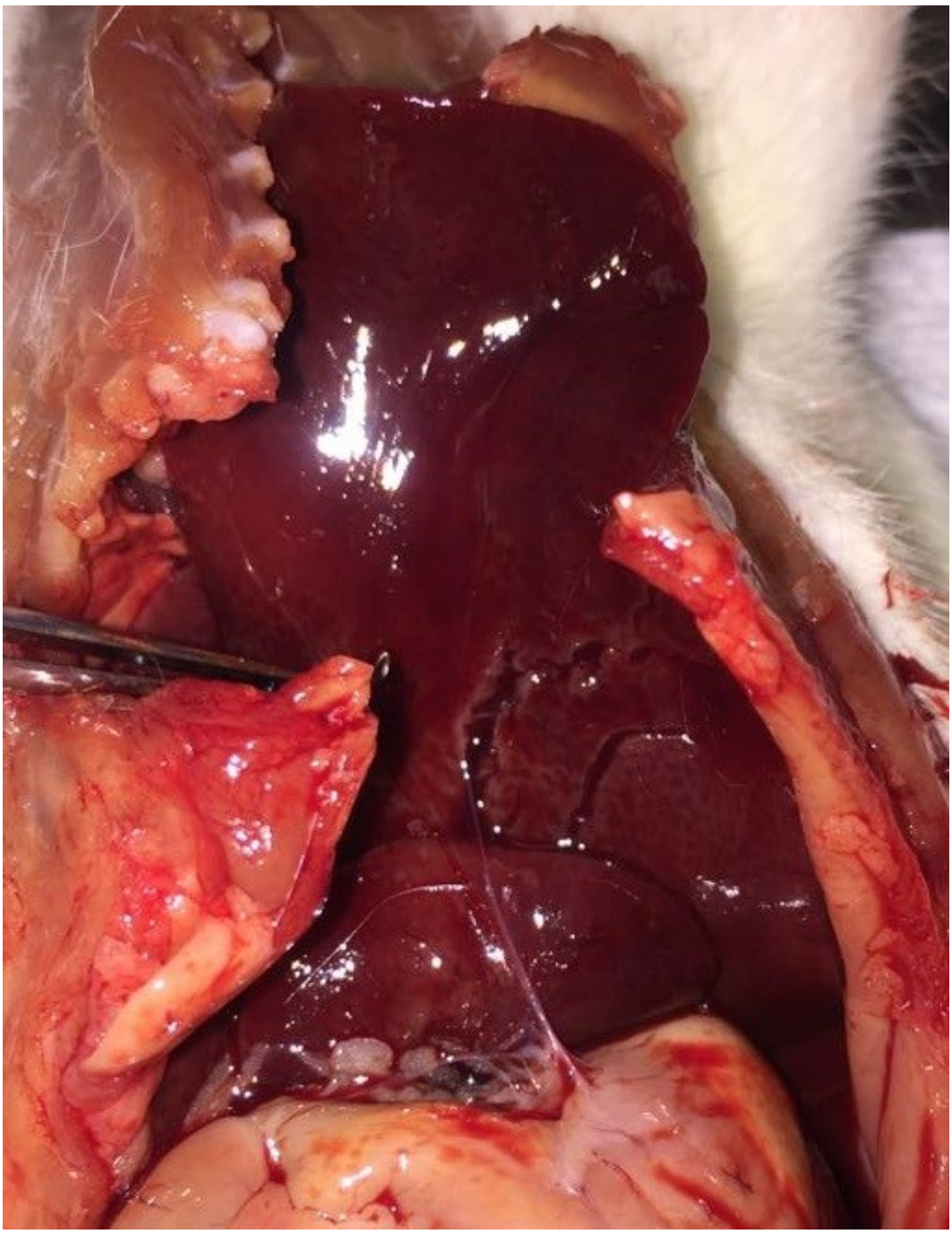

Figure 8.12: Liver injuries in response to vertical loading and as viewed from inferiorly thorough a laparotomy: laceration to the inferior surface of the lower left lobe in a rat exposed to peak velocity of 8.05m/s and

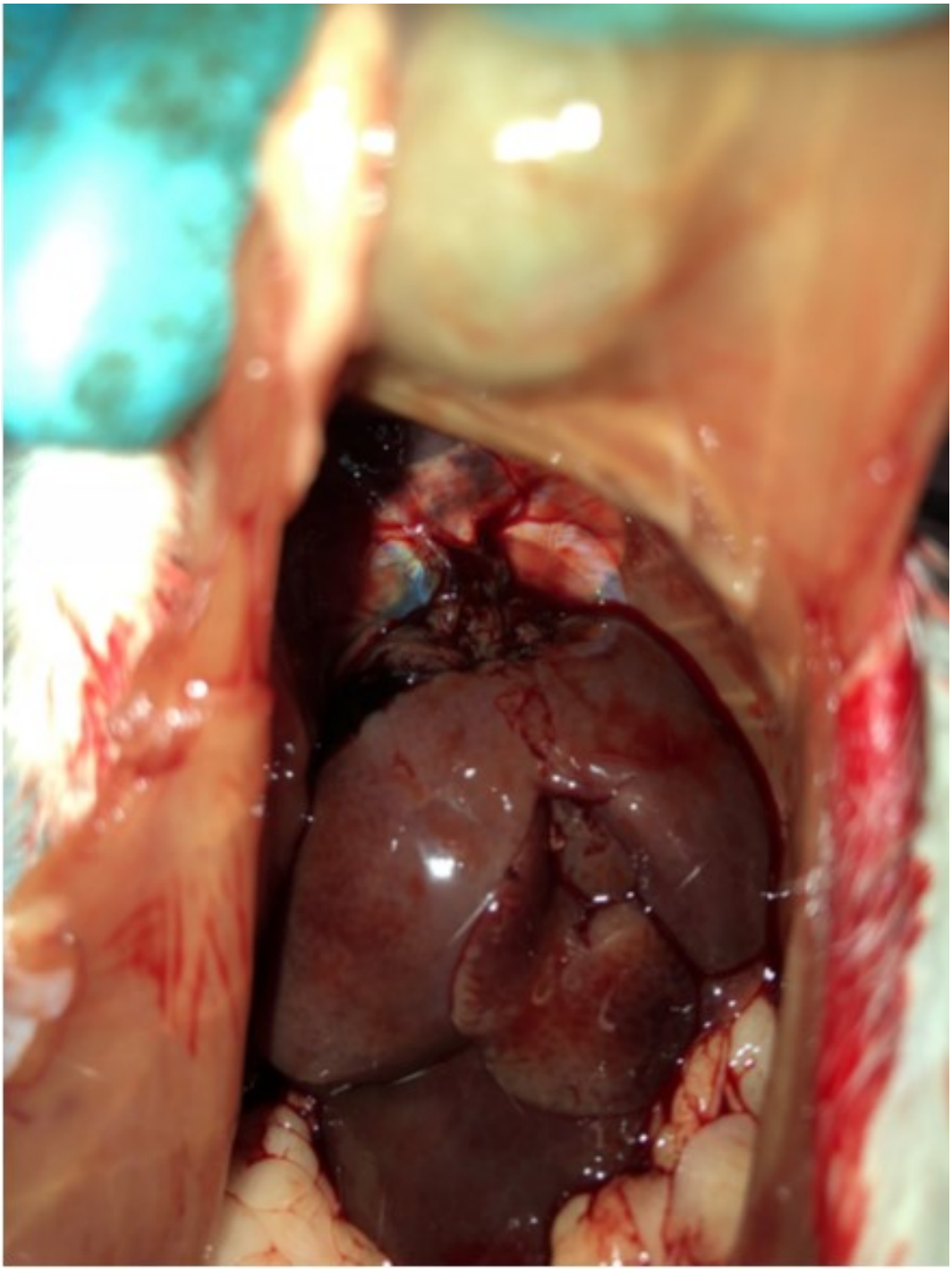

Figure 8.13: View of the liver (and inferior surface of the diaphragm as seen through a laparotomy incision). Severe liver injury is noted with avulsion of the liver from the IVC in a rat exposed to 12.06m/s vertical velocity change

Lung injury findings were similarly varied. Parenchymal haemorrhage was seen to occur in both localised patches around the base of the lungs (Figure 8.14) and at areas in contact with the ribs; or more widespread following higher loading (Figure 8.15).

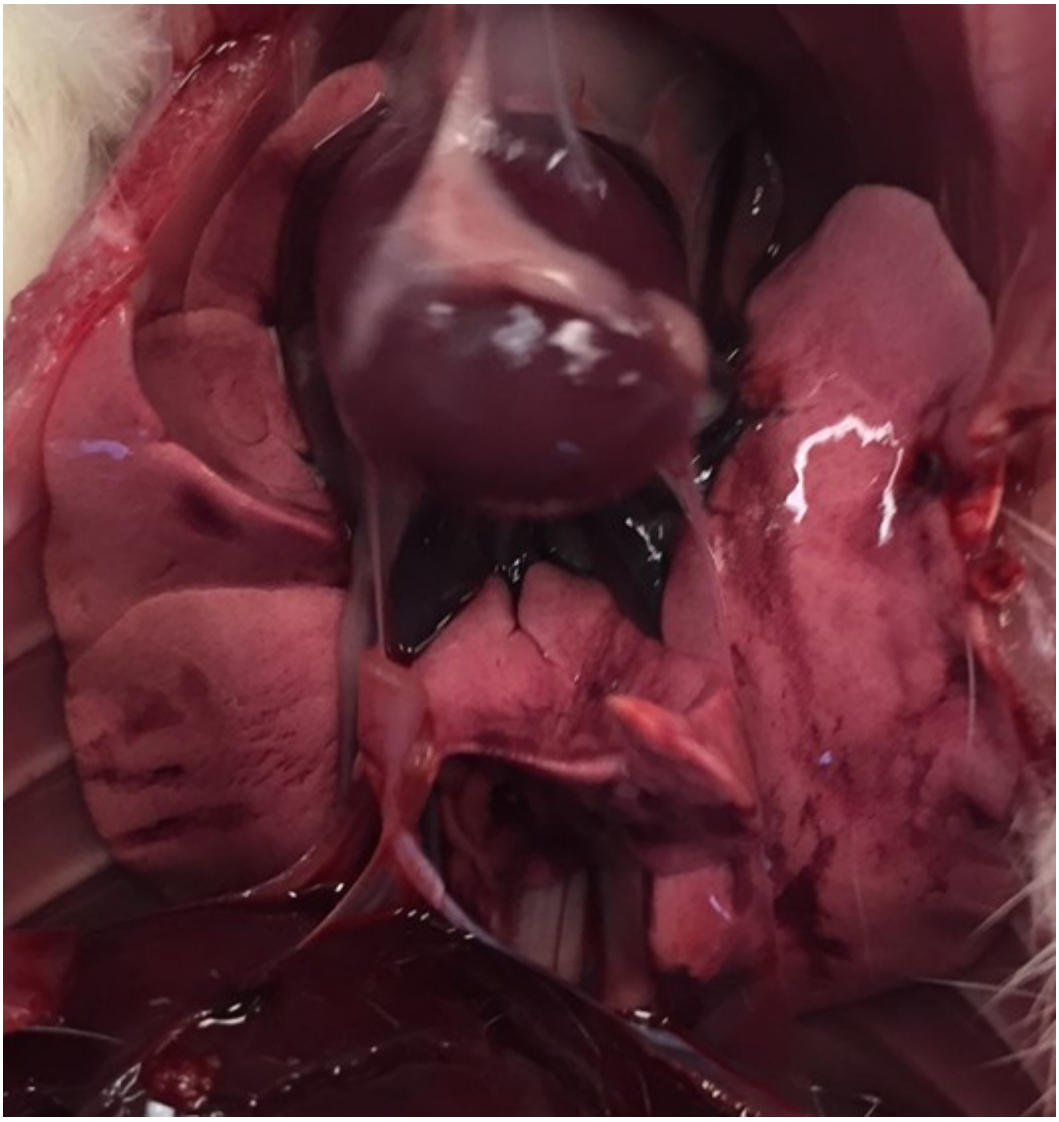

Figure 8.14: Necropsy views of parenchymal lung injury showing localised injury at the right lung base along with rib pattern injury to the left in an animal exposed to 9.64m/s.

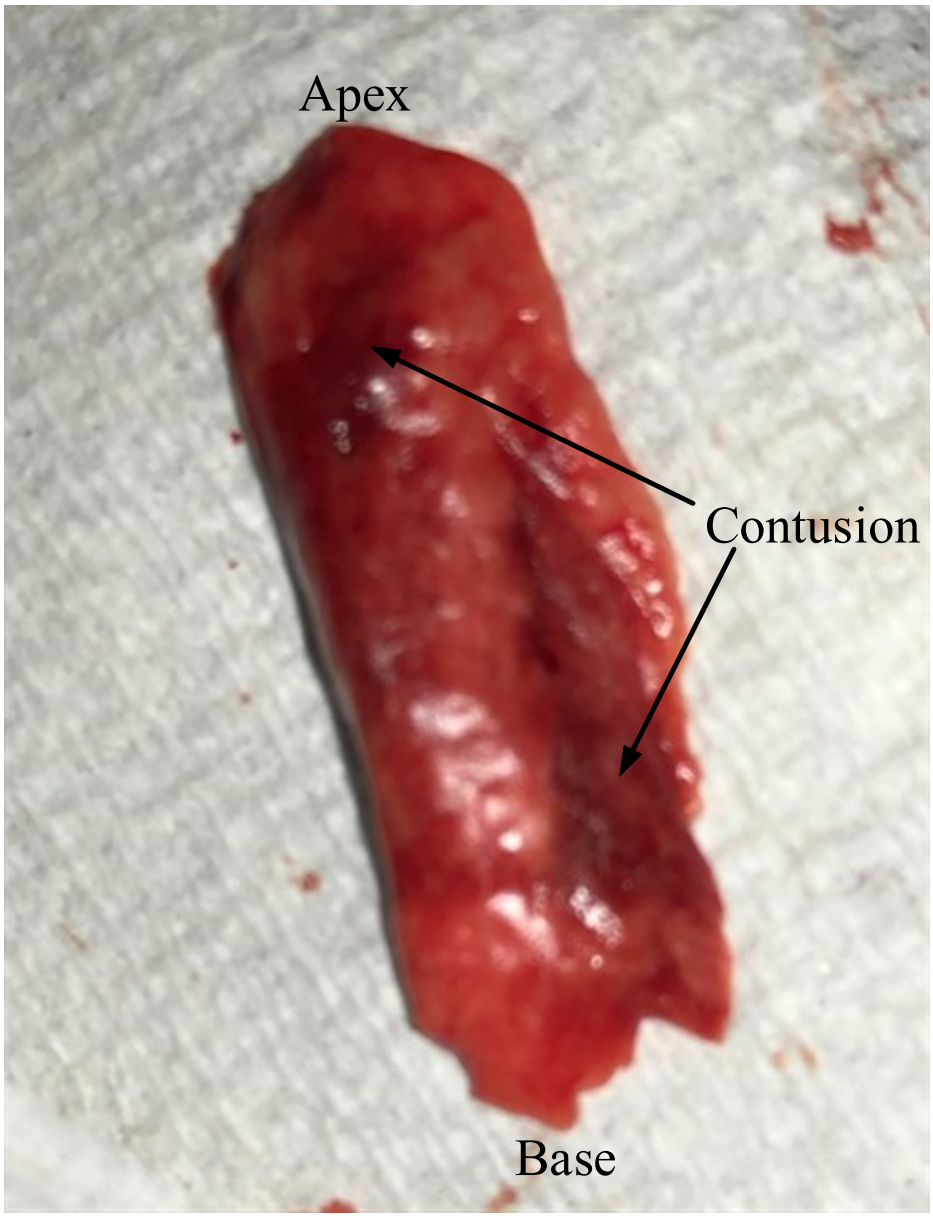

Figure 8.15: Widespread severe injury in an excised right lung specimen in an animal exposed to 12.05m/s loading.

Organs extracted at necropsy were weighed and masses compared to total body mass Table 8.2.

Sample Number	*Body mass (g)*	*Left lung mass (g)*	*Right lung mass (g)*	*Total lung mass (g)*	*Relative lung mass (%)*
16	262	0.422	0.839	1.261	0.48%
17	272.5	0.4	0.767	1.167	0.43%
18	279.6	0.477	0.897	1.374	0.49%
19	255.8	0.416	0.703	1.119	0.44%
20	312.1	0.528	0.821	1.349	0.43%
21	286.7	0.395	0.82	1.215	0.42%
22	306.4	0.465	0.947	1.412	0.46%
23	277.3	0.41	0.77	1.18	0.43%
24	299.4	0.46	0.924	1.384	0.46%
25	254.7	0.45	0.765	1.215	0.48%
26	283.8	0.39	0.79	1.18	0.42%
27	274.8	0.495	0.87	1.365	0.50%
28	263	0.42	0.79	1.21	0.46%
29	280	0.472	0.785	1.257	0.45%
30	260	0.46	0.815	1.275	0.49%
31	281	0.41	0.56	0.97	0.35%
32	295	0.45	0.91	1.36	0.46%
33	256	0.421	0.821	1.242	0.49%
34	293	0.47	0.89	1.36	0.46%
35	293	0.44	0.93	1.37	0.47%

Table 8.2: Body mass and lung masses of rats at necropsy.

No relationship was seen between either loading or presence of injury with changes in relative lung mass. Linear regression showed no effect of changing velocity upon the resultant lung mass (R^2 0.0025) while one way ANOVA testing revealed no significant difference in lung mass between those with and without macroscopic lung injuries (p= 0.818). The lack of increasing mass despite clinically apparent injury may be due to the short time scale to necropsy with little time for inflammatory change or venous congestion. Similarly, haemorrhage elsewhere (such as the liver) may reduce the circulating volume available to effect lung mass, bleeding from other sites may account for the lower total mass of the lungs when compared to literature values (nominally 0.6% of body mass (Treuting *et al.*, 2018)).

No injuries to the spleen or kidneys were noted. Similarly, and somewhat disappointingly, no injuries were noted to the heart or aorta. Transection of the azygous vein with haemothorax was seen in one test.

The cause of death for those animals with no signs of life at five minutes was not necessarily apparent. Although many of these animals had sustained liver or lung injuries, several had not. All animals had received a euthanizing injection at point of necropsy so lack of signs of life may be due to an impact apnoea (as described in rodents following primary blast injury) (Kirkman and Watts, 2011) or due to direct head impact described in the kinematic response below. No gross brain injuries were noted at necropsy although in-depth cranial investigations were not performed.

8.5.2 Micro CT

As can be seen from Table 8.1, the CT imaging was somewhat limited in the diagnosis of lung pathology. This limitation was due to the degree of contrast perfusion and likely a consequence of inadequate exsanguination of the lungs prior to perfusion. The quality of the images was insufficient to confidently describe or rule out lung pathology in three of the tests. Nevertheless, the image quality of the other scans was adequate to show parenchymal hyper density (noted primarily towards the lung bases), consistent with intra-parenchymal injury.

In comparison, the contrast was excellent for the diagnosis of significant liver injury with both injury site and haemoperitoneum obvious on these scans.

Although the secondary aim of the CT imaging was to accurately quantify the degree of injury, the quality of the imaging and protocol used precluded accurate measurement. Although previous work has suggested that measurement of haematoma size may be used as an injury metric, this measurement would undoubtedly be confounded by the injection of an additional contrast medium in relatively high volume. Examples of micro CT images are shown in Figure 8.16 and Figure 8.17.

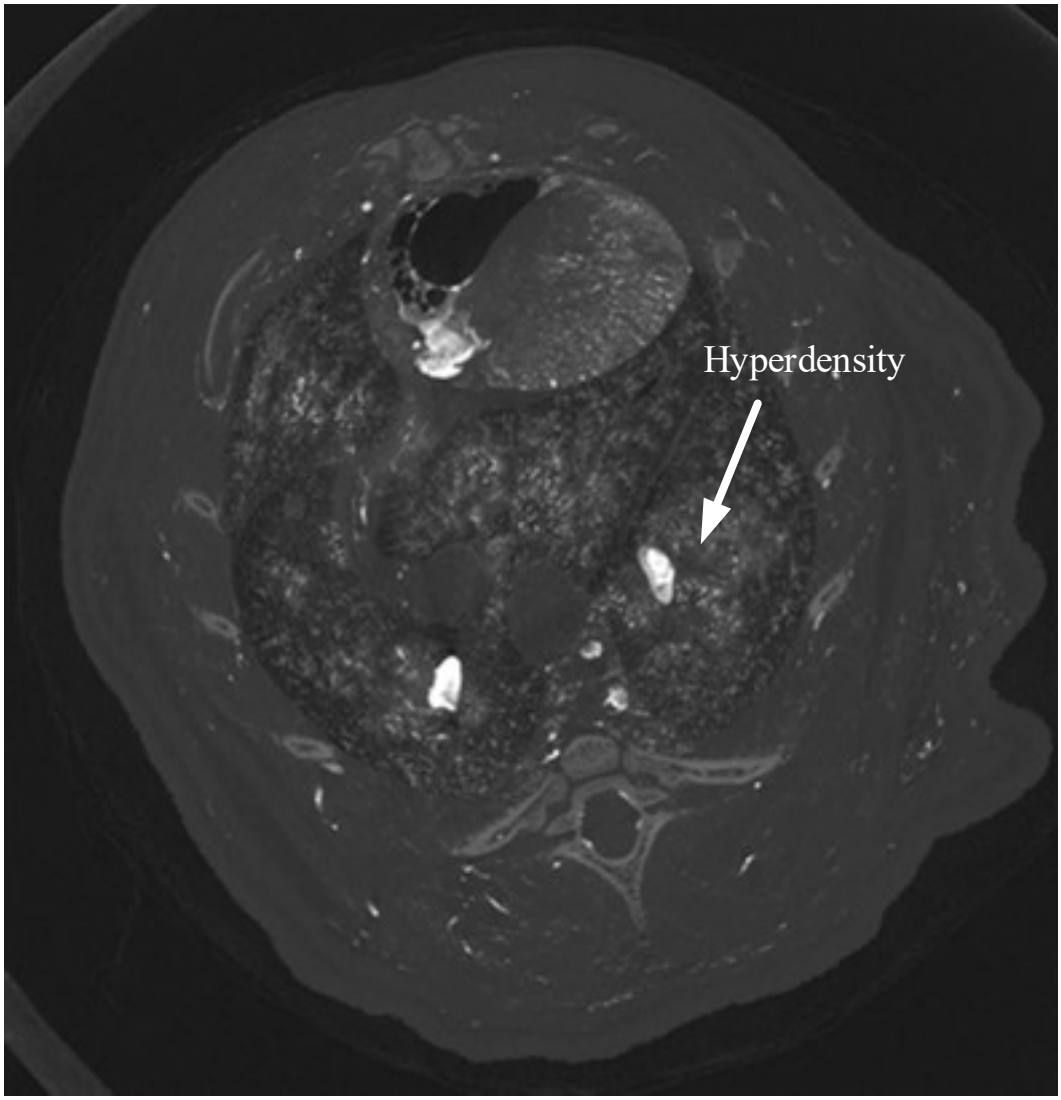

Figure 8.16: Micro CT images demonstrating regional hyperdensity consistent with parenchymal lung injury.

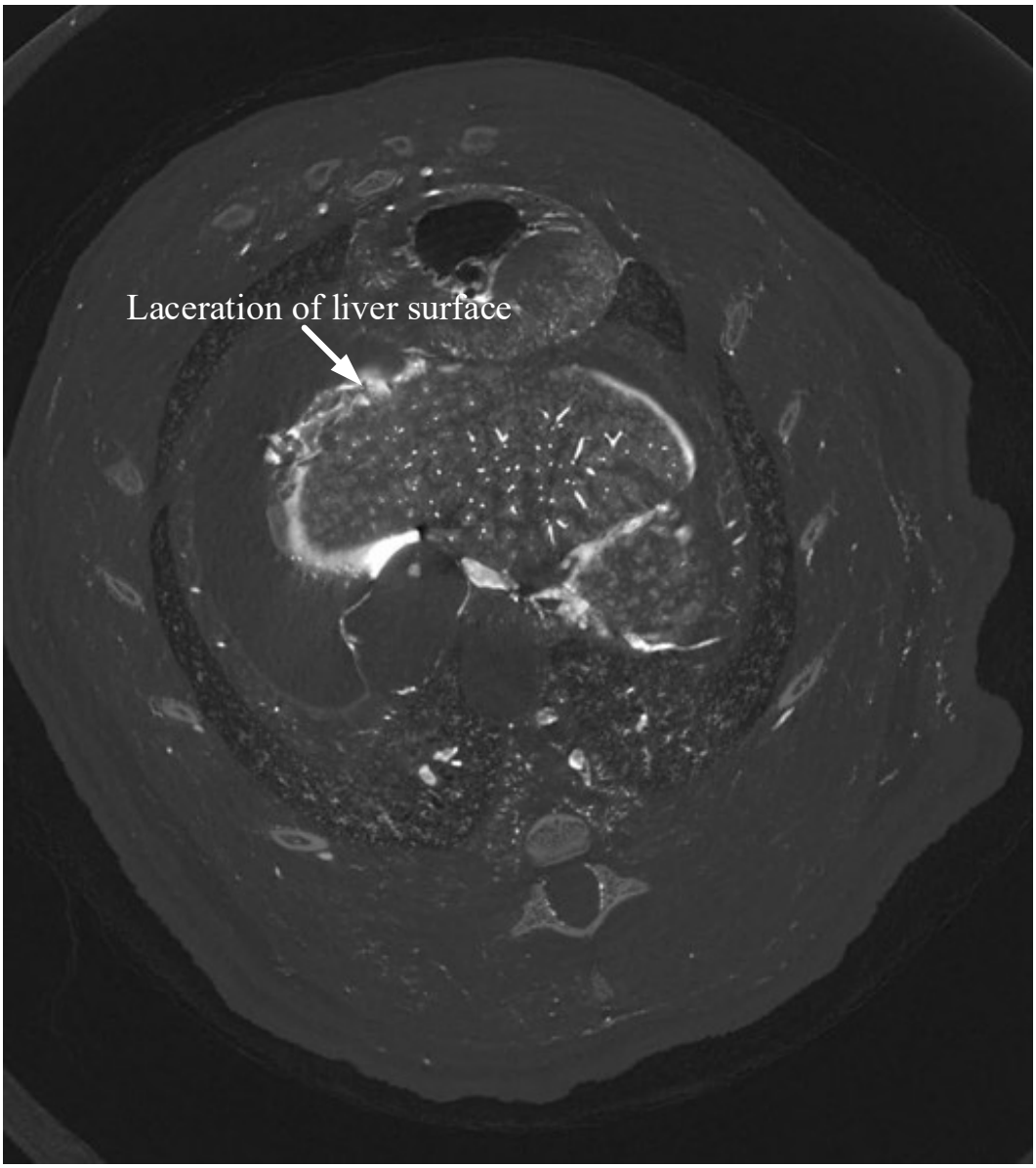

Figure 8.17: Micro CT showing laceration to the sub diaphragmatic liver surface with resultant haemoperitoneum. Both images are from a rat exposed to a peak velocity of 7.3m/s.

8.5.3 Histology

Samples from across the range of loading were processed for histology as described previously. Lung and liver samples from rats exposed to 3.5 ms, 9.7ms, and 10.3ms were processed and examined. Lung samples are shown in Figure 8.18.

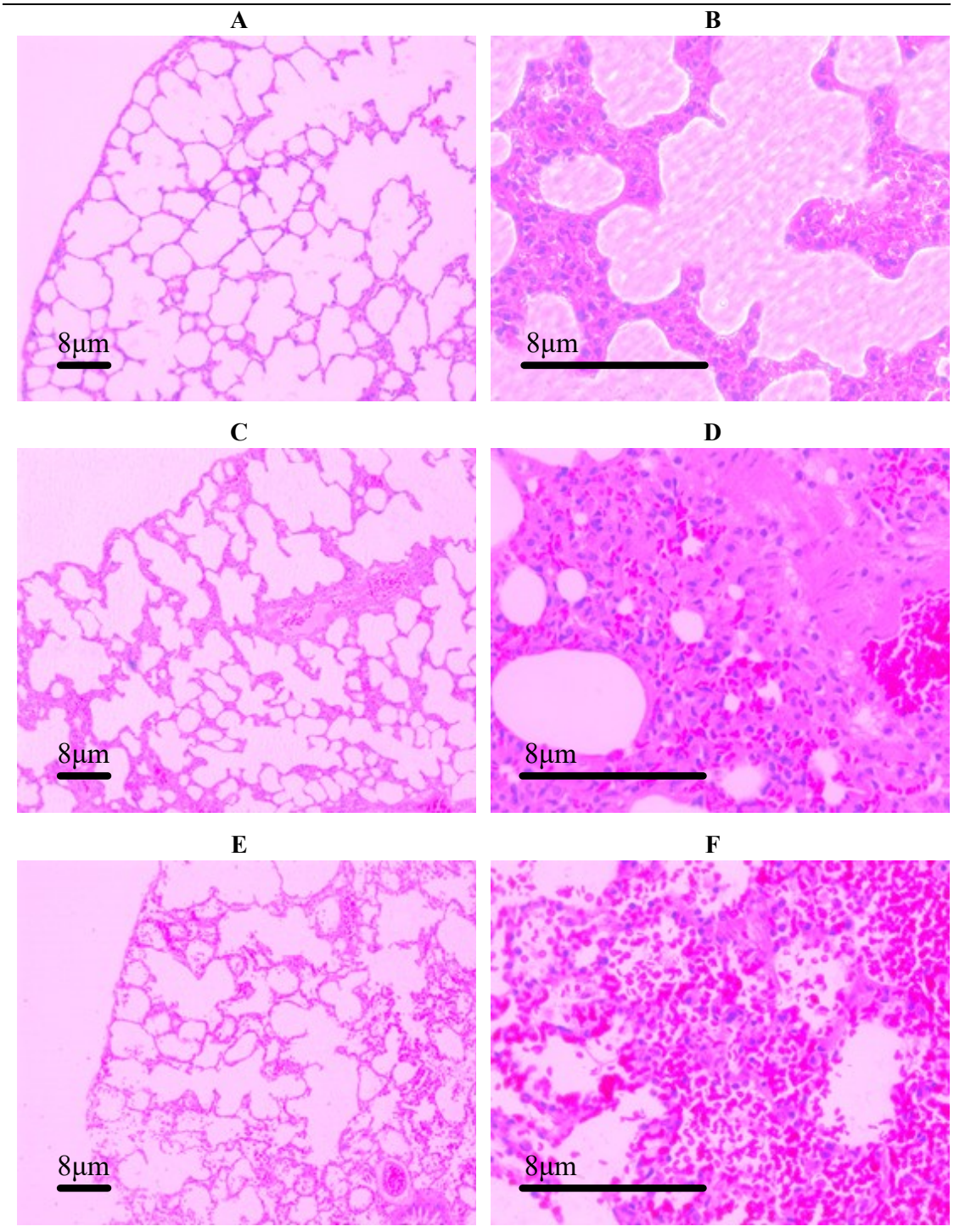

Figure 8.18: H and E stained lung histology. A) 10x view of lung from 3.5m/s rat. Alveoli are intact with no haemorrhage. B) 40X view of 3.5m/s shwoing intact alevoloar walls.. C) 10x view of 9.7m/s lung with minor alveolar break down. D) 40x of 9.7m/s lung shows scattered interstitial haemorrhage. E) 10x view of 10.3m/s lung shows widespread severe alveoli destruction. F) 40x view of 10.3ms lung shows both alveolar and interstitial haemorrhage.

Results of the histology, in those samples analysed, confirmed the macroscopic diagnosis of lung injury. The results also demonstrate the range of lung injury with qualitatively more severe injury in the highest loaded animal. As with the injury descriptions discussed above, there is a clear spectrum of lung injury with greater injury occurring in response to higher loading. The livers of the same animals were similarly examined (Figure 8.19).

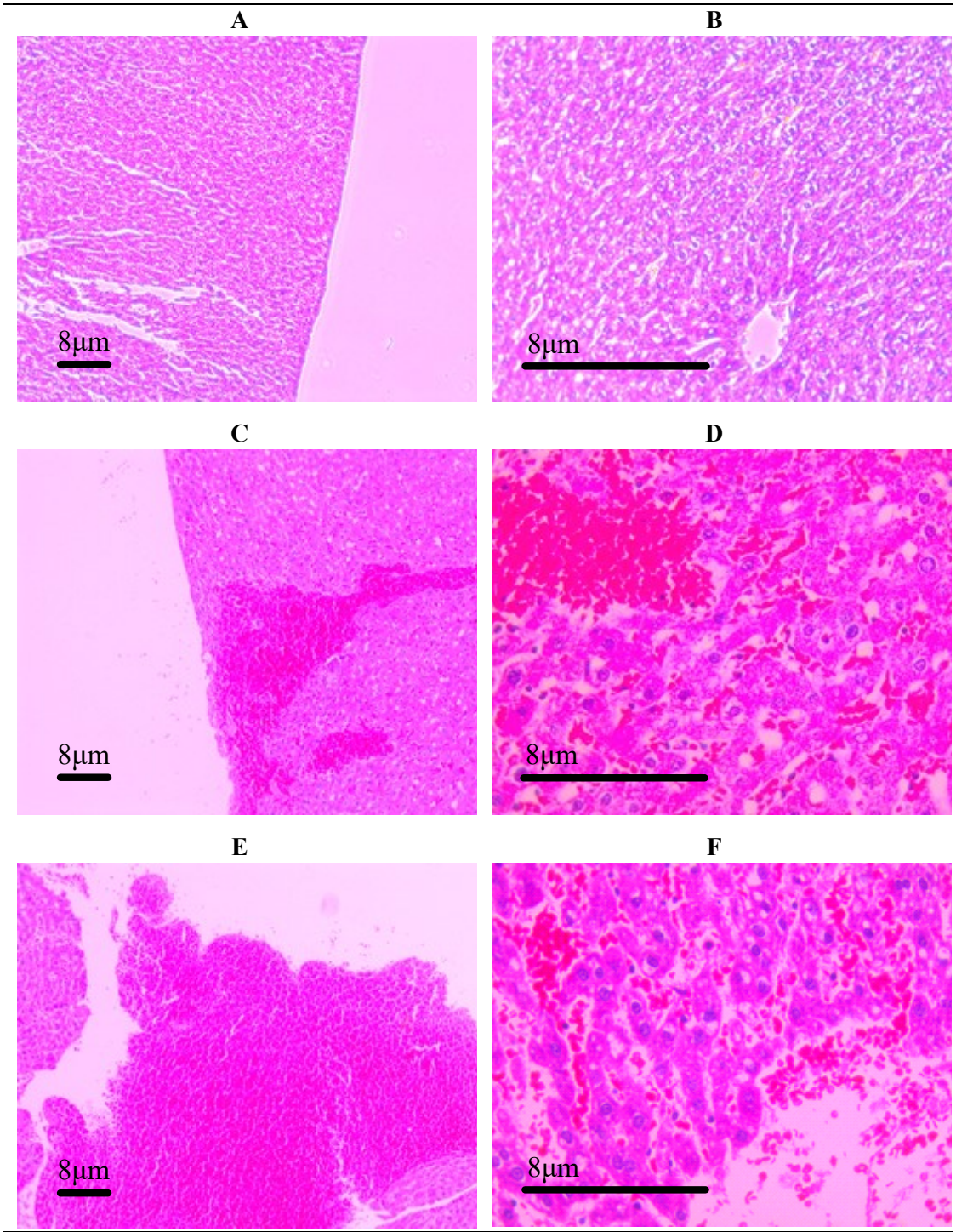

Figure 8.19: H and E stained liver histology. A) 10x view of liver from 3.5m/s rat with no apparent injury and smooth wall. B) 40X view confirms no interstitial haemorrhage C) 10x view of 9.7m/s lung with surface laceration (not seen macroscopically) D) 40x of 9.7m/s also shows scattered parenchymal haemorrhage. E) 10x view of 10.3m/s lung shows extensive severe laceration F) 40x view of 10.3ms lung shows widespread free parenchymal blood and parenchymal disruption.

As with the lung injury, the liver histology followed the loading with more severe injury seen at high rates. The limited surface laceration described in Figure 8.19 E and F was

not seen macroscopically and may not have been clinically significant but nevertheless shows progression of injury in response to increased loading.

8.5.4 Injury occurrence in relation to seat loading

The occurrence of liver and lung injuries in response to this loading is also demonstrated in Figure 8.20 below In addition to measuring injury, these tests were used to further characterise the performance of RivUL in regards to vertical acceleration.

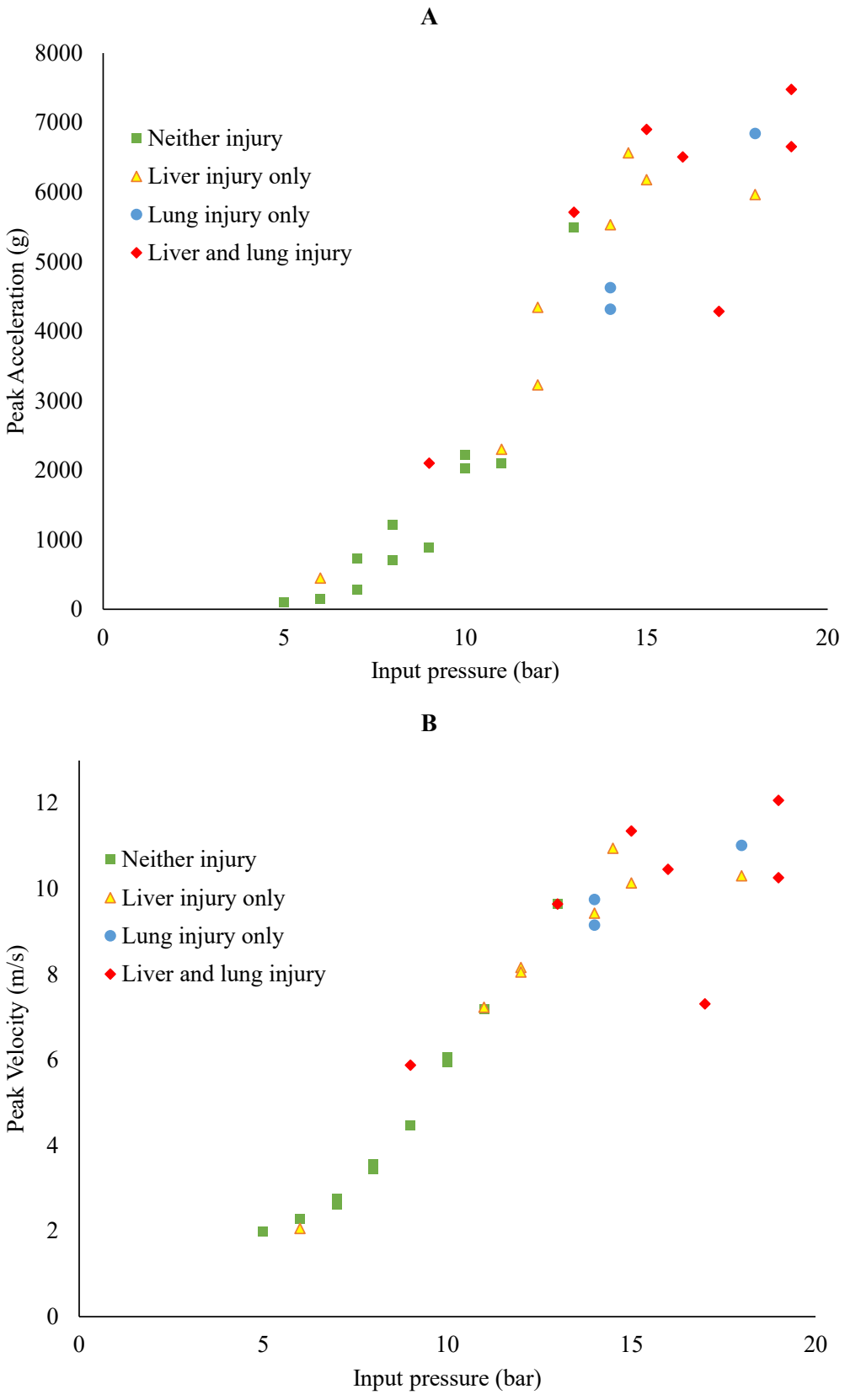

Figure 8.20 Occurrence of liver and lung injuries in response to altering input pressure and resultant loading expressed as A) peak acceleration and B) peak velocity.

As was seen during the characterisation experiments, both acceleration and velocity increased in response to increasing pressure. Both lung and liver injuries occur at higher acceleration and velocity. The loading threshold for liver injury is lower than lung with one such injury occurring at only 2.06 m/s. This may be due to the larger relative mass. Although one animal was exposed to an acceleration of almost 6000g with resultant velocity of 9.65m/s, it sustained neither injury.

8.5.5 Kinematic Response

As described above, high speed video footage of the animals during and immediately following the loading was used to describe the kinematic response to the loading. Stills from an example video (rat #25; 14bar input pressure and 9.7m/s seat velocity) are shown in Figure 8.21.

0ms

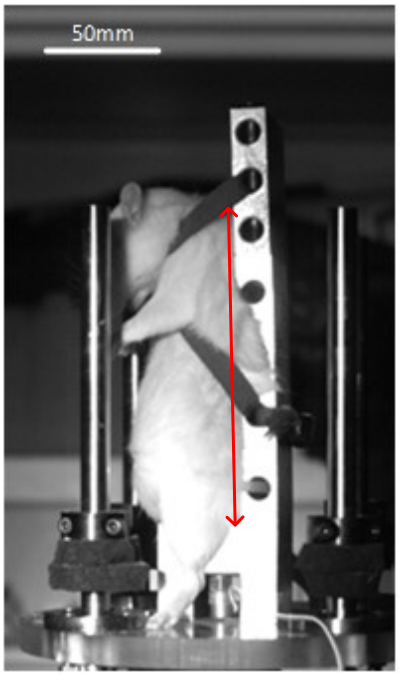

1ms

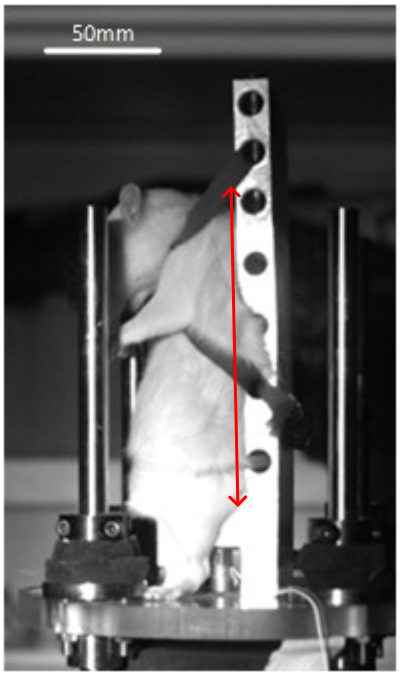

3ms

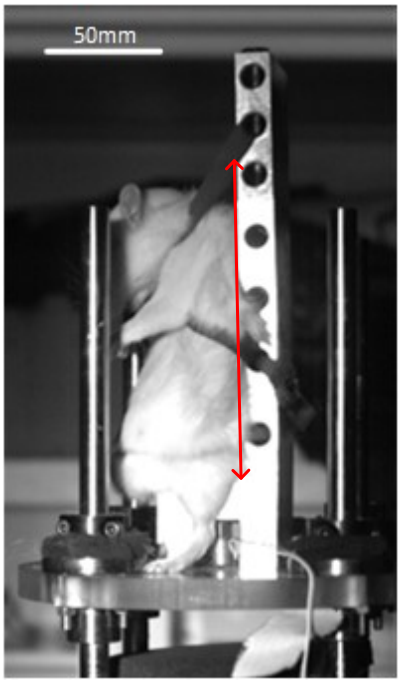

5ms

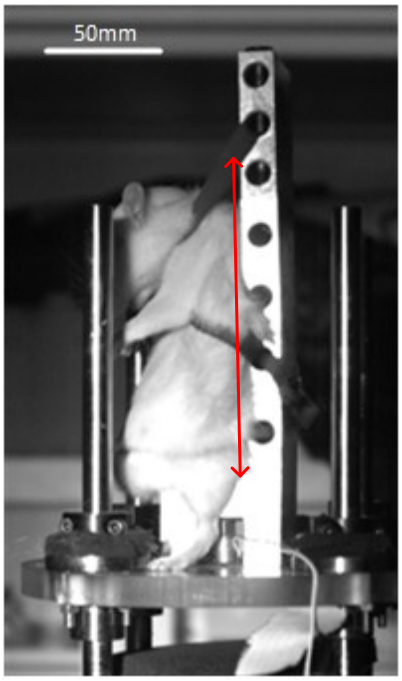

9ms

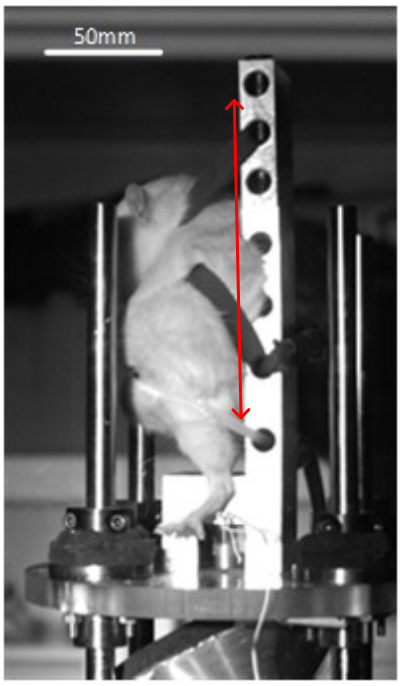

13ms

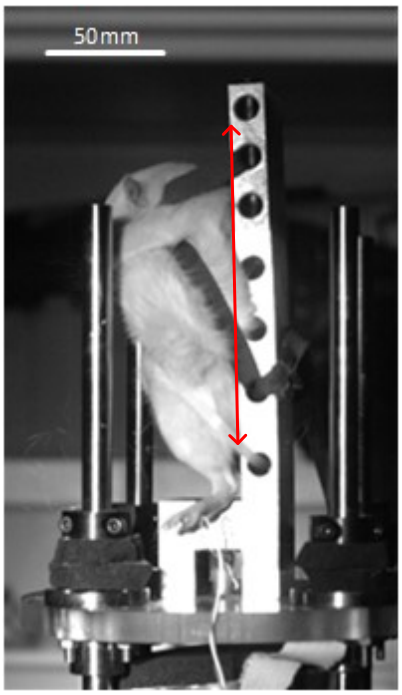

17ms

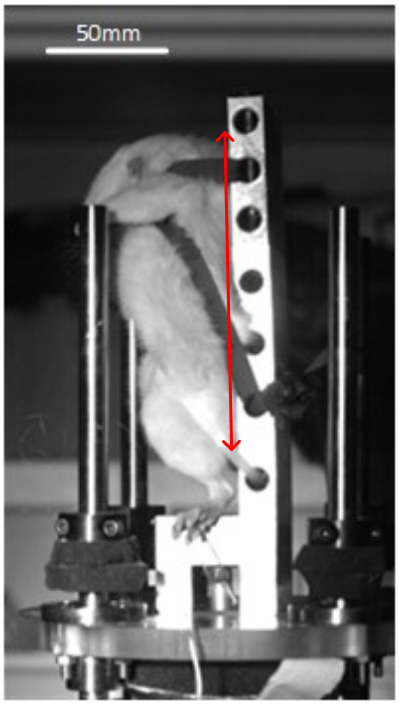

21ms

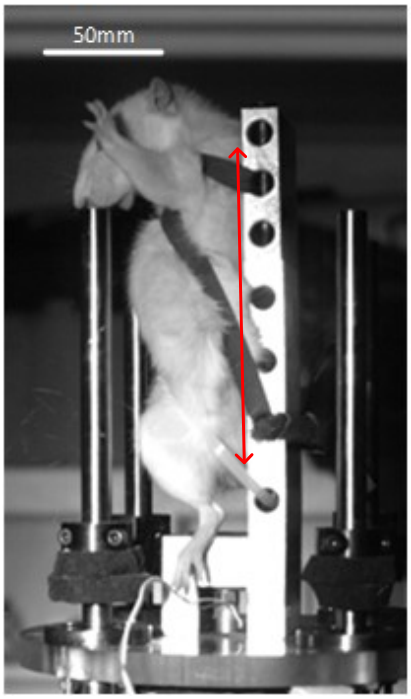

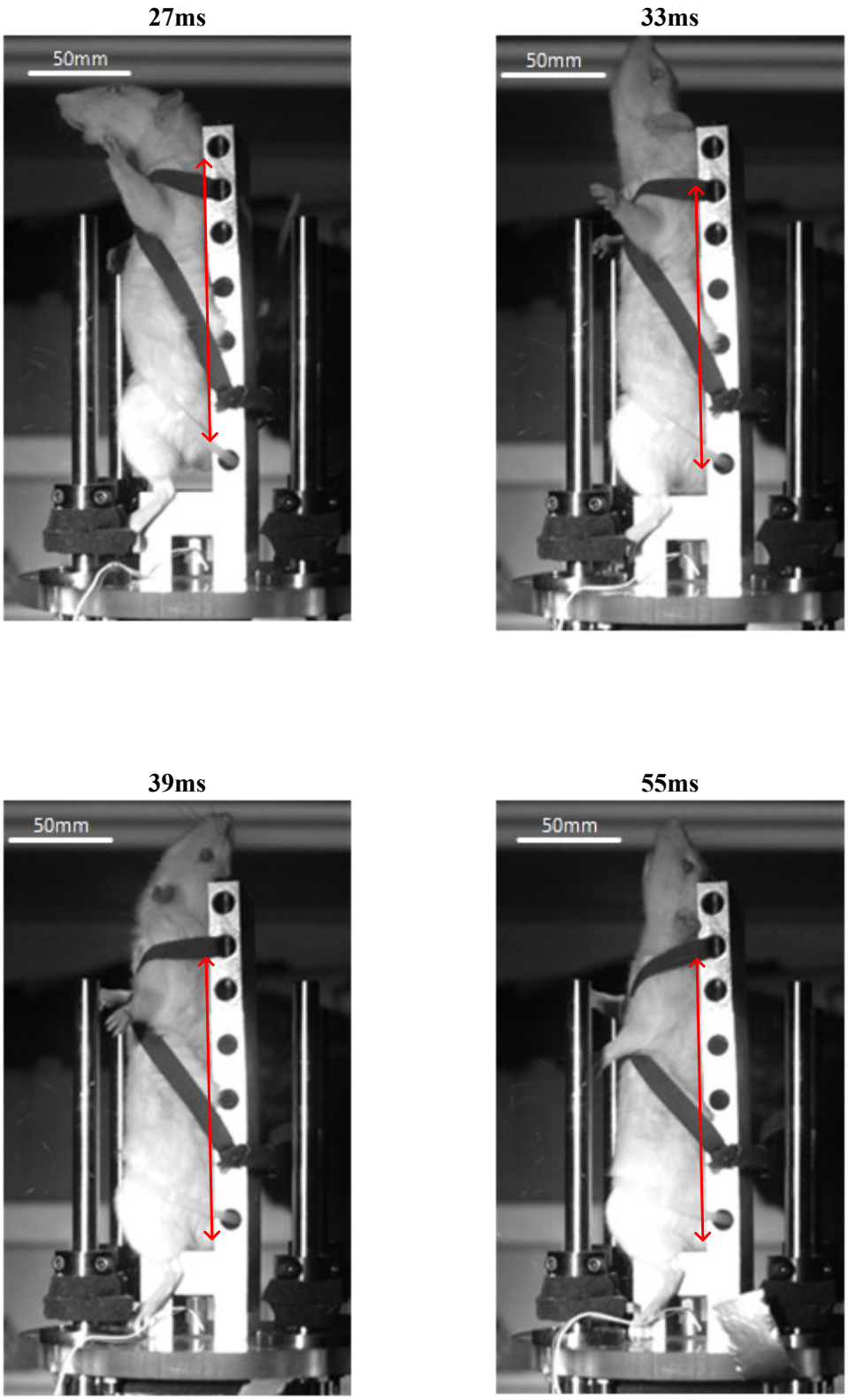

Figure 8.21: Stills from high speed camera of rat having undergone loading to peak seat velocity of 9.7m/s. Filming was performed at 10 000fps. Time above each still denotes the time from seat impact. The red line (as measured from the lowest torso point) indicates the original torso length.

In agreement with the seat accelerometer data, maximal acceleration and velocity of the plate and seat occurs in the first millisecond. During this time, the rat compresses at the torso to the same degree of the seat stroke with vertical movement of the pelvis and no movement of the head. The seat continues to move upwards (albeit more slowly) until 5ms, at which point the animal head has still not moved but the torso has compressed markedly. A surface wave phenomenon similar to that described by Kazarian *et al* occurs (Kazarian *et al.*, 1970). This surface wave is a thickening of the torso as it "pistons" upwards. At around 9ms, the pelvis of the animal moved away from the seat (which has stopped moving) and continues to move vertically. The torso of the animal reaches a maximal compression (around 9ms) and starts to elongate to just over normal length (around 27ms) and settling to normal length from around 30ms. This elongation phase occurs considerably slower than the compression phase. At this point, the head of the animal is slowly rotating dorsally and strikes the top of the seat before returning to rest. No anterior-posterior compression of the torso is evident although the tension in the restraint straps may increase in response to the apparent cross sectional increase at the point of the expanding surface wave.

The response of the torso may be defined using the metrics outlined above. As with seat acceleration and seat velocity, these were altered in response to varying input pressure. In each case, the maximum measurement of that metric (compression, compression rate, and viscous response) was used as the metric value. The measurement of each variable along with injury outcome of each test is shown in Figure 8.22 to Figure 8.24 below.

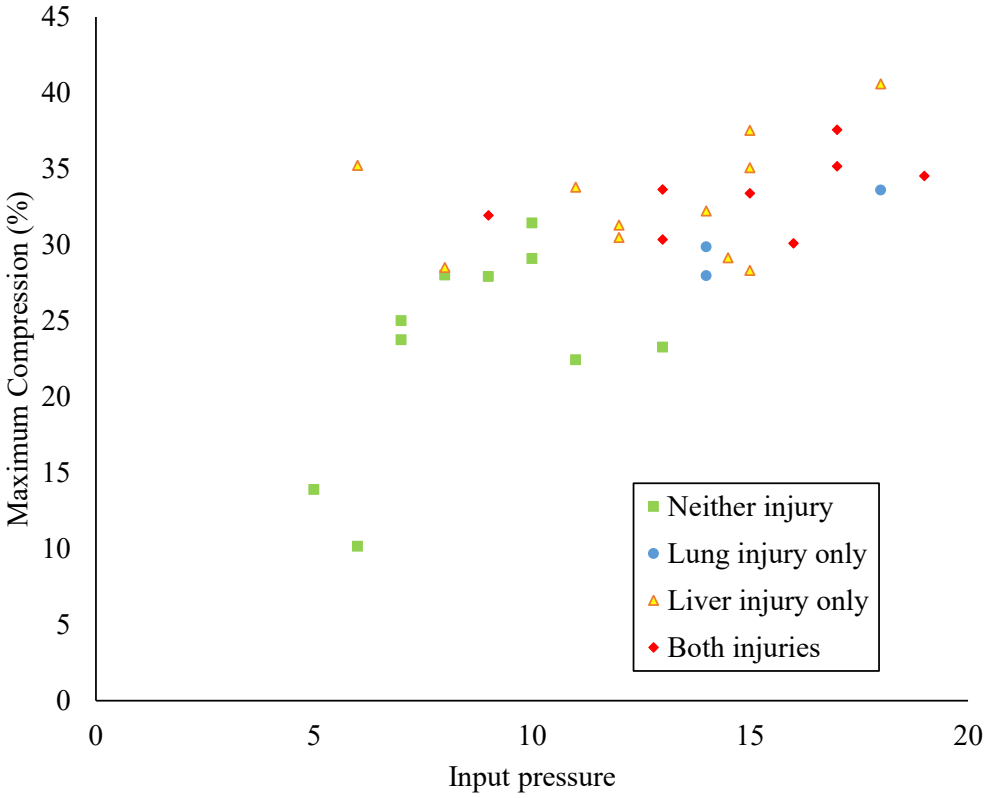

Figure 8.22: Change in maximum compression in response to changing pressure input. The injury status of each test is represented by the shape and colour of each point.

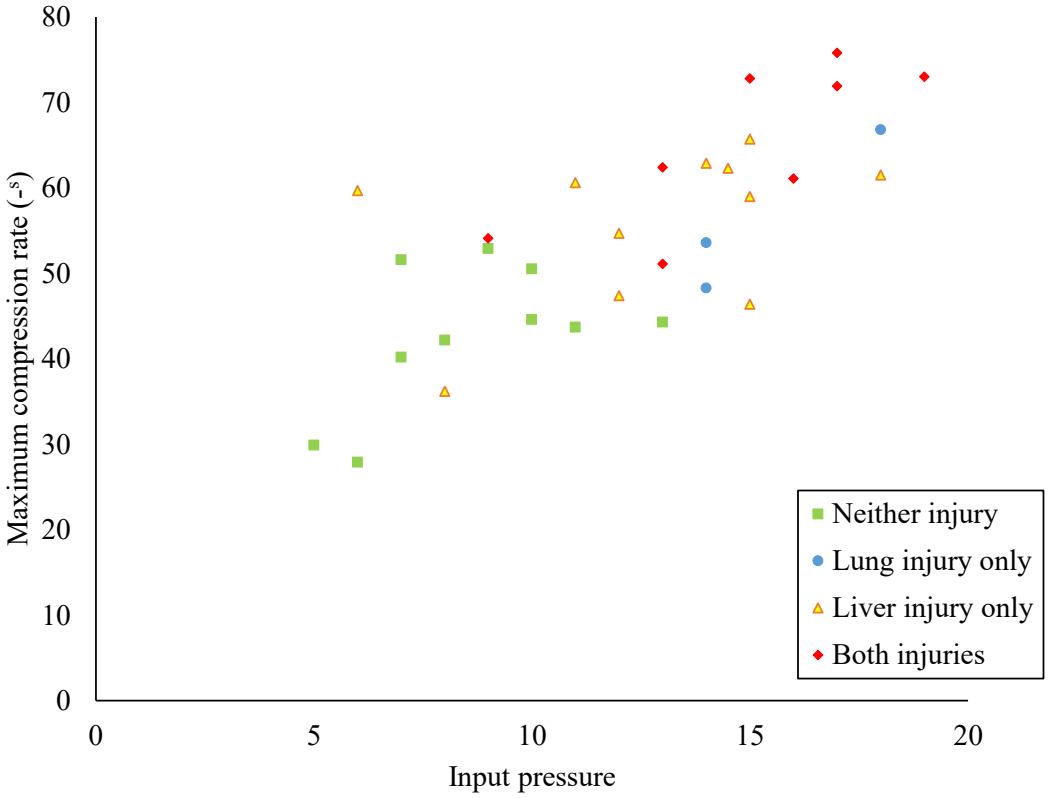

Figure 8.23: Change in maximum compression rate in response to changing pressure input. The injury status of each test is represented by the shape and colour of each point.

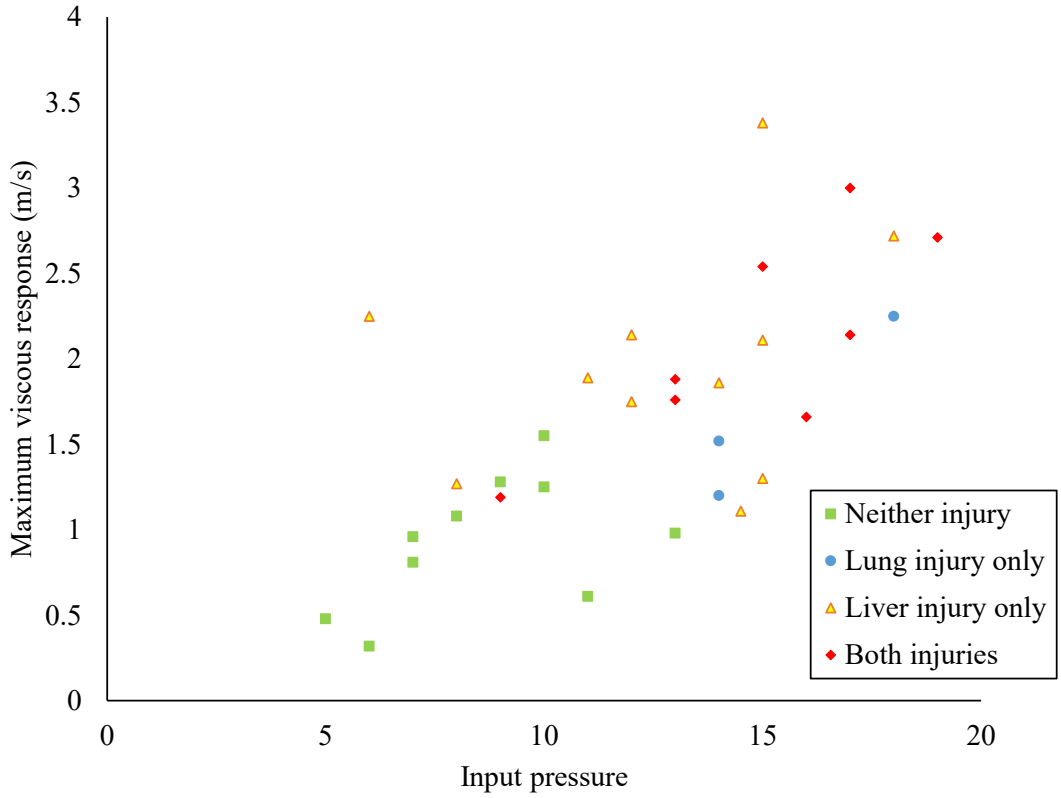

Figure 8.24: Change in maximum viscous response to changing pressure input The injury status of each test is represented by the shape and colour of each point.

Cross correlation of the physical and biomechanical metrics appear to show two groups (Table 8.3). Physical characteristics of the plate (acceleration and velocity) are closely correlated to each other (as described above by a linear regression model) but also closely correlated to the input pressure. The biomechanical criteria correlate less well with the input pressure and resultant plate characteristics but are well correlated with each other.

	Pressure	Acceleration	Velocity	Maximum compression	Compression rate	VC
Pressure	1	0.927	0.906	0.636	0.765	0.673
Acceleration	0.927	1	0.966	0.577	0.712	0.647
Velocity	0.906	0.966	1	0.581	0.663	0.598
Maximum compression	0.636	0.577	0.584	1	0.784	0.853
Compression rate	0.765	0.712	0.663	0.781	1	0.791
VC	0.673	0.647	0.598	0.853	0.791	1

Table 8.3: Correlation matrix showing Pearson correlation coefficient (r) between physical and biomechanical variables.

The relationship of the biomechanical variables to injury status was examined further. One way ANOVA with post hoc Tukey testing was used to compare the means of the maximum compression, compression rate, and axial viscous criterion across groups with no injury, isolated lung, isolated liver, or both injury modes (Figure 8.25, Figure 8.26, and Figure 8.27).

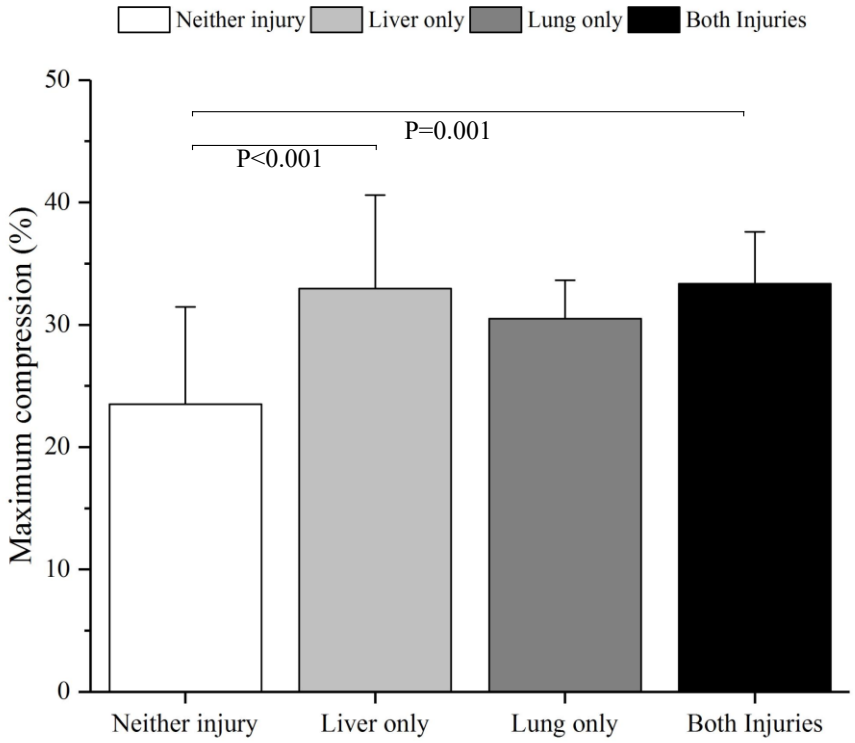

Figure 8.25: Mean maximum compression in each injury group. * denotes significant difference between two groups with one way ANOVA testing followed by Tukey's post hoc test ($p<0.05$).

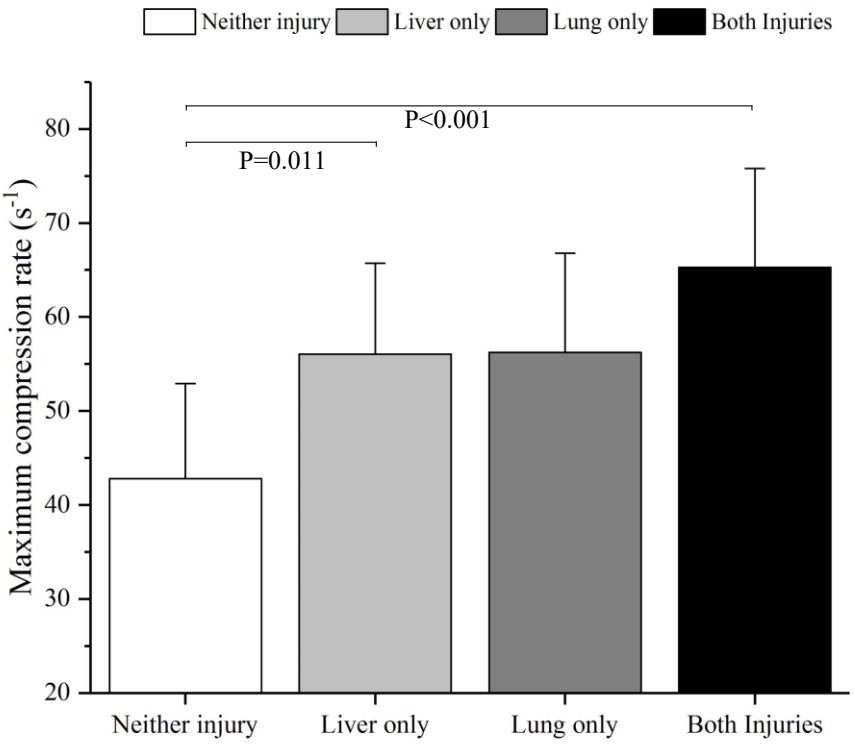

Figure 8.26: Mean maximum compression rate in each injury group. * denotes significant difference between two groups with one way ANOVA testing followed by Tukey's post hoc test ($p<0.05$).

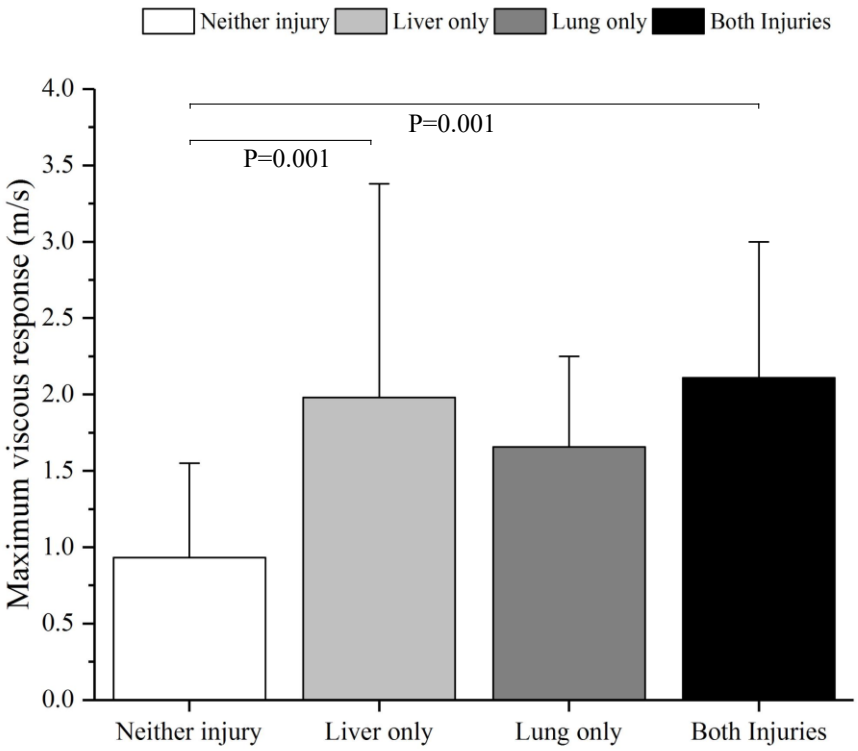

Figure 8.27: Mean maximum axial viscous response in each injury group. * denotes significant difference between two groups with one way ANOVA testing followed by Tukey's post hoc test ($p<0.05$).

Differences are seen in all three metrics between injurious and non-injurious tests. There is no significant difference in the mean of any of the parameters between non injured animals and those with isolated lung injuries. The mean value does differ however, and the lack of significance may be the result of a small number (only 3 animals with isolated lung injuries). The ability of injury metrics to predict a particular response will be considered further in Chapter 9.

8.6 Discussion

These results demonstrate torso injury in an *in vivo* rat model of high rate vertical loading in the absence of direct frontal or lateral loading. The primary injury outcomes were injuries to the lung and liver, both of which were deemed to be analogous to clinically relevant injuries. Impact injuries to the chest and abdomen have previously

been well described in *in vivo* animal studies. In nearly all cases, liver and lung trauma are the injuries of interest for abdominal and chest loading respectively (Viano *et al.*, 1978; Lau and Viano, 1981b, 1986 ; Stein *et al.*, 1983; Hoth *et al.*, 2006). These and similar studies have been used to characterise the injury mechanisms and develop injury metrics for soft tissue organ injury in response to these direct impacts. *In vivo* studies of high rate vertical loading are less common although other have previously demonstrated a variety of organ and vascular injuries from a similar, albeit slower, environment designed to replicate aviation crashes (Cook and Mosely, 1960; Hanson, 1967; Kazarian *et al.*, 1970).

This study has demonstrated these injuries with post mortem examination, histology, and CT imaging. The latter two modalities suggest a spectrum of injuries although the CT imaging was not adequate to relate the loading or injury metric to a more quantifiable measurement of lung injury. Future experiments could refine the imaging protocol to improve this injury measurement. The use of a nanoparticle blood pool agent would circumvent the difficulties posed of injecting a larger volume agent into an injured circulation.

The histological examination of both lung and liver confirmed the injuries diagnosed macroscopically and demonstrated a spectrum of injury across the loading range. The animals were culled and organs fixed at a very short time scale, so as expected, there was no evident immune infiltration into the injury region. Assuming a similar pathophysiological course to blast lung or pulmonary contusion, this immune response would be expected hours to days after the initial insult (Barnett-Vanes *et al.*, 2016).

Previous studies have been limited in their analysis of the kinematic response of the animal to vertical loading. Physical measures including acceleration have been used as the injury metric for these tests although the use of such measures may be limited by the positioning of suitable sensors and of the scalability of the metric (Cavanaugh and Yoganandan, 2015). The kinematic analysis of the experiments in this study demonstrate the poor correlation between seat acceleration and the response of the animal. Although acceleration and any similar measure of the physical loading may predict injury to a reasonable degree, they have little practical application for the understanding of the injury mechanism, and therefore for prevention of injury. A

previous rat model of UBB used acceleration as the injury threshold (Fiskum and Fourney, 2014). This group suggested a threshold vehicle acceleration of 2800g for around 0.5ms for causing unsurvivable injury. Animals in these experiments were in a prone position with acceleration therefore perpendicular to the long axis of the spine. These experiments aimed to replicate neurotrauma from hyper acceleration but there seems to be a marked difference in the injury threshold in the current study in which the threshold for lung injury appears closer to 5000g for a similar period of time. The difference may be that the Fiskum model caused direct loading of the chest, or that in a vertically orientate model, the input velocity of 5000g is attenuated by deformation of the body such that accelerations experience further up the body are significantly lower. The transmission of the input load from the loading platform (the seat) to the organs of interest in the abdomen and chest is therefore dependent upon the deformation of the torso in response to this load.

These results support the injury mechanisms proposed in Chapter 6. Internal organs are injured due to high rate vertical displacement with organ compression and tearing of attachments. Lung injuries are likely caused by craniad displacement of the abdominal viscera (most probably the liver) against the lung bases with subsequent lung compression and injury. The lung injury described resembles early contusion as caused by frontal loading. These injuries may be analogous to those described in post mortem studies of UBB and thought to be the result of a primary blast wave (Singleton *et al.*, 2013). These in vehicle PBLI injuries may actually be caused by vertical acceleration. Liver injuries are likely caused by compression against the diaphragm and lower ribs or tearing of the ligamentous attachments. The injuries are congruent with a simple mechanical model in which the degree of displacement is affected by the duration and magnitude of the acceleration. By measuring the physical response (the torso compression), the model negates the requirement to assume boundary conditions and spring/damper parameters of a complex system. Although organ movements themselves were not viewed radiologically, it is assumed the organs moved synchronously with the torso displacement as described by Weis and Mohr (1967).

No heart or great vessel injuries were sustained in these rat experiments. As discussed in Chapter 4, these injuries are of interest given that they are apparently a strong

predictor of death in the underbody environment. Several scenarios may account for this discrepancy between the battlefield and experimental data.

Firstly, the battlefield mediastinal injury itself may be phenomenological and not caused by vertical loading. Although efforts were made to examine only underbody blast, such incidents are complex and the possibility of this relatively small number of injuries to be caused by additional frontal loading is not inconceivable. Analogous injuries have certainly been described experimentally with craniad displacement of the diaphragm and heart attributed to be the cause of great vessel injuries caused by rapid G_z decelerations (Hanson, 1967).

A second scenario suggests accuracy of the battlefield data but failure of the experiment to adequately reproduce the necessary conditions. Although the vascular structure and relative cardiac masses of the rat and human are similar, what differences remain (such as the rounding of the rodent heart and reduced connective tissue within the vessel walls) might reduce the susceptibility of the rat to this injury mechanism. Although parenchymal injuries to the lungs may be caused by cranial movement of the abdominal viscera and compression against the lung bases, the superior position of the heart and damping effect of the abdomen may reduce the displacement of the heart and lungs such that no significant shear strain is generated at the structural attachments of these organs. Anatomical differences between the rat and human livers may also affect the susceptibility of the rat to mediastinal injury. The relatively large mass, and slightly more central position of the rat liver may offer some protection to the rodent heart and reduce the displacement of the heart and therefore of tensile strain to the aorta.

The third scenario is that while the battlefield data is accurate, and boundary conditions of the rat sufficiently similar, the loading created during these experiments was not great enough to cause these more severe injuries. This may suggest that a loading gap remains between the severe lung and liver injuries described in the experiment and the even more devastating heart and aortic injuries. Within the battlefield data, the vast majority of those with aortic and cardiac injuries sustained other concurrent torso trauma. Given the high mortality associated with lung and liver injuries in the battlefield environment, the bridging this gap would be desirable but not essential given the likely negligible improvement upon survivability should the liver and lung injuries be prevented.

This chapter has introduced novel injury metrics to reflect the importance of this torso deformation for the generation of injuries. Compression of the torso in the axial direction along with compression rate and axial viscous response. Compression rate and axial viscous response depend on a degree of displacement and are sensitive to increased rate. The internal organs are known to be rate sensitive, and the response of the organs to the vertical loading of the underbody blast environment (and that induced by the novel rig) is likely to lie somewhere on the viscous response spectrum between crush and blast described by Lau and Viano (1986). The viscous criterion (developed to predict injury following loading within this spectrum) assumed displacement at high velocity. The degree to which either displacement or velocity most influences the likelihood of injury is dependent on the relationship between the two with velocity mostly dictating injury at very high rates and low displacement (blast) and displacement contributing more when it is large and velocity is low (crush). In developing and validating the tool for frontal impact, Lau and Viano admitted that the application of linear mechanics to the understanding of such injuries may not be possible but that the criterion took the relevant aspects into account. The same appears to be true of torso injuries in response to high rate vertical loading. In these tests, the average of these metrics between injured and non-injured states differs although this analysis does not explore the ability of the metrics to accurately predict injury. Predicting injury must importantly take into account both injurious and non-injurious testing with appropriately censored data. This analysis will be carried out in Chapter 9.

The obvious limitation of this study is the translation of any conclusions from a rat to a human model of injury. The rationale for the use of an *in vivo* animal model is undeniable with organ injuries important to survival and not replicated by current cadaveric, surrogate, or computational models. As discussed earlier in the chapter, the general vascular and internal organ structure of the rat is similar to the human. The effect of what anatomical differences do exist (including the relative mass of lungs and liver) upon transmission of loading to those organs is unknown. Although scaling laws may be applied to overcome size and mass discrepancy, these laws apply assuming geometric similarity and there is no accurate measure of relevant similarity between the two species, particularly when tethering conditions of the relevant organs and tissues needs to be considered. These scaling laws, and the potential translation of animal derived data to human injury will be discussed further in Chapter 9. The kinematic response of the

human torso to UBB has not been well described. Compression of the torso length by 20% is described in one test by Danelson *et al* but this response was not compared either to varying loading or internal injury occurrence (Danelson *et al.*, 2015). Degree of torso compression must to some degree depend upon the spinal response. A reduction in torso length does not require an absolute reduction of the spinal length but upon reduction in the axial direction which can be achieved by a combination of intervertebral disc compression and by both sagittal and coronal flexion and extension. Although there is an existing metric for prediction of spina injury from vertical load (the Dynamic Response Index), this tool was developed for ejection seat loading and has been shown to be inaccurate for prediction of spinal injury from the higher rate UBB (Spurrier *et al.*, 2015)

This study has demonstrated the occurrence of relevant injuries in response to an *in vivo* model of UBB loading but prevention of the injuries requires prediction of risk. The limitations of using the loading itself as an injury metric is discussed above. Characterising the biomechanical response of the body to the loading and the link between response and injury accounts for coupling of the loading to the body and is essential. Changes in restraint, PPE, posture, body characteristics, or even seat material may affect injury without any change to the physical loading. This study has discussed the initial development of novel injury metrics which are based upon degree and rate of axial torso deformation. The application of these metrics for injury prevention depends upon their ability to predict injury. While the data above demonstrates difference in these values between injured and non-injured states, the next step is further statistical analysis of these variables and the development of injury risk models. This analysis will be considered in Chapter 9.

8.7 Conclusions

Torso injuries affect survivability in the UBB environment. This rat model replicates UBB relevant loading to a species with relative geometric similarity with subsequent occurrence of relevant torso injuries. Although mediastinal injuries did not occur in this study, both lung and liver injuries (both of which are more common in UBB) were commonly sustained. This chapter has demonstrated the kinematic response of the torso

to UBB which supports the proposed mechanism of organ injury; relative displacement of the chest and abdominal organs with generation of shear or compressive strain. The chapter has developed novel injury mechanisms based upon degree and rate of axial torso compression. The next chapter will discuss the translation of these injury metrics including the scaling of the metrics for humans and the development of injury risk curves to accurately predict torso injury.

CHAPTER 9

TRANSLATING THE MODEL: SCALING CONSIDERATIONS AND DEVELOPMENT OF INJURY RISK CURVES

9.1 Scope of the chapter

Chapter 8 demonstrated that high rate vertical loading generates clinically analogous torso injuries in a rat model of UBB. The chapter discussed the physical and kinematic variables which describe the input "dose" of the loading and the biomechanical response of the torso. This chapter will discuss the potential translation of these metrics with emphasis on scaling laws for physical parameters to facilitate understanding of the human response to injury, and of the development of injury risk curves which are used to predict likelihood of injury based upon a particular metric.

9.2 Introduction

The first part of this thesis showed that torso injuries are common in the UBB environment and that they have a strong influence upon survivability. Chapter 5 showed through injury association, that torso injuries are part of a seat loading complex and therefore most probably sustained due to high rate vertical loading of the torso through the pelvis. Chapters 7 and 8 have demonstrated that a custom designed rig to create seat driven high rate loading creates analogous injuries in a rat model used novel metrics to describe the kinematic response of the torso to this loading.

This chapter will discuss the utility of this model towards improving survival. As described within the early chapters of this thesis, improving survival can be achieved either through advancing treatment of severe injuries or by preventing or mitigating these injuries. The severity of the injuries, prolonged timescales, and already advanced management strategies suggest that greater improvement to survival can be achieved through prevention.

Preventing or mitigating injury requires that the risk between loading and injury is well characterised. Preventative measures for UBB may include changes to restraints, seats, posture, or vehicles. These changes may directly reduce the loading prior to transmission to the vehicle occupant or modify the loading such that the same injury mechanism does not occur to the same extent. For the purposes of designing and testing devices, and to ensure that they have a clinical effect, the change in risk of injury associated with a particular device or strategy must be known.

For the purposes of survival, we must therefore define the mitigative gap (which injuries need to be mitigated to improve survival) and the loading gap (how must the loading be changed or modified in order to cross this mitigative gap). This chapter will examine the thresholds of injury suggested by Chapter 8 and explore the use of scaling laws and injury risk curves to better define the necessary loading gap.

9.3 Scaling laws

Chapter 6 discussed the generalities of injury mechanisms: that injury occurs from deformation of biological tissues beyond a structural tolerance. Although environmental mechanical forces may act upon the body in different ways, be that: transmission from air, solid or liquid media; local or uniform loading; or through inertial forces, it is the resultant relative displacement of the tissues that generates strain and causes injury. Biological tissue response is rate dependent and generally higher loading rates produce failure at lower absolute levels of strain, that is, the tissues become more brittle. The detailed knowledge of how individual tissues respond is only known for some tissues and so general assumptions are frequently made when analysing failure at the tissue level. In addition, how to scale between different species is also a matter for debate in the scientific and clinical literature. The most common approach is to introduce scaling laws for injury; these examine the effect of changing dimensions and mass upon the resultant mechanical forces. Although there are definite differences in physiological, cellular, and metabolic responses between different species, a significant number of physical parameters can be scaled using uncomplicated allometric based scaling laws (Panzer *et al*., 2014). This section will explore existing scaling methodologies and determine the extent to which they may apply to a rodent model of UBB.

9.3.1 Air Blast

As discussed in Chapter 5, small animals have previously been used for impact and blast tolerance studies. The "Bowen curves" created by the Lovelace foundation examined the mammalian response to primary blast and determined the relationship between animal mass and air blast tolerance with an emphasis upon primary blast lung injury (Bowen *et al.*, 1968; Richmond *et al.*, 1968). The group examined the blast tolerance of 13 mammalian species, subsequently divided into "large" and "small" animals based upon body mass. The group formulated a general equation for expressing the interrelations between overpressure, duration of the blast wave, body mass, and probability of survival. This scaling was based upon dimensional analysis which assumed that the thoracic overpressure was caused by simultaneously acting chest wall and abdominal "pistons" (Bowen *et al.*, 1965). This model incorporated an air cavity

representing the gaseous volume of the lungs, two movable pistons and an orifice through which gas might pass in either direction. One of the pistons represented the chest wall and the other that portion of the abdomen which moves with the diaphragm to change the lung volume. Each piston was "assigned" an effective mass and area, a spring constant, and a damping factor (Figure 9.1).

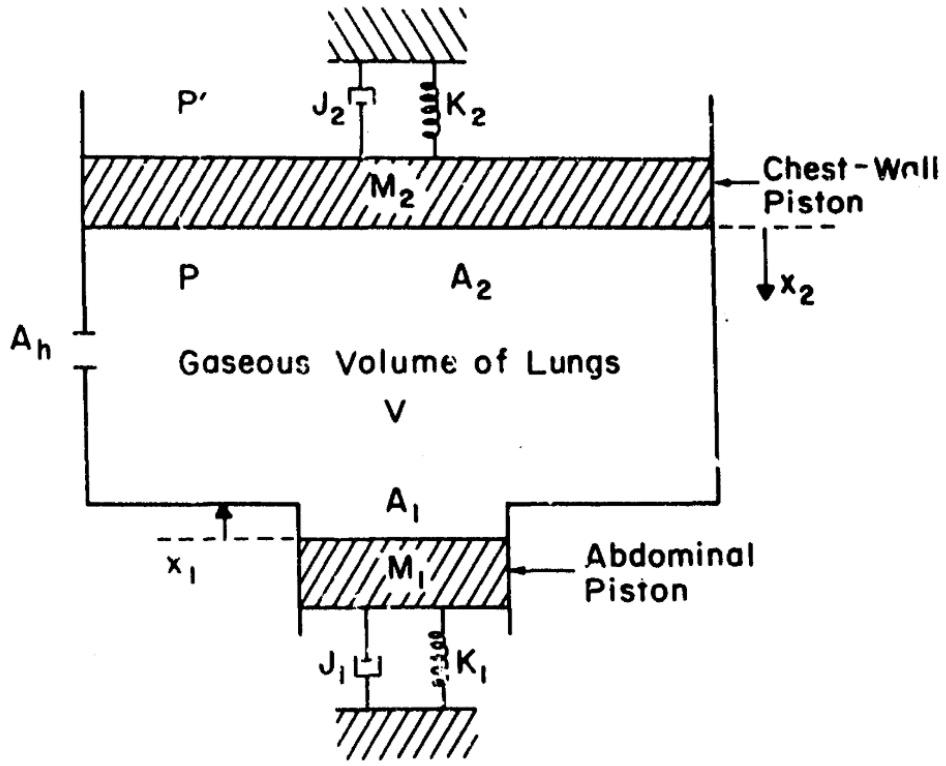

Figure 9.1: Mathematical model of the thoraco-abdominal system to simulate fluid mechanical response to rapid changes in environmental pressure. A_h represents the gaseous orifice, K_1 and K_2 are spring constants of the abdominal and chest wall pistons. J_1 and J_2 are the damping factors, A_1 and A_2 areas of the pistons, and M_1 and M_2 the masses. Reproduced with permission from Bowen *et al* (1965).

The volume change in this model following external pressure changes was based upon the displacements of the two pistons. The resultant pressure change is then a function of both the reducing availability of space and the airflow through the orifice. Dimensional analysis was then used to describe the influence of the mass upon the model. Experimental measurement of internal pressure was used to estimate specific spring and damper parameters which varied as a function of the animal mass (Bowen *et al.*, 1965). Although not further explored, it was assumed in the Bowen model that the damping

ratio, the tendency of the piston to reduce oscillation by dispersal of energy, was constant amongst species. Although normal physiological damping of the chest wall may be examined for typical respiration, the damping processes involved in the blast situation are more complex and cannot be related to conventional physiological studies (Bowen *et al.*, 1965). The spring system of the lung was modelled as a linear spring although the "air spring" of the lung with heterogeneous compressibility would make the system non-linear. Similarly, the damping of the abdomen in response to the external pressure change was modelled as a purely viscous sac rather than as individual masses.

Experimentally, the scaling laws applied to the time duration of the loading applied across the range of masses but two distinct groups ("large and small") of animals emerged for lung susceptibility to primary blast. The difference between these groups is in the initial scaled lung volume with considerably larger relative lung volume found in the larger group of animals (Figure 9.2).

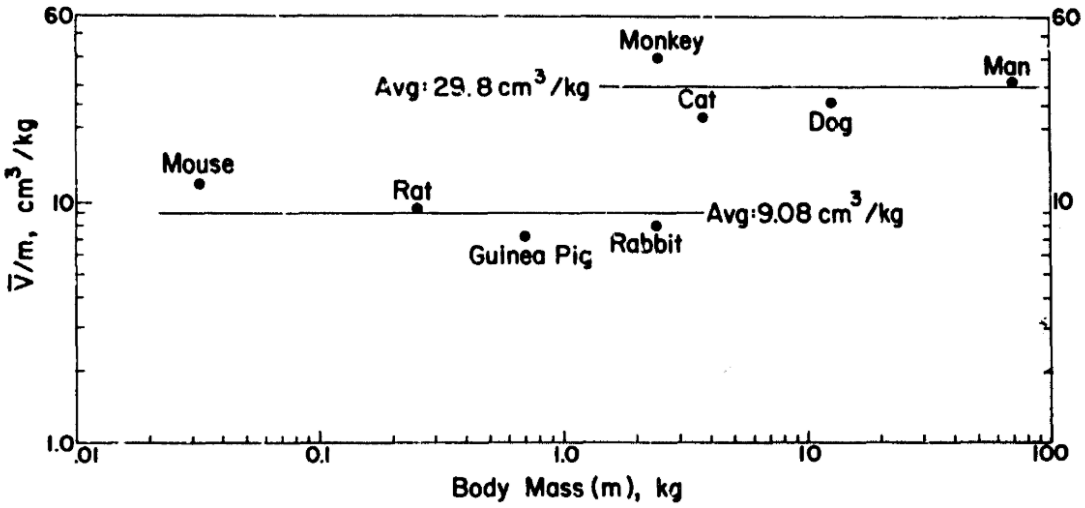

Figure 9.2: Average lung volume per kg of body mass across mammalian species. Reproduced with permission from Bowen *et al* (1965)

This model did not separate the effect of the abdominal and chest wall pistons assuming a uniform external pressure driving both pistons. This model, as an explanation of primary blast injury, also fits the proposed mechanism of UBB organ injury which the torso deformation results in the movement of an abdominal piston (without the chest

wall piston) towards the lungs. Given that compression of the lungs by the abdomen and diaphragm is physiological (to an extent), the rate that this compression occurs and the inability of the orifice to conduct the increased pressure away sufficiently quickly is a possible injury mechanism for UBB "blast lung".

The resultant injury curves generated by the Bowen group were summarised by Bass *et al* (2008) (Figure 9.3). Despite scaling of pressure and duration, a difference between large and small animals remains appreciable and is thought to result from the difference in relative lung mass.

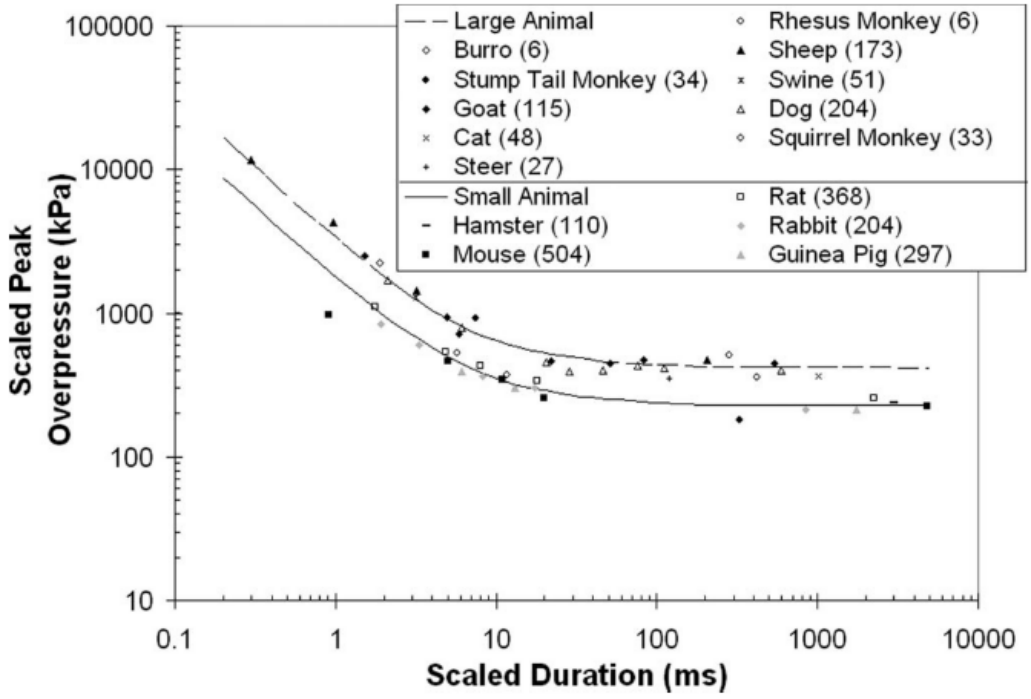

Figure 9.3: Bowen's Injury Risk Curve (number of animals in parentheses). Reproduced with permission from Bass *et al.* (2008) from Bowen *et al.* (1968).

These scaling laws are to some degree applicable for the rodent model of UBB torso injury. They demonstrate the relative geometric similarity of the two species without which the mathematically derived model above would not be validated. The derivation of the laws suggest that even with very high rate blast injury, an estimation of abdominal displacement can be used to predict injury. A number of assumptions were made during

the development of these laws, namely in the description of the damping qualities of the chest wall and abdomen to the loading. The piston displacement was calculated based upon changes in ambient pressure with assumed or mathematically derived spring and damping factors. Direct measurement of the piston movement following loading (the torso compression) may circumvent some of these assumptions. Of course, the primary direction and duration of loading in tertiary and UBB is different from primary blast and therefore scaling laws for impact loading should also be considered.

9.3.2 Impact loading

Scaling for impact testing is also reliant upon the development of a mechanical analogue of the bodies in question. For the purposes of examining impact tests, the relationship derived relates not to changes in pressure but directly to tissue strain and injury resultant from the input load. An ideal model is able to calculate the resultant strain from the input load based upon some measure of mechanical impedance. Precise mechanical and pressure impedances may be calculated at a component level from ex-vivo testing (von Gierke *et al.*, 1952; Shah *et al.*, 2006; Kemper *et al.*, 2010, 2012). Such experiments provide clues to the resonances of organs and to the mode of propagation of stress and shear waves (von Gierke, 1968). Direct impedance measures are not possible with *in vivo* testing but description of surface or internal movements may allow direct estimation of strain (Boorstin *et al.*, 1966; Kazarian *et al.*, 1969).

As with the model for primary blast, mechanical analogues for impact are based upon simple mass and spring systems in which an input (the impact) generates movement of the mass which is dependent upon basic mechanical parameters. Such a model can be used to simply describe tissue motions observed under linear accelerations and may be used to scale the relevant parameters between different masses of geometric similarity (Figure 9.4).

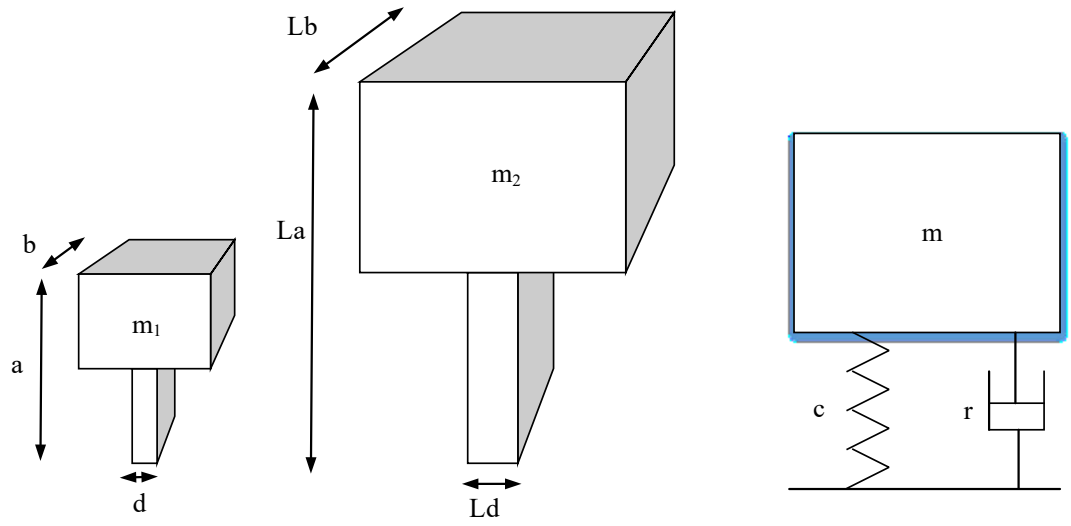

Parameter	Scaling
$\frac{m_2}{m_1}$	L^3
$\frac{c_2}{c_1}$	L
$\frac{r_2}{r_1}$	L
$\omega_0 = \sqrt{\frac{c}{m}}$	$\frac{1}{L}$

Figure 9.4: Scaling laws for geometrically similar structures such as mammals of different sizes. c and r refer to the spring and damping constants of the system and ω_0 is the natural resonance Adapted with permission from von Gierke (1968).

Von Gierke (1968) illustrated these laws by examining the resonance of bodies under vibration. He demonstrated that the main abdominal resonance of the system (the frequency at which the abdomen undergoes maximum displacement under linear vibration) alters predictably in response to changes in body mass or length Figure 9.5. Approximate acoustic resonance of the chest (as calculated) is also shown.

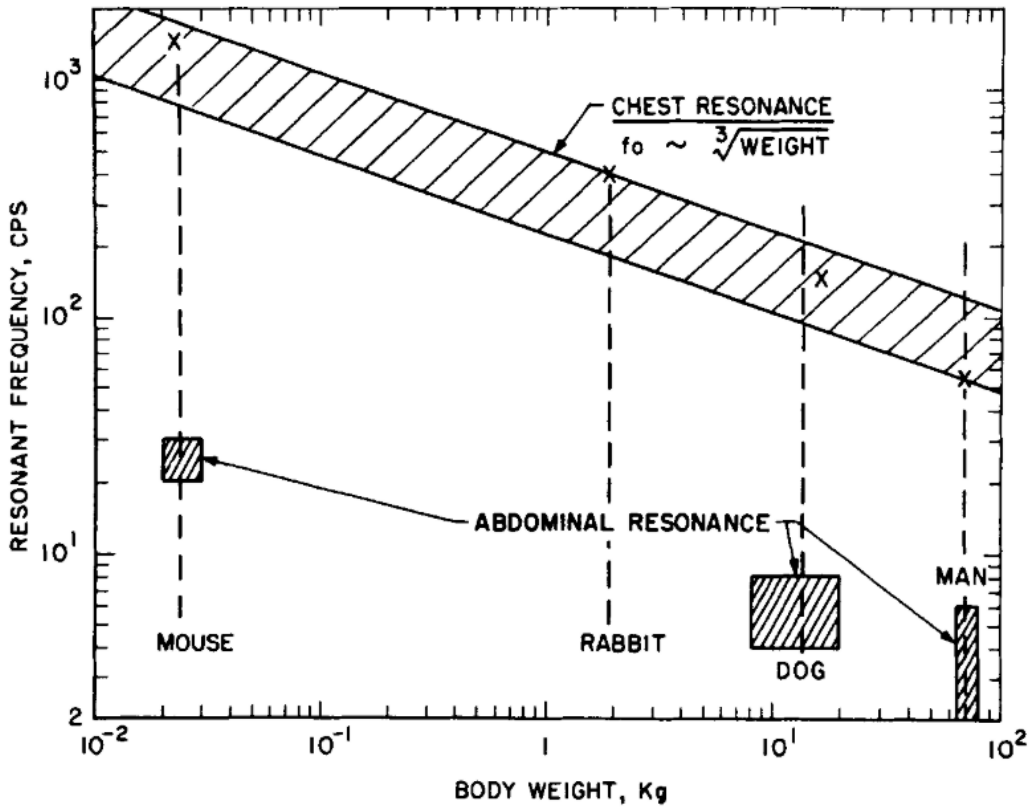

Figure 9.5: Approximate resonance frequencies of the abdomen of geometrically similar animals as a function of body mass. The calculated chest resonance is also shown. Reproduced with permission from von Gierke (1968).

Although it must be acknowledged that representing a human or rat organ system as a simple and passive linear system is an oversimplification, this model, particularly when used to express a single degree of freedom (as with torso compression to UBB) usefully describes the apparent phenomena. The complexities and non-linearity of the system are best measured experimentally.

Kornhauser and Lawton (1961) also used a mechanical analogue to describe the mammalian response to impact loading. Their model of mass and spring was first used to describe the performance of inertial mechanisms subjected to single short duration acceleration-time pulses. Both peak acceleration and change in velocity (representing the duration of the acceleration) may be used to describe the point at which the inertial mechanism (for which they substituted the occurrence of injury) occurs.

They described that for a particular system, the magnitude of acceleration required to induce the required response varied with the duration of the response.

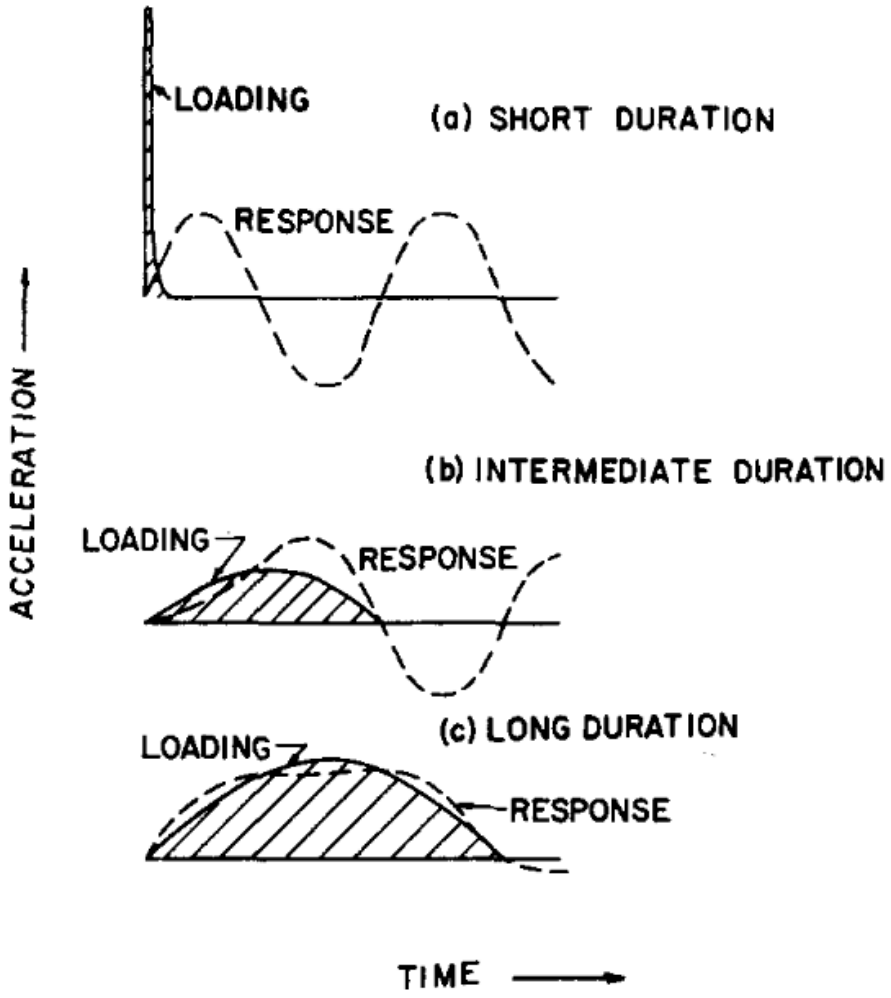

Figure 9.6: Changes in acceleration required to induce the required inertial "switch" in response to changing durations. Reproduced with permission from Kornhauser and Lawton (1961).

For each inertial or impact scenario, this data could be used to generate a sensitivity curve in which failure required both a minimal acceleration, and minimal velocity. Given the high rate nature of blast and related impact, the degree of injury would depend on a minimal time duration, below which sufficient change in velocity for a given acceleration would not be achieved.

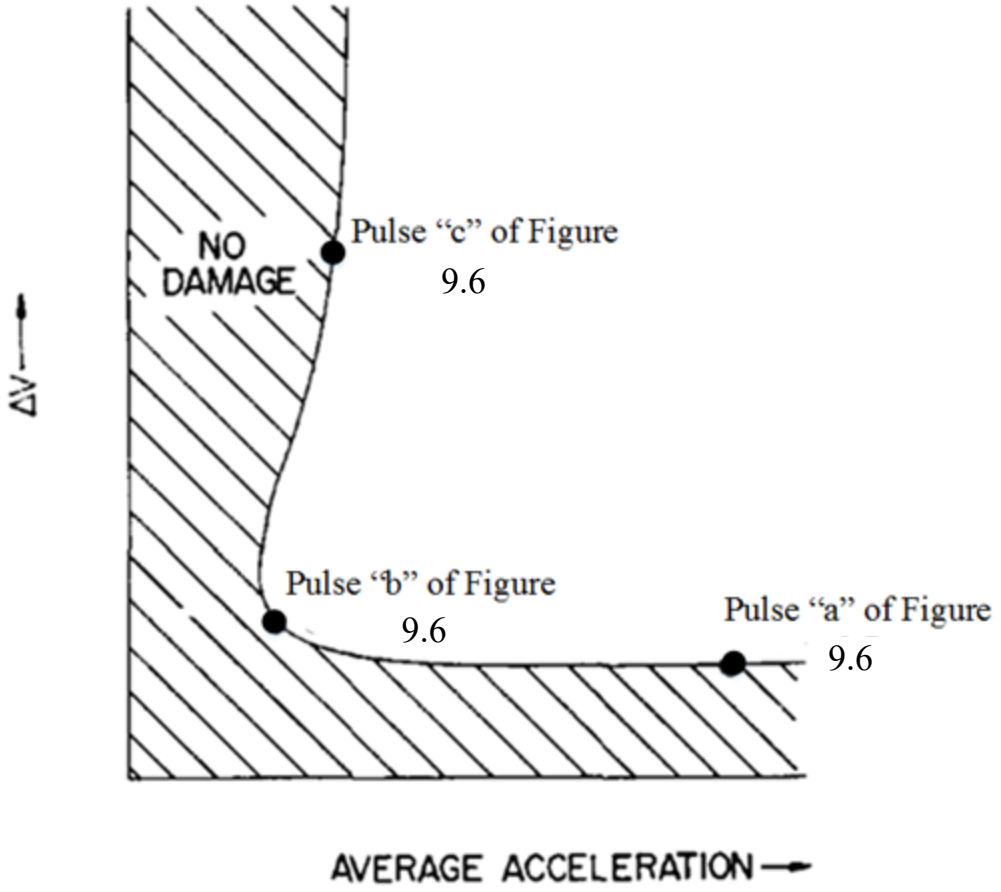

Figure 9.7: Sensitivity curve for mass-spring system subjected to impact loading scenarios as described in Figure 9.6. Adapted with permission from Kornhauser and Lawton (1961).

These sensitivity curves relate only to the parameter of input function and assume an otherwise identical loading scenario. The model takes no account of the coupling of the loading to the response. Although this coupling is represented in the occurrence of injury, it means that any particular sensitivity curve is valid only for a very specific loading scenario in which coupling of loading to the body remains consistent.

Kornhauser and Lawton used supinely positioned mice and a drop rig to demonstrate the existence of a vertical asymptote, which is the minimal velocity limit assuming short duration loading. Their tests were directed at mortality of the animal with cause unspecified.

Using low level human volunteer impact sensitivity (based on Col. Stapp's work as discussed in Chapter 5), Kornhauser extrapolated the sensitivity curve data to that of a the human and compared it to that of the mouse (Figure 9.8).

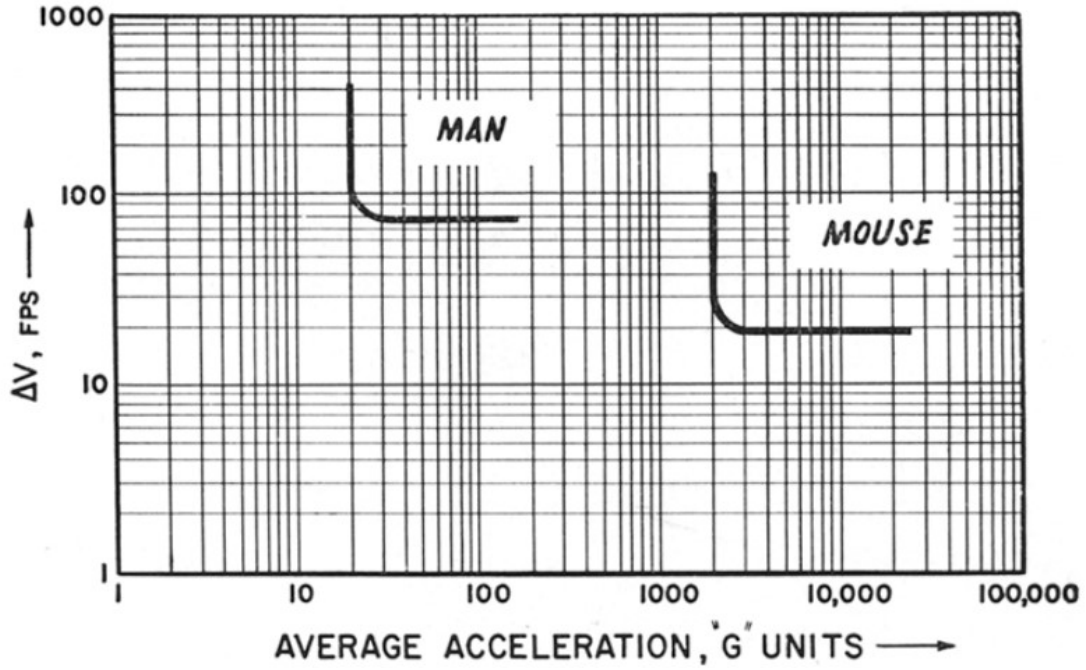

Figure 9.8: Comparison of mouse and human sensitivity curves. Reproduced with permission from Kornhauser and Lawton (1961).

The pronounced difference between the two curves is shown to be the required acceleration. The difference in mouse and human minimal velocity was unexpected as the mass-spring model would predict very similar thresholds for similar geometry. Differences between these two data sets could certainly arise from the experimental configuration. The mice were dropped in a fixed tube position with reducible (severe) loading onto a fixed point. Extrapolation of human volunteer tests (at much lower) accelerations and with far less severe injury endpoints is likely to result in large error.

However, Richmond *et al* (1961), when examining a range of dropped mammals determined that the "lethal dose" of velocity for dropped mammals was remarkably similar among different mammals (mice, rats, guinea, pigs, and rabbits) and to known (albeit not experimentally controlled) human data from falls.

The difference in the accelerative threshold relates therefore to the desired response and the natural resonance of the system or body in question. When a body is exposed to linear impact acceleration, it is the resonance that determines the shape of the sensitivity curve for pulse durations shorter than a critical duration such that the tolerable acceleration levels increase with decreasing pulse duration (von Gierke, 1968). The critical pulse duration is dependent primarily on the steady state natural frequency of the system and the damping of the structure in question. The smaller animal has the shorter critical duration (as described above) and therefore similarly increased acceleration threshold.

9.3.3 Application to current experiments

It may be inferred from this model and from von Gierke's data that the natural resonant frequency of the rat abdomen would be between that of a mouse and rabbit at around 10Hz and that scaling the response of the abdomen to that of a human could be done based either on mass or body length. Assuming an animal mass of 275g and a human mass of 70kg, the difference in natural frequency could be calculated determining the cube root of the ratio of masses (6.34 in this instance) or the ratio of torso lengths (around 5-6). In either case, the natural frequency of the system (between 2 and 60Hz depending on the species) is considerably greater than the impact duration of an UBB event.

This sensitivity curve can be applied to the experimental data from Chapter 8 (Figure 9.9).

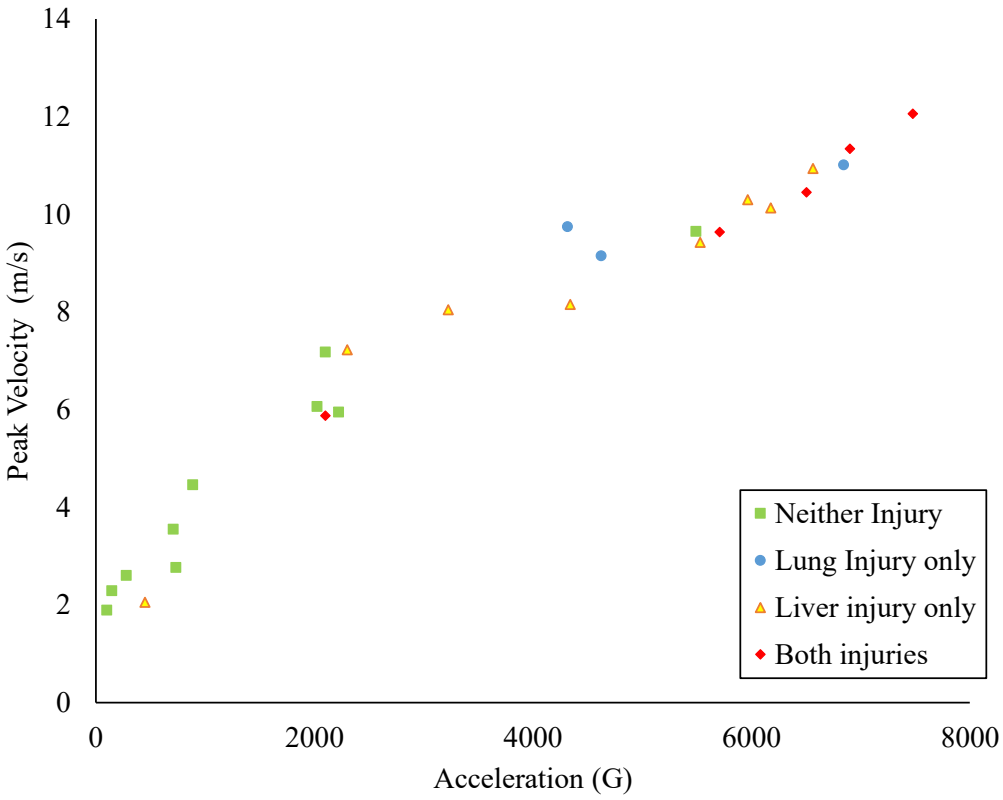

Figure 9.9: "Kornhauser" sensitivity curve as applied to high rate vertical loading of rats with torso injury as primary outcome (data from Chapter 8).

The data demonstrated in this thesis does not adequately describe the separate asymptotes given that since the duration of the acceleration remained fairly constant, acceleration and velocity have a fairly linear relationship.

The acceleration pulse in these tests occurred over a time duration (~0.5ms) which is considerably less than the expected critical duration of the animal (assuming 20ms for abdominal resonance based on the above data). Linear acceleration in this instance can be scaled based upon the ratio of lengths assuming similar mass density and modulus of elasticity (Panzer *et al.*, 2014). The threshold of injury in the animals was around 2000G with more severe injury around 6000G. These values would extrapolate to between 300 and 1000G for human injury (assuming a similar vertical asymptote) which should encompass the relevant range of UBB insult (Bailey *et al.*, 2015).

The description of the torso as a simple mechanical analogue certainly facilitates scaling comparisons between the two species. Although it must be acknowledged that representing a human or rat organ system as a simple and passive linear system is an oversimplification, this model, particularly when used to express a single degree of freedom (as with torso compression to UBB), usefully describes the apparent phenomena.

These mechanical models and sensitivity curves help to explain the effect and mechanism, and suggesting suitable values for scaling. They do not, however adequately describe the coupling of the body to the acceleration nor the organ and tissue level interactions. It is the properties of these tissue level interactions in response to this form of loading that are most uncertain in both human and animals.

The most appropriate way to account for the complexity and non-linearity (which is the predominant rationale underlying the use of an *in vivo* animal model) is to measure injury effect experimentally. As described by the kinematic analysis of the experiments in Chapter 8, there is a complex multimodal response of the animal to an accelerative input. The torso response is affected by restraint and posture. Any mechanical or computational model must make assumptions regarding factors along with non-linear tissue properties and of the coupling of the input to the response. Kinematic analysis enables direct measurement of the response and therefore takes each of these complicated factors into account. Although the previous chapter has described the injurious effect of the loading, the following section will use this data to predict risk of injury based upon both input and mechanical response of the affected body.

9.4 Principles of injury risk calculation

As described in Chapter 6, there may be many physical parameters that have some correlation with the injury outcome from a set of experiments. This may often reflect the fact that the physical parameter (such as the acceleration) is a measure of the occurrence of the event (Hardy *et al.*, 2015). All physical measurements are likely to increase as impact severity increases but this does not mean that a causal relationship

exists between each parameter and injury. These physical measures may have no biomechanical basis with regards to the injury mechanism.

Injury outcomes may be coupled to biomechanical metrics to generate risk curves. Such curves have frequently been used for PMHS testing for military and civilian crashworthiness evaluations and predict probability of outcome (injury or mechanical failure) for a given value of the metric of interest. Any curve or model will generate only a probability of injury with some degree of variability inherent to individual variability in injury tolerance. Injury risk curves may be used by regulatory bodies, vehicle manufacturers or suppliers to test vehicle or restraint design (Petitjean *et al.*, 2015). A further application of this information could be at a more tactical level for the military, given that a commander could estimate risk to personnel given a particular vehicle type and known explosive threat.

Several methods have been used for the derivation of injury curves with some models fitting the sample data to a simple binary regression model. One such technique, developed by Mertz and Weber based the curve solely on the strongest and weakest samples such that the mean of the distribution is the mean of the injury criterion of those two tests (Mertz and Weber, 1988). The curve is therefore highly influenced by these points and has little statistical basis.

Logistic regression has also been used to develop injury curves. This models the relationship between the binary variable (injured or non-injured) and one or more explanatory variables (biomechanical metric). This model assumes a logistic distribution and determines the best fit to maximise probability of injury for the injured tests and minimise the probability of injury of the non-injured tests (Petitjean *et al.*, 2015). Although used recently for injury curve derivation (Kuppa *et al.*, 2003) , logistic regression methods cannot take exact data or interval data (in which the precise input or narrow range of input is known) into account.

Survival analysis is a statistical technique commonly used in clinical studies to determine survival time after onset of disease. The major benefit of survival analysis is that it takes the censoring status of this time variable into account, i.e. that the exact time of an event may not be known but that it falls within a known range. For the purposes

of biomechanics studies, the time variable may be replaced by the injury criterion of interest. Survival analysis has been recommended by a working group (ISO/TC22/SC12/WG6) of the International Standards Organisation (ISO) as a standard method for producing curves (Yoganandan *et al.*, 2016). This method is recommended because of its ability to accommodate this differing censor status which incorporates biomechanical rationale better than simple sensor data.

The probability of risk generated by this method is shown in Equation 8.1, from (Petitjean *et al.*, 2015),

$$probability\ of\ risk = 1 - exp\left(-\int_0^x h(u)du\right) \quad [8.1]$$

where the probability of risk is expressed in terms of the hazard function *h*, where *h* is the instantaneous risk of injury and *h(u)du* is the probability of a subject being injured between *u* and *u+ Δu*, given that the subject is not injured until *u* (and *u* is the injury criterion value). Parametric survival analysis depends upon fitting the probability of risk to a known distribution. Examples of distribution are log-normal, log-logistic, and Weibull. Statistical simulation has shown that survival analysis using Weibull distribution is the most appropriate for generation of injury risk curves, generating the lowest error regardless of sample size.(Petitjean and Trosseille, 2011). The hazard function of this distribution is continuously increasing with the loading severity according to the shape and parameter coefficients (k and λ) generated by the data such that:

$$probability\ of\ risk = 1 - exp(-\left(\frac{x}{\lambda}\right)^k) \quad [8.2]$$

The injury curve can thus be reported by stating the distribution type and coefficients.

The ISO suggested a stepwise approach to the development of injury curves using survival analysis to assure methodological consistency (Petitjean *et al.*, 2015). These steps are:

1. Collection of data
2. Assigning censor status
3. Checking for multiple injury mechanisms
4. Separate data for multiple injury mechanism
5. Estimating distribution parameters
6. Identifying overly influential observations
7. Checking the distribution assumption.
8. Choosing the distribution
9. Checking the validity of the predictions against existing results
10. Calculating 95% confidence intervals
11. Assessing the quality
12. Recommending one curve per region

These steps have been described by some researchers as too simplistic. Yoganandan *et al* (2016) have argued that the ISO approach does not discuss the choice of biomechanical parameter for a particular model. They further argue that more quantitative measures should be used for choosing the distribution by identifying outliers and quantifying confidence interval gaps. Yoganandan *et al* suggest that the AUROC should be used to choose an optimal biomechanical metric, followed by use of the Akaike Information Criterion (which estimates the information lost when fitting data to a statistical model) to rank the best fitting statistical distributions.

McMurray and Poplin have argued against overcomplicating the procedure for producing these curves (McMurry and Poplin, 2017). They state that using AUROC to screen many biomechanical predictors is likely to over fit a model and that with limited sample sizes (as is often the case with PMHS testing), the AUROC value may alter significantly with additional tests. They instead recommend that researchers place significant emphasis on choosing predictors that best correspond to a physical understanding of the underlying biomechanics, such as the relation of the metric to tissue strain. They further argue that ranking the distribution using an additional criterion is not a reliable way to choose a model in most biomechanical experiments, that the Weibull distribution has biomechanical advantages (zero loading predicting zero risk by

default), and that any difference between competing distributions is likely insignificant (McMurry and Poplin, 2017).

Certainly, any injury risk curve should be generated based upon proposed injury. The coupling of the mechanical insult to the biomechanical and tissue level response should be considered in this metric choice. The use of AUROC scoring may seem to be more quantative but this seems only relevant when many different metrics are being evaluated and when the mechanism of injury in uncertain.

9.5 Deriving injury curves from novel *in vivo* data

With these considerations in mind, the decision was made to adopt a pragmatic approach to deriving injury curves from the available data. Large scale PMHS tests may collect dozens of data channels and derive many potential injury metrics. In contrast, the metrics collected in this experimental series were based either upon the input accelerometer data and reflect the loading of the seat (peak acceleration or peak velocity) of the animal torso response, which takes into account seat-restraint-animal coupling (maximum compression, maximum compression rate, and axial viscous response). These metrics were chosen on the basis of the proposed injury mechanism and presumed influence upon torso injury

Compression is an appropriate measure of torso deformation in the direction of interest. By measuring compression, the coupling of the seat to the animal, and the stiffness of the animal torso are taken into consideration.

The additional metrics build upon the compression metric but factor in rate of the loading. This is based on the known rate dependence of torso organs and upon the assumption that high rate loading may generate tissue failure at lower strain.

9.5.1 Collection of data

All data collection refers to the *in vivo* rat experiment detailed in Chapter 8. Seat parameters and kinematic data were obtained and calculated as previously described. Presence or absence of significant lung and liver injuries were the dependent variables.

9.5.2 Assigning of censor status

Censor status was defined on the basis of the injury outcomes. Given that the there was no real-time method to determine the exact injury parameter value at which an injury occurred, there was no exact data and data was considered either right censored (when injury did not occur), or left censored (when it had occurred during the test). Separate censoring for each test was done for each of the two injury types such that a particular test could be considered a right censored lung test and left censored liver test or vice versa.

9.5.3 Checking and separating of injury mechanisms

In all cases, the pattern of loading was observed to be high rate vertical acceleration with torso compression. No separation for different injury mechanism was carried out.

9.5.4 Choice of distribution, estimation of parameters, and identification of overly influential observations

As described above, the choice of distribution is unlikely to significantly alter the injury curve. The Weibull distribution was used based upon its appropriateness for injury risk curves (Petitjean and Trosseille, 2011). All distribution fitting was performed using NCSS 12 Statistical Software (2018) (NCSS, LLC. Kaysville, Utah, USA). The fit of these distribution for each potential metric was visually assessed using Q-Q plots (Appendix A). Good fits for each plot were observed.

9.5.5 Checking the validity of the predictions against existing results

Injury risk curves based on laboratory results should, where possible, be compared to real world results such as accident observations. Given the novelty of these metrics and difficulty in assessing UBB torso injuries, such a comparison is not currently available for human experiments and is certainly not available for rat UBB. The description of this relationship and use of the injury metrics may be used for injury predictions in future models. Retrospective application of the curves to previously observed tests (such as measuring torso deformation of human cadaveric tests from video footage) could be performed in the future.

9.5.6 Calculation of 95% confidence intervals

The injury risk curve represents the best estimate of the probability of risk. Depending upon samples size, censoring status, and distribution of the test data relative to the curve, confidence intervals to the curve may vary. Confidence intervals may be improved by increasing the number of tests, including exact data, and increasing the number of data points in the region of interest. Confidence intervals are calculated using the same methodology as the curve with the normal approximation of error (Petitjean *et al.*, 2015). The intervals may be calculated in the vertical direction (confidence in probability of injury for a stimulus) or horizontal (confidence in injury metric for a given injury probability). Both ways are appropriate depending upon the application (McMurry and Poplin, 2017). Although the ISO approach does not mandate one direction, it seems that the horizontal intervals are more frequently quoted.(Yoganandan *et al.*, 2016). The max likelihood injury risk and 95% confidence intervals for the five injury metrics compared to lung and liver injuries are shown in Figure 9.10 to Figure 9.19 . Shape and scale coefficients for each curve are included at Appendix B.

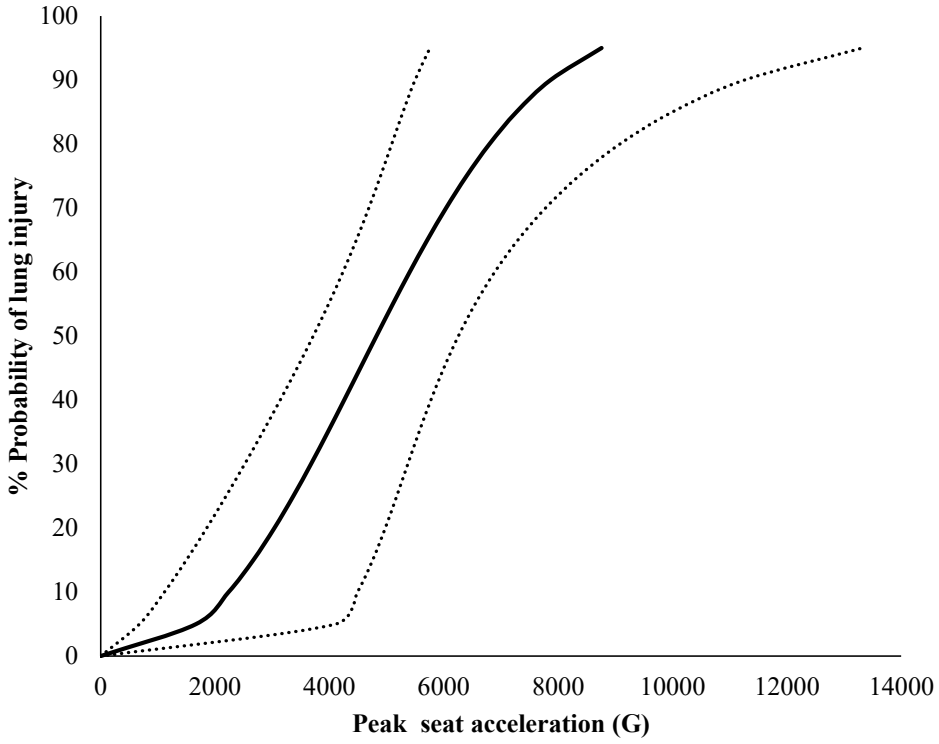

Figure 9.10 Injury risk curve for UBB loading in rats showing risk of lung injury based upon peak seat acceleration, In each case, the solid line shows the maximum likely risk of injury while the dotted lines show the 5% and 95% horizontal confidence intervals.

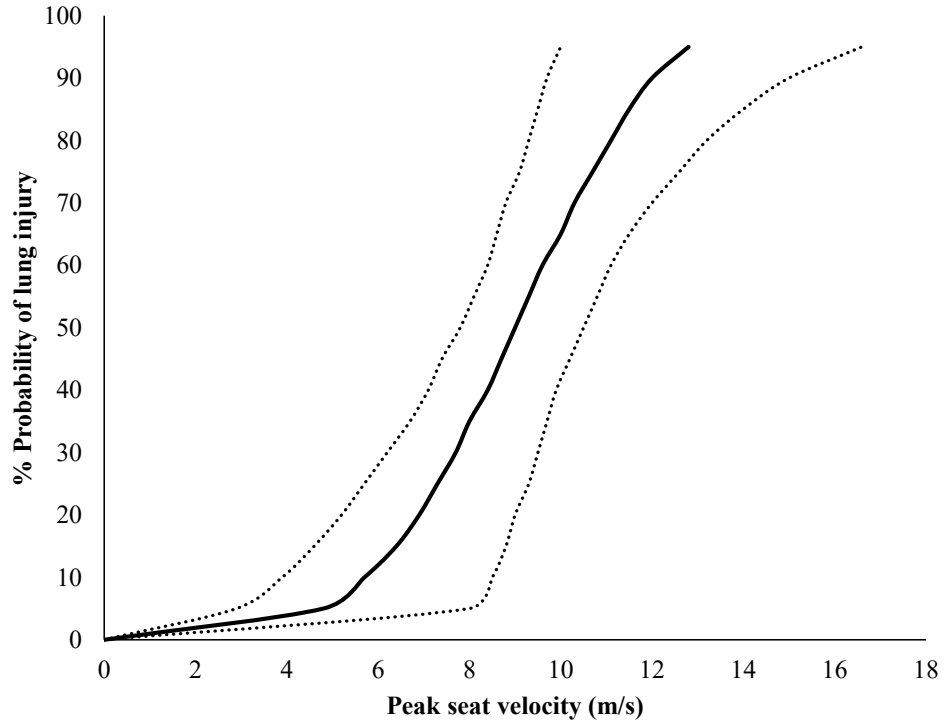

Figure 9.11: Injury risk curve for UBB loading in rats showing risk of lung injury based upon peak seat velocity. The solid line shows the maximum likely risk of injury while the dotted lines show the 5% and 95% horizontal confidence intervals.

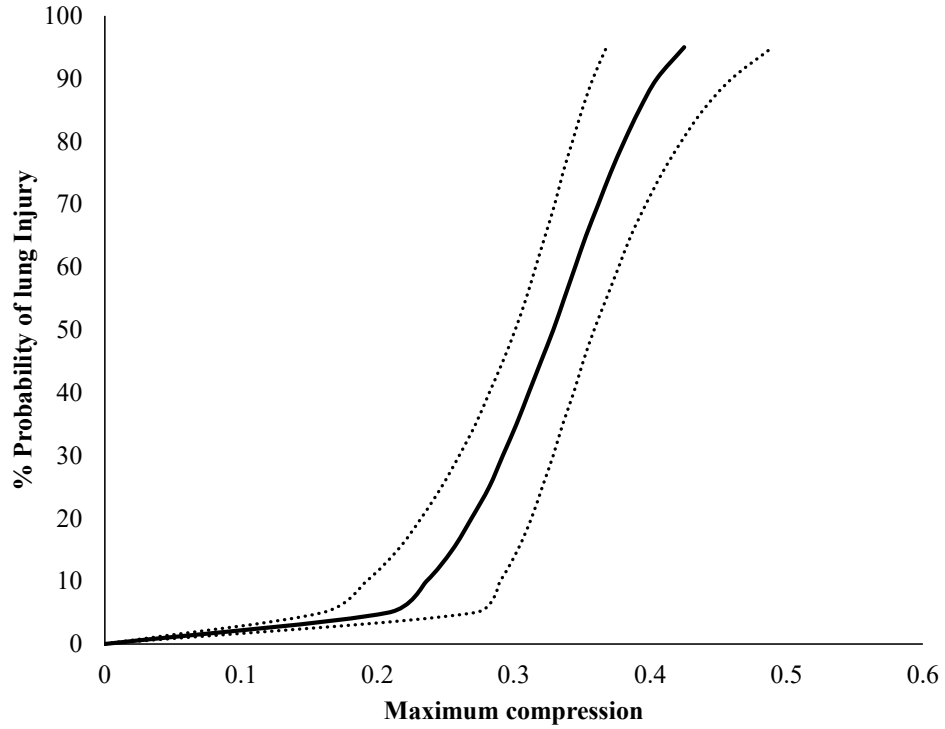

Figure 9.12: Injury risk curve for UBB loading in rats showing risk of lung injury based upon maximum axial torso compression. The solid line shows the maximum likely risk of injury while the dotted lines show the 5% and 95% horizontal confidence intervals.

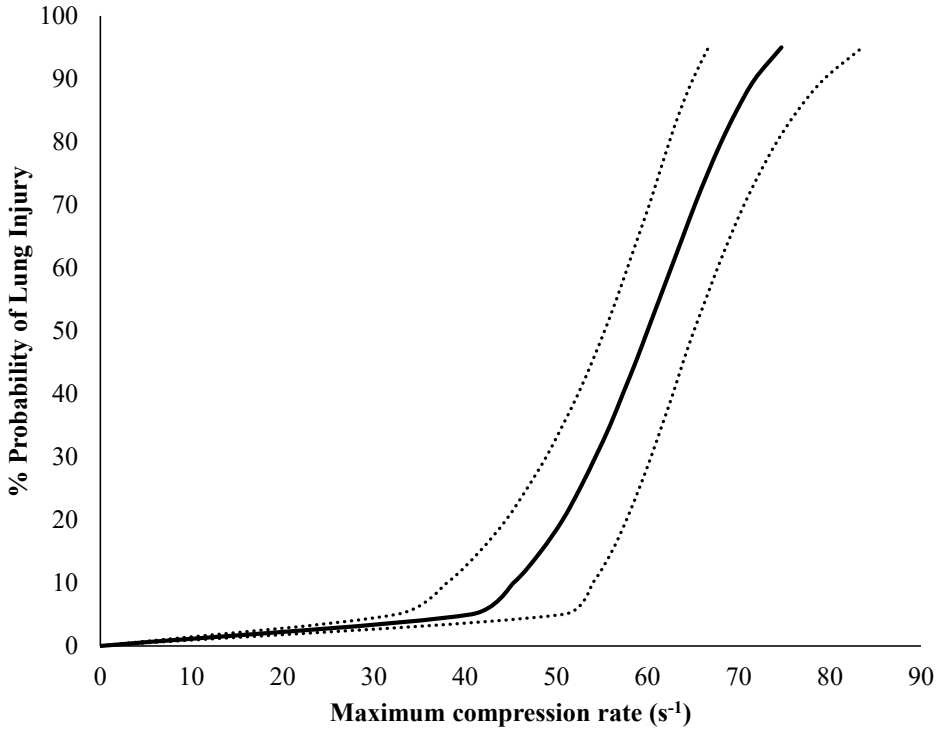

Figure 9.13: Injury risk curve for UBB loading in rats showing risk of lung injury based upon maximum axial torso compression rate. The solid line shows the maximum likely risk of injury while the dotted lines show the 5% and 95% horizontal confidence intervals.

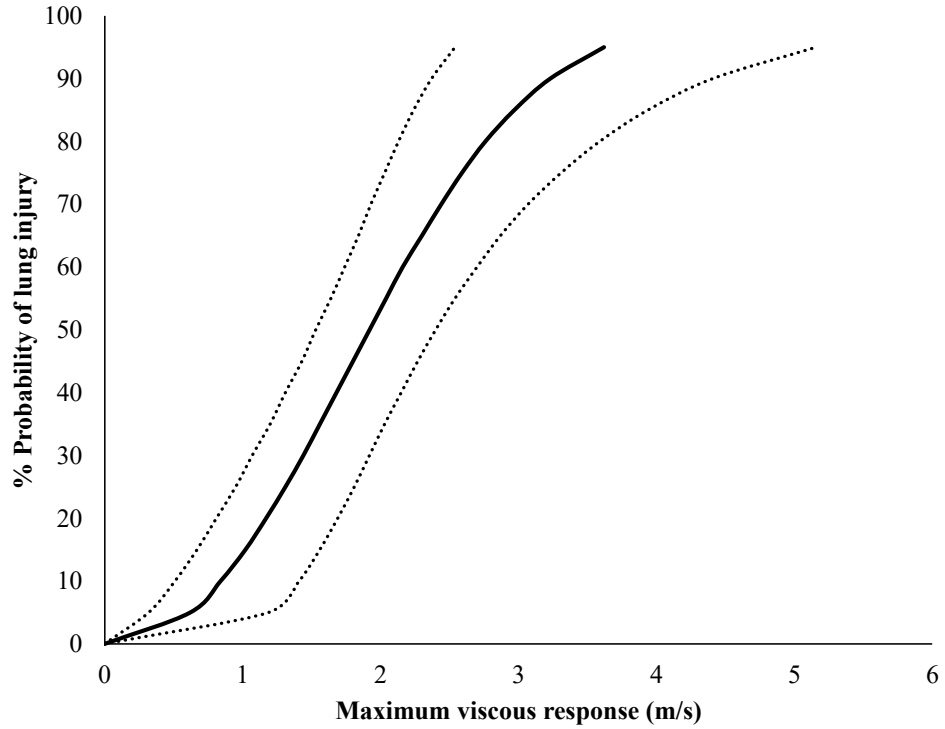

Figure 9.14: Injury risk curve for UBB loading in rats showing risk of lung injury based upon maximum axial viscous response. The solid line shows the maximum likely risk of injury while the dotted lines show the 5% and 95% horizontal confidence intervals.

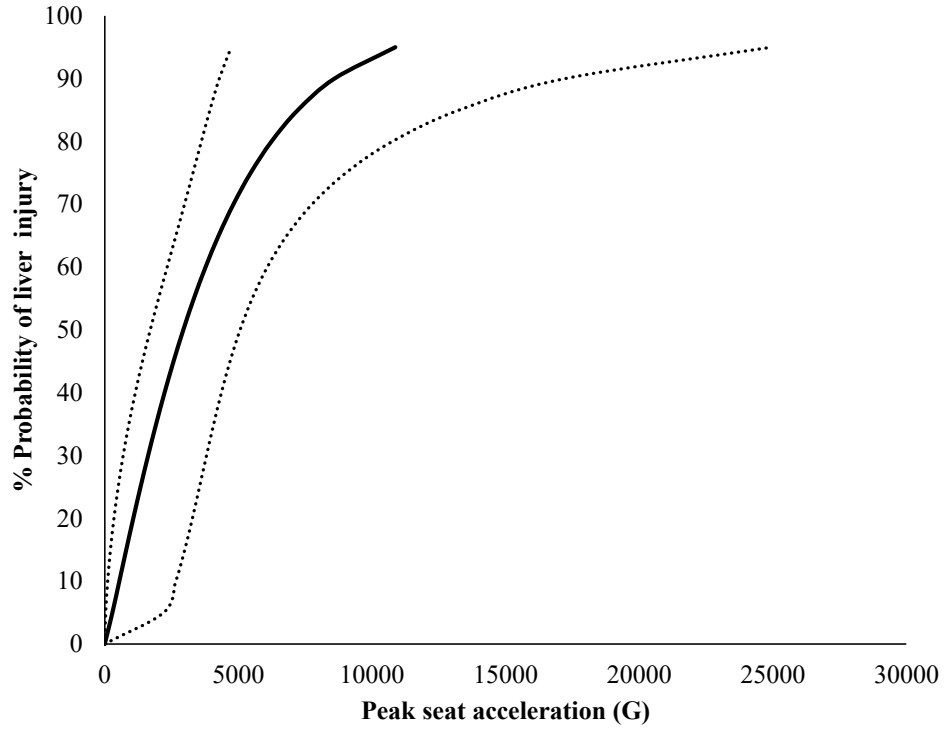

Figure 9.15: Injury risk curve for UBB loading in rats showing risk of liver injury based upon peak seat acceleration. The solid line shows the maximum likely risk of injury while the dotted lines show the 5% and 95% horizontal confidence intervals.

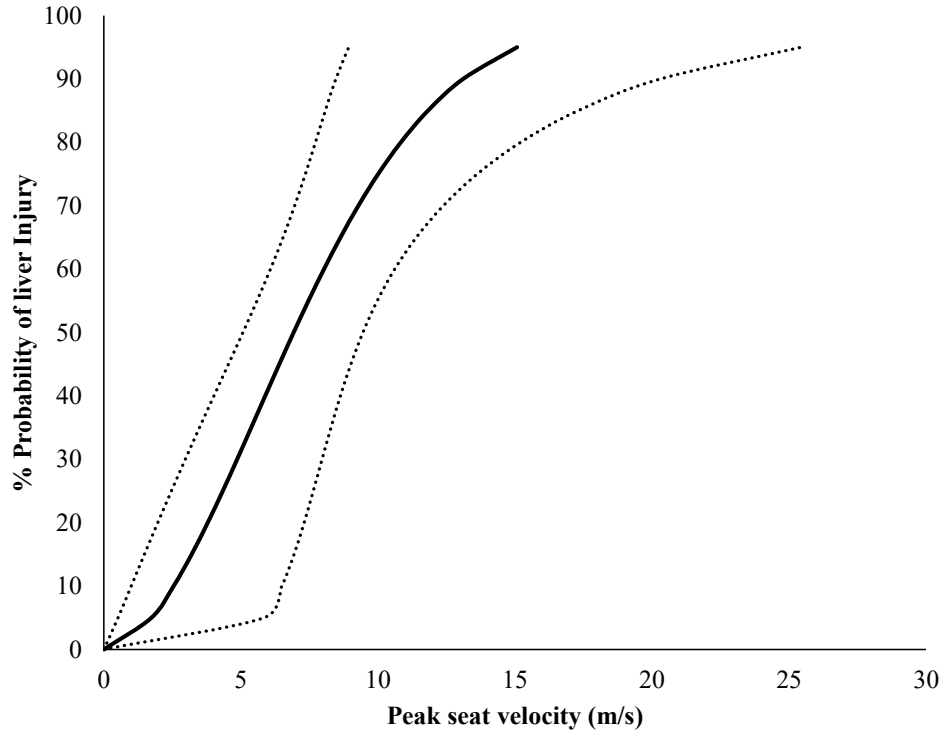

Figure 9.16: Injury risk curve for UBB loading in rats showing risk of liver injury based upon peak seat velocity. The solid line shows the maximum likely risk of injury while the dotted lines show the 5% and 95% horizontal confidence intervals.

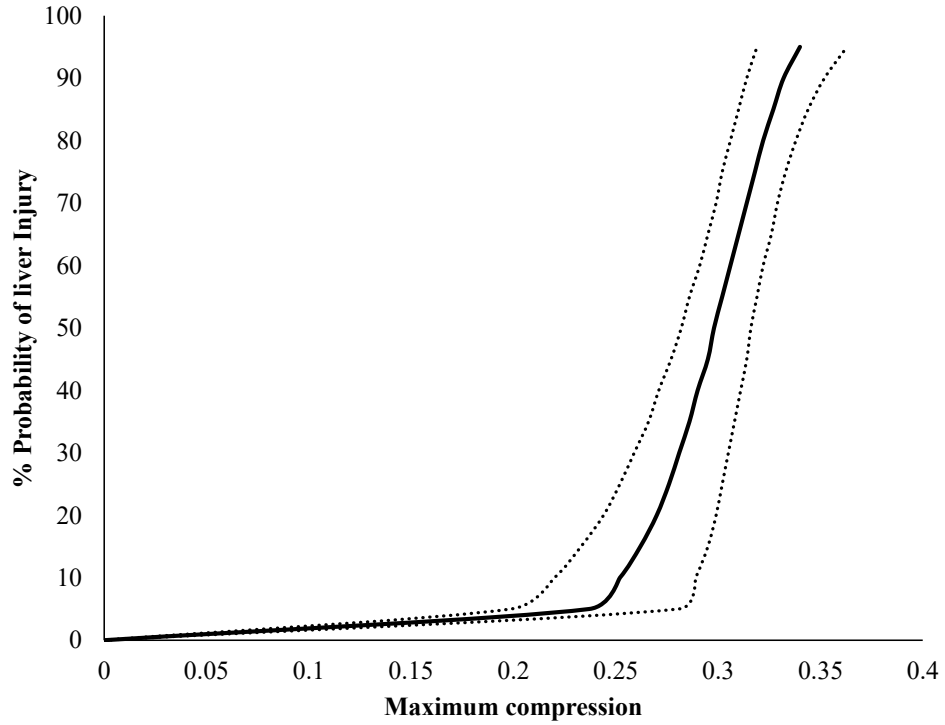

Figure 9.17: Injury risk curve for UBB loading in rats showing risk of liver injury based upon maximum axial torso compression. The solid line shows the maximum likely risk of injury while the dotted lines show the 5% and 95% horizontal confidence intervals.

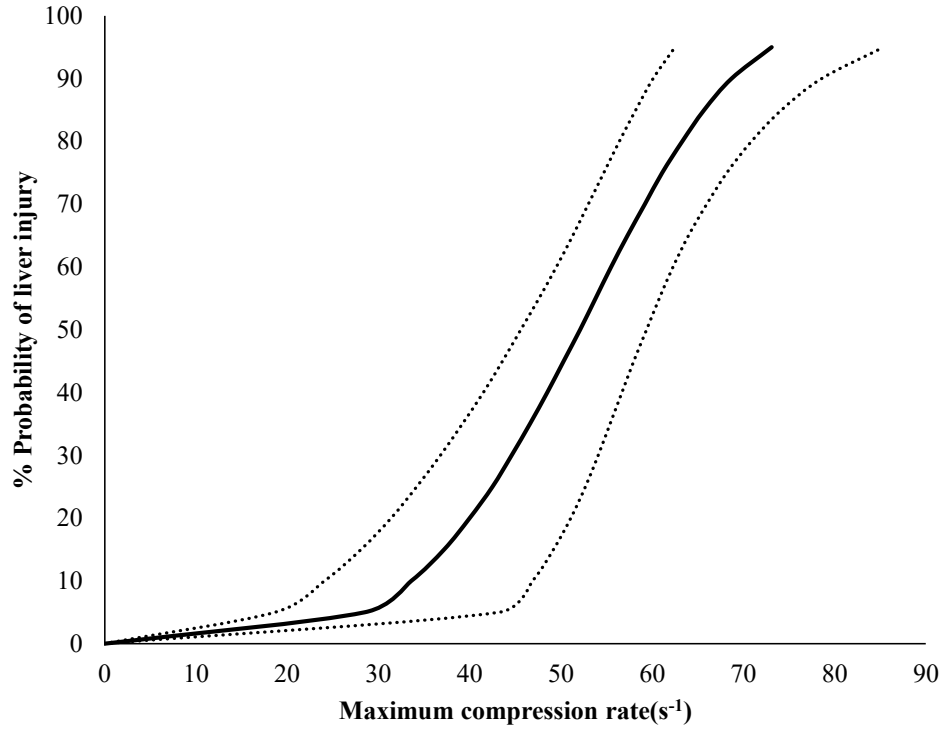

Figure 9.18: Injury risk curve for UBB loading in rats showing risk of liver injury based upon maximum axial torso compression rate. The solid line shows the maximum likely risk of injury while the dotted lines show the 5% and 95% horizontal confidence intervals.

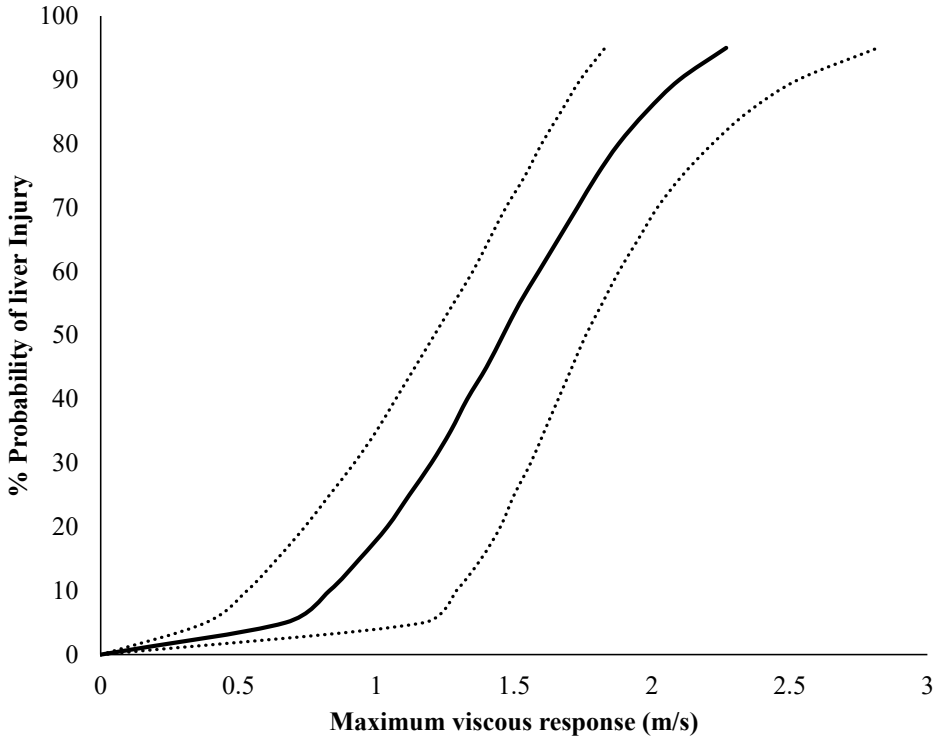

Figure 9.19: Injury risk curve for UBB loading in rats showing risk of liver injury based upon maximum axial viscous response. The solid line shows the maximum likely risk of injury while the dotted lines show the 5% and 95% horizontal confidence intervals.

9.5.7 Assessing the quality index of the injury risk curves

In addition to providing confidence in the data levels, the confidence intervals may be used to provide a quality index of the injury curve for a given metric (Petitjean *et al.*, 2015). A normalised confidence interval size (NCIS) may be generated by dividing the difference between the upper (95%) and lower (5%) confidence intervals by the size of the best estimate probability at that level. The NCIS provides a simple index of the validity of that injury curve at each level of risk, or of the need to increase sample sizes for future experiments.

Petitjean *et al* have suggested the following categories for NCIS (Table 9.1):

Quality Index	Normalised Confidence Interval Size
Good	0 to 0.5
Fair	0.5 to 1
Marginal	1 to1.5
Unacceptable	Over 1.5

Table 9.1: Categories of quality index based on the NCIS. Adapted with permission from Petitjean *et al* (2015)

For each curve, the NCIS may be compared at a variety of levels. NCIS indices for lung and liver injuries as described by the curves above are shown in Figure 9.20 and Figure 9.21.

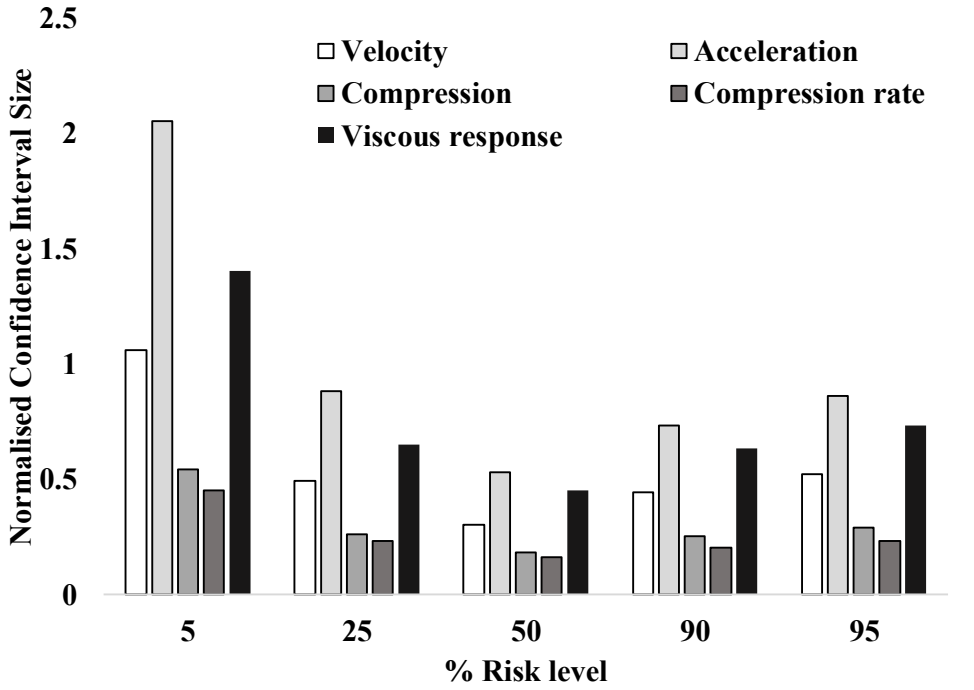

Risk level	Peak acceleration	Peak velocity	Maximum compression	Maximum compression rate	Maximum viscous response
0.05	2.05	1.06	0.54	0.45	1.4
0.25	0.88	0.49	0.26	0.23	0.65
0.5	0.53	0.3	0.18	0.16	0.45
0.9	0.73	0.44	0.25	0.20	0.63
0.95	0.86	0.52	0.29	0.23	0.73

Figure 9.20: NCIS indices for lung injury curves for UBB loading at varying levels of risk.

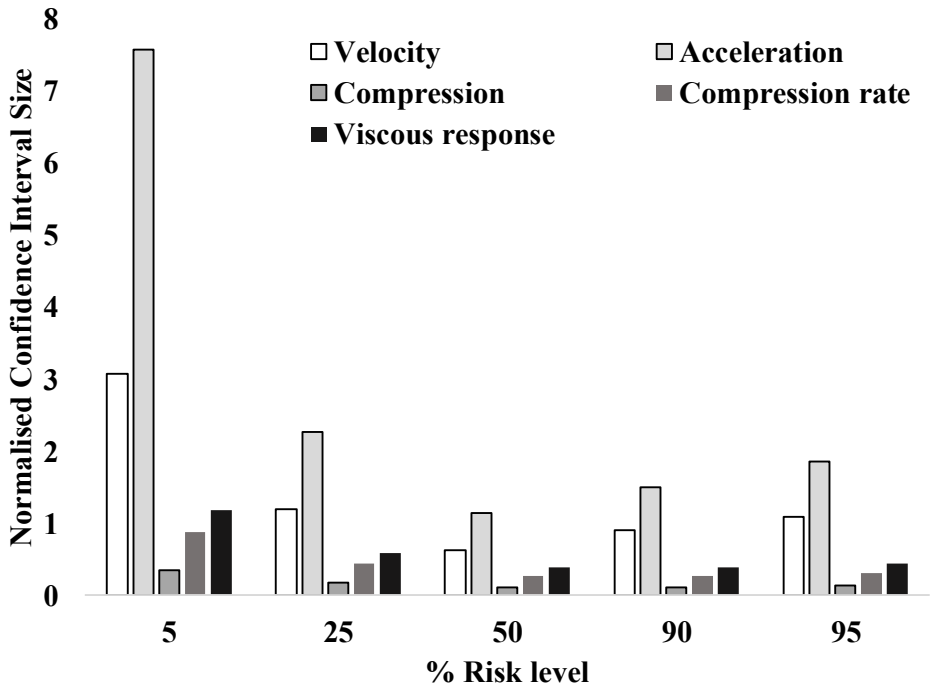

Risk level	Peak acceleration	Peak velocity	Maximum compression	Maximum compression rate	Maximum viscous response
0.05	7.58	3.07	0.34	0.87	1.18
0.25	2.27	1.19	0.18	0.44	0.59
0.5	1.14	0.63	0.11	0.27	0.38
0.9	1.5	0.90	0.11	0.27	0.38
0.95	1.86	1.09	0.13	0.31	0.44

Figure 9.21: NCIS indices for liver injury curves for UBB loading at varying levels of risk.

9.5.8 Recommendation of curves for region

There is considerable variation in the shape of each curve. All curves perform better at the intermediate risk levels with larger NCIS at both extremes of probability. The inferior ability of acceleration to accurately predict both modes of injury is apparent from the large NCIS. As with the mechanical models and sensitivity curves discussed earlier in this chapter, acceleration alone is seemingly a poor descriptor of the input "dose". The velocity change of the seat is a better predictor with good quality index for prediction of lung injury across the mid-range of injury risk. For both liver and lung injury, risk is best estimated using the mechanical response of the torso. Maximum compression rate is the best fitting and therefore recommended criterion for lung injury while maximum axial compression is the recommended criterion of liver injury although the small difference in NCIS for the metrics shows them to be very similar in predictive ability. The effectiveness of these criteria fits with the proposed injury mechanism and suggests that the effect of rate is most pronounced upon the lungs, whilst the degree of deformation (and therefore a greater initial response) has a greater influence on liver injuries. The actual difference between the two metrics in predicting injury for both injury types is small and suggests that the addition of the rate dependence to the metric is not essential when all experiments are performed at high rates. For both injury modes, the viscous response performs reasonably but it may be that combining compression velocity and degree somewhat dilutes the effect of the predominant factor in each case.

9.6 Discussion

Any injury biomechanics experiments require some degree of normalisation, or scaling to allow translation to a real life scenario. The aims of the experiments detailed in Chapters 7 and 8 was to create a novel small animal model of UBB and demonstrate the relationship of UBB loading to torso injury.

Scaling considerations for the experiment must be considered for two aspects. Firstly, the input load must be appropriate. Scaling of these parameters is somewhat hampered by the scarcity of data about real world UBB seat loading. As described in the rig specifications of Chapter 7, real world seat acceleration is likely to be at the range of

500G with velocity change of 9-10m/s. The scaling laws applied using a simple mechanical analogue and based upon the cubic root of the animal mass suggest that the experimental acceleration should be around 6-7 times greater. The rig achieves this and causes a similar overall change in velocity. Assuming a similar velocity asymptote (as described above), it is assumed that this loading is analogous to human scale input. The higher acceleration and shorter duration are thus beneath the critical duration of the presumed rat natural resonance and therefore considered to be analogous based upon historical scaling laws.

Scaling of the animal response must also be considered. As described in Chapter 8, despite some differences in anatomy, the two species have more in common with similar location, tethering, and relative masses of the torso viscera. With consideration of both bodies as mechanical analogues and assuming similar geometry, the response of the two bodies to this input may approximated by simple allometric scaling of the input parameters. In discussing the response of mammals to impact loading, Kornhauser dismissed the coupling of the input to the response of the animal, and assumed that this coupling would be factored into the injury response of the animal (Kornhauser and Lawton, 1961). Although this would remain true for a single set of experiments (assuming absolute consistency of the restraints and housing conditions), use of the acceleration metric has little translation between experiments or real world situation as the coupling of this acceleration to the organ or system of interest is fundamental to the injury mechanism. The importance of this coupling may be illustrated by comparison of the novel experiments to those of Fiskum and Fourney (2014). Their model simulated UBB in a rat model but animals were positioned prone within an enclosed housing with acceleration directed directly against the torso in an anterior-posterior direction. The group found almost ubiquitous lung injury at 2800G (for similar duration). In comparison, the presented data predicts around a 20% risk of lung injury at this same level. This difference is very likely to reflect the difference in coupling and restraint of the animal to the accelerating vehicle between the two tests.

This coupling is better factored into the injury risk by measuring the physical response of the animal. By devising and using new metrics based on torso compression, the animal response could be measured following modification of restraint or housing. The need to measure the physical response to the stimulus is well known to those who

develop surrogates or ATDs for injury biomechanics work. Current ATDs are designed to be biofidelic such they mimic human physical characteristics in regard to size, shape, mass, stiffness, and energy transfer. The purpose of ATDs for testing of vehicles and restraint systems means that a response which closely resembles that of the human is desirable. Although the rat may geometrically resemble the human and scaling laws may be used to demonstrate the relationship of UBB relevant input parameters to analogous injuries, the rat is not closely biofidelic to the human. It would be foolish to directly transfer the numerical values of injury risk from an animal to human.

The development of rat injury curves for these experiments demonstrates the use of novel injury metrics based upon the coupled torso response. A pragmatic approach has been taken for the development of these injury curves, with metrics and statistical distribution chosen which seem applicable to the relevant biomechanics. Both lung and liver injuries are considerably more reliably predicted by measures of torso compression than by either acceleration or velocity change. NCIS indices for lung injury are best when using axial torso compression rate. This metric is not only a good predictor, but makes good biomechanical sense with the hypothesised injury mechanism of UBB lung haemorrhage related to high rate displacement of the abdominal visceral "piston" against the lungs with relatively little displacement of the lungs.

Rat liver injury is best predicted by maximal compression, although compression rate is also a reliable indicator. Again, this makes reasonable biomechanical sense with relative movement of the liver to its tethering points thought to be the predominant mode of injury. As with cineradiographic experiments by Weis and Mohr, the liver likely follows this compression which is therefore a maker of its displacement (Weis and Mohr, 1967). Although there was no rate dependence calculated as part of the metric itself, it is assumed that the same levels of compression are unlikely to cause the same injury at low rates.

The axial viscous response is good to fair predictor of both injury types across the mid to upper risk of injury. It is better than velocity or acceleration for liver injury and better than acceleration for lung injury but with higher NCIS than the other kinematic markers. Given that all compression in these experiments occurred at a high rate, both compression rate and the viscous response may be better measures across a greater range

of loading rates. At lower loading rates, a fall in compression rate and viscous response would be expected and not reflected by the maximum compression. Further experiments could be used firstly to generally reduce the confidence intervals (which are inherently influenced by sample size), and secondly to decouple the effects of compression and rate. Of course, this decoupling is somewhat unnecessary for the UBB environment (which will always be high rate), in which case axial compression may be a useful translatable metric.

An advantage of using kinematic data is that it can be normalised, which may make translatability to the human easier. The measure of compression is normalised by the torso length and is unitless. Using a similar metric for the human would rely on scaling not by size but by the difference in stiffness of the human torso. Maximum compression of the rat torso was found to be around 40% of the initial length in the rat. Compression of the human torso of around 20% during cadaveric testing has been reported although this has not been studied further and no maximum torso response has been investigated (Danelson *et al.*, 2015). There is certainly a likely difference in the overall stiffness of the torso in this direction. A biofidelic ATD would need to allow this torso compression (by means of both soft tissue compression and combined flexion/extension/compression of the spine).

How then do we use this data to prevent injury in humans? Future work should focus first upon characterising the analogous deformation of the human torso to UBB. Relating the tissue level response (and injury) to the degree of deformation remains difficult but could be approximated using computational models with assumptions of tissue properties.

9.7 Conclusion

These experiments and subsequent analyses have demonstrated the occurrence of relevant injuries in a geometrically similar mammalian model and demonstrated the relationship of this injury occurrence to simple physical parameters and kinematic torso metrics. Input parameters are analogous to those known in UBB assuming a similar velocity threshold and scaled acceleration threshold for mammals. Development of

injury curves using these metrics shows that high rate compression of the torso in an axial direction is a superior predictor of both chest and lung injuries than using simple input parameters. These metrics have not previously been described in this scenario. Although axial torso compression has been demonstrated in cadaveric UBB experiments, no similar metric has been used to evaluate the risk of soft tissue torso injury in the UBB environment. Direct extrapolation of the predicted values to human injuries would be over simplistic but these results demonstrate a robust relationship between severe injuries and easily measured biomechanical metrics. The relationship is explained by the previously hypothesised mechanisms of injury in the torso.

The translatability of this work is apparent. Novel metrics of severe torso injury should be applied in order to develop protective and mitigative strategies for UBB. The next chapter will summarise the thesis and discuss the future work which could be used to improve survivability in this environment.

CHAPTER 10

SUMMARY, DISCUSSION AND FUTURE WORK

10.1 Scope of the chapter

This chapter summarises and discusses the research presented in the previous chapters and makes recommendations for future work.

10.2 Summary

Explosions are the most common cause of battlefield death and injury. Patterns of injury and causes of death differ between mounted and dismounted blast incidents. Death from mounted blast injury is commonly due to torso injury. The overall aim of this thesis has been to describe the pattern of torso injury following underbody blast and to define the relationship between UBB loading parameters and injury.

Previous research into UBB has focused upon skeletal injury with particular regard to the lower limb. Although this research has led to development and recommendation for protective strategies such as combat boots and mats, it has not addressed the issue of survival.

After an introduction, the first part of this thesis defined the clinical problem and placed this within the context of modern warfare. The second chapter provided an overview of the current understanding of blast and underbody blast physics and demonstrated the increasing ubiquity of explosives as a wartime weapon. Chapter 3 discussed contemporary descriptions of survivability. An important point to reiterate from this chapter is that future improvements to survival may best be gained from prevention and mitigation of injury rather than novel therapies. Chapter 4 further examined survivability but with focus upon a particular environment. The aim of this chapter was to identify those injuries which have an influence upon survival. UBB research has not previously focussed upon torso injuries and the chapter developed the "mitigation gap", the injury burden which must be mitigated or prevented in order to influence survival.

With relevant injuries in mind, mitigation relies upon understanding the relationship between loading and injury. Chapter 5 placed torso injuries within the context of other known UBB injury patterns in order to determine the loading pathway. The association of torso injuries (for which non-compressible torso haemorrhage was used as a marker) with spinal and pelvic injuries, and not with foot and ankle injuries implies that high rate loading through the seat is the pathway of interest.

The second part of the thesis concerned the biomechanics of UBB mediated torso injury. Chapter 6 reviewed the relevant anatomy of the torso with particular emphasis upon the vulnerabilities of organs to injury and a demonstration of relevant injury mechanisms. Given the lack of research into UBB torso injury, existing and historical models of impact and accelerative loading to the torso from a variety of environments was discussed. The chapter discussed current criteria for torso injury and those criteria currently recommended for the UBB environment were not developed or validated for this type of loading. Chapter 6 concluded with proposed mechanism of torso injury from high rate seat mediated vertical acceleration and defined the need for a novel in vivo model of UBB with which to explore the relationship of this loading to relevant injury.

Chapter 7 covered the specification, design and construction of a novel rig for UBB loading of a small animal (RivUL). Characterisation of the rig showed it to be able to meet and exceed those specifications. Chapter 8 detailed the use of the RivUL system upon a rat model. This chapter discussed the rationale for, and limitations of, using a small animal for the experiments. The relevant anatomy was compared to that of the human. The chapter details the experimental procedure for the tests from the point of anaesthesia through to necropsy or imaging. The chapter described the loading associated with each test and therefore with the resultant injuries.

Chapter 9 discussed the translatability of this model to human injury. Firstly, the chapter reviewed scaling laws and the use of mechanical analogues to scale up relevant loading. Secondly, the chapter detailed the process required to develop injury risk curves and applied this process to the new experimental results. In doing so, the work showed that: torso injury is predictable within the UBB environment, basic input parameters (velocity and acceleration) are poor predictors of injury and, novel measures of rate related axial torso compression (which conform to the proposed mechanisms of injury) are better predictors of injury and should be used to predict severe injuries due to high rate vertical loading.

10.3 Discussion and future work

Battlefield injury is undoubtedly complicated and varied. Improving survival across the entire spectrum of conflict trauma requires a range of interventions used at different points along the timeline. Separation of injury by weapon type (explosive), environment (mounted), and body region (torso) allows precise examination of the causes and outcomes of injury. This detailed understanding allows the formation of a biomechanical hypothesis and description of the link to loading and therefore of what must be required to prevent injury.

UBB research is not a new topic. Academic, clinical, and military interest in the particular environment has been reinvigorated by operations in Afghanistan and Iraq but anti-vehicle mines and IEDs are not a modern invention. Attempts to increase mine-protection of vehicles occurred during the Second World War in which sandbags were

added to the vehicle floors to prevent secondary fragmentation and reduce vertical acceleration (Ramasamy *et al.*, 2009). This review by Ramasamy provides a good overview of the history of vehicle development. Several factors are identified to be important for mitigation and protection. Basic principles for mitigating the effect of UBB are of a V-shaped hull to vent the detonation products and reduce impulse transfer, increased spacing of wheels with increasing ground clearance, and removing the crew compartment from zone of injury. Analysis of casualty data from the Rhodesian War (1972-1980) examined the effects of these basic vehicle modifications on injury rates (Arul Ramasamy, Hill, *et al.*, 2011). Cumulative effects of these modifications were demonstrated with reduction of both injury and mortality rates.

These protective modification are incorporated into modern US and UK military patrol vehicles (Ramasamy *et al.*, 2009). The main design feature in mine protection remains to increase the distance between the occupants and the blast centre. However, incorporating this increased standoff will necessitate a larger vehicle, which introduces further complications. From a personnel threat perspective, a taller vehicle platform increases its visibility, thereby making the vehicle more vulnerable to ambush. Similarly, in large population centres, the streets are often too narrow for these vehicles to enter. Therefore, vehicle designers must be aware of these conflicting needs, as there will always be a requirement for the Armed Forces to develop a suite of vehicles that can cater for both the environment and the current threat state. Certainly, fatal incidents are less likely in very large, heavily armoured platforms but these vehicles are simply unfeasible for many operations in which high mobility (both on the ground, and by air lift) and low visibility are essential for success. Such operational focus may be even more important in a future operating environment where complex urban spaces are expected to be the most challenging (MOD, 2015) .

Despite the incorporation of modifications into current military vehicles, deaths and injuries in such vehicles have certainly not been eliminated. It could be argued that increased protection can be overcome by more sophisticated weapon technology (or simply larger explosive charges). Within the UBB community, the term “overmatch” is common although frustratingly poorly defined. The term relates to those explosive events in which the protective vehicle was not adequately protective. What is apparent from both review of clinical data and from discussion with previously deployed

surgeons is that "overmatch" of a vehicle does not necessarily equate to "overmatch" of the occupant. The Centre for Blast Injury studies was partly instigated by a particular incident in Afghanistan in which one occupant died on scene, one occupant required an amputation for severe lower limb injury, and the final occupant sustained no serious injuries. To describe such an incident (as many are) as overmatch is far too simplistic.

The approach by much of the underbody blast research community has been to focus upon the prevention of injury. Test standards used for military vehicles design are based upon a "pass or fail" methodology (NATO Research and Technology Organisation, 2012). For each injury region, an injury criterion value has been selected with in most cases represents a 10% chance of AIS2+ injury to that region. Vehicles tested pass or fail for each injury region depending upon the injury criteria value measured (and as sustained by an ATD).

This system has shortcomings with regards to both torso injuries and as a general approach. The shortcomings of torso injury criteria for UBB have already been discussed in Chapter 6; these criteria are not based on vertical loading. It would be reasonable to expect many vehicles to pass the torso injury criteria (and thus suggest minimal risk of torso injury) simply because no frontal or lateral loading to the torso has occurred.

As a general approach, this pass/fail system with a minimal injury threshold is inflexible. For the operational reasons discussed above, there must be a range of protective level for vehicles. Judging vehicles by the same pass or fail methodology does not incorporate the operational requirements. It is for those smaller, more mobile, less visible, and by necessity less protected vehicles that assessing the risk of severe life threatening injuries is more important. In using a smaller platform, both the operational command and the service personnel involved are accepting a larger risk of injury. For these vehicles, preventing all AIS2+ injuries using the same technology and same threats is not feasible. Such vehicles are therefore likely to fail a test using the same methodology. Although these vehicles may not be designated as mine-resistant, they may face the same threats, and if required for the operation, will deploy regardless.

Quantification of risk in these circumstances is even more important but using methodology and criteria which estimate the probability of a minor to moderate lower limb injury is clearly inappropriate. Given that these operations must accept the likelihood of injury following an explosive incident, test methodology should instead focus upon improving survivability by comparing the likely loading to measures of severe injury such as those developed by this thesis. This comparison would yield the mitigation gap. Protective strategies should then be focussed upon mitigating the injury burden such that it is survivable.

The following sections will discuss the potential for further work. Suggested work will include not only improvements of the model and criteria developed but suggest a more holistic strategy for improving survivability in the underbody blast environment.

10.3.1 Clinical data analysis

The first part of this thesis interrogated the clinical data to determine the pattern and importance of torso injuries to UBB. As discussed in the relevant chapters, there are limitations to this data collection and analysis. The design of these analyses was retrospective. This is in keeping with most of the military clinical research published from conflicts in Iraq and Afghanistan (including Ramasamy *et al.*, 2009; Morrison *et al.*, 2013; Beranger *et al.*, 2017). There are inherent weaknesses based on retrospective analysis of a database, even one such as JTTR which is prospectively maintained. There are, of course, significant logistical and ethical difficulties in conducting prospective research in an operational environment. Research conducted during conflict operations tends to be conducted once some relative stability has been achieved. Despite the conflict in Afghanistan starting in 2001, the first randomised controlled trial was not started until 2010 (Fries *et al.*, 2014). A much greater number of observational studies were carried out during the intervening period (Naumann *et al.*, 2017). This lag period includes the requirement to formulate a research question, design appropriate trials, seek ethics approval, and implement potentially complicated trial logistics. It has been proposed that rather than waiting for a conflict to begin , and only then to consider research, many relevant research questions are predictable to the extent that a panel or protocols could be designed and approved prior to a hypothetical future deployment (Naumann *et al.*, 2017).

The application of such a process to UBB may be more complicated. Observational studies (including those within this thesis) are important for defining injury patterns and generating hypotheses. Future work however, should focus upon the clinical effect of protective strategies. A randomised control trial under such circumstances may not be possible when the outcome is mortality; there must exist equipoise between different protections in order to overcome an obvious ethical problem. It must be acknowledged however, that the value of a protective strategy or device as described by laboratory data, may not equate to a real world scenario. Formal prospective study of vehicles, protection, incidents, and injuries is unfeasible (and not conducted in analogous automotive or aeronautic industries) but improvement requires rapid classification or quantification of the effect of any changes upon the functionality and role of the vehicle. Once again, an interdisciplinary approach is required in which both the clinical importance, and biomechanical significance of all injuries is directly fed back to those responsible for the design of vehicles and to military commanders so that modification (of both vehicles or military strategy) can be conducted without significant lag time.

Such research in the UBB community is also limited by security considerations. The injury analysis in this thesis has purposefully not separated out injury patterns by vehicle type to avoid revealing any specific vulnerabilities. Although not publishable, a panel of UK military and academic scientists, engineers, and clinicians has previously been convened to examine a subset of UBB incidents. This panel was put together in order to support the design of an international surrogate and found to be useful for the understanding of injury mechanisms and future mitigation strategies. This interdisciplinary panel should perhaps be pre-approved and ready to convene to consider all future blast incidents.

What is apparent from the discussion of scoring systems in Chapter 3 is the limitation of current systems for quantifying severe injury. These systems have been created and validated to stratify injury burden to allow comparison for research and governance although they are also widely (and frequently inappropriately) used for triage and prediction. No system has been used which adequately describes injury burden beyond the point of death. Such a system would have little use for predicting success of a medical treatment but is essential for design of mitigation. The Anatomic Profile (Copes *et al.*, 1990), given that it includes all injuries and does not "max out", may have

potential to better stratify death. Further work could use this (or a novel score) to determine the extent of fatal injury and quantify the "distance" from the uninjured state for fatalities in the UBB (or any other) environment. The potential of such a system to illustrate the "mitigation gap" could be used across all forms of military and civilian trauma.

Future trauma registries should may be improved by the inclusion of real time date. This thesis has described the relationship between physical parameters and injury. The use of real time physiological monitoring should be coupled to real time measurement of physical parameters using wearable technology. It is entirely possible that future trauma registries will be able to detail the precise physical insult sustained by patients with simultaneous measurement of physiological and anatomical injury. Such data would be invaluable for improving both pre-injury protection and post-injury management.

10.3.2 *In vivo* models

The rat model discussed in this thesis has been used to demonstrate the occurrence of relevant injuries to UBB load and the prediction of these injuries from both existing and novel parameters. The limitations of the model with regard to scaling and anatomical differences have been discussed but future work with the same model could be used to further demonstrate some of the relationships which underpin the injuries of interest.

The restraint system in the model is fundamental to the generation of injuries. The restraint was made to closely resemble an analogous human restraint in its appearance and function. The material properties of the restraint itself were not tested but could have important implications. Following the UBB loading, the torso is accelerated upwards by the seat. It is the restraint acting upon the shoulder of the animal which couples the torso to this acceleration. The compliance of the restraint will dictate the limit to which the body is compressed. It is apparent that the compression of the torso depends upon the overall stiffness of the torso being less than that of the restraint such that the torso compresses rather than the restraint deforming upwards and allowing a greater upwards stroke of the torso. Similarly, the compression of the body would alter in response to the inertial effects between the different component masses. The effect of helmets and armour in altering these component masses could be evaluated. As with the

experiments described, precise values would be of little use but understanding the changes in mechanical response of the torso (and therefore in injury pattern) caused by changes in restraint compliance and in component masses would inform the design of such devices for humans. In this case, any changes would have to be balanced against upwards displacement of the occupant and an increased risk of head injury. The relative contribution of these two effects – restraint and inertia – would have to be assessed at all threat levels.

The novel injury criteria developed in this thesis are based upon axial torso compression. Maximum compression alone outperformed the viscous response which included the rate of compression. The reason of this is likely to be that all tests were performed at high rate and thus 'topped out' the rate effects. Future work could aim to decouple these factors to examine low rate compression. These tests could also be used to calculate the torso-stiffness of the animal, which could be compared to a similar metric in the human to aid in scaling. The converse of low rate compression would be examining high rate loading with minimal deformation, although the real life analogue of this is unlikely given that the human torso certainly is deformable, even at high rates if loading.

The existing model could be improved with additional data acquisition. Difficulties in obtaining quantifiable CT imaging have been discussed in Chapter 8. Use of other agents (such as heavy metal nano-particles injected prior to loading) could increase the quantative yield of these tests. This may allow a more continuous measure of injury and therefore a subtler prediction of risk. Additional data could also include the measurement of pressure from inside body cavities, solid organs, or blood vessels. Intrahepatic pressure has been shown to be a good predictor of injury during component tests (Sparks *et al.*, 2007b). Performing pressure measurement at both component level and during in vivo testing could be used for real time injury prediction and allow the addition of exact data for the formation of injury curves. The use of fine fibre-optic intra-arterial pressure probes (Chavko *et al.*, 2007) was contemplated for these tests but the poor ability of these sensors to withstand the likely deformation combined with their cost made the test unfeasible.

Further real time data could be obtained using cineradiography. A high-speed camera, operating in conjunction with an x-ray source and image intensifier may be used to

create high speed x-ray videos and observe the movement of the internal organs. Although similar systems have been used historically (Boorstin *et al.*, 1966; Hanson, 1966; Weis and Mohr, 1967), such systems were comparatively slow (around 40fps). Modern systems would be able to provide footage at over 10000 fps. If combined with contrast agents, such a system could provide real time images of injury and allow for precise calculations of strain. Discussions with several manufacturers of these systems showed them to be prohibitively expensive for this work alone but the collaboration with other projects could make this economically feasible in the future.

A further consideration of in vivo modelling is to change the animal type. Porcine models are well described for biomechanical and blast experiments. Performing a similar set of experiments in a pig model would aid scaling, given a closer size of the animal to a human. The disadvantages to using a pig model are also apparent. The cost of the animals themselves is greater and so using a similar number of pigs as rats (and therefore gaining the same statistical power) would be a great deal more expensive. The logistics of using a pig model are also difficult; housing and maintenance of pigs requires additional specified infrastructure. The rig required to simulate the requisite loading would be large (effectively human sized), requiring a large amount of both physical space and money. Although similar in size to human organs, there are still differences in the anatomy of the pig to the human. Note is made of a recent porcine model of axial loading (Guan *et al.*, 2018). This study used a lateral sled model of loading, with 21 pigs in a supine position. The position affects relative organ displacement. Only 2 impacts speeds (8m/s and 11m/s) were used. The measured biomechanical metrics for the study were peak acceleration of the pelvis and intra-abdominal pressure (measured within the peritoneum). No attempt was made to construct injury curves although the authors did comment on the degree of spinal flexion. Abdominal deformation in animals was noted but not measured. The use of a large animal model by other researchers is encouraging but further in vivo work should focus upon sufficiently powered studies to determine injury risk; and translating this to humans.

Now established, the rodent model used in this work could be used for other projects. TBI remains a major concern following UBB. The previously discussed model by Fiskum and Fourney (2014) aimed to reproduce the TBI caused by the hyper-

acceleration alone. Their projected future work includes developing a model of secondary head impact (to simulate the roof of the vehicle) although such work has not yet been published and is complicated given the totally enclosed nature of their model. Although unintended, the rotation of the rodent head in this current model and subsequent impact with the seat may be a suitable analogue of this secondary impact. The rotational aspect is likely to differ to humans (given the increased anterior-posterior length and therefore moment of the rat head) but this could be overcome by adapting the seat to add a "roof".

Similarly, the rodent model could be used to examine the biological changes caused by the loading and compared to blast. The physiological effect upon the respiratory and cardiovascular systems along with the immune response of the lungs to blast has been well characterised (Guy *et al.*, 1998; Kirkman and Watts, 2011; Barnett-Vanes *et al.*, 2016; Eftaxiopoulou *et al.*, 2016). Although the lung injuries described by the experiments in this thesis are similar to blast lung and may account for blast lung previously described following mounted blast, the physiological and cellular responses to underbody loading have not been described.

The experimental phase of this thesis has focused upon injuries to the lungs and liver. The importance of these injuries to clinical outcome is well described but future work should examine injury to other organs. A recovery model of *in vivo* blast could be used to examine for both macroscopic anatomical disruption of other organs but of also microscopic disruption and physiological dysfunction.

As discussed in Chapter 6, a great deal of existing UBB research has been conducted using human cadavers. As stated, the great advantage of these models is biofidelity. However, limitations of human cadavers for study of soft tissue and internal organs persist, with pressurisation of vessels, ventilation of lungs, and inverse positioning required to approximate the living torso for impact experiments (Hardy *et al.*, 2008; Howes *et al.*, 2013), and the influence of death on biological tissue properties is simply not known for many tissues. The degree to which such experimental modifications are feasible when subjecting the model to UBB loading is uncertain but clearly difficult. Currently, no model in the literature has resolved the problem. Cadaveric work could be simplified, however, by examining the deformation of the torso in the absence of these

measures. Axial compression of the torso has been observed in PMHS UBB testing but only measured in a simple test (Danelson *et al.*, 2015). Although not documented, it is assumed that this compression (as in the rat model) is predominantly comprised of abdominal deformation, given that the rib cage and chest wall is likely to make the thoracic component of the torso stiffer than the abdomen. Further tests in an un-perfused cadaver may definitively link in vivo injury to loading but would be useful to demonstrate the mechanical response of the torso to different loads. As with animal experiments, changes in this response with different seats and restraints can be measured.

The range of cadaveric testing must be great enough to cross over into the "overmatch" region. It is expected that loading severe enough to cause torso injuries are likely to result in skeletal injuries. Experiments should be aimed at investigating the response of the torso and the performance of protective devices and strategies in this severe loading region.

10.3.3 Anthropomorphic test devices

The same "overmatch" testing should be a consideration for the use of test dummies. As discussed above with regard to NATO standardised test methodology, testing should not be limited to those low level tests likely to cause a 10% risk of an AIS2+ injury. Using dummies at severe loading is contentious. A major focus of contemporary ATD development is upon human biofidelity. It is this focus which led to the recognition that those dummies used for automotive collision testing are not appropriate for UBB. The Warrior Injury Assessment Mannequin (WIAMan) is currently under development to fulfil this gap (Pietsch *et al.*, 2016). Certainly, improving the biofidelity of ATDs to blast is important but increasingly the complexity of the device incurs an increased cost. As with PMHS, dummies should be used not only at sub-injurious and up to the NATO pass/fail mark, but to assess severe and lethal injury risk for lesser protection. The cost of a new generation WIAMan may preclude their use for such tests. Consideration should perhaps be given towards use of "overmatch dummies" which sacrifice some degree of complexity and are either robust enough to undergo very severe loading, or disposable. A simple ATD for torso injury may require only comparable axial stiffness to that measured from a cadaver with injury risk based upon degree of compression. A

frangible surrogate, in which components actually fail at realistic levels may be useful to demonstrate secondary injuries (those which do not occur without the deformation resulting from failure of another tissue).

10.3.4 Computational models

This thesis has not focussed at all upon the computational modelling of torso injury biomechanics. The role of such models is clear: by creating an accurate in silico model, numerous simulated tests can be performed without the need for physical experimentation. A key point in the design of any computational model is that it be validated against experimental data and shown to be accurate. Finite element models of the human thorax for impact and primary blast loading already exist (Shah *et al.*, 2001; Richens *et al.*, 2004; Gayzik *et al.*, 2007; Goumtcha *et al.*, 2016). The validation of these models is difficult with aortic models being validated against the prediction of chest wall deflection rather than against aortic stresses.

Computational models for UBB have focussed upon skeletal injuries with finite element models and include models of the foot, lower limb, and pelvis (Weaver and Stitzel, 2015; Grigoriadis *et al.*, 2016; Newell *et al.*, 2016). These models may be formulated based upon material properties derived from component level testing and validated against PMHS testing.

A finite element approach to UBB torso injuries is complicated by firstly, the mostly unknown material properties and boundary conditions imposed by the organs when in situ, and secondly by inability to validate the work (given that no PMHS models of UBB torso injury exist). Although the material properties of most internal organs have been well characterised at a component level (as described in Chapter 6), the properties of their attachments and relationships to surrounding organs is just as important. Predicting the response of the lungs to seat loading using a computational model would require detailed mechanical properties of every tissue between the point of loading and the lungs.

A more feasible approach may be to consider a simpler analogue of the body and use a computational rigid body dynamics model. This form of model can approximate organs

and structures as simple masses with spring and damper models representing tissue attachments. For the torso, these values could be adjusted until the gross mechanical response of the torso resembles that seen in a cadaveric model. The complexity of the model could vary. The spine could be represented as a single spring (as for the Dynamic Response Index) or separated into spinal regions or individual vertebrae. Although not as representative as a detailed finite element model (and unable to predict the stresses and deformations within organs), a rigid body model could be used to predict relative movement which is the likely mechanism of torso injuries. This would, therefore, be a computational model of a surrogate of the injury mechanism; the validation of such models that are two steps removed from reality is difficult and there is no robust and accepted framework for this type of validation.

10.3.5 Other injuries

Although this thesis has focussed upon torso injuries, the relevance of other injuries to UBB survivability should not be overlooked. In contrast to dismounted blast, lower limb and pelvic injuries have been shown not to be an important contributor to UBB mortality (Singleton *et al.*, 2013; Webster *et al.*, 2015). Head injuries are important. Along with selected injuries to the torso, outcomes from severe head injuries are unlikely to be improved by novel medical therapies. Prevention and mitigation of these head injuries are once again key. Fatal head injuries from UBB are likely due to severe parenchymal brain injury (Stewart *et al.*, 2018). As discussed in Chapter 4, these injuries are associated with other axial injuries following UBB and likely the result of seat loading. In contrast to torso injuries, however, the injury mechanism is likely to be impact of head with the roof above. The importance of this somewhat separate injury mechanism is that any preventative or mitigative strategy must take both into account. Allowing greater upwards stroke of the torso may reduce the inertial displacement of chest and abdominal organs but increase the risk of head impact. Likewise, increasing the mass and size of a helmet may convey greater protection to the head but increase the mass acting upon the torso and exaggerate this inertial response.

10.3.6 Interdisciplinary research

This thesis concerned one particular injury pattern caused by one particular loading environment. Improved survival from this form of incident would result from mitigating these injuries using strategies which reduce the axial deformation of the torso. The approach used in this thesis has been to first examine the clinical data and determine the relevance of injuries to the environment and to the outcome. Understanding the injury in relation to the loading has required the proposal of a mechanism, replication of the analogous loading, and quantification of the mechanical affect and injury outcome. Although most of these steps are inherent to injury biomechanics research, understanding the relevance of the injuries is key. The separation of clinicians, scientists, and engineers is not conducive to carrying out relevant and impactful research. Clinicians should be in a position to inform scientific and engineering endeavours from the outset to ensure that research programmes are clinically and operationally relevant.

This same approach should be applied to all aspects of combat casualty survival. The spectrum of injury should be considered to span from pre-injury to rehabilitation with the effect of intervention in one domain considered upon all other domains (Figure 10.1).

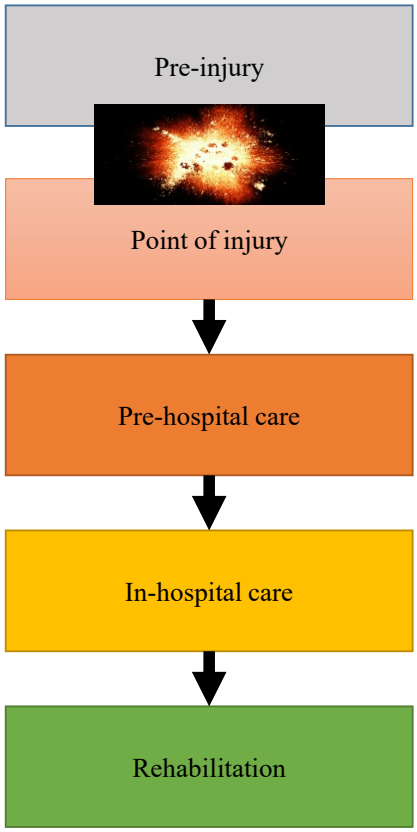

Figure 10.1: The domains of care including a pre-injury phase.

Improved survival of UBB (or any other kinetic event) may be affected not only by medical interventions but also by mitigating and protective measures which may affect the patient cohort received into medical treatment facilities. Mitigation which prevents unsurvivable injuries may result in proportionally higher numbers of severely injured personnel. Although the cohort of "unexpected survivors" is testament to the ability of the medical services to care for such patients, this ability may be stretched and require change if the previously KIA cohort survive to hospital.

This paradigm is not reflected by the current roles or echelons of care. Role 1 care may be at the point of injury but more consideration should be given to the effect of "Role 0" upon the later phases. Modifications at the pre-injury phase may affect each stage afterwards and as such should be an important consideration for clinicians and engineers alike. Further improvement across all aspects of trauma care can best be achieved with an interdisciplinary approach.

10.4 Conclusions

This thesis has explored the effect of torso injury upon survivability following underbody blast. This work has contributed to the knowledge of this complicated environment by demonstrating the extent and effect of particular injuries. The work includes development of a novel in vivo rig which reproduces an analogous loading to UBB and creates analogous injuries in a rodent model. Importantly, the data derived from these experiments show that axial torso deformation is an important (and previously undescribed) injury criterion for these injuries.

Further work should aim to:

- better stratify injury beyond point of death in order to define the mitigation gap which may be a target for protective technologies;
- characterise the degree of torso compression in a PMHS or computational model of severe UBB loading;
- determine the effect of external factors (including PPE, restraint, and posture) upon this deformation;
- validate the relationship between deformation an tissue injury using perfused PMHS or large animal model; and
- utilise axial torso compression as an injury metric for torso injury in either novel ATD or computational models of UBB loading.

REFERENCES

Aboudara, M., Mahoney, P. F., Hicks, B. and Cuadrado, D. (2014) 'Primary blast lung injury at a NATO Role 3 hospital', *Journal of the Royal Army Medical Corps*, 160(2), pp. 161–166.

Aharonson-Daniel, L., Giveon, A., Stein, M. and Peleg, K. (2006) 'Different AIS Triplets: Different Mortality Predictions in Identical ISS and NISS', *The Journal of Trauma: Injury, Infection, and Critical Care*, 61(3), pp. 711–717.

Alanezi, K., Milencoff, G. S., Baillie, F. G., Lamy, A. and Urschel, J. D. (2002) 'Outcome of major cardiac injuries at a Canadian trauma center', *BMC Surgery*, 2(1), pp. 4.

Ambrose, G., Barrett, L. O., Angus, G. L. ., Absi, T. and Shaftan, G. W. (2000) 'Main pulmonary artery laceration after blunt trauma: accurate preoperative diagnosis', *The Annals of Thoracic Surgery*. 70(3), pp. 955–957.

Andersen, R. C., Fleming, M., Forsberg, J. A., Gordon, W. T., Nanos, G. P., Charlton, M. T. and Ficke, J. R. (2012) 'Dismounted Complex Blast Injury.', *Journal of Surgical Orthopaedic Advances*, 21(1), pp. 2–7.

Andres, J., Scott, J. and Giannoudis, P. V. (2016) 'Resuscitative endovascular balloon occlusion of the aorta (REBOA): What have we learned?', *Injury*, 47(12), pp. 2603–2605.

Atanasijevic, T. C., Popovic, V. M. and Nikolic, S. D. (2009) 'Characteristics of chest injury in falls from heights.', *Legal Medicine (Tokyo, Japan)*, 11 Suppl 1, pp. S315-7.

Avidan, V., Hersch, M., Armon, Y., Spira, R., Aharoni, D., Reissman, P. and Schecter, W. P. (2005) 'Blast lung injury: clinical manifestations, treatment, and outcome.', *American Journal of Surgery*, 190(6), pp. 927–931.

Ayubi, E. and Safiri, S. (2017) 'Mediastinal injury is the strongest predictor of mortality in mounted blast amongst UK deployed forces: Methodological issues', *Injury*, pp. 7348.

Bailey, A. M., Christopher, J. J., Brozoski, F. and Salzar, R. S. (2015b) 'Post Mortem Human Surrogate Injury Response of the Pelvis and Lower Extremities to Simulated Underbody Blast', *Annals of Biomedical Engineering*. 43(8), pp. 1907–1917.

Bailey, A. M., Christopher, J. J., Salzar, R. S. and Brozoski, F. (2015) 'Comparison of Hybrid-III and postmortem human surrogate response to simulated underbody blast loading.', *Journal of Biomechanical Engineering*, 137(5), p. 051009.

Baker, S. P., O'Neill, B., Haddon, W. and Long, W. B. (1974) 'The injury severity score: a method for describing patients with multiple injuries and evaluating emergency care', *Journal of Trauma*, 14(3), pp. 187–196.

Barnett-Vanes, A., Sharrock, A., Eftaxiopoulou, T., Arora, H., Macdonald, W., Bull, A. M. and Rankin, S. M. (2016) 'CD43Lo classical monocytes participate in the cellular immune response to isolated primary blast lung injury', *Journal of Trauma and Acute Care Surgery*, 81(3), pp. 500–511.

Bass, C. R., Rafaels, K. a. and Salzar, R. S. (2008) 'Pulmonary Injury Risk Assessment for Short-Duration Blasts', *The Journal of Trauma: Injury, Infection, and Critical Care*, 65(3), pp. 604–615.

Benesch, B. (2011) 'Utilizing vehicle response data from underbody blast tests', in *Ballistics 2011: 26th International Symposium.*

Benzinger, T. (1950) *Physiological effects of blast in air and water in German Aviation Medicine World War II*.

Beranger, F., Lesquen, H. De, Aoun, O., Roqueplo, C., Meyrat, L., Natale, C. and Avaro, J. P. (2017) 'Management of war-related vascular wounds in French role 3 hospital during the Afghan campaign', *Injury*, pp. 1906–1910.

Berwick, D. M., Downey, A. S. and Cornett, E. A. (2016) 'A National Trauma Care System to Achieve Zero Preventable Deaths After Injury', *JAMA*. American Medical Association, 316(9), pp. 927.

Bhattacharjee, Y. (2008) 'NEUROSCIENCE: Shell Shock Revisited: Solving the Puzzle of Blast Trauma', *Science*, 319(5862), pp. 406–408.

Bonner, T. J., Newell, N., Karunaratne, A., Pullen, A. D., Amis, A. A., M.J. Bull, A.

and Masouros, S. D. (2015) 'Strain-rate sensitivity of the lateral collateral ligament of the knee', *Journal of the Mechanical Behavior of Biomedical Materials*. 41, pp. 261–270.

Boorstin, J., Hayes, J. and Goldman, D. (1966) 'Injury mechanism of internal organs of animals exposed to sinusoidal vibration.', *Aerospace Medicine*, 37, pp. 22–28.

Boris, K., Forat, S., Itamar, A., Oded, O., Kobi, P., Adi, G., Igor, J., Ricardo, A. and Ricardo, A. (2014) 'Increasing number of fractured ribs is not predictive of the severity of splenic injury following blunt trauma: An analysis of a National Trauma Registry database', *Injury*, 45(5), pp. 855–858.

Bouamra, O., Wrotchford, A., Hollis, S., Vail, A., Woodford, M. and Lecky, F. (2006) 'A New Approach to Outcome Prediction in Trauma: A Comparison With the TRISS Model', *The Journal of Trauma: Injury, Infection, and Critical Care*, 61(3), pp. 701–710.

Bowen, I. G., Fletcher, E. R. and Richmond, D. R. (1968) *Estimate of man's tolerance to the direct effects of air blast*, *DASA 2113*.

Bowen, I., Holladay, A., Fletcher, E., Richmond, D. and White, C. (1965) *A Fluid-Mechanical Model of the Thoraco- Abdominal System with Applications to Blast Biology*. DTIC

Boyd, C. R., Tolson, M. A. and Copes, W. S. (1987) 'Evaluating trauma care: the TRISS method. Trauma Score and the Injury Severity Score.', *The Journal of Trauma*, 27(4), pp. 370–8.

Brathwaite, C. and Rodriguez, A.(1990) 'Blunt traumatic cardiac rupture. A 5-year experience.', *Annals of Surgert.*, 212, pp. 701–704.

Breeze, J. and Carr, D. J. (2016) 'Energised Fragments, Bullets and Fragment Simulating Projectiles', in *Blast Injury Science and Engineering*. Springer International Publishing, pp. 219–226.

Brun-Cassan, F., Pincemaille, Y. and MacK, P. (1987) 'Contribution and evaluation of criteria proposed for thorax-abdomen protection in lateral impact', in *SAE Technical Paper 876040*.

Brunon, A., Bruyère-Garnier, K. and Coret, M. (2010) 'Mechanical characterization of liver capsule through uniaxial quasi-static tensile tests until failure.', *Journal of Biomechanics*. 43(11), pp. 2221–7.

Burkhart, H. M., Gomez, G. A., Jacobson, L. E., Pless, J. E. and Broadie, T. A. (2001) 'Fatal blunt aortic injuries: a review of 242 autopsy cases.', *The Journal of Trauma*, 50(1), pp. 113–5.

Cannon, J. W., Hofmann, L. J., Glasgow, S. C., Potter, B. K., Rodriguez, C. J., Cancio, L. C., Rasmussen, T. E., Fries, C. A., Davis, M. R., Jezior, J. R., Mullins, R. J. and Elster, E. A. (2016) 'Dismounted Complex Blast Injuries: A Comprehensive Review of the Modern Combat Experience', *Journal of the American College of Surgeons*. 223(4), pp. 652–664.e8.

Carney, N., Totten, A. M., O'Reilly, C., Ullman, J. S., Hawryluk, G. W. J., Bell, M. J., Bratton, S. L., Chesnut, R., Harris, O. A., Kissoon, N., Rubiano, A. M., Shutter, L., Tasker, R. C., Vavilala, M. S., Wilberger, J., Wright, D. W. and Ghajar, J. (2016) 'Guidelines for the Management of Severe Traumatic Brain Injury, Fourth Edition', *Neurosurgery*. 80(1), pp. 6-15.

Casali, M. B., Bruno, C. M., Battistini, A., Alessio, B., Blandino, A., Alberto, B., Cattaneo, C. and Cristina, C. (2014) 'The injury pattern in fatal suicidal falls from a height: an examination of 307 cases.', *Forensic Science International*, 244, pp. 57–62.

Cavanaugh, J. M., Nyquist, G. W., Goldberg, S. J. and King, A. I. (1986) 'Lower Abdominal Tolerance and Response', in *SAE Transactions*. pp. 611–633.

Cavanaugh, J. M. and Yoganandan, N. (2015) *Thorax injury biomechanics*, *Accidental Injury: Biomechanics and Prevention*. New York, NY: Springer New York.

Cavanaugh, J. M., Zhu, Y., Huang, Y. and King, A. I. (1993) 'Injury and Response of

the Thorax in Side Impact Cadaveric Tests', *Stapp Car Crash Conference*, 37, pp. 199–221.

Champion, H. R., Holcomb, J. B. and Young, L. A. (2009) 'Injuries From Explosions: Physics, Biophysics, Pathology, and Required Research Focus', *The Journal of Trauma: Injury, Infection, and Critical Care*, 66(5), pp. 1468–1477.

Champion, H. R., Sacco, W. J., Copes, W. S., Gann, D. S., Gennarelli, T. A. and Flanagan, M. E. (1989) 'A revision of the Trauma Score.', *The Journal of Trauma*, 29(5), pp. 623–9.

Chandler, R. (1988) 'Human Injury Criteria Relative to Civil Aircraft Seat and Restraint Systems', in *Society of Automotive Engineers*.

Chang, J. C., Holloway, B. C., Zamisch, M., Hepburn, M. J. and Ling, G. S. F. (2015) 'ResQFoam for the Treatment of Non-Compressible Hemorrhage on the Front Line', *Military Medicine*. 180(9), pp. 932–933.

Chavko, M., Koller, W. A., Prusaczyk, W. K. and McCarron, R. M. (2007) 'Measurement of blast wave by a miniature fiber optic pressure transducer in the rat brain', *Journal of Neuroscience Methods*., 159(2), pp. 277–281.

Chawda, M. ., Hildebrand, F., Pape, H. . and Giannoudis, P. . (2004) 'Predicting outcome after multiple trauma: which scoring system?', *Injury*, 35(4), pp. 347–358.

Christensen, A. M. and Smith, V. A. (2013) 'Rib Butterfly Fractures as a Possible Indicator of Blast Trauma', *Journal of Forensic Sciences*. Wiley/Blackwell (10.1111), 58, pp. S15–S19.

Clark, D. P. and Badea, C. T. (2014) 'Micro-CT of rodents: State-of-the-art and future perspectives', *Physica Medica*, 30(6), pp. 619–634.

Coermann, R. R., Ziegenruecker, G. H., Wittwer, A. L. and von Gierke, H. E. (1960) 'The passive dynamic mechanical properties of the human thorax-abdomen system and of the whole body system.', *Aerospace Medicine*, 31, pp. 443–55.

Cohn, S. M. and DuBose, J. J. (2010) 'Pulmonary Contusion: An Update on Recent Advances in Clinical Management', *World Journal of Surgery*. 34(8), pp. 1959–1970.

Collins, M. P. and Robinson, G. C. (1989) 'Traumatic rupture of the pulmonary artery', *The Annals of Thoracic Surgery*. 47(4), pp. 612–613.

Cook, J. and Mosely, J. (1960) 'Visceral displacement in black bears subjected to abrupt deceleration.', *Aerospace Medicine*.31 pp.1.

Cooper, C. F. and Taylor, P. A. (2015) 'Virtual Simulation of Blast, Behind-Armor Blunt Trauma, and Projectile Penetration Leading to Injury of Life-Critical Organs in the Human Torso', in *Volume 3: Biomedical and Biotechnology Engineering*. ASME,

Cooper, G. J., Pearce, B. P., Stainer, M. C. and Maynard, R. L. (1982) 'The biomechanical response of the thorax to nonpenetrating impact with particular reference to cardiac injuries.', *The Journal of Trauma*, 22(12), pp. 994–1008.

Cooper, G. J. and Taylor, D. E. (1989) 'Biophysics of impact injury to the chest and abdomen.', *Journal of the Royal Army Medical Corps*, 135(2), pp. 58–67.

Cooper, G. J., Townend, D. J., Cater, S. R. and Pearce, B. P. (1991) 'The role of stress waves in thoracic visceral injury from blast loading: modification of stress transmission by foams and high-density materials.', *Journal of Biomechanics*, 24(5), pp. 273–85.

Copes, W. S., Champion, H. R., Sacco, W. J., Lawnick, M. M., Gann, D. S., Gennarelli, T., Mackenzie, E. and Schwaitzberg, S. (1990) 'Progress in characterizing anatomic injury', *Journal of Trauma - Injury, Infection and Critical Care*, 30(10), pp. 1200–1207.

Copes, W. S., Lawnick, M., Champion, H. R. and Sacco, W. J. (1988) 'A comparison of Abbreviated Injury Scale 1980 and 1985 versions.', *The Journal of Trauma*, 28(1), pp. 78–86.

Courtney, A. C. and Courtney, M. W. (2009) 'A thoracic mechanism of mild traumatic brain injury due to blast pressure waves', *Medical Hypotheses*., 72(1), pp. 76–83.

Courtney, A. and Courtney, M. (2015) 'The Complexity of Biomechanics Causing Primary Blast-Induced Traumatic Brain Injury: A Review of Potential Mechanisms', *Frontiers in Neurology*. 6, p. 221.

Crandall, J. R., Bose, D., Forman, J., Untaroiu, C. D., Arregui-Dalmases, C., Shaw, C. G. and Kerrigan, J. R. (2011) 'Human surrogates for injury biomechanics research', *Clinical Anatomy*. 24(3), pp. 362–371.

Crass, J. R., Cohen, A. M., Motta, A. O., Tomashefski, J. F. and Wiesen, E. J. (1990) 'A proposed new mechanism of traumatic aortic rupture: the osseous pinch.', *Radiology*, 176(3), pp. 645–649.

Culver, R., Bender, M., Stelnaker, R. and Melvin, J. (1977) 'Feasibiltiy of investigating the Mechanisms of Aortic Trauma Using High-Speed Cineradiography'. *SEA Technical report*

Danelson, K. A., Kemper, A. R., Mason, M. J., Tegtmeyer, M., Swiatkowski, S. A., Bolte, J. H. and Hardy, W. N. (2015) 'Comparison of ATD to PMHS Response in the Under-Body Blast Environment.', *Stapp Car Crash Journal*, 59, pp. 445–520.

Davis, K. A., Fabian, T. C., Ragsdale, D. N., Trenthem, L. L. and Proctor, K. G. (2000) 'Endogenous adenosine and secondary injury after chest trauma.', *The Journal of Trauma*, 49(5), pp. 892–8.

Dehghan, N., de Mestral, C., McKee, M. D., Schemitsch, E. H. and Nathens, A. (2014) 'Flail chest injuries', *Journal of Trauma and Acute Care Surgery*, 76(2), pp. 462–468.

Demetriades, D. *et al.* (2008) 'Operative Repair or Endovascular Stent Graft in Blunt Traumatic Thoracic Aortic Injuries: Results of an American Association for the Surgery of Trauma Multicenter Study', *The Journal of Trauma: Injury, Infection, and Critical Care*, 64(3), pp. 561–571.

DuBose, J. J., Scalea, T. M., Brenner, M., Skiada, D., Inaba, K., Cannon, J., Moore, L., Holcomb, J., Turay, D., Arbabi, C. N., Kirkpatrick, A., Xiao, J., Skarupa, D., Poulin, N. and AAST AORTA Study Group (2016) 'The AAST prospective Aortic Occlusion for

Resuscitation in Trauma and Acute Care Surgery (AORTA) registry', *Journal of Trauma and Acute Care Surgery*, 81(3), pp. 409–419.

Eastridge, B.J., Mabry, R.L., Seguin, P., Cantrell, J., Tops, T., Uribe, P., Mallett, O., Zubko, T., Oetjen-Gerdes, L., Rasmussen, T.E. and Butler, F.K. (2012). Death on the battlefield (2001–2011): implications for the future of combat casualty care. *Journal of Trauma and Acute Care Surgery*, 73(6), pp.S431-S437.

Edwards, D. and Clasper, J. (2016) 'Blast Injury Mechanism', in *Blast Injury Science and Engineering: A Guide for Clinicians and Researchers*. Springer International pp. 89–103.

Edwards, D. S., Guthrie, H. C., Yousaf, S., Cranley, M., Rogers, B. A. and Clasper, J. C. (2016) 'Trauma-related amputations in war and at a civilian major trauma centre—comparison of care, outcome and the challenges ahead', *Injury*. 47(8), pp. 1806–1810.

Edwards, D. S., McMenemy, L., Stapley, S. A., Patel, H. D. L. and Clasper, J. C. (2016) '40 years of terrorist bombings - A meta-analysis of the casualty and injury profile.', *Injury*. 47(3), pp. 646–52.

Eftaxiopoulou, T., Barnett-Vanes, A., Arora, H., MacDonald, W., Nguyen, T. T. N., Itadani, M., Sharrock, A. E., Britzman, D., Proud, W. G., Bull, A. M. J. and Rankin, S. M. (2016) 'Prolonged but not short-duration blast waves elicit acute inflammation in a rodent model of primary blast limb trauma', *Injury*, 47(3), pp. 625–632.

Eiband, M. (1959) 'Human Tolerance to Rapidly Applied Accelerations: A Summary of the Literature', *NASA Memorandum 5-19-59E*, , pp. 1–57.

Eppinger, R., Marcus, J. and Morgan, R. (1984) Development of dummy and injury index for NHTSA's thoracic side impact protection research program, *SAE International*.

Fabian, T.C., Richardson, J.D., Croce, M.A., Smith, J.S., Rodman, G., Kearney, P.A., Flynn, W., Ney, A.L., Cone, J.B., Luchette, F.A. and Wisner, D.H., 1997. Prospective study of blunt aortic injury: multicenter trial of the American Association for the

Surgery of Trauma. *The Journal of Trauma and Acute Care Surgery*, 42(3), pp.374-383,

Fazekas, I. G., Kósa, F., Jobba, G. and Mészáros, E. (1971) 'Die Druckfestigkeit der menschlichen Leber mit besonderer Hinsicht auf die Verkehrsunfälle', *Zeitschrift für Rechtsmedizin*. Springer-Verlag, 68(4), pp. 207–224.

Ficke, J. R., Eastridge, B. J., Butler, F. K., Alvarez, J., Brown, T., Pasquina, P., Stoneman, P. and Caravalho, J. (2012) 'Dismounted complex blast injury report of the army dismounted complex blast injury task force', *Journal of Trauma and Acute Care Surgery*, 73(6), pp. S520–S534.

Fiskum, G. and Fourney, W. (2014) *Underbody Blast Models of TBI Caused by Hyper-Acceleration and Secondary Head Impact*. DTIC

Franklyn, M. and Lee, P. (2017) *Military Injury Biomechanics: The Cause and Prevention of Impact Injuries*.

Freedman, B. A., Serrano, J. A., Belmont, P. J., Jackson, K. L., Cameron, B., Neal, C. J., Wells, R., Yeoman, C. and Schoenfeld, A. J. (2014) 'The combat burst fracture study—results of a cohort analysis of the most prevalent combat specific mechanism of major thoracolumbar spinal injury', *Archives of Orthopaedic and Trauma Surgery*, 134(10), pp. 1353–1359.

Friedman, R., Epstein, Y. and Gefen, A. (2016) 'Traumatic Brain Injury in the Military: Biomechanics and Finite Element Modelling', Springer, pp. 209–233.

Fries, C. A., Ayalew, Y., Penn-Barwell, J. G., Porter, K., Jeffery, S. L. A. and Midwinter, M. J. (2014) 'Prospective randomised controlled trial of nanocrystalline silver dressing versus plain gauze as the initial post-debridement management of military wounds on wound microbiology and healing', *Injury*, 45(7), pp. 1111–1116.

Fung, Y. C., Yen, R. T., Tao, Z. L. and Liu, S. Q. (1988) 'A Hypothesis on the Mechanism of Trauma of Lung Tissue Subjected to Impact Load', *Journal of Biomechanical Engineering*. American Society of Mechanical Engineers, 110(1), p. 50.

Fung, Y. and Yen, M. (1984) 'Experimental investigation of lung injury mechanisms. Topical report', *US Army Medical Research and Development*

Galarneau, M. R., Woodruff, S. I., Dye, J. L., Mohrle, C. R. and Wade, A. L. (2008) 'Traumatic brain injury during Operation Iraqi Freedom: findings from the United States Navy–Marine Corps Combat Trauma Registry', *Journal of Neurosurgery*, 108(5), pp. 950–957.

Gayzik, F. S., Hoth, J. J., Daly, M., Meredith, J. W. and Stitzel, J. D. (2007) 'A finite element-based injury metric for pulmonary contusion: investigation of candidate metrics through correlation with computed tomography.', *Stapp Car Crash Journal*, 51, pp. 189–209.

Gibson, T., Shewchenko, N. and Whyte, T. (2017) 'The Skull and Brain : Test Methods, Behind Armour Blunt Trauma and Helmet Design'. CRC Press, pp. 119–158.

von Gierke, H. E. (1968) 'Response of the Body To Mechanical Forces - an Overview', *Annals of the New York Academy of Sciences*, 152(1), pp. 172–186.

von Gierke, H. E., Oestreicher, H. L., Franke, E. K., Parrack, H. O. and von Wittern, W. W. (1952) 'Physics of Vibrations in Living Tissues', *Journal of Applied Physiology*. American Physiological Society Bethesda, MD, 4(12), pp. 886–900.

Gotzen, L., Flory, P. and Otte, D. (1980) 'Biomechanics of Aortic Rupture at Classical Location in Traffic Accidents', *The Thoracic and Cardiovascular Surgeon*, 28(01), pp. 64–68.

Goumtcha, A. A., Bodo, M., Taddei, L. and Roth, S. (2016) 'From military to civil loadings: Preliminary numerical-based thorax injury criteria investigations.', *International Journal for Numerical Methods in Biomedical Engineering*, 32(3), p. e02738.

Grabherr, S., Hess, A., Karolczak, M., Thali, M. J., Friess, S. D., Kalender, W. A., Dirnhofer, R. and Djonov, V. (2008) 'Angiofil®-mediated visualization of the vascular system by microcomputed tomography: A feasibility study', *Microscopy Research and*

Technique. 71(7), pp. 551–556.

Gray, H., Lewis, W. H. (Warren H. and Bartleby.com, I. (1918) *Anatomy of the Human Body*. Available at bartleby.com.

Grigoriadis, G., Carpanen, D., Bull, A. M. and Masouros, S. D. (2016) 'A Finite Element Model of the Foot and Ankle for Prediction of Injury in Under-Body Blast', *IRCOBI Conference Proceedings*.

Grigoriadis, G., Carpanen, D., Webster, C., Newell, N. and Masouros, S. (2017) 'The Effect of the Posture of the Lower Limb in Anti-Vehicular Explosions', *IRCOBI Conference Proceedings.*

Grujicic, M., B. Pandurangan, G. M. Mocko, S. T. Hung, B. A. Cheeseman, W. N. Roy, and R. R. Skaggs. (2008) 'A combined multi-material Euler/Lagrange computational analysis of blast loading resulting from detonation of buried landmines', *Multidiscipline Modeling in Materials and Structures*, 4, pp. 105–124.

Guan, S., Liao, Z., Xiang, H., Zhu, X., Wang, Z., Zhao, H., Liu, P. and Lai, X. (2018) 'Experimental Study of Thoracoabdominal Injuries Suffered from Caudocephalad Impacts Using Pigs', *Applied Bionics and Biomechanics*. Hindawi, 2018, pp. 1–10.

Guy, R. J., Kirkman, E., Watkins, P. E. and Cooper, G. J. (1998) 'Physiologic responses to primary blast.', *The Journal of Trauma*, 45(6), pp. 983–7.

Hamra, G. B., Loomis, D. and Dement, J. (2014) 'Examining the association of lung cancer and highly correlated fibre size-specific asbestos exposures with a hierarchical Bayesian model.', *Occupational and Environmental Medicine*., 71(5), pp. 353–7.

Hanson, C. P. G. (1966) Radiographic Studies of Cardiac Displacement During Abrupt Deceleration, *SAE Technical paper 660799*.

Hanson, P. (1967) 'Cardiac displacement and thoracic vascular trauma resulting from abrupt deceleration of dogs.', *Aerospace Medi*cine 12 pp. 1259.

Hardy, W. N., Howes, M. K., Kemper, A. R. and Rouhana, S. W. (2015) *Impact and injury response of the abdomen*, *Accidental Injury: Biomechanics and Prevention*. New York, NY: Springer New York.

Hardy, W. N., Schneider, L. W. and Rouhana, S. W. (2001) 'Abdominal impact response to rigid-bar, seatbelt, and airbag loading.', *Stapp Car Crash Journal*, 45, pp. 1–32.

Hardy, W. N., Shah, C. S., Mason, M. J., Kopacz, J. M., Yang, K. H., King, A. I., Van Ee, C. A., Bishop, J. L., Banglmaier, R. F., Bey, M. J., Morgan, R. M. and Digges, K. H. (2008) 'Mechanisms of traumatic rupture of the aorta and associated peri-isthmic motion and deformation.', *Stapp Car Crash Journal*, 52, pp. 233–65.

Harrison, C. D., Bebarta, V. S. and Grant, G. a. (2009) 'Tympanic Membrane Perforation After Combat Blast Exposure in Iraq: A Poor Biomarker of Primary Blast Injury', *The Journal of Trauma: Injury, Infection, and Critical Care*, 67(1), pp. 210–211.

Harwood, P. J., Giannoudis, P. V., Probst, C., Van Griensven, M., Krettek, C. and Pape, H.-C. (2006) 'Which AIS Based Scoring System is the Best Predictor of Outcome in Orthopaedic Blunt Trauma Patients?', *The Journal of Trauma: Injury, Infection, and Critical Care*, 60(2), pp. 334–340.

Henderson, K. a, Bailey, A. M., Christopher, J. J., Brozoski, F. and Salzar, R. S. (2013) 'Biomechanical Response of the Lower Leg under High Rate Loading', *IRCOBI Conference 2013*, pp. 145–157.

Holcomb, J. B. (2018) 'Transport Time and Preoperating Room Hemostatic Interventions Are Important: Improving Outcomes After Severe Truncal Injury', *Critical Care Medicine*., 46(3), pp. 447–453.

Holcomb, J. B., McMullin, N. R., Pearse, L., Caruso, J., Wade, C. E., Oetjen-Gerdes, L., Champion, H. R., Lawnick, M., Farr, W., Rodriguez, S. and Butler, F. K. (2007) 'Causes of death in U.S. Special Operations Forces in the global war on terrorism: 2001-

2004.', *Annals of Surgery*., 245(6), pp. 986–91.

Hollister, M., Stern, E. J. and Steinberg, K. P. (1995) 'Type 2 pulmonary laceration: a marker of blunt high-energy injury to the lung.', *AJR. American Journal of Roentgenology*, 165(5), p. 1126.

Hooker, D. R. (1924) 'Physiological Effects Of Air Concussion', *American Journal of Physiology-Legacy Content*, 67(2), pp. 219–274.

Horrocks, C. L. (2001) 'Blast injuries: biophysics, pathophysiology and management principles.', *Journal of the Royal Army Medical Corps*, 147, pp. 28–40.

Horsch, J. D., Lau, I. V., Viano, D. C. and Andrzejak, D. V. (1985) 'Mechanism of Abdominal Injury by Steering Wheel Loading', in *29th Stapp Car crash Conference*.

Hoth, J. J., Stitzel, J. D., Gayzik, F. S., Brownlee, N. A., Miller, P. R., Yoza, B. K., McCall, C. E., Meredith, J. W. and Payne, R. M. (2006) 'The Pathogenesis of Pulmonary Contusion: An Open Chest Model in the Rat', *The Journal of Trauma: Injury, Infection, and Critical Care*, 61(1), pp. 32–45.

Howes, M. K., Hardy, W. N. and Beillas, P. (2013) 'The effects of cadaver orientation on the relative position of the abdominal organs.', *Annals of advances in automotive medicine. Association for the Advancement of Automotive Medicine. Annual Scientific Conference*. Association for the Advancement of Automotive Medicine, 57, pp. 209–24.

Huelke, D. F., Nusholtz, G. S. and Kaiker, P. S. (1986) 'Use of quadruped models in thoraco-abdominal biomechanics research', *Journal of Biomechanics*, 19(12), pp. 969–977.

Johnson, A., & Strother, C. E. (1972). The effect of deck deceleration on man's response to ship shock motions. *Journal of Biomechanics*, 5(6), 621-628.

Karamercan, A., Yilmaz, T. U., Karamercan, M. A. and Aytaç, B. (2008) 'Blunt abdominal trauma: evaluation of diagnostic options and surgical outcomes.', *Turkish*

journal of trauma & emergency surgery : TJTES, 14(3), pp. 205–10.

Kazarian, L. E. (1975) 'The Primate as a Model for Crash Injury', *SAE Technical Paper 751172*.

Kazarian, L. E., Hahn, J. W. and Von Gierke, H. E. (1970) 'Biomechanics of the Vertebral Column and Internal Organ Response to Seated Spinal Impact in the Rhesus Monkey', *SAE Technical Paper 700898*.

Keating, C. (1944) 'Wounds in naval action', *Bailey H Surgery of modern warfare. 3rd ed. Edinburgh*

Kehoe, A., Smith, J. E., Edwards, A., Yates, D. and Lecky, F. (2015) 'The changing face of major trauma in the UK.', *Emergency medicine journal :*, 32(12), pp. 911–5.

Keller, W. K., Dillihunt, R. C., Fenner, H. A., Jolley, F. L., Keeney, A. H., Weygandt, P. L. and Hames, L. N. (1971) 'Rating the Severity of Tissue Damage: I. The Abbreviated Scale', *JAMA: The Journal of the American Medical Association*. American Medical Association, 215(2), pp. 277–280.

Kemper, A. R., Santago, A. C., Stitzel, J. D., Sparks, J. L. and Duma, S. M. (2010) 'Biomechanical response of human liver in tensile loading.', *Annals of advances in automotive medicine. Association for the Advancement of Automotive Medicine. Annual Scientific Conference*. Association for the Advancement of Automotive Medicine, 54, pp. 15–26.

Kemper, A. R., Santago, A. C., Stitzel, J. D., Sparks, J. L. and Duma, S. M. (2012) 'Biomechanical response of human spleen in tensile loading.', *Journal of Biomechanics*, 45(2), pp. 348–55.

Kemper, A. R., Santago, A. C., Stitzel, J. D., Sparks, J. L. and Duma, S. M. (2013) 'Effect of strain rate on the material properties of human liver parenchyma in unconfined compression.', *Journal of Biomechanical Engineering*, 135(10), pp. 104503–8.

Khan, M., Streets, C., Tai, N. and Rickard, R. (2017) 'United Kingdom military surgical

preparedness for contingency operations.', *Journal of Trauma and Acute Care Surgery* 83(51), pp. S142-S144.

Kheirabadi, B. S., Terrazas, I. B., Hanson, M. A., Kragh, J. F., Dubick, M. A. and Blackbourne, L. H. (2013) 'In vivo assessment of the Combat Ready Clamp to control junctional hemorrhage in swine', *Journal of Trauma and Acute Care Surgery*, 74(5), pp. 1260–1265.

Kilgo, P. D., Osler, T. M. and Meredith, W. (2003) 'The Worst Injury Predicts Mortality Outcome the Best: Rethinking the Role of Multiple Injuries in Trauma Outcome Scoring', *The Journal of Trauma: Injury, Infection, and Critical Care*, 55(4), pp. 599–607.

Kindig, M. W., Lau, A. G., Forman, J. L. and Kent, R. W. (2010) 'Structural response of cadaveric ribcages under a localized loading: stiffness and kinematic trends.', *Stapp Car Crash Journal*, 54, pp. 337–80.

Kirkman, E. and Watts, S. (2011) 'Characterization of the response to primary blast injury', *Philosophical Transactions of the Royal Society B: Biological Sciences*, 366(1562), pp. 286–290.

Kohl, P., Nesbitt, A. D., Cooper, P. J. and Lei, M. (2001) 'Sudden cardiac death by Commotio cordis: role of mechano–electric feedback', *Cardiovascular Research*., 50(2), pp. 280–289.

Kornhauser, M. and Lawton, R. W. (1961) 'Impact tolerance of mammals', *Planetary and Space Science*., 7, pp. 386–394.

Kotwal, R. S., Butler, F. K., Gross, K. R., Kragh, J. J. F., Kheirabadi, B. S., Baer, D. G., Dubick, M. A., Rasmussen, T. E., Weber, M. A. and Bailey, J. A. (2013) 'Management of Junctional Hemorrhage in Tactical Combat Casualty Care: TCCC Guidelines-Proposed Change 13-03'.DTIC

Kragh, J. F., Walters, T. J., Baer, D. G., Fox, C. J., Wade, C. E., Salinas, J. and Holcomb, J. B. (2008) 'Practical Use of Emergency Tourniquets to Stop Bleeding in Major Limb

Trauma', *The Journal of Trauma: Injury, Infection, and Critical Care*, 64(Supplement), pp. S38–S50.

Kragh, J. F., Walters, T. J., Baer, D. G., Fox, C. J., Wade, C. E., Salinas, J. and Holcomb, J. B. (2009) 'Survival With Emergency Tourniquet Use to Stop Bleeding in Major Limb Trauma', *Annals of Surgery*, 249(1), pp. 1–7.

Kroell, C. K., Pope, M. E., Viano, D. C., Warner, C. Y. and Allen, S. D. (1981) 'Interrelationship of velocity and chest compression in blunt thoracic impact to swine', 25th *Stapp Car Crash Conference*, pp. 549–582.

Kroell, C. K., Schneider, D. C. and Nahum, A. M. (1974) 'Impact Tolerance and Response of the Human Thorax II', *SAE Technical Pape 741187.*

Kudsk, K. A., Bongard, F. and Lim, R. C. (1984) 'Determinants of survival after vena caval injury. Analysis of a 14-year experience.', *Archives of surgery* 119(9), pp. 1009–12.

Kuppa, S., Eppinger, R. H., McKoy, F., Nguyen, T., Pintar, F. A. and Yoganandan, N. (2003) 'Development of Side Impact Thoracic Injury Criteria and Their Application to the Modified ES-2 Dummy with Rib Extensions (ES-2re).', *Stapp Car Crash Journal*, 47, pp. 189–210.

Lapostolle, F., Gere, C., Borron, S. W., Pétrovic, T., Dallemagne, F., Beruben, A., Lapandry, C. and Adnet, F. (2005) 'Prognostic factors in victims of falls from height*', *Critical Care Medicine*, 33(6), pp. 1239–1242.

Lau, I. V. and Viano, D. C. (1986) 'The Viscous Criterion - Bases and Applications of an Injury Severity Index for Soft Tissues', in *30th Stapp Car Crash Conference* .

Lau, I. and Viano, D. (1986) 'The viscous criterion-bases and applications of an injury severity index for soft tissues'. *SAE Technical paper 861882*

Lau, V. K. and Viano, D. C. (1981) 'Influence of impact velocity on the severity of nonpenetrating hepatic injury.', *The Journal of Trauma*, 21(2), pp. 115–23.

Lim, J. Y., Wolf, A. S. and Flores, R. M. (2013) 'Thoracic vessel injury.', *Minerva chirurgica*, 68(3), pp. 251–62.

Link, M. S., Maron, B. J., VanderBrink, B. A., Takeuchi, M., Pandian, N. G., Wang, P. J. and Estes, N. A. M. (2001) 'Impact directly over the cardiac silhouette is necessary to produce ventricular fibrillation in an experimental model of commotio cordis', *Journal of the American College of Cardiology*. Journal of the American College of Cardiology, 37(2), pp. 649–654.

Lobdell, T. E., Kroell, C. K., Schneider, D. C., Hering, W. E. and Nahum, A. M. (1973) 'Impact Response of the Human Thorax', in *Human Impact Response*. Boston, MA: Springer US, pp. 201–245.

Lundevall, J. (1964) 'The mechanism of traumatic rupture of the aorta.', *Acta Pathologica et Microbiologica Scandinavica*, 62, pp. 34–46.

Mabry, R. L. and DeLorenzo, R. (2014) 'Challenges to improving combat casualty survival on the battlefield', *Military Medicine*, 179(5), pp. 477–482.

Mackenzie, I., Tunnicliffe, B., Clasper, J., Mahoney, P. and Kirkman, E. (2013) 'What the Intensive Care Doctor Needs to Know about Blast-Related Lung Injury', *Journal of the Intensive Care Society*. 14(4), pp. 303–312.

Mamczak, C. N. and Elster, E. A. (2012) 'Complex dismounted IED blast injuries: the initial management of bilateral lower extremity amputations with and without pelvic and perineal involvement.', *Journal of Surgical Orthopaedic Advances*, 21(1), pp. 8–14.

Martins, P. N. A. and Neuhaus, P. (2007) 'Surgical anatomy of the liver, hepatic vasculature and bile ducts in the rat.', *Liver international : official journal of the International Association for the Study of the Liver*, 27(3), pp. 384–92.

Mason, M. J., Shah, C. S., Maddali, M., Yang, K. H., Hardy, W. N. and Ee, C. a Van (2005) 'A New Device for High-Speed Biaxial Tissue Testing : Application to Traumatic Rupture of the Aorta', *SAE Technical Paper 2005-01-0741*

Masouros, S. D., Newell, N., Ramasamy, A., Bonner, T. J., West, A. T. H., Hill, A. M., Clasper, J. C. and Bull, A. M. J. (2013) 'Design of a traumatic injury simulator for assessing lower limb response to high loading rates', *Annals of Biomedical Engineering*, 41(9), pp. 1957–1967.

Masuda, R., Nakagawa, T., Hamamoto, A., Inoue, Y., Iwazaki, M. and Inoue, H. (2007) 'A case of deep pulmonary laceration associated with blunt chest trauma treated by emergency room thoracotomy.', *The Tokai Journal of Experimental and Clinical Medicine*, 32(3), pp. 75–7.

Mattox, K. L. (1988) 'Thoracic great vessel injury.', *The Surgical Clinics of North America*, 68(4), pp. 693–703.

Mays, E. T. (1966) 'Bursting Injuries of the Liver', *Archives of Surgery*. American Medical Association, 93(1), p. 92.

McDonald Johnston, A. and Ballard, M. (2015) 'Primary Blast Lung Injury', *American Journal of Respiratory and Critical Care Medicine*., 191(12), pp. 1462–1463.

Mcelhaney, J. H., Stalnaker, R. L., Roberts, V. L. and Snyder, R. G. (1971) 'Door Crashworthiness Criteria', *SAE Technical Paper*. 710864.

McKay, B. J. and Bir, C. A. (2009) 'Lower extremity injury criteria for evaluating military vehicle occupant injury in underbelly blast events.', *Stapp Car Crash Journal*, 53, pp. 229–49.

McMurry, T. L. and Poplin, G. S. (2017) 'A note on"Deriving injury risk curves using survival analysis from biomechanical experiments', *Journal of Bbiomechanics*., 52, pp. 187–188.

Melvin, J. (1985) Review of biomechanical response and injury in the automotive environment. *UMTRI report* 85-3.

Melvin, J., Mohan, D. and Stalnaker, R. (1975) 'Occupant injury assessment criteria'. *SAE Technical Paper* 750914

Melvin, J. W., Stalnaker, R. L., Roberts, V. L. and Trollope, M. L. (1973) 'Impact Injury Mechanisms in Abdominal Organs', in *Proceedings: Stapp Car Crash Conference*. Society of Automotive Engineers SAE,p.

Mertz, H. J. and Gadd, C. W. (1971) 'Thoracic Tolerance to Whole-Body Deceleration', *Proceedings of the 15th Stapp Car Crash Conference*, pp. 135–157.

Mertz, H. J. and Weber, D. A. (1988) "Interpretations of the impact responses of a 3-year-old child dummy relative to child injury potential". *SAE Technical Pape*r, 826048

Miller, R. T., Nazir, N., McDonald, T. and Cannon, C. M. (2017) 'The modified rapid emergency medicine score: A novel trauma triage tool to predict in-hospital mortality.', *Injury*. 48(9), pp. 1870–1877.

Ministry of Defence (2015) *Strategic Trends Programme Future Operating Environment 2035 First Edition*.

Mohan, D. and Melvin, J. W. (1982) 'Failure properties of passive human aortic tissue. I—Uniaxial tension tests', *Journal of Biomechanics*, 15(11), pp. 887–902.

Mohan, D. and Melvin, J. W. (1983) 'Failure properties of passive human aortic tissue. II—Biaxial tension tests', *Journal of Biomechanics*, 16(1), pp. 31–44.

Molina, D. K. and DiMaio, V. J. M. (2012a) 'Normal Organ Weights in Men', *The American Journal of Forensic Medicine and Pathology*, 33(4), pp. 368–372.

Molina, D. K. and DiMaio, V. J. M. (2012b) 'Normal Organ Weights in Men', *The American Journal of Forensic Medicine and Pathology*, 33(4), pp. 362–367.

Molina, D. K. and DiMaio, V. J. M. (2015) 'Normal Organ Weights in Women', *The American Journal of Forensic Medicine and Pathology*, 36(3), pp. 182–187.

Moore, E. E., Cogbill, T. H., Malangoni, M. A., Jurkovich, G. J., Champion, H. R., Gennarelli, T. A., McAninch, J. W., Pachter, H. L., Shackford, S. R. and Trafton, P. G. (1990) 'Organ injury scaling, II: Pancreas, duodenum, small bowel, colon, and rectum.',

The Journal of Trauma, 30(11), pp. 1427–9.

Moore, E. E., Shackford, S. R., Pachter, H. L., McAninch, J. W., Browner, B. D., Champion, H. R., Flint, L. M., Gennarelli, T. A., Malangoni, M. A. and Ramenofsky, M. L. (1989) 'Organ injury scaling: spleen, liver, and kidney.', *The Journal of Trauma*, 29(12), pp. 1664–6.

Morrison, J. J. and Rasmussen, T. E. (2012) 'Noncompressible Torso Hemorrhage. A Review with Contemporary Definitions and Management Strategies', *Surgical Clinics of North America*, 92(4), pp. 843–858.

Morrison, J. J., Ross, J. D., Rasmussen, T. E., Midwinter, M. J. and Jansen, J. O. (2014) 'Resuscitative endovascular balloon occlusion of the aorta: a gap analysis of severely injured UK combat casualties.', *Shock (Augusta, Ga.)*, 41(5), pp. 388–93.

Morrison, J. J., Stannard, A., Rasmussen, T. E., Jansen, J. O., Tai, N. R. M. and Midwinter, M. J. (2013) 'Injury pattern and mortality of noncompressible torso hemorrhage in UK combat casualties', *Journal of Trauma and Acute Care Surgery*, 75(2 Suppl 2), pp. S263–S268.

Nahum, A. M., Schneider, D. C. and Kroell, C. K. (1975) 'Cadaver Skeletal Response to Blunt Thoracic Impact', *SAE Transactions*: pp. 3160-3177.

Nakagawa, A., Manley, G. T., Gean, A. D., Ohtani, K., Armonda, R., Tsukamoto, A., Yamamoto, H., Takayama, K. and Tominaga, T. (2011) 'Mechanisms of Primary Blast-Induced Traumatic Brain Injury: Insights from Shock-Wave Research', *Journal of Neurotrauma*. , 28(6), pp. 1101–1119.

NATO Research and Technology Organisation (2012) *RTO-TR-HFM-148*. Available at: https://www.sto.nato.int/publications/STO

Naumann, D. N., Eisenstein, N., Burns, D. S. and Stapley, S. A. (2017a) 'Towards research combat readiness: prepared, prospective and preapproved.', *Journal of the Royal Army Medical Corps*. 163(4), pp. 233–234.

Neschis, D. G., Scalea, T. M., Flinn, W. R. and Griffith, B. P. (2008) 'Blunt Aortic Injury', *New England Journal of Medicine*., 359(16), pp. 1708–1716.

Newell, N., Pearce, A. P., Spurrier, E., Gibb, I., Webster, C. E., Masouros, S. D. and Clasper, J. C. (2018) 'Analysis of isolated transverse process fractures sustained during blast related events.', *The Journal of Trauma and Acute Care Surgery* 85, pp. S129-S133.

Newell, N., Salzar, R., Bull, A. M. J. and Masouros, S. D. (2016) 'A validated numerical model of a lower limb surrogate to investigate injuries caused by under-vehicle explosions', *Journal of Biomechanics*. 49(5), pp. 710–717.

Nguyen, T.-T. N., Wilgeroth, J. M. and Proud, W. G. (2014) 'Controlling blast wave generation in a shock tube for biological applications', *Journal of Physics: Conference Series*, 500(14), p. 142025.

Nusholtz, G. and Kaiker, P. (1994) 'Abdominal response to steering wheel loading', in *4th International Technical Conference on Enhanced Safety of Vehicles*.

Office for National Statistics (2016) *Deaths registered in England and Wales (series DR) - Office for National Statistics*. (Accessed: 17 April 2018).

Osler, T., Rutledge, R., Deis, J. and Bedrick, E. (1996) 'ICISS: an international classification of disease-9 based injury severity score.', *The Journal of Trauma*, 41(3), pp. 380-6;.

Owens, B. D., Kragh, J. F., Wenke, J. C., Macaitis, J., Wade, C. E. and Holcomb, J. B. (2008) 'Combat Wounds in Operation Iraqi Freedom and Operation Enduring Freedom', *The Journal of Trauma: Injury, Infection, and Critical Care*, 64(2), pp. 295–299.

Owers, C., Morgan, J. L. and Garner, J. P. (2011) 'Abdominal trauma in primary blast injury.', *The British journal of surgery*, 98(2), pp. 168–79.

Panzer, M. B., Wood, G. W. and Bass, C. R. (2014) 'Scaling in neurotrauma: How do

we apply animal experiments to people?', *Experimental Neurology*., 261, pp. 120–126.

Parmley, L. F., Mattingly, T. W., Manion, W. C. and Jahnke, E. J. (1958) 'Nonpenetrating traumatic injury of the aorta.', *Circulation*, 17(6), pp. 1086–101.

Pearce, A. P., Bull, A. M. J. and Clasper, J. C. (2017) 'Mediastinal injury is the strongest predictor of mortality in mounted blast amongst UK deployed forces', *Injury*. 48(9), pp. 1900–1905.

Peng, J., Wheeler, K., Shi, J., Groner, J. I., Haley, K. J. and Xiang, H. (2015) 'Trauma with Injury Severity Score of 75: Are These Unsurvivable Injuries?', *PLOS ONE*. Edited by C. Lazzeri, 10(7), p. e0134821.

Penn-Barwell, J. G., Roberts, S. A. G., Midwinter, M. J. and Bishop, J. R. B. (2015) 'Improved survival in UK combat casualties from Iraq and Afghanistan', *Journal of Trauma and Acute Care Surgery*, 8(5) :pp. 1014-1020..

Petitjean, A. and Trosseille, X. (2011) 'Statistical simulations to evaluate the methods of the construction of injury risk curves.', *Stapp Car Crash Journal*, 55, pp. 411–40.

Petitjean, A., Trosseille, X., Yoganandan, N. and Pintar, F. A. (2015) 'Normalization and Scaling for Human Response Corridors and Development of Injury Risk Curves', in *Accidental Injury*. New York, NY: Springer New York, pp. 769–792.

Petrucelli, E., States, J. D. and Hames, L. N. (1981) 'The abbreviated injury scale: Evolution, usage and future adaptability', *Accident Analysis & Prevention*. 13(1), pp. 29–35.

Pietsch, H. A., Bosch, K. E., Weyland, D. R., Spratley, E. M., Henderson, K. A., Salzar, R. S., Smith, T. A., Sagara, B. M., Demetropoulos, C. K., Dooley, C. J. and Merkle, A. C. (2016) 'Evaluation of WIAMan Technology Demonstrator Biofidelity Relative to Sub-Injurious PMHS Response in Simulated Under-body Blast Events.', *Stapp Car Crash Journal*, 60, pp. 199–246.

Polfer, E. M., Hope, D. N., Elster, E. A., Qureshi, A. T., Davis, T. A., Golden, D., Potter,

B. K. and Forsberg, J. A. (2015) 'The development of a rat model to investigate the formation of blast-related post-traumatic heterotopic ossification', *The Bone & Joint Journal*, 97–B(4), pp. 572–576.

Poplin, G. S., McMurry, T. L., Forman, J. L., Hartka, T., Park, G., Shaw, G., Shin, J., Kim, H. joo and Crandall, J. (2015) 'Nature and etiology of hollow-organ abdominal injuries in frontal crashes', *Accident Analysis & Prevention*, 78, pp. 51–57.

Prasad, P. and Daniel, R. P. (1984) 'A Biomechanical Analysis of Head, Neck, and Torso Injuries to Child Surrogates Due to Sudden Torso Acceleration', in *SAE transactions* pp.784-799..

Proctor, J. L., Fourney, W. L., Leiste, U. H. and Fiskum, G. (2014) 'Rat model of brain injury caused by under-vehicle blast-induced hyperacceleration', *Journal of Trauma and Acute Care Surgery*, 77(3 Suppl 2), pp. S83–S87.

Proud, W. (2013) 'The physical basis of explosion and blast injury processes', *Journal of the Royal Army Medical Corps*, 159(suppl_1), pp. i4–i9.

Proud, W. G. (2016) 'The Fundamentals of Blast Physics', in *Blast Injury Science and Engineering*. Cham: Springer International Publishing, pp. 3–16.

Radonić, V., Giunio, L., Biocić, M., Tripković, A., Lukcić, B. and Primorac, D. (2004) 'Injuries from Antitank mines in Southern Croatia.', *Military Medicine*, 169(4), pp. 320–4.

Raghavendran, K., Notter, R. H., Davidson, B. A., Helinski, J. D., Kunkel, S. L. and Knight, P. R. (2009) 'Lung contusion: inflammatory mechanisms and interaction with other injuries.', *Shock* 32(2), pp. 122–30.

Rajab, T. K. (2018) 'Anastomotic techniques for rat lung transplantation.', *World Journal of Transplantation*. 8(2), pp. 38–43.

Ramasamy, A., Hill, A. M., Masouros, S., Gibb, I., Bull, a. M. J. and Clasper, J. C. (2011) 'Blast-related fracture patterns: a forensic biomechanical approach', *Journal of*

The Royal Society Interface, 8(58), pp. 689–698.

Ramasamy, A., Harrisson, S. E., Clasper, J. C. and Stewart, M. P. M. (2008) 'Injuries From Roadside Improvised Explosive Devices', *The Journal of Trauma: Injury, Infection, and Critical Care*, 65(4), pp. 910–914.

Ramasamy, A., Hill, A. M. and Clasper, J. C. (2009) 'Improvised explosive devices: pathophysiology, injury profiles and current medical management.', *Journal of the Royal Army Medical Corps*, 155 (4) pp. 265–272.

Ramasamy, A., Hill, A. M., Hepper, A. E., Bull, A. M. and Clasper, J. C. (2009) 'Blast mines: physics, injury mechanisms and vehicle protection.', *Journal of the Royal Army Medical Corps*, 155(4), pp. 258–264.

Ramasamy, A., Hill, A. M., Masouros, S. D., Gordon, F., Clasper, J. C. and Bull, A. M. J. (2011) 'Evaluating the effect of vehicle modification in reducing injuries from landmine blasts. An analysis of 2212 incidents and its application for humanitarian purposes', *Accident Analysis & Prevention*. 43(5), pp. 1878–1886.

Ramasamy, A., Hill, A. M., Masouros, S., Gibb, I., Phillip, R., Bull, A. M. J. and Clasper, J. C. (2013) 'Outcomes of IED foot and ankle blast injuries.', *The Journal of bone and joint surgery. American volume*. 95(5), p. e25.

Ramasamy, A., Hill, A. M., Phillip, R., Gibb, I., Bull, A. M. J. and Clasper, J. C. (2011) 'The Modern "Deck-Slap" Injury—Calcaneal Blast Fractures From Vehicle Explosions', *The Journal of Trauma: Injury, Infection, and Critical Care*, 71(6), pp. 1694–1698.

Ramasamy, A., Masouros, S. D., Newell, N., Hill, A. M., Proud, W. G., Brown, K. a, Bull, A. M. J. and Clasper, J. C. (2011) 'In-vehicle extremity injuries from improvised explosive devices: current and future foci.', *Philosophical transactions of the Royal Society of London. Series B, Biological sciences*, 366, pp. 160–170.

Ramasamy, Harrisson, S., Lasrado, I. and Stewart, M. P. M. (2009) 'A review of casualties during the Iraqi insurgency 2006–A British field hospital experience', *Injury*,

40(5), pp. 493–497.

Rasmussen, T. E., Gross, K. R. and Baer, D. G. (2013) 'Where do we go from here?', *Journal of Trauma and Acute Care Surgery*, 75, pp. S105–S106.

Rasmussen, T. E. and Kellermann, A. L. (2016) 'Wartime Lessons — Shaping a National Trauma Action Plan', *New England Journal of Medicine*. 375(17), pp. 1612–1615.

Reed, M. P. (2014) *The Seated Soldier Study: Posture and Body Shape in Vehicle Seats*. DTIC

Richens, D., Field, M., Hashim, S., Neale, M. and Oakley, C. (2004) 'A finite element model of blunt traumatic aortic rupture.', *European journal of cardio-thoracic surgery : official journal of the European Association for Cardio-thoracic Surgery*, 25(6), pp. 1039–47.

Richens, D., Field, M., Neale, M. and Oakley, C. (2002) 'The mechanism of injury in blunt traumatic rupture of the aorta.', *European journal of cardio-thoracic surgery : official journal of the European Association for Cardio-thoracic Surgery*, 21(2), pp. 288–93.

Richens, D., Kotidis, K., Neale, M., Oakley, C. and Fails, A. (2003) 'Rupture of the aorta following road traffic accidents in the United Kingdom 1992-1999. The results of the co-operative crash injury study.', *European journal of cardio-thoracic surgery : official journal of the European Association for Cardio-thoracic Surgery*, 23(2), pp. 143–8.

Richmond, D. R., Bowen, I. G. and White, C. S. (1961) 'Tertiary Blast effects: The effect pf impact on mice, rats, guinea pigs, and rabbits. DTIC.

Richmond, D. R., Damon, E. G., Fletcher, E. R., Bowen, I. G. and White, C. S. (1968) 'The relationship between selected blast-wave parameters and the response of mammals exposed to air blast', *Annals of the New York Academy of Sciences*, 152(1), pp. 103–121.

Roberto, M., Hamernik, R. P. and Turrentine, G. A. (1989) 'Damage of the Auditory System Associated with Acute Blast Trauma', *Annals of Otology, Rhinology & Laryngology*, 98(5_suppl), pp. 23–34.

Rodriguez, R. M., Friedman, B., Langdorf, M. I., Baumann, B. M., Nishijima, D. K., Hendey, G. W., Medak, A. J., Raja, A. S. and Mower, W. R. (2016) 'Pulmonary contusion in the pan-scan era', *Injury*. 47(5), pp. 1031–1034.

Rosenfeld, J. V. and Ford, N. L. (2010) 'Bomb blast, mild traumatic brain injury and psychiatric morbidity: A review', *Injury*, pp. 437–443.

Rostas, J. W., Lively, T. B., Brevard, S. B., Simmons, J. D., Frotan, M. A. and Gonzalez, R. P. (2017) 'Rib fractures and their association With solid organ injury: higher rib fractures have greater significance for solid organ injury screening', *The American Journal of Surgery*, 213(4), pp. 791–797.

Rouhana, S. W., Lau, I. V and Ridella, S. A. (1985) 'Influence of velocity and forced compression on the severity of abdominal injury in blunt, nonpenetrating lateral impact.', *The Journal of Trauma*, 25(6), pp. 490–500.

Russell, R., Halcomb, E., Caldwell, E. and Sugrue, M. (2004) 'Differences in Mortality Predictions Between Injury Severity Score Triplets: A Significant Flaw', *The Journal of Trauma: Injury, Infection, and Critical Care*, 56(6), pp. 1321–1324.

Russell, R., Hunt, N. and Delaney, R. (2014) 'The Mortality Peer Review Panel: a report on the deaths on operations of UK Service personnel 2002-2013.', *Journal of the Royal Army Medical Corps*. 160(2), pp. 150–4.

Russell, R. J., Hodgetts, T. J., McLeod, J., Starkey, K., Mahoney, P., Harrison, K. and Bell, E. (2010) 'The role of trauma scoring in developing trauma clinical governance in the Defence Medical Services', *Philosophical Transactions of the Royal Society of London B: Biological Sciences*, 366(1562).

Russell, R. J., Hodgetts, T. J., McLeod, J., Starkey, K., Mahoney, P., Harrison, K. and Bell, E. (2011) 'The role of trauma scoring in developing trauma clinical governance in

the Defence Medical Services', *Philosophical Transactions of the Royal Society B: Biological Sciences*, 366(1562), pp. 171–191.

Russo, R. M., Williams, T. K., Grayson, J. K., Lamb, C. M., Cannon, J. W., Clement, N. F., Galante, J. M. and Neff, L. P. (2016) 'Extending the golden hour: Partial resuscitative endovascular balloon occlusion of the aorta in a highly lethal swine liver injury model.', *The Journal of Trauma and Acute Care Surgery*, 80(3), pp. 372–80.

Rutledge, R., Hoyt, D. B., Eastman, A. B., Sise, M. J., Velky, T., Canty, T., Wachtel, T. and Osler, T. M. (1997) 'Comparison of the Injury Severity Score and ICD-9 diagnosis codes as predictors of outcome in injury: analysis of 44,032 patients.', *The Journal of Trauma* 42(3) pp 477-489

Santago, A. C., Kemper, A. R., McNally, C., Sparks, J. L. and Duma, S. M. (2009) 'Freezing affects the mechanical properties of bovine liver - biomed 2009.', *Biomedical Sciences Instrumentation*, 45, pp. 24–9.

Schambach, S. J., Bag, S., Groden, C. and Schilling, L. (2010) 'Vascular imaging in small rodents using micro-CT', *Methods*. 50(1), pp. 26–35.

Schardin, H. (1950) 'The physical principles of the effects of a detonation', *US Government Printing Office*

Schluter, P. J., Nathens, A., Neal, M. L., Goble, S., Cameron, C. M., Davey, T. M. and McClure, R. J. (2010) 'Trauma and Injury Severity Score (TRISS) Coefficients 2009 Revision', *The Journal of Trauma: Injury, Infection, and Critical Care*, 68(4), pp. 761–770.

Sevitt, S. (1977) 'The mechanisms of traumatic rupture of the thoracic aorta', *British Journal of Surgery*, 64(3), pp. 166–173.

Shah, C. and Mason, M. (2005) 'High-speed biaxial tissue properties of the human cadaver aorta', *ASME 2005*

Shah, C. S., Hardy, W. N., Mason, M. J., Yang, K. H., Van Ee, C. A., Morgan, R. and

Digges, K. (2006) 'Dynamic biaxial tissue properties of the human cadaver aorta.', *Stapp Car Crash Journal*, 50, pp. 217–46.

Shah, C. S., Yang, K. H., Hardy, W., Wang, H. K. and King, A. I. (2001) 'Development of a computer model to predict aortic rupture due to impact loading.', *Stapp Car Crash Journal*, 45, pp. 161–82.

Sharma, O. P. and Rawitscher, R. E. (1999) 'Blunt vena azygos trauma: report of a case and review of world literature.', *The Journal of Trauma*, 46(1), pp. 192–5.

Sharpnack, D., Johnson, A. and Phillips, Y. (1991) 'The pathology of primary blast injury', *Textbook of Military Medicine*. Borden Institute

Shorr, R. M., Crittenden, M., Indeck, M., Hartunian, S. L. and Rodriguez, A. (1987) 'Blunt thoracic trauma. Analysis of 515 patients.', *Annals of Surgery*. 206(2), pp. 200–5.

Shuker, S. T. (2013) 'Effect of biomechanism mine explosion on children: craniofacial injuries and management.', *The Journal of Craniofacial Surgery*, 24(4), pp. 1132–6.

Siegel, J. H., Belwadi, A., Smith, J. A., Shah, C. and Yang, K. (2010) 'Analysis of the mechanism of lateral impact aortic isthmus disruption in real-life motor vehicle crashes using a computer-based finite element numeric model: with simulation of prevention strategies.', *The Journal of Trauma*, 68(6), pp. 1375–95.

Siegel, J. H., Smith, J. A. and Siddiqi, S. Q. (2004) 'Change in Velocity and Energy Dissipation on Impact in Motor Vehicle Crashes as a Function of the Direction of Crash: Key Factors in the Production of Thoracic Aortic Injuries, Their Pattern of Associated Injuries and Patient Survival A Crash Injury Research Engineering Network (CIREN) Study', *The Journal of Trauma: Injury, Infection, and Critical Care*, 57(4), pp. 760–778.

Siegel, J. H., Smith, J. A., Tenenbaum, N., McCammon, L., Siddiqi, S. Q., Presswalla, F., Pierre-Louis, P., Williams, W., Zaretski, L., Hutchins, K., Perez, L., Shaikh, J. and Natarajan, G. (2002) 'Deceleration energy and change in velocity on impact: key factors

in fatal versus potentially survivable motor vehicle crash (mvc) aortic injuries (AI): the role of associated injuries as determinants of outcome.', *Annual proceedings / Association for the Advancement of Automotive Medicine. Association for the Advancement of Automotive Medicine*, 46, pp. 315–38.

Singleton, Gibb, Hunt, Bull and Clasper, J. C. (2013) 'Identifying future "unexpected" survivors: a retrospective cohort study of fatal injury patterns in victims of improvised explosive devices', *BMJ Open*, 3(8), pp. e003130–e003130.

Singleton, Gibb, I. E., Bull, A. M. J., Mahoney, P. F. and Clasper, J. C. (2013) 'Primary blast lung injury prevalence and fatal injuries from explosions: Insights from postmortem computed tomographic analysis of 121 improvised explosive device fatalities', *Journal of Trauma and Acute Care Surgery*, 75(2 SUPPL. 2), pp. S269–S274.

Sırmalı, M., Türüt, H., Topçu, S., Gülhan, E., Yazici, Ü., Kaya, S. and Taştepe, I. (2003) 'A comprehensive analysis of traumatic rib fractures: morbidity, mortality and management', *European Journal of Cardio-Thoracic Surgery*. Oxford University Press, 24(1), pp. 133–138.

Smith, J., Hodgetts, T., Mahoney, P., Russell, R., Davies, S. and McLeod, J. (2007) 'Trauma governance in the UK defence medical services.', *Journal of the Royal Army Medical Corps*. 153(4), pp. 239–242; discussion 243.

Smith, M. R., Amberger, M. A., Pavalonis, A. G., Onursal, E. M., Lee, S., Phillips, P. A. and Edwards, J. S. (2017) 'Some patients live after trauma: Re-examining the lethality of vertical deceleration injuries', *Trauma*. 19(4), pp. 294–301.

Smith, M. and Withnall, R. (2017) 'Developing prolonged field care for contingency operations', *Trauma*. 20(2) pp 108-112

Smith, S., Devine, M., Taddeo, J. and McAlister, V. C. (2017) 'Injury profile suffered by targets of antipersonnel improvised explosive devices: prospective cohort study.', *BMJ open*. 7(7), p. e014697.

Snyder, R. G. (1970) Human Impact Tolerance - American Viewpoint, *SAE Technical*

Paper 700398.

Society of Automotive Engineers (1995) Surface Vehicle recommended practices J211/1*: Instrumentation for Impact Test - Part 1 - Electronic Instrumentation - SAE International*.

Sparks, J. L., Bolte, J. H., Dupaix, R. B., Jones, K. H., Steinberg, S. M., Herriott, R. G., Stammen, J. A. and Donnelly, B. R. (2007) 'Using pressure to predict liver injury risk from blunt impact.', *Stapp Car Crash Journal*, 51, pp. 401–32.

Spurrier, E., Gibb, I., Masouros, S. and Clasper, J. (2016) 'Identifying spinal injury patterns in underbody blast to develop mechanistic hypotheses', *Spine* 41, no. 5 (2016): E268-E275..

Spurrier, E., Singleton, J. A. G., Masouros, S., Gibb, I. and Clasper, J. (2015) 'Blast Injury in the Spine: Dynamic Response Index Is Not an Appropriate Model for Predicting Injury', *Clinical Orthopaedics and Related Research*, 473(9), pp. 2929–2935.

Stalnaker, R. L. and Ulman, M. S. (1985) 'Abdominal Trauma-Review, Response, and Criteria', in *29th Stapp Car Crash Conference*.

Stannard, A., Eliason, J. L. and Rasmussen, T. E. (2011) 'Resuscitative Endovascular Balloon Occlusion of the Aorta (REBOA) as an Adjunct for Hemorrhagic Shock', *The Journal of Trauma: Injury, Infection, and Critical Care*, 71(6), pp. 1869–1872.

Stannard, A., Morrison, J. J., Scott, D. J., Ivatury, R. a., Ross, J. D. and Rasmussen, T. E. (2013) 'The epidemiology of noncompressible torso hemorrhage in the wars in Iraq and Afghanistan', *Journal of Trauma and Acute Care Surgery*, 74(3), pp. 830–834.

Stapp, J. P. (1957) 'Human tolerance to deceleration', *The American Journal of Surgery*, 93(4), pp. 734–740.

Staruch, R. M. T., Jackson, P. C., Hodson, J., Yim, G., Foster, M. A., Cubison, T. and Jeffery, S. L. A. (2016) 'Comparing the surgical timelines of military and civilians

traumatic lower limb amputations', *Annals of Medicine and Surgery*. 6, pp. 81–86.

Stein, P. D., Sabbah, H. N., Hawkins, E. T., White, H. J., Viano, D. C. and Vostal, J. J. (1983) 'Hepatic and splenic injury in dogs caused by direct impact to the heart.', *The Journal of Trauma*, 23(5), pp. 395–404.

Stevenson, M., Segui-Gomez, M., Lescohier, I., Di Scala, C. and McDonald-Smith, G. (2001) 'An overview of the injury severity score and the new injury severity score.', *Injury prevention : Journal of the International Society for Child and Adolescent Injury Prevention*, 7(1), pp. 10–13.

Stewart, S. K., Pearce, A. P. and Clasper, J. C. (2018) 'Fatal head and neck injuries in military underbody blast casualties.', *Journal of the Royal Army Medical Corps*. p. jramc-2018-000942.

Steyerberg, E. W., Borsboom, G. J. J. M., van Houwelingen, H. C., Eijkemans, M. J. C. and Habbema, J. D. F. (2004) 'Validation and updating of predictive logistic regression models: a study on sample size and shrinkage', *Statistics in Medicine*. 23(16), pp. 2567–2586.

Stuhmiller, J., Phillips, Y. and Richmond, D. . R. (1991b) 'The Physics and Mechanisms of Primary Blast Injury', *Conventional Warfare Ballistic, Blast and Burn Injuries*, pp. 241–270.

Tai, N. R. M. and Dickson, E. J. (2009) 'Military junctional trauma.', *Journal of the Royal Army Medical Corps*, 155(4), pp. 285–92.

Teixeira, P. G. R., Georgiou, C., Inaba, K., DuBose, J., Plurad, D., Chan, L. S., Toms, C., Noguchi, T. T. and Demetriades, D. (2009) 'Blunt Cardiac Trauma: Lessons Learned From the Medical Examiner', *The Journal of Trauma: Injury, Infection, and Critical Care*, 67(6), pp. 1259–1264.

Teixeira, P. G. R., Inaba, K., Barmparas, G., Georgiou, C., Toms, C., Noguchi, T. T., Rogers, C., Sathyavagiswaran, L. and Demetriades, D. (2011) 'Blunt Thoracic Aortic Injuries: An Autopsy Study', *The Journal of Trauma: Injury, Infection, and Critical*

Care, 70(1), pp. 197–202.

Tinkoff, G., Esposito, T. J., Reed, J., Kilgo, P., Fildes, J., Pasquale, M. and Meredith, J. W. (2008) 'American Association for the Surgery of Trauma Organ Injury Scale I: Spleen, Liver, and Kidney, Validation Based on the National Trauma Data Bank', *Journal of the American College of Surgeons*. Elsevier, 207(5), pp. 646–655.

Tohira, H., Jacobs, I., Mountain, D., Gibson, N. and Yeo, A. (2012) 'Systematic review of predictive performance of injury severity scoring tools.', *Scandinavian Journal of Trauma, Resuscitation and Emergency Medicine*. Scandinavian Journal of Trauma, Resuscitation and Emergency Medicine, 20(1), p. 63.

Tremblay, J., Bergeron, D. M. and Gonzalez, R. (1998) 'Protection of Soft-Skinned Vehicle Occupants from Landmine Effects.le', *Defence Research Establishment Valcartier, Quebec, Canada.*

Treuting, P. M., Dintzis, S. M., Frevert, C. W. and Denny Liggitt, P. D. (2018) *Comparative Anatomy and Histology: A Mouse and Human Atlas*.).

Viano, D. C. (1978) 'Evaluation of biomechanical response and potential injury from thoracic impact.', *Aviation, Space, and Environmental Medicine*, 49(1 Pt. 2), pp. 125–35.

Viano, D. C. (1983) 'Biomechanicans of non-penetrating aortic trauma: a review". *SAE Technical Paper* 831608.

Viano, D. C. (2011) 'Chest Impact aimed at producing aortic rupture', *Clinical anatomy (New York, N.Y.)*, 24(3), pp. 339–49.

Viano, D. C., King, A. I., Melvin, J. W. and Weber, K. (1989) 'Injury biomechanics research: An essential element in the prevention of trauma', *Journal of Biomechanics*. 22(5), pp. 403–417.

Viano, D. C. and Lau, I. V. (1988) 'A viscous tolerance criterion for soft tissue injury assessment', *Journal of Biomechanics*, 21(5), pp. 387–399.

Viano, D. C. and Stalnaker, R. L. (1980) 'Mechanisms of femoral fracture', *Journal of Biomechanics*. 13(8), pp. 701–715.

Viano, D. C., Warner, C. Y., Hoopes, K., Mortenson, C., White, R. and Artinian, C. G. (1978) 'Sensitivity of Porcine Thoracic Responses and Injuries to Various Frontal and A Lateral Impact Site', *SAE Transactions* : 3176-3192..

Viano, D. and Warner, C. (1976) 'Thoracic impact response of live porcine subjects' *SAE Technical Pap*er 760823.

Viano, Lau, I. V., Asbury, C., King, A. I. and Begeman, P. (1989) 'Biomechanics of the human chest, abdomen, and pelvis in lateral impact', *Accident Analysis & Prevention*. Pergamon, 21(6), pp. 553–574.

Voigt, G. and Wilfert, K. (1969) 'Mechanisms of injuries to unrestrained drivers in head-on collisions'. *SAE Transactions:* pp. 2635-2645.

Wagner, R. B., Crawford, W. O. and Schimpf, P. P. (1988) 'Classification of parenchymal injuries of the lung.', *Radiology*, 167(1), pp. 77–82.

Walfisch, G., Fayon, A., Tarriere, C., Rosey, J. P., Guillon, F., Got, C., Patel, A. and Stalnaker, R. L. (1980) 'Designing of a dummy's abodmen for detecting injuries in side impact collisions", i*nternational IRCOBI Conference on the Biomechanics of Impacts (5th) Proceedings,.*, p. 149–64.

Walker, N. M., Eardley, W. and Clasper, J. C. (2014) 'UK combat-related pelvic junctional vascular injuries 2008–2011: Implications for future intervention', *Injury*, 45(10), pp. 1585–1589.

Walker, W. and Homberger, D. (1997) *Anatomy and Dissection of the Rat*. 3rd edn. W.H.Freeman and Company.

Wallace, T. F., Swearingen, J. J., Wallace, T. F. and Swearingen, J. J. (1971) 'Crash Injury Severity as Related to Aircraft Attitude During Impact Crash Injury Severity as Related to Aircraft Attitude During Impact', *SAE Technical Paper* 710399.

Wang, J., Bird, R., Swinton, R., technology, A. K. battlefield and 2001, undefined (2001) 'Protection of lower limbs against floor impact in army vehicles experiencing landmine explosion', *Journal of Battlefield Technology*, 4, pp. 8–12.

Wang, J., Liu, H., Jiang, N. Q., Jiang, B. and Wei, N. (2015) 'A rat model of aortic arch aneurysm with excellent survival', *Asian Cardiovascular and Thoracic Annals*, 23(6), pp. 652–657.

Warner, K. G. and Demling, R. H. (1986) 'The pathophysiology of free-fall injury', *Annals of Emergency Medicine*. 15(9), pp. 1088–1093.

Weaver, A. A., Gayzik, F. S. and Stitzel, J. D. (2009) 'Biomechanical analysis of pulmonary contusion in motor vehicle crash victims: a crash injury research and engineering network (ciren) study.', *Biomedical sciences instrumentation*, 45, pp. 364–9.

Weaver, C. M. and Stitzel, J. D. (2015) 'Pelvic Response of a Total Human Body Finite Element Model During Simulated Under Body Blast Impacts', *IRCOBI Conference*, IRC-15-82, pp. 1–2.

Webster, C., Masouros, S., Gibb, I. and Clasper, J. C. (2015) "Fracture patterns in pelvic blast injury: a retrospective analysis and implications for future protective strategies"', *Orthopaedic Proceedings,* vol. 97, no. SUPP_8, pp. 14-14.

Weis, E. B. and Mohr, G. C. (1967) 'Cineradiographic analysis of human visceral responses to short duration impact.', *Aerospace Medicine*, 38(10), pp. 1041–4.

Yoganandan, N., Banerjee, A., Hsu, F.-C., Bass, C. R., Voo, L., Pintar, F. A. and Gayzik, F. S. (2016) 'Deriving injury risk curves using survival analysis from biomechanical experiments', *Journal of Biomechanics*. 49(14), pp. 3260–3267.

Yoganandan, N., Pintar, F. A., Gennarelli, T. A. and Maltese, M. R. (2000a) 'Patterns of abdominal injuries in frontal and side impacts.', *Annual proceedings. Association for the Advancement of Automotive Medicine*., 44, pp. 17–36.

Yoganandan, N., Pintar, F. A., Gennarelli, T. A. and Maltese, M. R. (2000b) 'Patterns of abdominal injuries in frontal and side impacts.', *Annual proceedings / Association for the Advancement of Automotive Medicine. A* 44, pp. 17–36.

APPENDIX A: Q-Q PLOTS FOR WEIBULL INJURY RISK CURVES

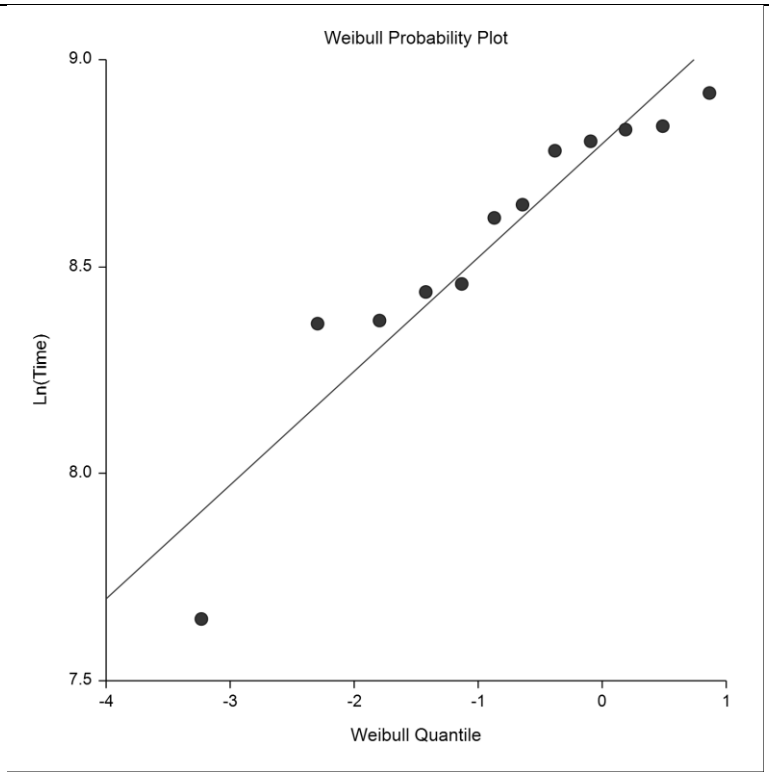

Figure A.1: Q-Q plot for Weibull distribution fit- Lung injury and seat acceleration

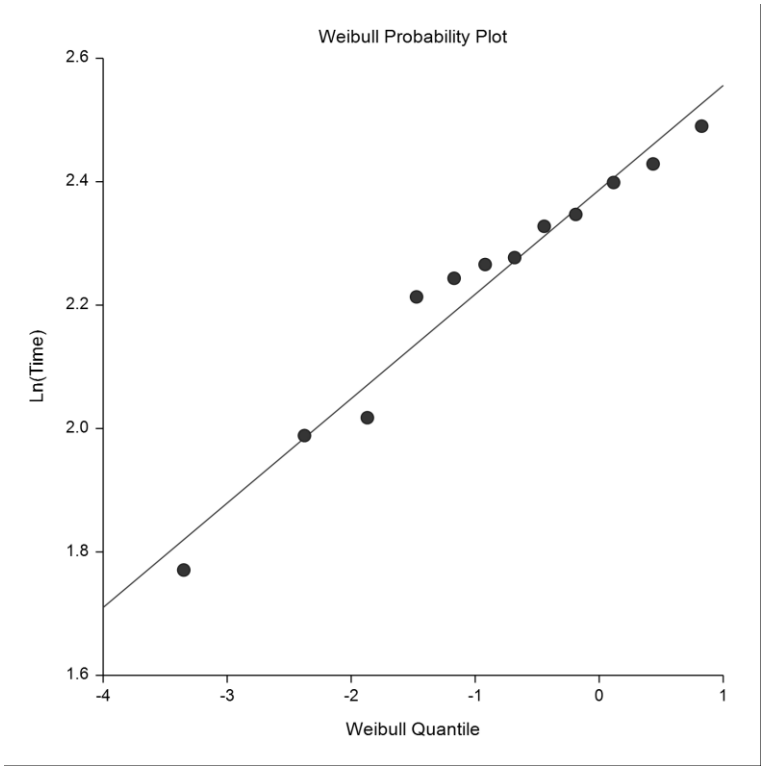

Figure A.2: Q-Q plot for Weibull distribution fit- Lung injury and seat velocity

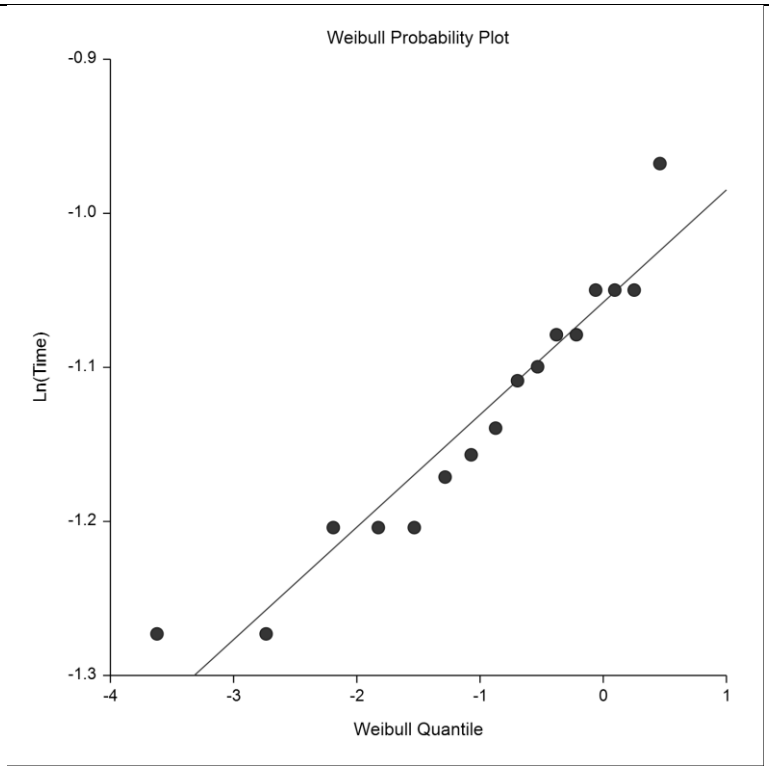

Figure A.3:Q-Q plot for Weibull distribution fit- Lung injury and maximum compression

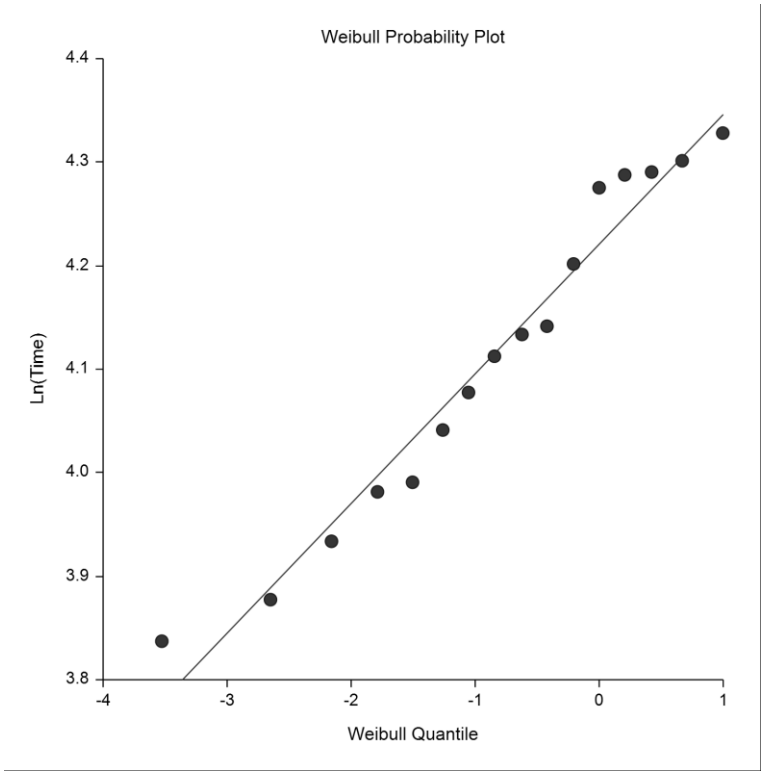

Figure A.4: Q-Q plot for Weibull distribution fit- Lung injury and compression rate

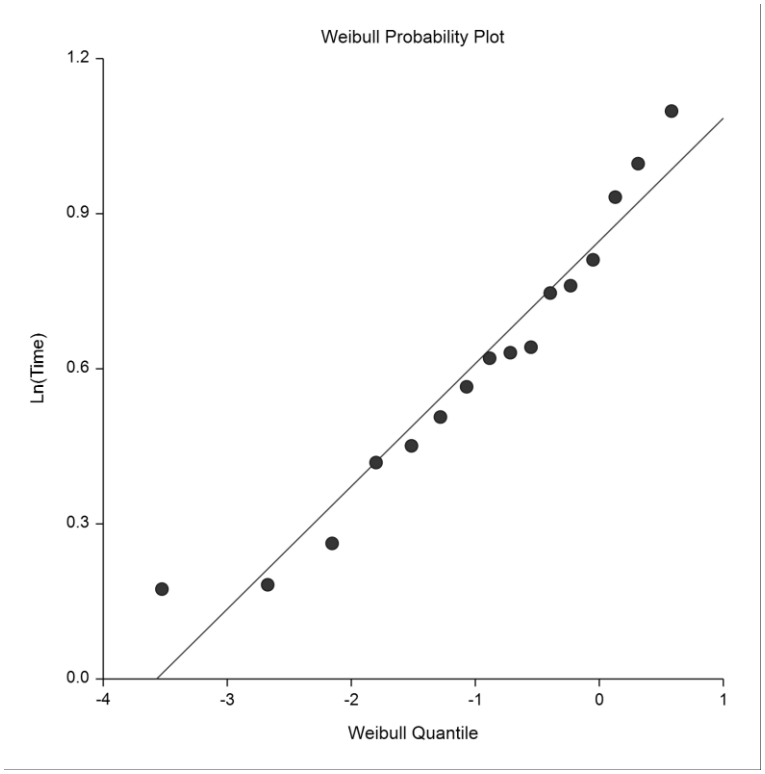

Figure A.5: Q-Q plot for Weibull distribution fit- Lung injury and viscous response

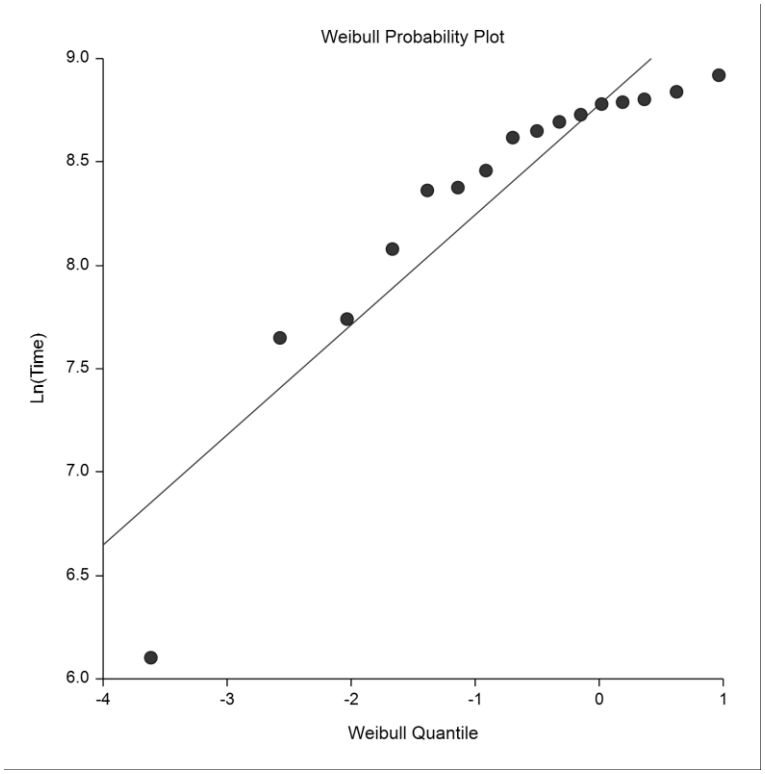

Figure A.6: Q-Q plot for Weibull distribution fit- Liver injury and seat acceleration

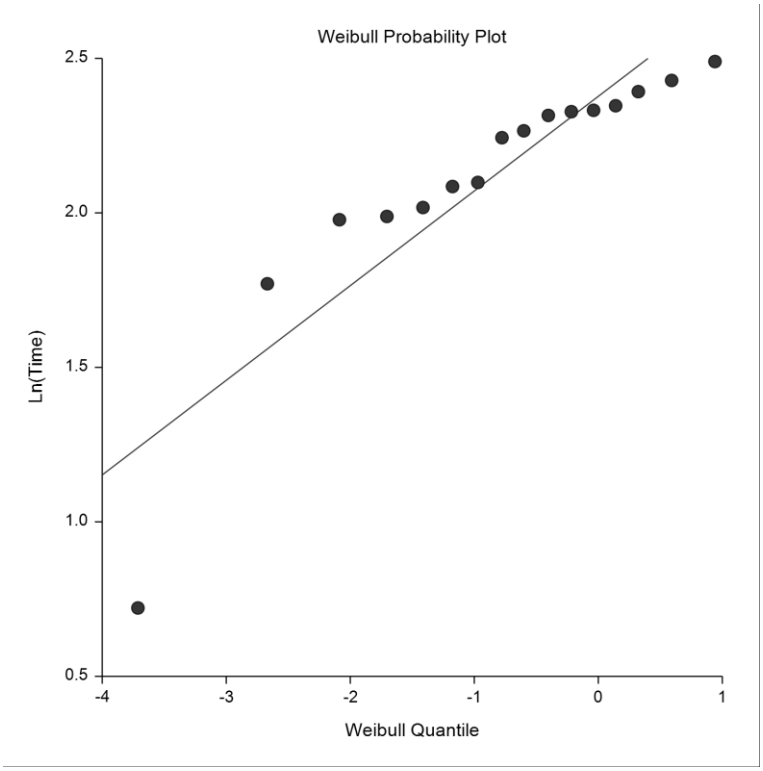

Figure A.7: Q-Q plot for Weibull distribution fit- Liver injury and seat velocity

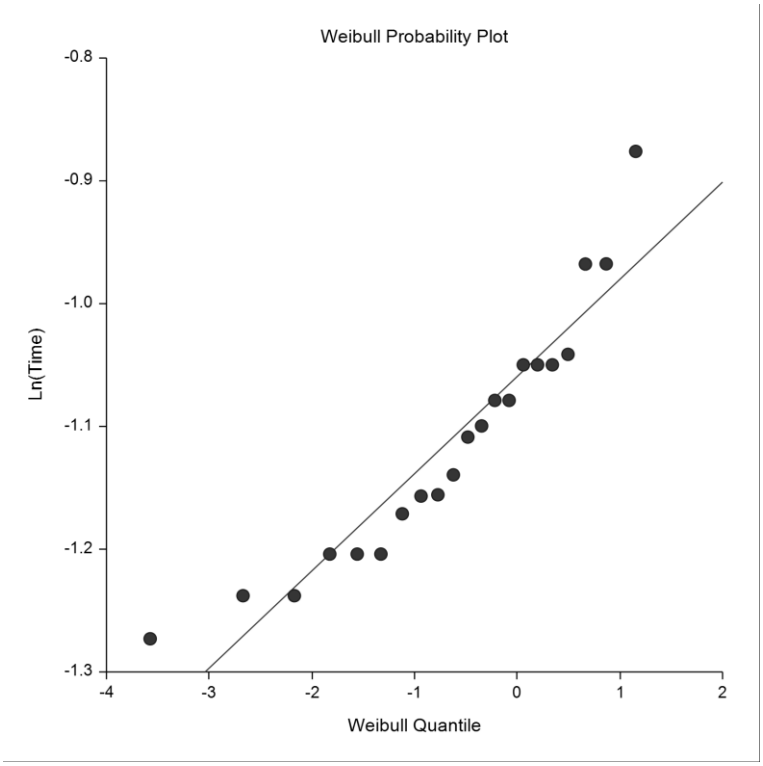

Figure A.8: Q-Q plot for Weibull distribution fit- Liver injury and maximum compression

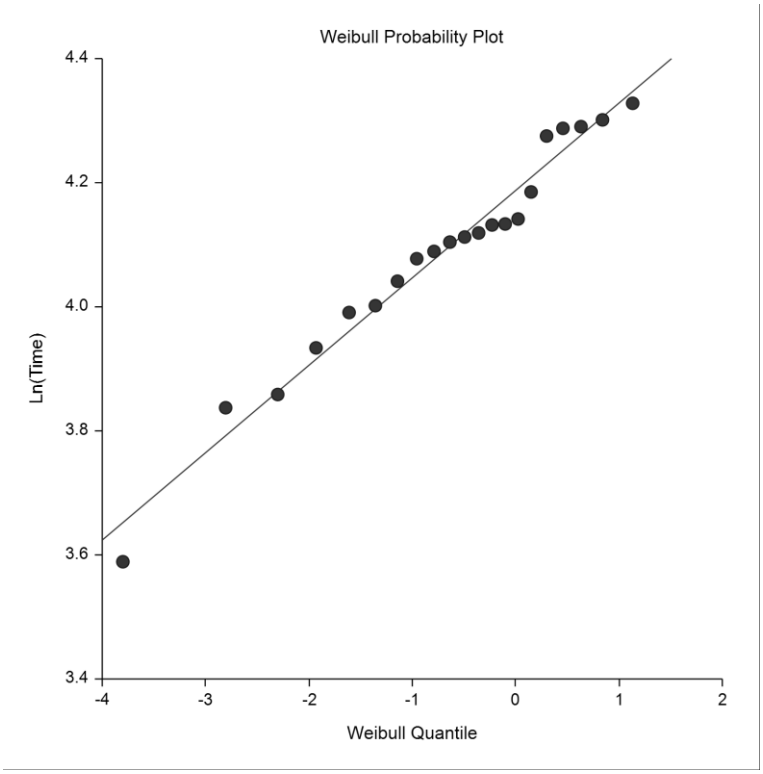

Figure A.9: Q-Q plot for Weibull distribution fit- Liver injury and compression rate

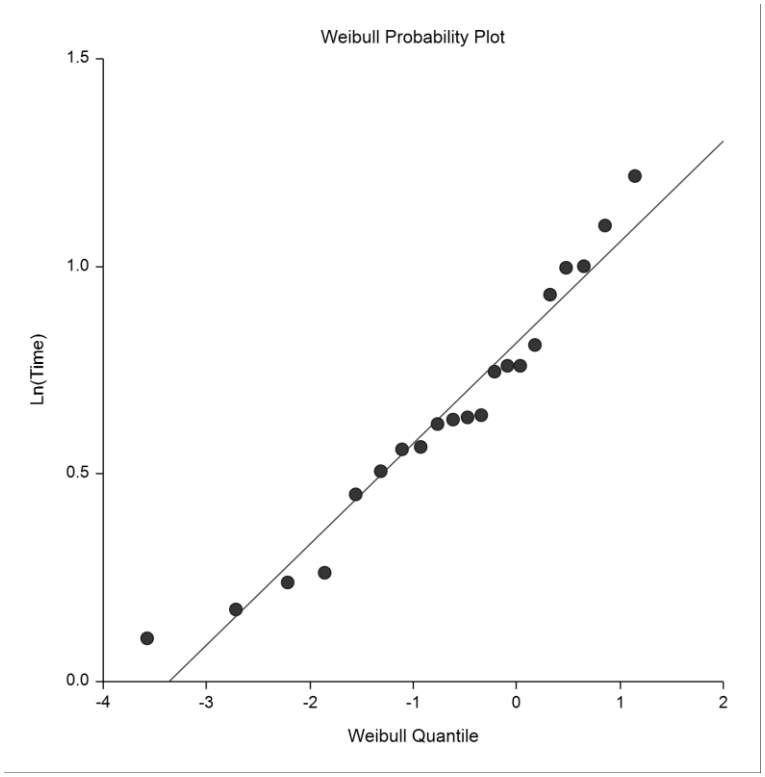

Figure A.10: Q-Q plot for Weibull distribution fit- Liver injury and viscous response

APPENDIX B: SHAPE AND SCALE PARAMETERS FOR INJURY RISK CURVES

Injury Type	Injury Criterion	Shape Parameter (k)	Scale Parameter (λ)
Lung	Acceleration	2.45	5600
Lung	Velocity	4.13	9.85
Lung	Compression	5.71	0.35
Lung	Compression rate	6.68	63.4
Lung	Axial viscous response	2.30	2.25
Liver	Acceleration	1.12	4079
Liver	Velocity	1.88	8.41
Liver	Compression	11.19	0.31
Liver	Compression rate	4.31	56.7
Liver	Axial viscous response	3.31	1.63

Table B.1: Weibull shape and scale parameters for maximum likelihood injury risk curves from UBB loading in an *in vivo* rodent model.